Solar heating plants with flat plate collectors and parabolic trough collectors

Tian, Zhiyong

Publication date:
2018

Document Version
Publisher's PDF, also known as Version of record

Solar heating plants with flat plate collectors and parabolic trough collectors

Zhiyong Tian

PhD Thesis

Department of Civil Engineering
2018

DTU Civil Engineering Report-BYG R-394

DTU Civil Engineering
Department of Civil Engineering

Solar heating plants with flat plate collectors and parabolic trough collectors

Zhiyong Tian

PhD Thesis

12/07/2018

Technical University of Denmark

DTU-BYG

Supervisors:

Simon Furbo, Associate Professor, Department of Civil Engineering, Technical University of Denmark

Jianhua Fan, Associate Professor, Department of Civil Engineering, Technical University of Denmark

Assessment Committee:

Toke Rammer Nielsen, Associate Professor, Department of Civil Engineering, Technical University of Denmark

Jørgen Schultz, Senior Sustainability Consultant, Steensen Varming Aps, Denmark

Alexander Thür, Assistant Professor, University of Innsbruck, Austria

Solar heating plants with flat plate collectors and parabolic trough collectors

Cover photo: *Aalborg CSP A/S*

Publisher: Department of Civil Engineering,

Technical University of Denmark,

Brovej, Building 118,

2800 Kgs. Lyngby, Denmark

ISBN: 9788778774910

ISSN: 1601-2917

Report: BYG R-394

Preface

This thesis was submitted as fulfilment of the requirements for the Degree of Doctor of Philosophy at the Department of Civil Engineering, Technical University of Denmark. The thesis is the result of research on **solar heating plants with flat plate collectors and parabolic trough collectors**.

This page is intentionally left blank.

Acknowledgement

The PhD study has been financed by China Scholarship Council, and the EUDP project “Kombineret Teknisk Solenergi Demonstration”, supported by the Danish Energy Agency.

During my PhD in Denmark, I have been supported by many people who I want to say thank you to here. Simon Furbo and Jianhua Fan are my supervisors. They were patient with me all the time during the study. They are always available to discuss and have good comments to the project. Special thanks are expressed to Jianhua Fan for the efforts making my PhD study possible in DTU. I also got a lot of help and advices from Bengt Perers. Bengt always gave me very good comments in a simple and positive way.

I also want to say thank you to the whole Solar Group, colleagues in Section of Building Energy (Section of Energy and Services) in the Technical University of Denmark, and Daniel Tschopp from AEE INTEC for the discussions. Especially, I would like to say thanks to Mark Dannemand for translating the abstract to Danish for the thesis and always providing tips patiently when I encountered problems on Danish language during the last three years.

I spent some time in Spain for my external stay. Loreto Valenzuela, Rafael Gongora Vizcaino and Carmen Montesinos Carretero from PSA (Plataforma Solar de Almería - CIEMAT), Fabienne Sallaberry and Leticia Aldaz Asurmendi from National Renewable Energy Centre of Spain, provided a lot of help to accommodation and work. I want to say thank you to all of you.

I would like to say thanks to Andreas Zourellis from Aalborg CSP A/S for prompt response all the time, if I needed some information from Aalborg CSP A/S. Many thanks are also expressed to Aalborg CSP A/S for the shared information within the project cooperation.

I participated several Expert meeting workshops of IEA-SHC Task 55 project - Towards the Integration of Large SHC Systems into District Heating and Cooling (DHC) Networks. Thanks to all of you for fruitful discussions.

I also would like to say thank you to all of my friends in both China and Denmark for accompany (Too many names to mention here).

Last but not the least, I would like to express my very profound gratitude to my parents, my sister and brother for continuous support during my years of study. I cannot come to this accomplishment without your encouragement.

Zhiyong Tian,

Technical University of Denmark

DK-2800 Kgs. Lyngby.

Abstract

Denmark is the frontrunner country worldwide on the total installed capacity and numbers of large solar district heating plants. By the end of 2017, more than 1.3 million m^2 solar collector fields have been constructed in Denmark. Denmark is also the first and only country with a mature-commercial market of large solar heating plants in the world. Most collectors in the existing solar district heating plants in Denmark are flat plate collectors. The thermal performance of flat plate collectors decreases with the increase of operation temperature in the plant. Parabolic trough collectors have attracted lots of attention in the temperature level 70-150 ℃ in recent years, due to the good efficiency at high temperatures. A hybrid solar district heating plant with flat plate collectors and parabolic trough collectors in series was investigated in this study.

Firstly, as large-scale solar district heating plants have been witnessed sustainable growth in magnitude and number, requiring significant initial investment in Denmark, the importance of the "bankability" of the solar radiation data and collector field yield used to plan, design and operate solar heating plants increases as well. Solar radiation analysis was carried out in this study. Total solar radiation on a tilted surface is one of the most important variables used to simulate the thermal performance of flat plate collectors, while direct normal irradiance is the main input for parabolic trough collectors. Calculated direct normal irradiance from global radiation based on empirical models for Danish solar radiation conditions was introduced and the method was validated by measurements. Calculated total radiation on a tilted surface based on the hybrid empirical models only from available global radiation was proposed and has good agreements against measurements.

A numerical model based on TRNSYS-GenOpt was set up and validated. Both measured and simulated thermal performances of a hybrid solar heating plant with flat plate collectors and parabolic trough collectors in series were investigated. Comparisons on the thermal performance of both collector types was carried out. Potential of the hybrid solar heating plant based on weather data from the design reference year was also presented for Denmark.

Thermal-economic optimization of the hybrid solar heating plant based on Levelised Cost of Heat was carried out. Optimal solar collector areas in hybrid solar heating plants was determined based on the current investment costs. Furthermore, analysis on different future scenarios, such as different parabolic trough collector price levels and heat demand,

was carried out to determine optimal configurations for hybrid solar heating plants in the near future. It is found that hybrid solar heating plants are feasible in Denmark.

This study shows the potential thermal performance of the investigated hybrid solar heating plant with flat plate collectors and parabolic trough collectors in series in Denmark. The new concept might also be used for other regions.

This PhD thesis consists of 2 parts: **Part I** is the summary of main results achieved; **Part II** is the peer-review scientific papers.

Resume

Danmark er førende vedrørende store solvarmecentraler i fjernvarmeområder, både med hensyn til installeret kapacitet og antal solvarmecentraler. Ved udgangen af 2017 var der installeret mere end 1,3 millioner m^2 solfangere i danske solvarmecentraler. Danmark er også det første og eneste land i verden med et modent kommercielt marked for store solvarmeanlæg. De fleste solfangere i de eksisterende solvarmecentraler i Danmark er plane solfangere. Den termiske ydeevne af plane solfangere reduceres når driftstemperaturen i anlægget stiger. Koncentrerende parabolske solfangere har tiltrukket opmærksomhed de seneste år på grund af den høje effektivitet i temperaturniveauet 70-150 ℃. En hybrid solvarmecentral med plane solfangere og koncentrerende solfangere i serie er blevet undersøgt i dette studium.

Storskala solvarmeanlæg i Danmark har været i vedvarende vækst i størrelse og antal. Disse anlæg kræver en betydelig investering og derfor er korrektheden af solstrålingsdata brugt til at beregne det samlede udbytte af solfangerfeltet vigtig for planlægning, design og drift af solvarmeanlægget. Der er blevet udført en solstrålingsanalyse i dette studium. Den samlede solindstråling på en skrå flade er vigtig da den bruges til at simulere termiske ydelser af plane solfangere, mens den direkte stråling er vigtigst for koncentrerende solfangere. En model til beregning af direkte stråling ud fra global stråling baseret på empiriske modeller under danske solstrålingsforhold er foreslået og valideret ved målinger. En beregning af total stråling på en skrå flade baseret på hybrid-empiriske modeller fra global stråling blev analyseret. Modellen resulterer i små forskelle mellem målt og beregnet solstråling.

En numerisk model baseret på TRNSYS-GenOpt blev udviklet og valideret. Både de målte og simulerede termiske ydelser af et hybrid-solvarmeanlæg med plane solfangere og parabolske trug solfangere blev undersøgt. Den termiske ydeevne af begge solfangertyper blev undersøgt og sammenlignet. Baseret på vejrdata fra designreferenceåret for Danmark blev potentialet for hybrid-solvarmeanlægget bestemt.

En termisk-økonomisk analyse af hybrid-solvarmeanlægget baseret på ”Levelised Cost of Heat” blev udført. De optimale solfangerarealer for hybrid-solvarmeanlæg blev bestemt ud fra investeringsomkostningerne. Desuden blev der gennemført analyser af forskellige fremtidige scenarier, med forskellige prisniveauer og efterspørgselsbehov for de koncentrerende solfangere, for at bestemme optimale konfigurationer for hybrid-solvarmeanlæg. Det konstateret at hybridvarmeanlæg er mulige i Danmark.

Denne undersøgelse viser potentiellet for hybrid-solvarmeanlæg med plane solfangere og paraboliske solfangere i Danmark. Designkonceptet kan også bruges til andre regioner.

Denne ph.d.-afhandling består af 2 dele: Del I er et resumé af de vigtigste resultater. Del II er de offentliggjorte peer review videnskabelige artikler.

Following papers have been included directly or indirectly in the thesis

[1] **Zhiyong Tian**, Bengt Perers, Simon Furbo, Jianhua Fan, Jie Deng and Janne Dragsted. A Comprehensive Approach for Modelling Horizontal Diffuse Radiation, Direct Normal Irradiance and Total Tilted Solar Radiation Based on Global Radiation under Danish Climate Conditions, **Energies**, vol. 11, no. 5, May 2018.

[2] **Zhiyong Tian**, Bengt Perers, Simon Furbo and Jianhua Fan, Analysis and validation of a quasi-dynamic model for a solar collector field with flat plate collectors and parabolic trough collectors in series for district heating, **Energy**, vol. 142, pp. 130–138, 2018.

[3] **Zhiyong Tian**, Bengt Perers, Simon Furbo and Jianhua Fan, Annual measured and simulated thermal performance analysis of a hybrid solar district heating plant with flat plate collectors and parabolic trough collectors in series, **Applied Energy**, vol. 205, pp. 417–427, 2017.

[4] **Zhiyong Tian**, Bengt Perers, Simon Furbo and Jianhua Fan, Thermo-economic optimization of a hybrid solar district heating plant with flat plate collectors and parabolic trough collectors in series. **Energy Conversion and Management**, vol. 165, pp. 92–101, 2018.

[5] Fabienne Sallaberry, **Zhiyong Tian**, Odei Goñi Jauregi, Simon Furbo, Bengt Perers, Andreas Zourellis and Jan Holst Rothmann, Evaluation of the Tracking Accuracy of Parabolic-Trough Collectors in a Solar Plant for District Heating, **Proceedings of SolarPACES 2017 conference**.

[6] Benjamin Ahlgren, **Zhiyong Tian**, Bengt Perers, Janne Dragsted, Emma Johansson, Kajsa Lundberg, Jonatan Mossegård, Joakim Byström, Olle Olsson. A simplified model for linear correlation between annual yield and DNI for parabolic trough collectors. **Energy Conversion and Management**, vol. 174, pp. 295–308, 2018.

Publications that are part of the PhD study but not included in the thesis are the following:

[1] Jie Deng, **Zhiyong Tian**, Jianhua Fan, Ming Yang, Simon Furbo, Zhifeng Wang. Simulation and optimization study on a solar space heating system combined with a low temperature ASHP for single family rural residential houses in Beijing. **Energy and Buildings**. 2016;126:2-13.doi:10.1016/j.enbuild.2016.05.019.

[2] Bengt Perers, Simon Furbo, **Zhiyong Tian**, Egelwisse Jörn, Federico Bava, Jianhua Fan. Tårs 10000 m^2 CSP + flat plate solar collector plant - cost-performance optimization of the design. **Energy Procedia**. 2016;91:312-316. doi:10.1016/j.egypro.2016.06.224.

[3] **Zhiyong Tian**, Bengt Perers, Simon Furbo and Jianhua Fan, Analysis of measured and modeled solar radiation at the Taars solar heating plant in Denmark. **Proceeding of the 11th ISES Eurosun 2016 conference**.

[4] Simon Furbo, Bengt Perers, Weiqiang Kong, **Zhiyong Tian**, Hans-Erik Kiil, Anders William Larsen, René Bang Madsen, New CPC based hybrid collector for solar heating plants, **International Solar District Heating Conference 2016**.

[5] **Zhiyong Tian**, Bengt Perers, Simon Furbo and Jianhua Fan, Thermal performance of a combined solar heating plants with parabolic trough collectors and flat plate collectors, **Proceeding of International Solar District Heating Conference 2016**.

[6] Bengt Perers, Simon Furbo, Guofeng Yuan, **Zhiyong Tian**, Federico Bava, Peter Kvis, Jan Holst Rothmann , Thorkil Neergaard , Jørgen Røhr Jensen, Per Alex Sørensen, Niels From, Fabienne Sallaberry. A CSP plant combined with biomass CHP using ORC-technology in Brønderslev Denmark, **Proceedings of the ISES EuroSun 2016 conference**.

[7] Bengt Perers, Simon Furbo, **Zhiyong Tian**, Jan Holst Rothmann, Jacob Juul, Thorkil Neergaard, Poul Vestergaard Jensen, Jørgen Røhr Jensen, Per Alex Sørensen, Niels From. Performance of the 27000 m^2 parabolic trough collector field, combined with Biomass ORC Cogeneration of Electricity, in Brøndeslev Denmark. **Proceeding of International Solar District Heating Conference 2018**.

[8] Bengt Perers, Janne Dragsted, Simon Furbo, **Zhiyong Tian**, Jonatan Mossegård, Joakim Byström, Olle Olsson, Benjamin Ahlgren, Emma Johansson, Kajsa Lundberg. A novel simulation model, for the annual yield of parabolic trough collectors, including shading in the field. Simulation and validation. **Proceeding of International Solar District Heating Conference 2018.**

Contents

List of Figures

List of Tables

This page is intentionally left blank.

Part I Summary

1 Introduction

In December of 2015, Conference of Parties (COP) 21, also known as the 2015 United Nations Climate Change Conference (Paris), has achieved a legally binding and universal agreement on climate, with the aim of keeping global warming below 2°C, for the first time after over 20 years of UN negotiations [1].

The building sector is responsible for approximately 40% of energy consumption and 36% of CO_2 emissions in the EU [2]. Space heating and domestic hot water systems consume about 80% of total energy consumption in the EU building sector [3]. 84 % of heating and cooling energy consumption in the EU is still produced by fossil fuel systems while only 16 % is generated from renewable energy sector [3]. In order to fulfil EU's climate and energy goals, the heating and cooling sector in EU must sharply cut down its energy demand and scale down its use of fossil fuels in the coming decades [4]. Use of renewable energy can reduce the fossil energy consumption in the building sector, particularly solar energy. Solar energy is the most commercial and market-driven energy source used among renewable energy sources in the building sector. Solar heat technology can play a crucial role in the 2050 Europe energy mix. Solar heat technology can cover up to 47% of the energy demand at low temperature levels with a favorable policy framework [5].

Efficient district energy systems can play a key role in the energy transition towards a low-carbon economy, acting as an evaluative backbone towards efficient local energy systems [4]. Different energy system configurations were optimized and the results showed that solar collector fields should be included in the energy supply system to achieve both an economic and environmental optimization [6].

The vision of the Solar Heating and Cooling (SHC) Programme of the International Energy Agency (IEA) is "By 2050 a worldwide capacity of 5 kW_{th} per capita of solar thermal energy systems installed and significant reductions in energy consumption achieved by using passive solar and daylighting: thus solar thermal energy meeting 50% of low temperature heating and cooling demand (heat up to 250 °C)" [7]. IEA-SHC Task 7 - Central Solar Heating Plants with Seasonal Storage, Task 45 - Large Systems: Large Solar Heating/Cooling Systems, Seasonal Storage, Heat Pumps and Task 55- Towards the Integration of Large SHC Systems into District Heating and Cooling (DHC) Networks, has focused on the application of large solar heating and cooling systems in district heating.

Guadalfajara et al. [8] did dynamic simulations to investigate the potential of large solar district heating plants in 10 cities in Spain. It was concluded that solar district heating plants with seasonal storage could be an interesting alternative for Spain compared to traditional natural gas boiler systems. Carotenuto et al. [9] carried out simulations on a novel solar-geothermal district heating, cooling and domestic hot water system in Italy. It was found that the studied system achieved a significant saving of primary energy consumption compared with the traditional reference system. Urbaneck et al. [10] found that it could be very attractive to realize about 10% solar fraction in many German district heating systems. A 500,000 m² solar heating plant for 20% solar fraction is planned in Graz, Austria [11]. Sirén et al. [12]–[14] did the feasibility study of solar district heating plants in Finland. It was found that solar thermal energy can be used to provide a significant fraction of heat demand even in high latitude Nordic countries, like Finland. Soloha et al. [15] found that it was possible to achieve 10-78% solar fraction in a typical district heating networks in Latvia. Furthermore, the Drake Landing Solar Community in Canada is the first major implemented solar district heating system with seasonal solar thermal energy storage in North America [16][17]. Drake Landing Solar Community achieves consistent solar fractions above 90% over the last 5 years, with an average of 96% for the period 2012-2016 [18]. Reed et al. [19] investigated the pathways to commercial viability of solar district heating systems with underground thermal energy storage in America based on the Drake Landing Solar Community model. In addition, Denmark is the most successful country worldwide in solar district heating plants and attracts lots of attention.

1.1 Energy policy in Denmark

The objective of the Danish energy policy as a whole is that Denmark should cease to be dependent on fossil fuels (coal, oil and gas) by 2050 [20]. In 2015, 56% of electricity consumption and about 51% of district heating consumption was covered by renewable energy, compared to 16% and 19%, respectively, in 2000 [21]. Renewable energy is expected to cover about 72% of electricity consumption and 71 % of district heating consumption in 2020, compared with about 56% and 51% respectively in 2015 [21]. The heating requirements of 64% of Danish households are provided by district heating networks [22], consisting of space heating and domestic hot water. District heating systems are an interesting opportunity for the increase of renewable energy share in the heating and cooling sector [23]. District heating in Denmark is expected to play an important role in reaching the following EU and Danish energy goals [24]:

• 2020 climate & energy package: a 20% reduction in CO_2 emissions compared to 1990 levels, an increase in the share of renewables to 20% of the energy (Denmark’s share is 30%), and a 20% increase in energy efficiency.

• In 2020, half of the domestic electricity consumption should be supplied by wind energy in Denmark.

• By 2030, 50% of the Danish gross energy consumption comes from renewable energy sector.

• In the 2050, the whole energy systems in Denmark are to be independent of fossil fuels.

District heating in the Nordic area has a long history. During the 1920's and 1930's, a collective district heating system was developed based on waste heat from local electricity production in Denmark [25]. Around 4% of the Danish heat demand of some urban areas was covered by district heating networks at that time. From here on, district heating network from combined heat and power (CHP) plants expanded in the larger Danish cities and in the 1970's, around 30 % of all households were connected with district heating systems [26]. After the energy crisis in 1973 and 1974, cost-effectiveness and security of energy supply became a significant priority of energy policy by the Danish Government. Then the government supported district heating and combined heating and power through favorable energy policies in order to decrease dependency on imported oil. The first law on heat supply in Denmark started a new era in public heat planning in 1979, which still exists today [24]. The Heat Supply Act from 1979 (revised extensively in 1990, 2000 and 2005) empowered Danish Energy Authority to ban use of electric heating systems in new buildings located within district heating or natural gas supply networks [27]. A political majority in the Danish Parliament decided to improve conditions for 250 small- and medium-sized CHP plants outside the major cities for the period from 1993 to 2000 [28]. In 2008, political agreements were made to promote wind energy and other renewable energy sources in Danish energy systems. In 2012, Major political agreement about Danish energy policy for the period 2012-2020 were agreed upon containing a wide range of ambitious initiatives and investments within energy efficiency, renewable energy and the energy system [24]. A number of initiatives from Danish government will reduce individual heating based on oil and gas in buildings and promote renewable alternatives. These include a halt to installation of oil-fired and gas-fired boilers in new buildings from 2013 and a halt to installation of oil-fired boilers in existing buildings from 2016 in areas with district heating or natural gas [24].

The key aspects for development of district heating in Denmark can be as summarized below [4]:

• Non-profit principle: All the district heating companies under the **Heat Supply Act** are non-profit. The price of heat is only allowed to include the necessary costs for production

and distribution for end-uses. Most of the district heating companies are owned and controlled by the consumers through the cooperation or local municipalities.

- Heat planning and cost effective zoning.
- Protection of consumers.
- General ban on electric and oil boilers.
- Subsidies and Taxes.
- Financial instruments.
- Price competitiveness.

Few solar heating plants connected to district heating systems was found in Denmark before 2005. However, the technological development of solar heating plants combined with a change in regulatory setup for small-scale CHP plants expanded a huge potential emerging market of solar heating plants, specifically for district heating sector. Large-scale solar heating plants in Denmark are experiencing a very rapid expansion from 2006. In the long term energy scenarios, the Danish Energy Agency predicts a heat production from solar heating plants of 6,000 TJ in 2025, which is approximately 7 times as the amount in 2015 [24].

1.2 Solar district heating plants in Denmark

The first solar collector arrays for district heating networks were constructed in Sweden in 1980s [29]. Then, large solar district heating plants developed rapidly in Denmark, Germany [30], and Austria, particularly in Denmark [31].

During the last ten years, the annual growth in the total solar collector area has been an average of 42% and the corresponding increase of solar heating plants has been 29% in Denmark [32]. By the end of 2017, more than 1.3 million square meter solar collector arrays are in operation in Denmark for district heating networks, see Fig. 1. Denmark is the global-leader country for large solar district heating plants. Denmark is also the first and the only country with a commercial mature-market for large solar district heating plants [31]. Most of the largest solar district heating plants worldwide are constructed in Denmark, such as Marstal (33300 m^2), Dronninglund (37573 m^2), Vojens (70000 m^2) and Silkeborg (156694 m^2), as is shown in Fig. 2.

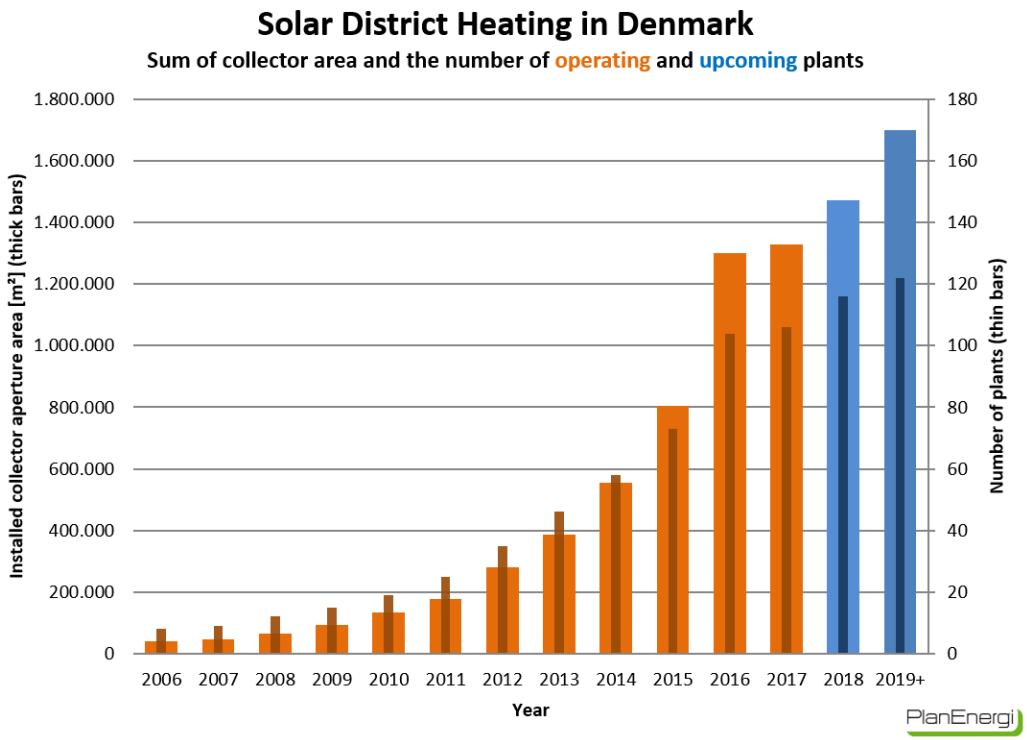

Fig. 1 Development of solar district heating plants in Denmark from 2006 [32].

Fig. 2a Marstal plant (33300 m^2)

Fig. 2c Vojens plant (70000 m^2)

Fig. 2b Dronninglund plant (37573 m^2)

Fig. 2d Silkeborg plant (156694 m^2)

Fig. 2 Typical large solar heating plants in Denmark (source: Arcon-Sunmark A/S).

Fig. 3 Typical large flat plate collectors without/with FEP foils used in solar heating plants (Source: Arcon-sunmark A/S) [33].

The main successful key factors for solar district heating plants in Denmark can be summarized as follows: sound low temperature district heating networks, favourable cost-performance of ground mounted flat plate collectors, long lifetime of solar collectors of at least 30 years, cheap land, high heat price from natural gas boiler systems.

Solar collectors are the core components of solar district heating plants. Annual solar heat yield of solar heating plants on average is around 400-460 kWh/m^2 in Denmark [34][35]. Most solar collectors in the large solar district heating plants in Denmark are ground-mounted flat plate collectors, see Fig. 2. Arcon-Sunmark A/S is the main manufacturer of the large flat plate collectors for district heating in Denmark. Arcon-Sunmark A/S has installed more than 80% of the world's large solar heating plants connected to district heating networks. Typical flat plate collectors delivered by Arcon-Sunmark A/S in Danish solar heating plants can be seen in Fig. 3. Flat plate collectors without and with FEP foils are usually used together in series in the solar district heating plants to get more energy output. Large flat plate collector is the most mature-commercialized solar collector technology in large solar district heating plants so far.

The flat plate collector field supplies the heat to the district heating networks via a heat exchanger. Therefore the operation temperature of flat plate collectors is 3-4 K higher than the temperatures on the district heating side. The required supply temperature is 85-95 ℃ for typical Danish district heating networks. The efficiency of flat plate collectors decreases sharply at these temperature levels. Solar collectors include flat plate collectors, evacuated tube collectors, compound parabolic collectors and concentrating solar power collectors. Compared to flat plate collectors, the heat loss of parabolic trough collectors is very low at these temperature levels. And the efficiency of the parabolic trough collectors is almost constant for low-medium temperature application. More and more parabolic trough collectors are used in the industrial process heat in the last decades [36].

Frank et al. [37] evaluated the daily and monthly performance of two solar plants with parabolic trough collectors in Switzerland. The apertures of both the solar heating plants are 115 m^2 and 630 m^2. The second plant is located at an altitude of 1000 m. Even though

the yearly DNI is low (1183 kWh/m^2/a), both the daily and the monthly evaluation presented that the collector field performance could be high when the operation temperature of parabolic trough collectors is low, such as 125℃. Silva et al. [38], [39] did simulations and thermo-economic design optimization on parabolic trough collectors for heat production for industrial processes. LCOE (Levelized Cost Of Energy) of 5 c€/kWh and a PBT (payback time) of 8 years could be achieved at the base scenario conditions considered. Kizilkan et al. [40] proposed a parabolic trough solar collector-based integrated system for an ice-cream factory in Turkey and discussed the thermal performance. The payback period of the proposed integrated system was found to be 8.5 years. The payback period was similar as reported by Silva et al [38], [39].

On the one hand, flat plate collectors are cheaper and have higher efficiency than parabolic trough collectors at low temperature levels. On the other hand, parabolic trough collectors retain high efficiency at high temperature levels of the district heating networks. Thirdly parabolic trough collectors can use more beam radiation during the daytime, due to the tracking. A hybrid solar district heating plant consisting of flat plate collectors and parabolic trough collectors in series can harvest the good performance of both solar collector technologies. The barrier of parabolic trough collectors for application in district heating networks is the high price. The yearly DNI in Denmark is not high and Denmark has not been regarded as a suitable place for concentrating solar power technologies for a long time. So a techno-economic analysis of hybrid solar district heating plants should be determined in order to figure out which collector type and field design is the most favourable one.

A preliminary case study of parabolic trough collectors for district heating at high latitudes with low solar radiation resources was carried out in 2000 [41]. The economic comparison indicated that parabolic trough systems could be competitive with flat plate collectors. But few practical projects with parabolic trough collectors for district heating are found during the last decades. The Danish company Aalborg CSP A/S [42] and Technical University of Denmark (DTU) [43] started to investigate the feasibility of parabolic trough collector for district heating networks in large solar heating plants through an Energy Technology Development and Demonstration Programs project (EUDP) supported by Danish Energy Agency in 2013. A hybrid solar district heating plant with flat plate collectors and parabolic trough collectors in series was constructed in Taars, in the northern Jutland of Denmark in 2015 [44].

1.3 Development of PTCs for solar district heating

1.3.1 Parabolic trough collectors

As is shown in Fig. 4, concentrating solar power collector technologies consist of parabolic trough collector (Fig. 4a), linear Fresnel collector (Fig. 4b), central receiver system with dish collector (Fig. 4c), and central receiver system with distributed reflectors (Fig. 4d). Another concentrating collector type is Compound Parabolic Concentrator (CPC). The CPC can be non-tracking. Parabolic trough collector is one of the most promising concentrating solar power technologies in the commercial market. IEA-SHC Task 49 has focused on solar heat for industrial processes (SHIP) [36]. It is indicated that parabolic trough collectors are more suitable than other solar collector technologies in industrial processes. Parabolic trough collector consists of parabolic trough receivers, mirrors and tracking device. Parabolic trough collector can track the sun from sunrise to sunset during the daytime, see Fig. 5. The sunlight reaching the mirror parallel to its plane of symmetry is focused along the focal line, where the receiver is located. Today the absorber tube is often enclosed in a vacuum glass tube to further reduce the heat loss. Parabolic trough collectors also are the most suitable solar collectors for the temperature level 90-150 ℃ [36]. The heat loss of parabolic trough collectors is low at temperature level 80-150 ℃ because of the vacuum condition around the receiver.

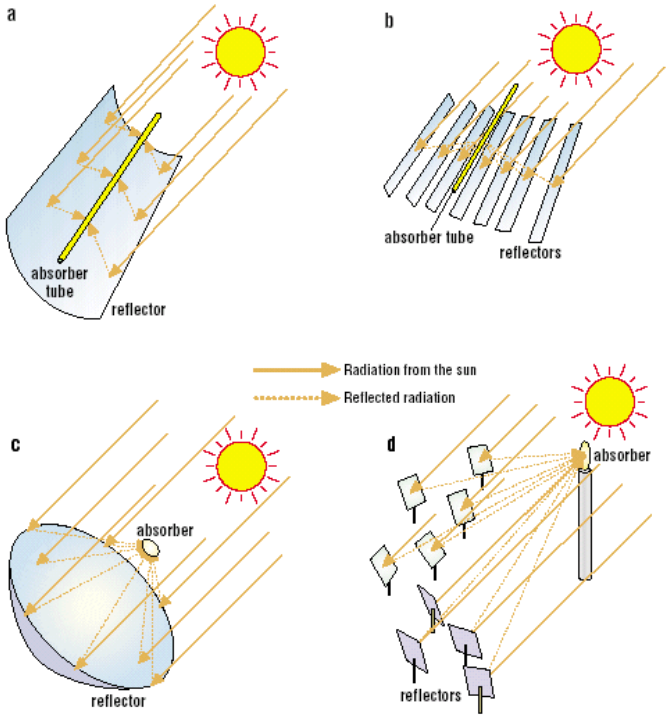

Fig. 4 Concentrating solar power collector technologies: (a) parabolic trough collector (b) linear Fresnel collector (c) central receiver system with dish collector and (d) central receiver system with distributed reflectors [45].

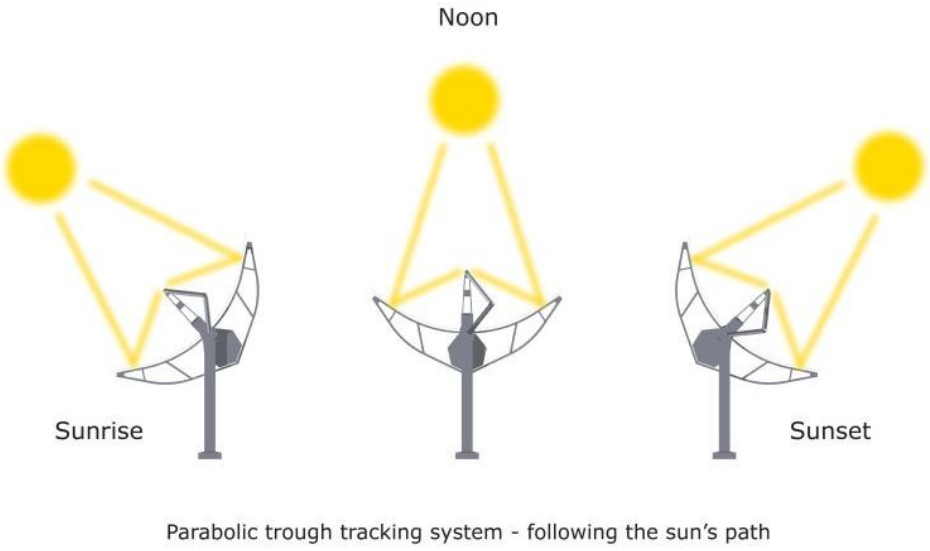

Fig. 5 Principle of parabolic trough collector during the daytime [42].

1.3.2 Demonstration projects in Denmark

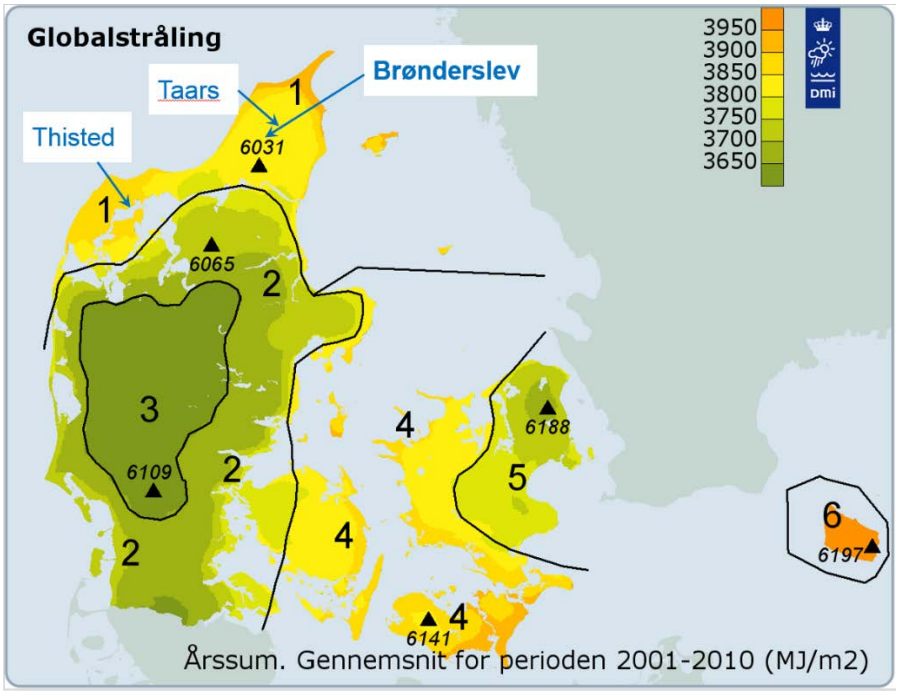

Fig. 6 Location of solar district heating demonstration projects with concentrating solar collectors in Denmark (Source: Danish Meteorological Institute) [46].

Fig. 7 The pilot parabolic trough collector loop in Thisted, Denmark (Source: Aalborg CSP A/S).

Three pilot parabolic trough collector plants have been installed in Denmark in recent years, as is shown in Fig. 6. There are 6 solar radiation zones in Denmark. The pilot parabolic trough collector plants are in the first solar radiation zone, north part of Denmark. The yearly global solar radiation on the horizontal surface in Denmark is around 1000-1150 kWh/m^2. Fig. 7 shows the first pilot parabolic trough collector loop for district heating in Thisted, Denmark [42]. The Thisted collector array is connected to a boiler plant and it has been operated at relatively high temperatures in the range of 100°C -120°C [43]. The aperture area of parabolic trough collector field is 808 m^2. The heat transfer fluid is water.

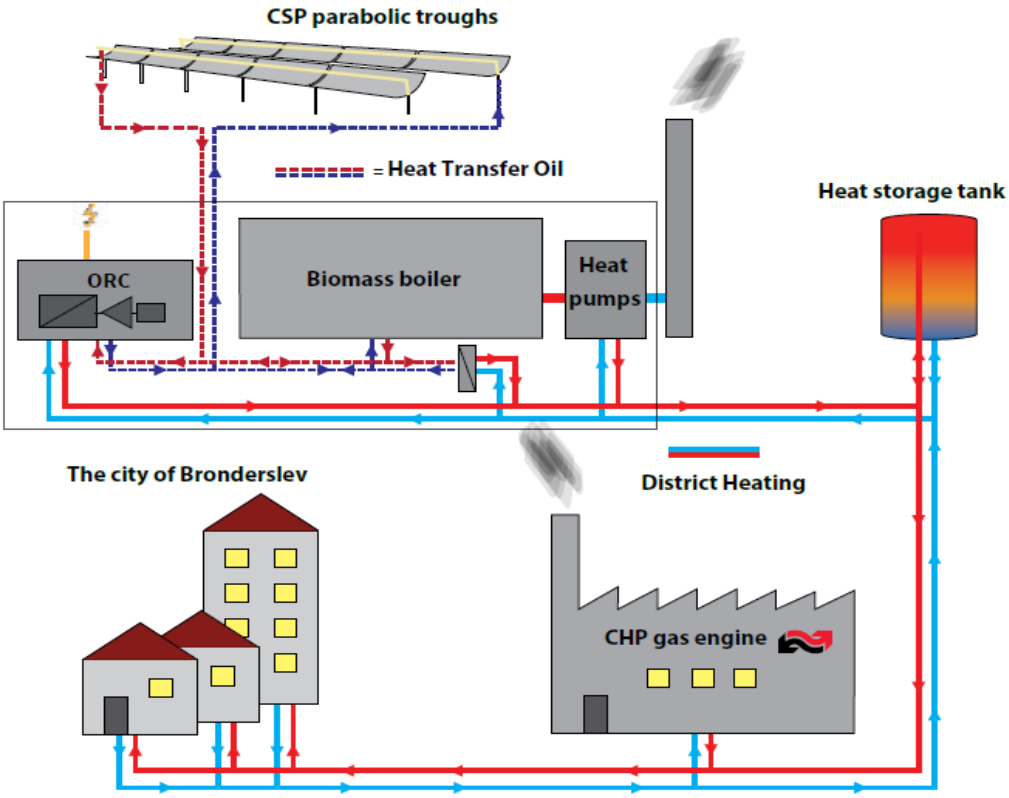

Fig. 8 Concentrated solar power integrated with a biomass-ORC plant (Source: Aalborg CSP A/S).

Fig. 9 The parabolic trough collector array in Brønderslev, Denmark (Source: Aalborg CSP A/S).

A concentrating solar power (CSP) plant with biomass combined heating and power (CHP), using Organic Rankine Cycle (ORC) was constructed in Brønderslev in the northern part of Denmark, as is shown in Fig. 8. The aperture area of the parabolic trough collector field is about 27000 m^2, see Fig. 9. The heat transfer fluid is oil. The design power is 16.6 MW_{th}. The plant was put into operation in 2017.

Furthermore, a hybrid solar district heating plant with flat plate collectors and parabolic trough collectors in series was constructed and put into operation in August 2015, in Taars. This study is mainly related to the hybrid solar district heating plant in Taars. Detailed information about the pilot hybrid solar district heating plant can be found in Chapter 2.

1.4 Aim and scope

The focus of this PhD study is on hybrid solar heating plants with flat plate collectors and parabolic trough collectors. As most collectors in existing solar heating plants are mass produced flat plate collectors after reliable development during many years, parabolic trough collectors were not considered as the suitable technology for solar district heating plants in the current market, particularly for high latitudes. However, with the rapid development of parabolic trough collectors, reliable tracking accuracy and high efficiency at high temperature, parabolic trough collectors can be cost-effectively today. Parabolic trough collectors are more and more interesting for the solar thermal market, especially in series with flat plate collectors.

Denmark is located at high latitudes and has relatively low average solar radiation compared to many other regions. Given that the most successful market worldwide for large solar district heating plants with flat plate collectors is Denmark, it is interesting to analyze the potential of parabolic trough collectors in solar district heating plants in Denmark.

A new design concept for large solar district heating plants with flat plate collectors and parabolic trough collectors in series is introduced in this study. The aim of this PhD study is to investigate the technical-economic feasibility of solar heating plants with both types of collectors in Denmark. Four hypotheses will be investigated in this study.

(I) Is there enough DNI for the application of parabolic trough collectors in Denmark?

This is addressed in Paper 1.

(II) Can standard collector test parameters be used to simulate the thermal performance of large flat plate collector and parabolic trough collector fields?

This is addressed in Paper 2.

(III) Can the principle of hybrid solar district heating plants with flat plate and parabolic trough collectors in series work in Denmark?

This is addressed in Paper 3.

(IV) Is it technical-economically feasible to use hybrid solar district heating plants?

This is addressed in Paper 4.

The outline of this study is summarized as follows:

Chapter 1: Introduction of this study.
Chapter 2: The pilot hybrid solar district heating plant.
Chapter 3: Model description and validation.
Chapter 4: Solar radiation and thermal performances.
Chapter 5: Optimizations.
Chapter 6: Discussion.
Chapter 7: Conclusions.
Chapter 8: Future work.

2 Taars hybrid solar district heating plant

Taars plant is the first large-scale demonstration project with flat plate collectors and parabolic trough collectors in series developed for district heating in Europe, even worldwide. The plant was put into operation in the middle of August, 2015. The return water from the district heating network is preheated up to 65 - 75°C by the heat exchanger connected to the flat plate collector field. Then the preheated water from the flat plate collector field is heated to the required temperature by going through the parabolic trough collector field, see Fig. 10. The solar collector fluid of the parabolic trough collectors is water, while that of FPC is a glycol/water mixture (35%). The aperture areas of the flat plate collector field and the parabolic trough collector field are 5960 m^2 and 4039 m^2, respectively. The flat plate collector field consists of flat plate collectors half without and half with FEP foils. The flat plate collectors were delivered by Arcon-Sunmark A/S [33]. Geometry parameters of the flat plate collectors and parabolic trough collectors can be found in Table 1 and 2. The parabolic trough collectors were delivered by Aalborg CSP A/S [42]. Two natural gas boilers with 9.1 MW in total are used as the back-up systems. Two tanks with 2430 m^3 in total in the existing boiler system are used as short-term storage. The district heating network supplies hot water for space heating and domestic hot water for about 850 buildings with about 1900 residents.

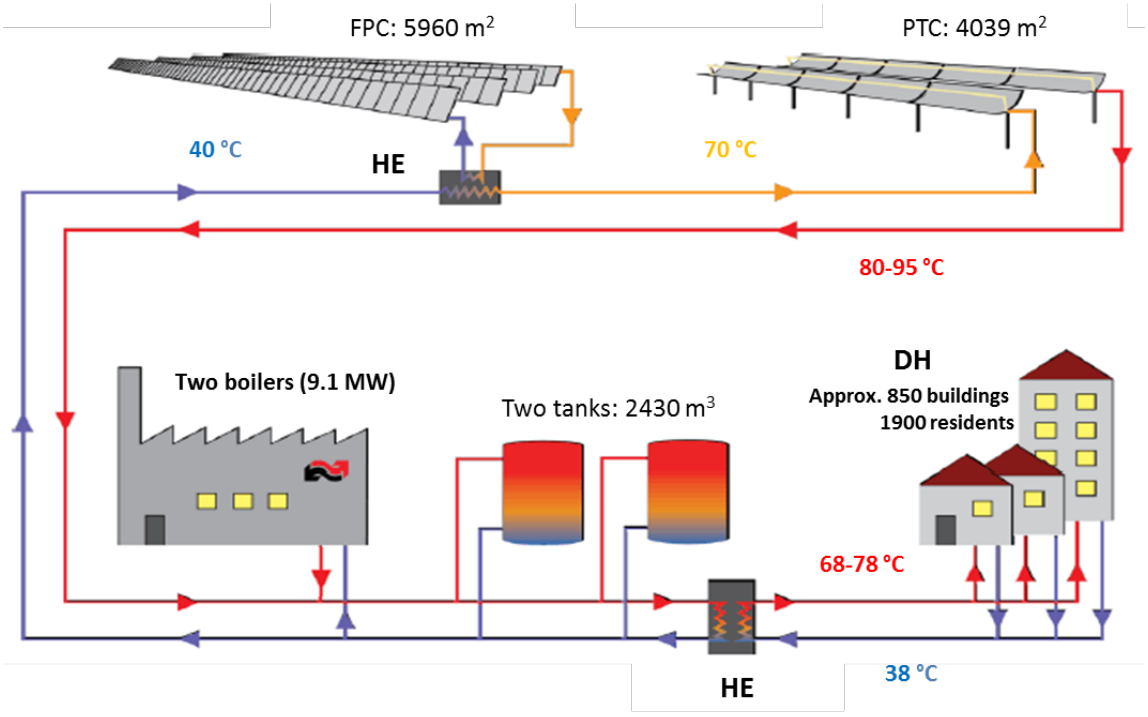

Fig. 10 Simplified illustration chart of the Taars plant.

Fig. 11 The hybrid solar collector field of the Taars plant (Source: Aalborg CSP A/S).

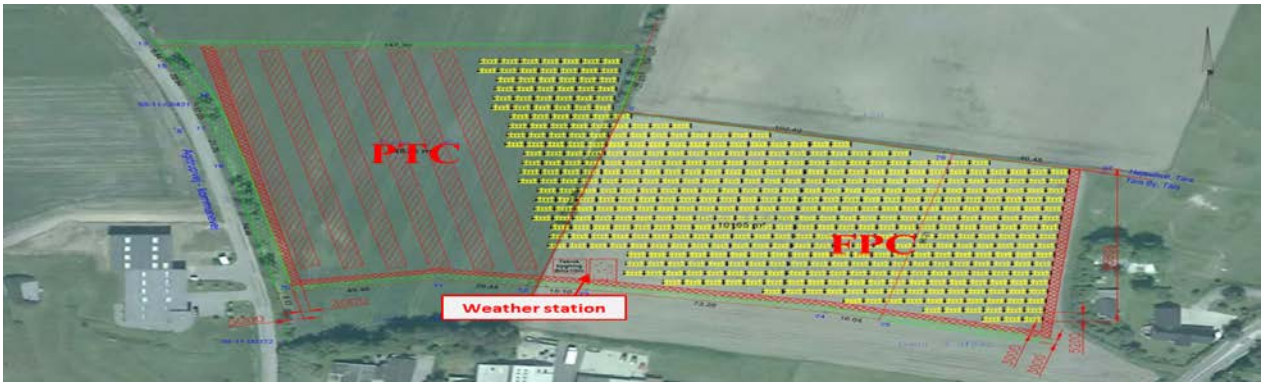

Fig. 12 Layout of the hybrid solar collector field in Taars (Source: Aalborg CSP A/S).

Table 1 Geometry parameters of the flat plate collectors.

Geometrical parameters for the FP collector		
Length, m		5.96
Width, m		2.27
Thickness, m		0.14
Gross area, m^2		13.57
Aperture area, m^2		12.60
Solar collector volume, L		10.6
Absorber	Material	Cu pipe /Al plate
	Absorption	0.95
	Emission	0.05
Insulation	Backside	75 mm mineral wool
	Side	30 mm mineral wool
Cover(s)	Atireflex glass(AR:3.2mm)-with/without FEP foil	

Table 2 Geometry parameters of the parabolic trough collectors.

Geometrical parameters for the PTC collector	
Absorber tube outer diameter (m)	0.070
Absorber tube inner diameter (m)	0.066
Glass envelope outer diameter (m)	0.125
Glass envelope inner diameter (m)	0.119
Parabola width (m)	5.77
Numbers of modules per row	10
Mirror length in each module (m)	12
Geometric concentration ratio	26.2

Fig. 11 shows the photo of the hybrid solar collector field in Taars. Fig. 12 illustrates the layout of the flat plate collector field and parabolic trough collector field. The row distance of parabolic trough collector field and flat plate collector field is 12.6 and 5.67 m, respectively. The parabolic trough collector field consists of six rows of around 125 m collector loop. The orientation of parabolic trough collectors is 13.4° towards west from south. The tilt of flat plate collectors is 50 °.

3 Model description, measurements and validation

3.1 Empirical models for solar radiation analysis

Dragsted et al. analyzed solar radiation measurements from the climate station at Technical University of Denmark from 2006 to 2010 [47]. A DTU model was developed to determine diffuse radiation based on global radiation on the horizontal surface. The reduced Reindl model (RR model) developed in two steps was used to determine the diffuse fraction by means of the clearness index and the solar altitude angle [48]. Both the DTU model and the RR model were used to calculate diffuse radiation on a horizontal surface.

Five other empirical models (one isotropic model and four anisotropic models) were used to calculate total solar radiation on the tilted flat plate collector surface. The isotropic model, also called by “Liu-Jordan model”, was developed by Liu et al. [49]. The isotropic model assumes that the diffuse radiation from a complete sky dome is distributed uniformly. Four anisotropic models (HD, HDKR, Perez I and II) were further developed by Hay, Davies, Reindl, and Perez, et at. [50]. HD model considered circumsolar diffuse radiation by using an anisotropy index. HDKR model adds a horizon brightening diffuse term to HD model. Perez models use empirically derived "reduced brightness coefficients" to calculate circumsolar, horizon brightening, and isotropic diffuse radiation. Mathematical description of the models can be found in paper 1.

3.1.1 Solar radiation measurements

A weather station was set up in the Taars plant, as shown in Fig. 13. Global radiation, DNI, total radiation on the tilted solar collectors were measured from middle of August, 2015.

Fig. 13 Used weather station and pyrheliometer of the Taars solar heating plant.

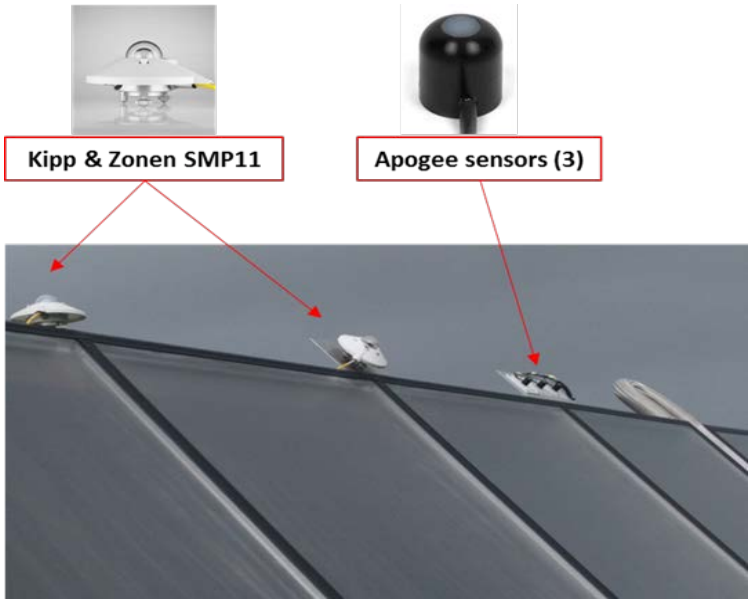

Fig. 14 Pyranometers and pyrheliometer in Taars plant.

As shown in Fig. 14, four south facing pyranometers with a tilt of 50° were installed on the top of a flat plate collector plane in the middle of the flat plate collector field. Three Apogee pyranometers were used as backup sensors to double-check the measured total solar radiation on the tilted surface. Two of the pyranometers to measure solar radiation on the horizontal surface and solar radiation on the titled collector plane were Kipp&Zonen SMP11, see Fig. 14 left. DNI was measured with a PMO6-CC pyrheliometer with the sun tracking platform Sunscanner SC1 in the weather station next to the solar heating plant, see Fig. 13.

3.1.2 Model validation on the solar radiation

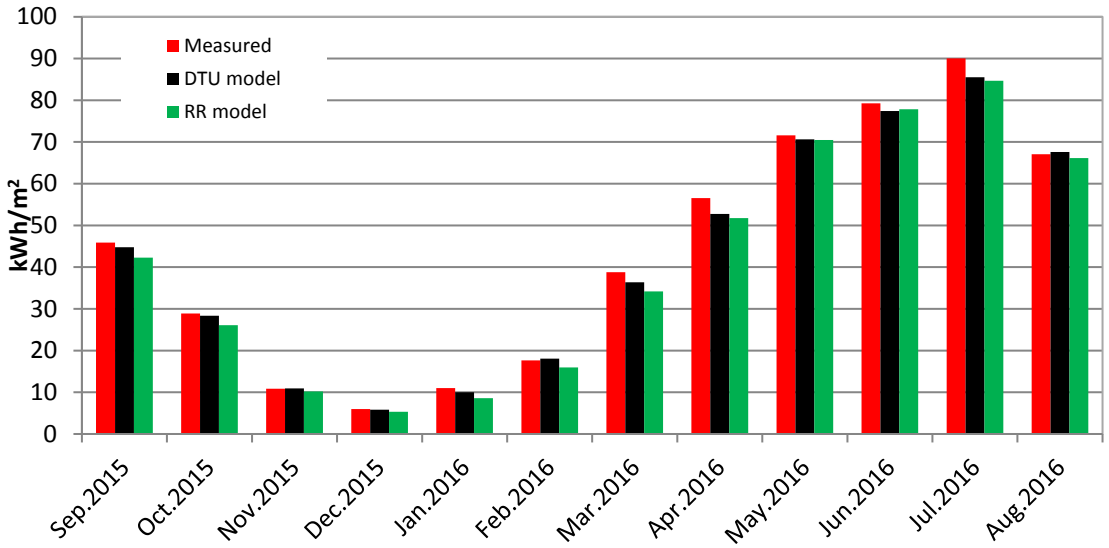

Fig. 15 Measured and modelled horizontal diffuse radiation for the period Sep.2015-Aug.2016.

Diffuse radiation was not measured directly in Taars. The diffuse radiation can be obtained from measured global radiation and DNI indirectly, which is called by "measured diffuse radiation" in this study. DTU model and classic Reduced Reindl Correlation model (RR model) in type 16a of TRNSYS were used to calculate the horizontal diffuse radiation from measured global radiation. Fig. 15 shows the monthly measured and calculated diffuse radiation by both mentioned models for the period Sep.2015-Aug.2016. Yearly measured diffuse radiation is 524 kWh/m^2. The yearly calculated diffuse radiation of the DTU model and RR model are 514 kWh/m^2 and 490 kWh/m^2. It can be concluded that the DTU model was more accurate than the classic RR model.

Fig. 16 shows the comparison between measured and modelled total solar radiation on the tilted flat plate collector surface. The calculated total solar radiation on the collector plane by the isotropic and anisotropic models was based on measured global radiation and DNI. The calculated monthly total radiation levels according to the isotropic model were much lower than the measured values compared to the anisotropic models. The measured yearly total radiation on the collector was 1170 kWh/m^2. The monthly total solar radiation on the tilted surface in November 2015 and January 2016, was around 20 kWh/m^2. For the four anisotropic models, the calculated total radiation on the tilted surface according to the Perez II model and the Perez I model gave results closest to the measured values, with small average differences, which is similar to the results reported by Andersen E., et al. [51]. It is suggested that the Perez models were the most suitable models to calculate total solar radiation on the collector compared to other models.

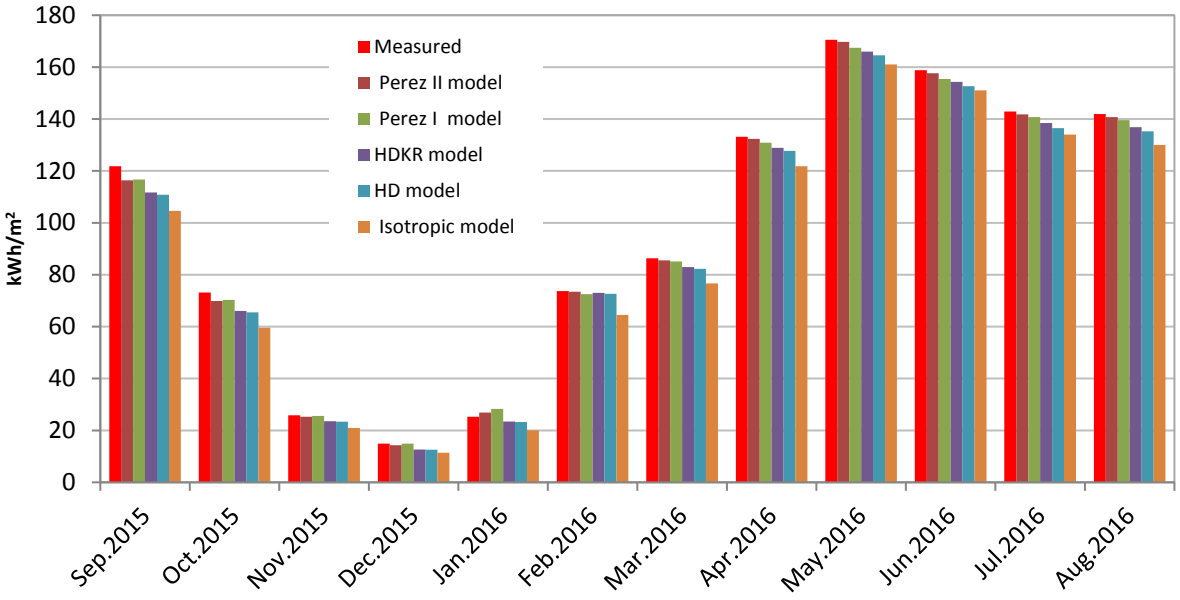

Fig. 16 Comparison of measured and modelled total tilted solar radiation from isotropic and anisotropic models based on measured global radiation and DNI.

To sum up, it is concluded that the DTU model can be used for calculation of diffuse radiation on horizontal surfaces in Denmark. DNI can be derived from global radiation on the horizontal surface by means of DTU model, see Chapter 4.1.1. Anisotropic models can be used to calculate total radiation on tilted surfaces with better accuracy than the isotropic model under Danish conditions. Anisotropic models together with the DTU model can be a new method to determine total radiations on tilted surfaces for Danish conditions, see Chapter 4.1.2. The only input for the mentioned method is global radiation measurement. The proposed method is very simple, cost-effective and gives relatively accurate total radiation on tilted surfaces and DNI under Danish conditions.

Further details are given in the attached paper 1.

3.2 Solar heating plant model

(1) Quasi-dynamic model

The quasi-dynamic model was used to simulate the thermal performance of both flat plate collectors and parabolic trough collectors in this study, as shown in Equation 1 and 2. The technical parameters of flat plate collector without/with FEP foil and parabolic trough collector based on aperture area used in the model were shown in Table 3.

$$\frac{Q}{A} = \eta_0 K_{\theta b}(\theta) G_b + \eta_0 K_{\theta d} G_d - c_1(T_m - T_a) - c_2(T_m - T_a)^2 - c_3 \frac{dT_m}{dt} \qquad (01)$$

$$K_{\theta b}(\theta) = 1 - b_0 \left(\frac{1}{cos\theta} - 1\right), \theta \leq 60^{\circ} \qquad (02)$$

When θ >60°, the IAM is linearized from the value at 60° to a value of zero at 90° [48].

Table 3 Parameters based on aperture area for the investigated solar collectors [43] [52].

η_0	b_0	$K_{\theta d}$	c_1, [W/(m²·K)]	c_2, [W/(m²·K²)]	c_3, [kJ/(m²·K)]	
0.839	0.1	0.98	2.596	0.016	7.321	HEATboost 35/10
0.802	0.1	0.93	2.226	0.010	7.876	HEATstore 35/10
0.75	0.27	0.038	0.04	0	4.00	PTC

(2) Levelized cost of heat (LCOH)

LCOH not only considers cost of the energy systems, but also take the energy output of these systems into consideration at the same time [53]. Equation 03 shows the general definition of LOCH. LCOH was used to evaluate the flat plate collectors and parabolic trough collectors on the same basis. The results can also be used to compare with fossil energy systems from an economy point of view. There are two boundary conditions when the LCOH was used in solar district heating plants. One is that only solar heat and storage are considered. This is called "Net LCOH" (nLCOH) in this study. The nLCOH can be expressed as Equation 04. The other one is that not only solar heat and storage are considered, but also the backup fossil energy systems are included. The latter is called "System LCOH" (sLOCH) in this study. The sLCOH can be calculated based on Equation 5.

$$LCOH = \frac{I_0 - S_0 + \sum_{t=1}^{T} \frac{C_t \cdot (1-TR) - DEP_t \cdot TR}{(1+r)^t} - RV \cdot (1+r)^{-T}}{\sum_{t=1}^{T} E_t \cdot (1+r)^{-t}} \quad (03)$$

$$nLCOH = \frac{I_s + C_{storage} + \sum_{t=1}^{T} P_s \cdot (1+r)^{-t}}{\sum_{t=1}^{T} SE \cdot (1+r)^{-t}} \quad (04)$$

$$sLCOH = \frac{I_s + C_{storage} + I_b + \sum_{t=1}^{T} (P_s + P_b) \cdot (1+r)^{-t}}{\sum_{t=1}^{T} (SE + NE) \cdot (1+r)^{-t}} \quad (05)$$

A detailed TRNSYS-GenOpt model was set up to simulate the performance of the hybrid solar heating plant. TRNSYS is the popular and common dynamic platform for solar thermal systems [54]. Main components used in TRNSYS can be found in Table 4. Type 1290 is used to simulate the thermal performance of both the flat plate collector and parabolic trough collector field. Type 30 is employed to simulate shadows between the collectors. Type 9 is used to make use of measured heat demand from the district heating

network. Type 659 is used to simulate the backup natural gas boilers. The type 31 is used for forward and return pipes for the solar collector field.

Table 4 Main TRNSYS components and parameter settings (default condition).

Name	Type	Main Parameters	Descriptions
Weather data	Type 15	North Jutland of Denmark, Design Reference Year	Solar radiation mode 1: fixed surface for FPC; Solar radiation mode 2: the surface rotates around a fixed (user-defined) axis for PTC
FPC	Type 1290	5960 m^2	Flat plate collectors without/with FEP foils
PTC	Type 1290	4039 m^2	Parabolic trough collectors
Shadow	Type 30	Model 1: row distance : 5.67 m Model 2: row distance: 12.6 m	Model 1: flat plate collectors; Model 2: parabolic trough collectors.
Tank	Type 4	2430 m^3	Short-term storage.
Boilers	Type 659	9100 kW	Natural gas boiler systems
Pipe	Type 31	DN 150	Supply/return pipe
Pump	Type 3	Varied parameters	-
Heat load	Type 9	Return temperature and Heat load	Measured return temperature and heat load from the district heating system (approximately 850 buildings with about 1900 residents).

3.2.1 Measured ambient temperature and heat demand

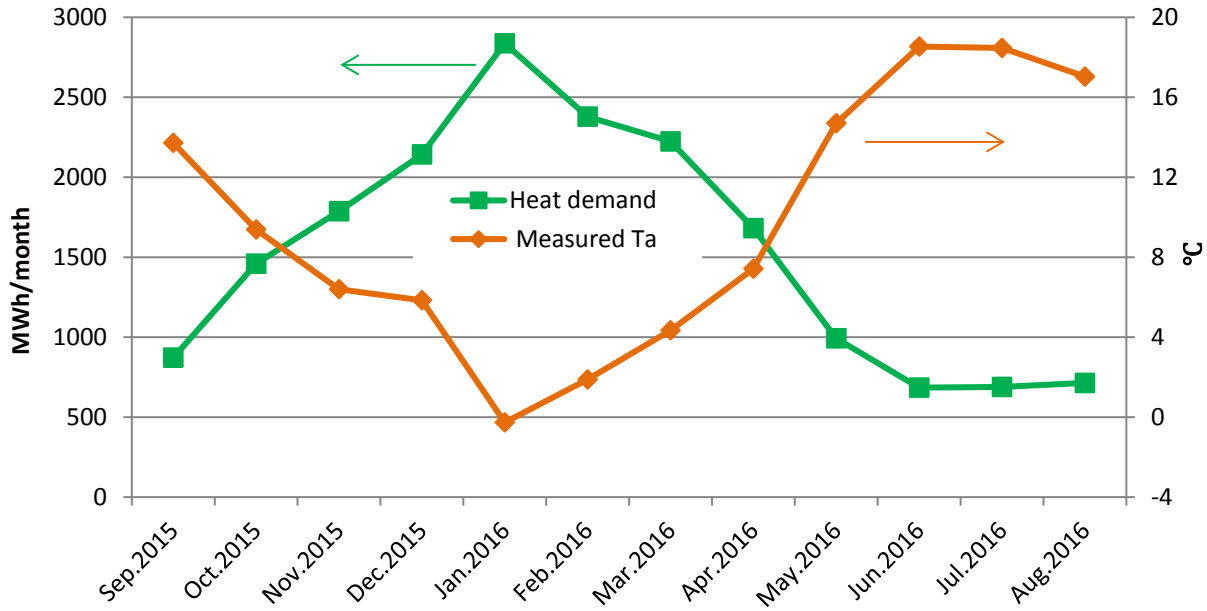

Fig. 17 Monthly heat demand and average ambient temperature in the Taars solar heating plant (Sep.2015-Aug.2016).

Fig. 17 illustrates the monthly heat demand of the district heating network and the average ambient temperature. The coldest weather took place at Jan.2016 with around 0 ℃ and the heat demand exceeded 2500 MWh. The yearly heat demand from Sep.2015 to Aug.2016 is 18460 MWh. The average ambient temperature in summer is between 15℃ and 20 ℃, while the heat demand was low.

3.2.2 Model validation on the solar heating plant

Inlet and outlet temperature, flow rate of the flat plate collector field and the parabolic trough collector field are also measured in the Taars plant to obtain the measured thermal performance of the plant. Dynamic performance on typical cloudy and sunny days, daily performances for a full year, and monthly performance for a full year from the model show a good agreement with the measured data in Taars. Fig. 18 and Fig. 19 show the comparison between modelled and measured daily solar heat energy output for flat plate collector field and parabolic trough collector field, respectively. Modelled energy output of both collector fields have good agreement against the measurements. As there were defocus of parabolic trough collectors in some sunny days in the period May 2016-August 2016 in order to avoid boiling (decided by the local operator), these periods were excluded in Fig. 19. By the comparison of Fig. 18 and Fig. 19, it is clearly observed that the daily

solar heat output of the flat plate collector field cannot exceed 5 kWh/m^2. This may be because the average operation temperature was relatively high, around 60℃ during the studied period due to the oversized collector field and the relatively high collector tilt of 50° results in shadows and relative low radiation on the collectors. The daily solar heat output of the parabolic trough collector field can be higher than 5 kWh/m^2, even if the field is operating at a high temperature level of around 80 ℃.

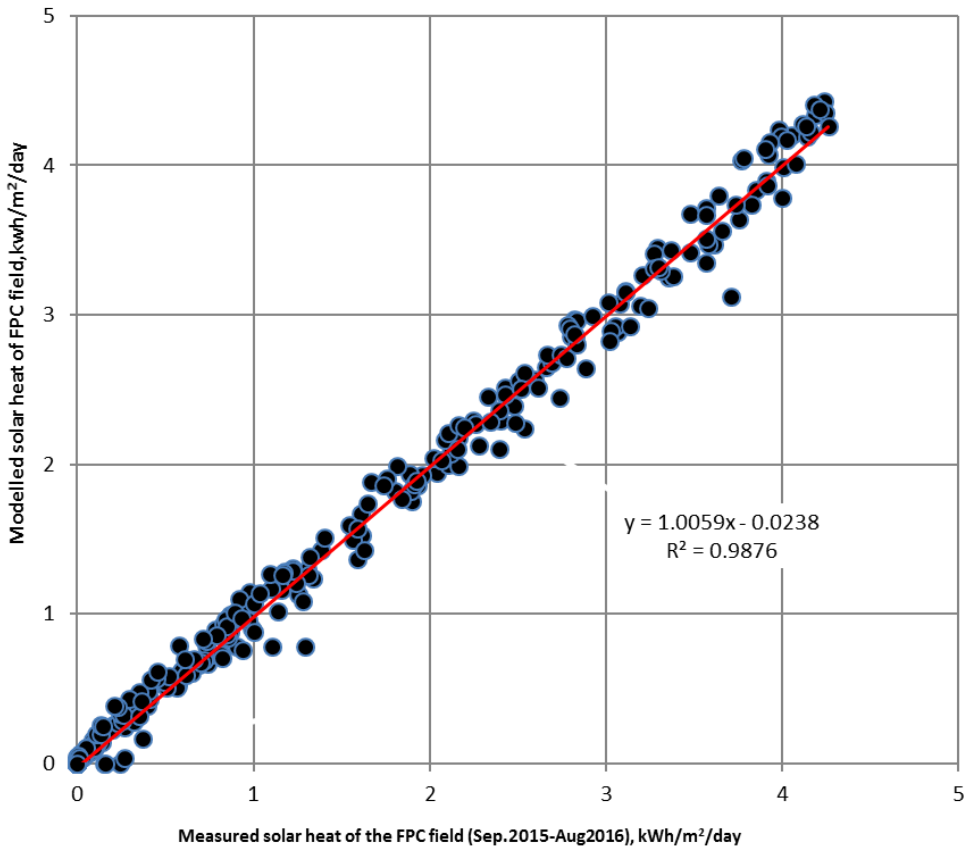

Fig. 18 Daily modelled solar energy output as a function of daily measured solar energy output of the FPC field for the period Sep.2015-Aug.2016.

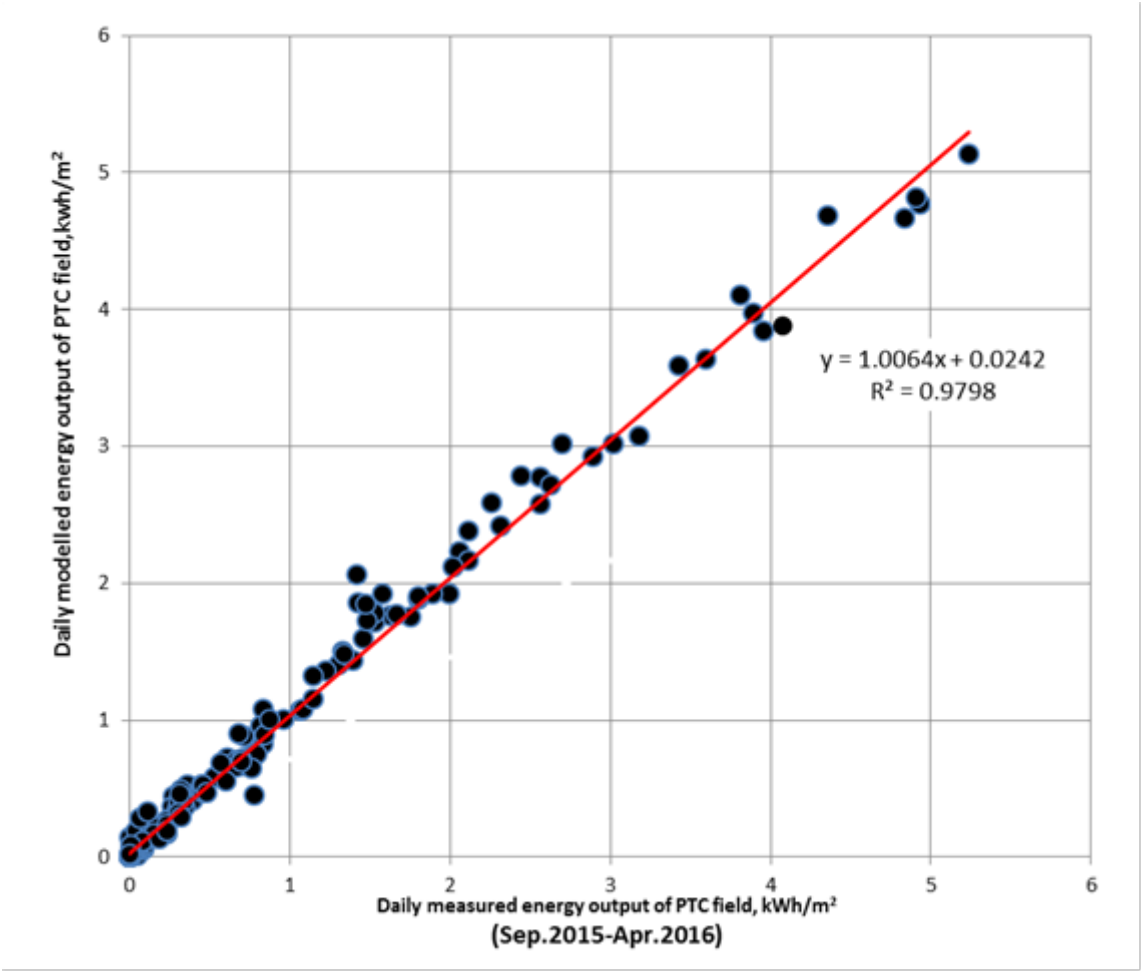

Fig. 19 Daily modelled solar energy output as a function of daily measured solar energy output of the FPC field for the period Sep.2015-Apr.2016.

Further details on the validation are given in the attached paper 2.

4 Yearly solar radiation and thermal performance

4.1 Solar radiation

Accurate solar radiation data is the core information for designers to design solar energy systems. There are many empirical formulas to split global radiation into beam radiation and diffuse radiation [55]. DTU has developed empirical formulas for Danish solar radiation conditions. Five other empirical models (one isotropic model and four anisotropic models) used to calculate total solar radiation on the tilted flat plate collector surface were shown in Chapter 3. These empirical formulas were validated by using the measured hourly data for a full year period in Taars. DNI and total radiation on the tilted surface are the main inputs to simulate the performance of parabolic trough collector field and flat plate collector field, respectively. To make sure that the inputs of solar radiation are reliable, calculated DNI and total radiation on the tilted surface only based on global radiation on a horizontal surface by means of the selected models are shown in section 4.1.1 and 4.1.2, respectively.

4.1.1 DNI

Global radiation is always available from climate stations of Danish Meteorological Institute (DMI). But DNI is not measured at climate stations sometimes and only very seldom in solar heating plants. Moreover, DNI is a very important design parameter for concentrating collectors, such as the parabolic trough collectors in Taars. As is shown in section 3.1, diffuse radiation calculated by the DTU model is more accurate than the RR empirical model under Danish conditions. So the DTU model was used in this section to predict DNI. The diffuse radiation calculated by the DTU model was used to calculate DNI and beam radiation. Fig. 20 shows monthly calculated DNI (DTU) and measured DNI from Sep.2015 to Aug.2016. The calculated total DNI (997 kWh/m^2) is about 1% larger than measured total DNI (990 kWh/m^2) for the period from Sep.2015 to Aug.2016, which is within the measuring accuracy.

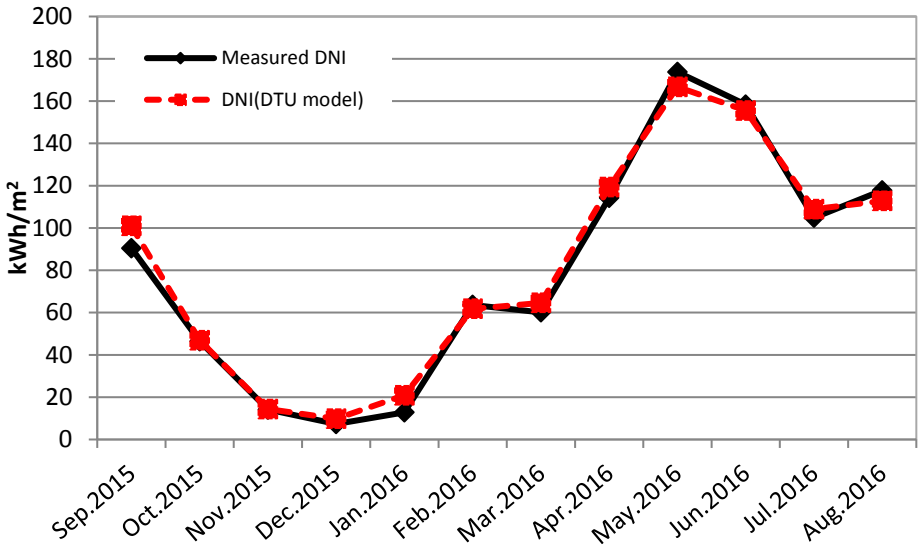

Fig. 20 Measrued and calculated DNI for the period Sep.2015-Aug.2016.

4.1.2 Total solar radiation on tilted surface

As mentioned, normally global radiation from the Danish Meteorological Institute is available. Total radiation on collector surfaces are measured at most solar heating plants but with a poor accuracy in some cases. By the DTU model, calculated diffuse radiation and beam radiation could be obtained only based on measured global radiation on a horizontal surface. The Perez models were selected as the optimal models based on calculated diffuse radiation and beam radiations from the DTU model in this section. As the classic isotropic model is simple and widely used, the isotropic model was also included in this section. Fig.21 shows the measured and calculated total solar radiation on a tilted surface from the combined models (the DTU & the isotropic model, the DTU & Perez I model and the DTU & Perez II model) only from the global radiation on the horizontal surface. The calculated total solar radiation on a tilted surface of the DTU & Perez models had very good agreements against the measured values.

In the past, in most cases, inexpensive and inaccurate solar radiation sensors have been used to measure solar radiation on collector planes in solar district heating plants in Denmark. Few technicians onsite in solar heating plants have paid much attention to the accuracy of measurements of solar radiation. Poor solar radiation measurements may also result in wrong control strategies for large solar collector fields, since the flow rate is determined as a function of solar radiation. Consequently, a decrease of thermal performance due to poor solar radiation measurements can be the result. The combined model for accurately modelling total solar radiation on the collector surface can be used to double-check solar radiation measurements onsite, in a cost-effective and fast way.

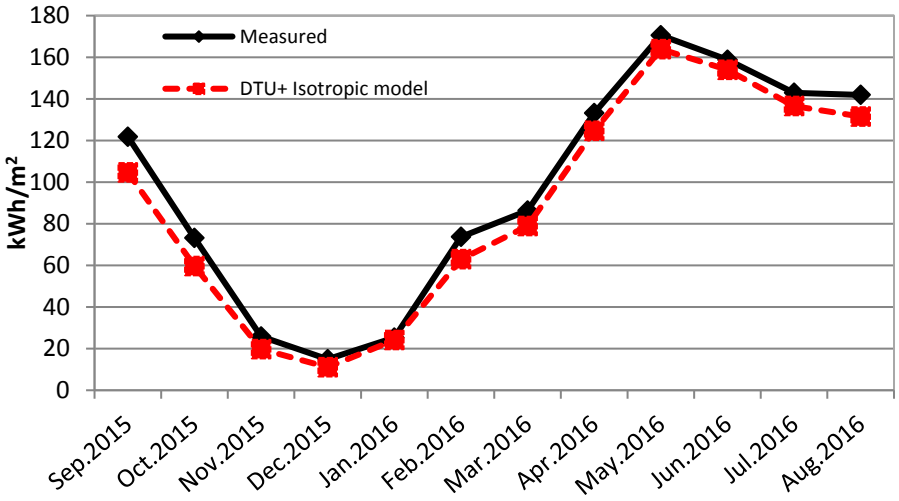

a

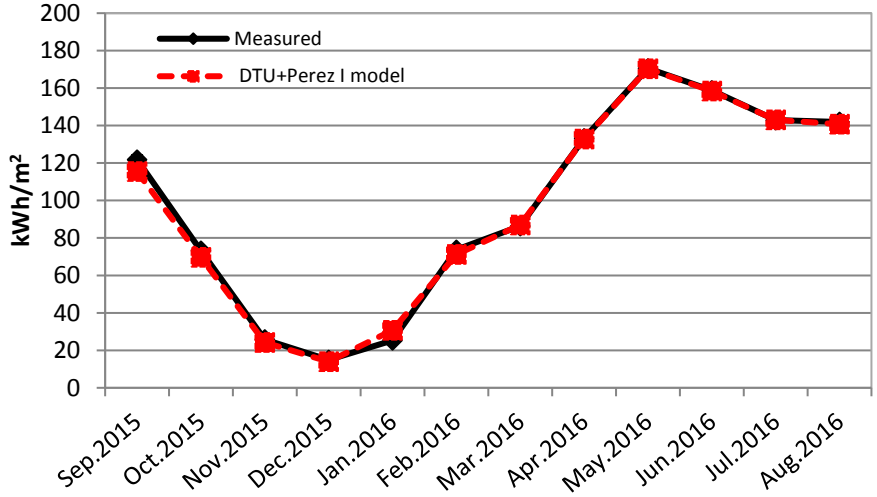

b

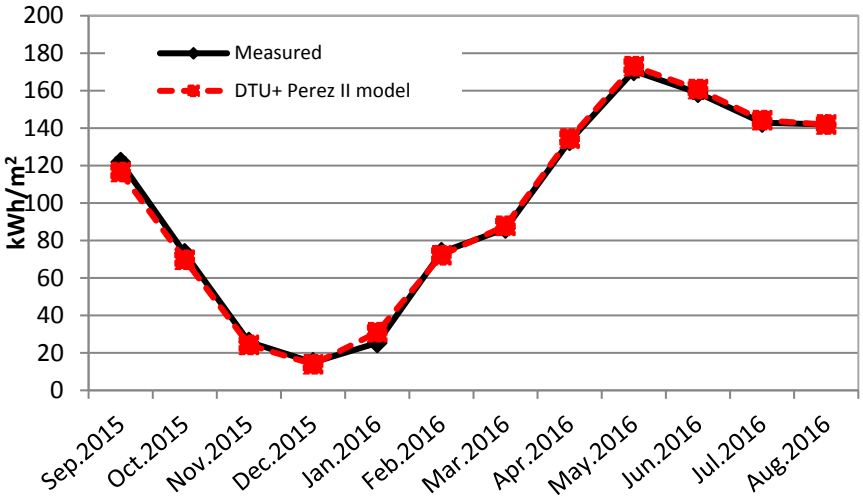

c

Fig. 21 Measured monthly total radiation and calculated total radiation on tilted surface. The calculations are based on calculated diffuse radiation and beam radiation (Sep.2015 – Aug.2016: a-DTU model & isotropic model, b- DTU model & Perez I model, c- DTU model & Perez II model.)

4.2 Thermal performance

Measured and simulated thermal performances of the hybrid solar heating plant for the first operation year from September 2015 to August 2016 are shown in this section, see Table 5. The weighted average operation temperature of the parabolic trough collectors is 80 °C. The weighted average operation temperature of the flat plate collector collectors is in the range of 50 -60 °C.

Table 5 Monthly measured and simulated heat output for the flat plate collector field and parabolic trough collector field (kWh/m^2).

	Sep. 2015	Oct. 2015	Nov. 2015	Dec. 2015	Jan. 2016	Feb. 2016	Mar. 2016	Apr. 2016	May. 2016	Jun. 2016	Jul. 2016	Aug. 2016	Sum	
Measured	53.0	22.8	1.9	0.4	0.9	22.4	30.2	53.3	76.0	66.8	58.7	61.7	448	FPC
Modelled	51.2	21.1	2.28	0.4	0.6	22.9	28.6	52.3	77.5	68.6	60.1	62.4	448	
Measured	38.3	13.9	1.51	0.3	1.5	15.4	24.4	57.6	59.3	29.0	54.7	58.2	354	PTC
Modelled without defocus	40.4	15.3	2.01	0.18	0.9	16.7	25.1	60.0	101.8	96.9	64.4	66.8	490	

4.2.1 Flat plate collector field

As is shown in Fig. 22 and Fig. 23, both the flat plate collector field and the parabolic trough collector field produced not much solar heat from Nov.2015 to Jan.2016, in which period the backup natural gas boiler systems were main heat sources for the district heating network. Measured and modelled yearly thermal performances of flat plate collector field were about 450 kWh/m^2. The solar heat of the flat plate collector field in the summer could be higher than 60 kWh/m^2 in May, June and August of 2016, as shown in Fig. 22.

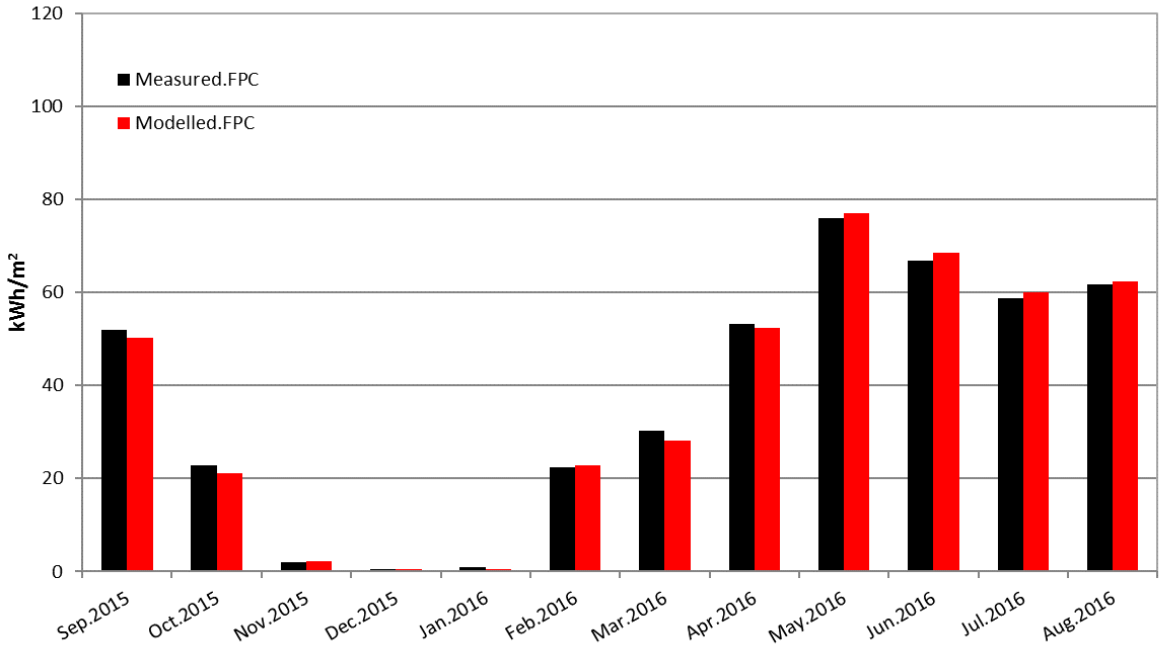

Fig. 22 Measured and modelled energy output of flat plate collector field for the period Sep.2015-Aug.2016.

4.2.2 Parabolic trough collector field

In the summer of 2016, the heat demand is low and the storage volume is too small. Therefore, the parabolic trough collectors were defocused in some sunny days, which resulted in a low energy output for the parabolic trough collector field. The measured monthly thermal performance and simulated thermal performance without defocus of parabolic trough collector field can be seen in Fig. 23. The yearly measured thermal performance of parabolic trough collector field is 354 kWh/m^2 for the period Sep.2015-Aug.2016. If there were not defocus, the thermal performance can reach close to 490 kWh/m^2 in the studied period. The potential monthly energy output of parabolic trough collector field in the summer can be higher than 90 kWh/m^2. Tracking accuracy of the parabolic trough collector field excluding the defocus period has been determined in the paper 5.

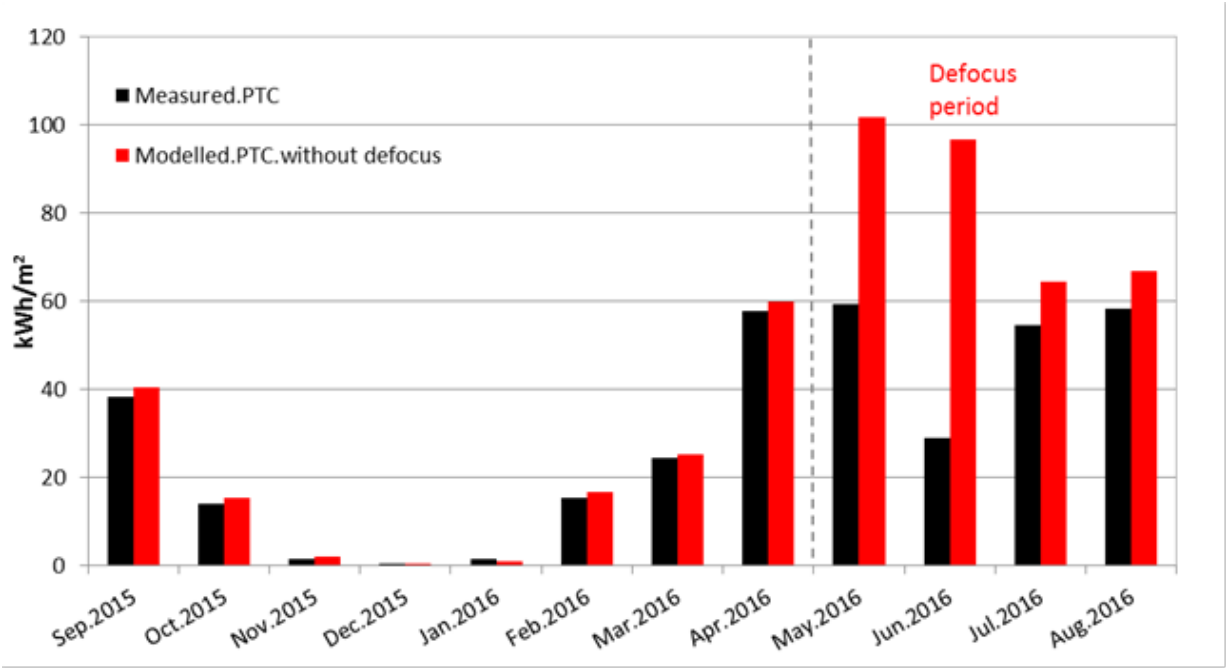

Fig. 23 Measured and modelled energy output of parabolic trough collector field for the period Sep.2015-Aug.2016.

4.2.3 Utilized efficiency

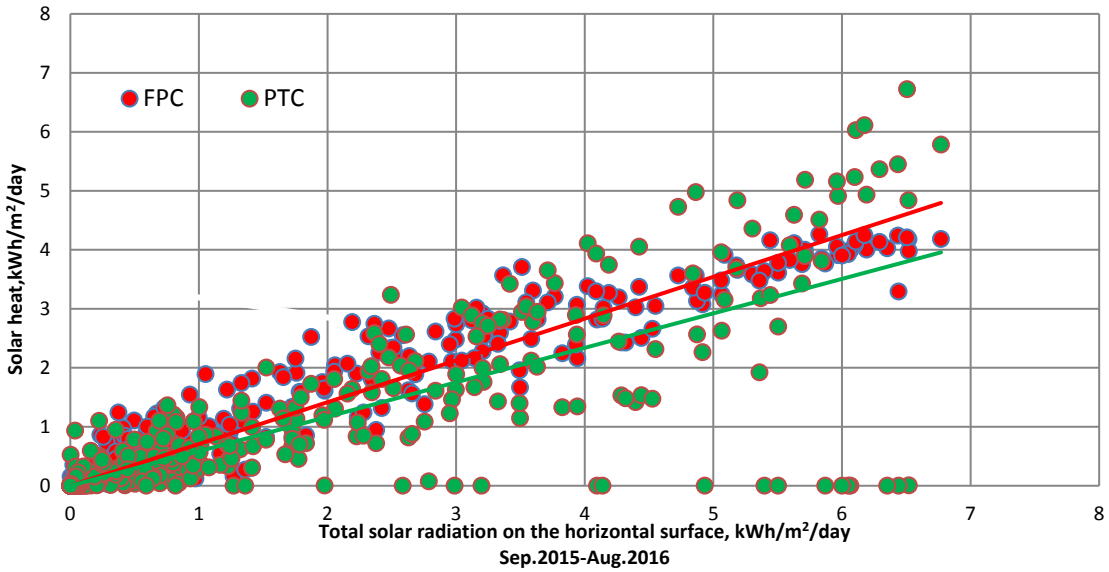

Fig. 24 Measured daily solar heat as a function of daily global radiation for both collector fields.

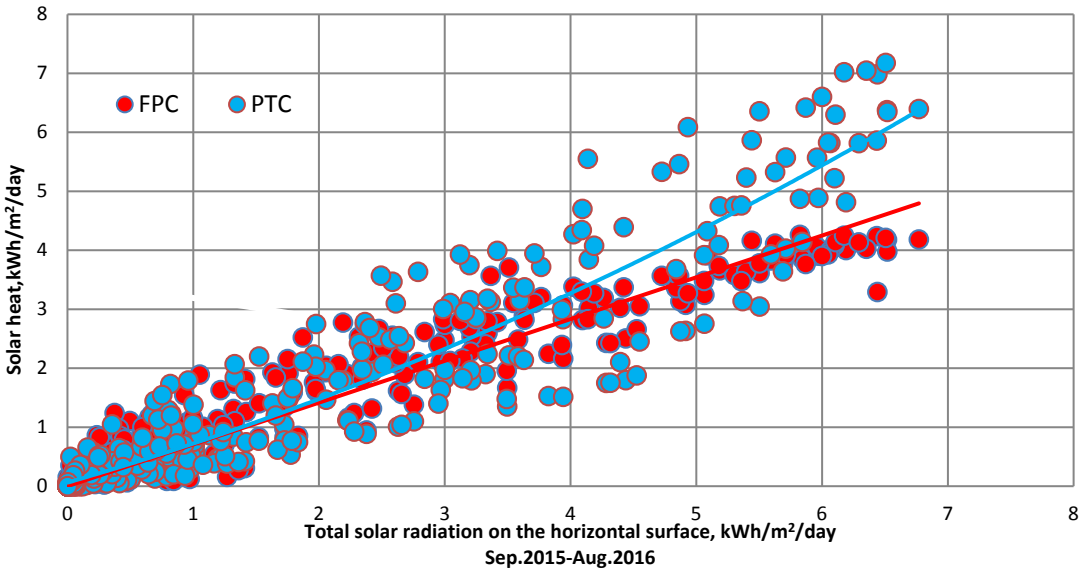

Fig. 25 Modelled daily solar heat as a function of daily global radiation for both collector fields.

Flat plate collectors utilize total radiation on the tilted collector plane, while parabolic trough collectors mainly utilize beam radiation on the collector plane. To compare the thermal performances of both collector technologies on the same basic, solar heat as a function of global radiation on the horizontal surface for both collector fields was shown in Fig. 24 and Fig. 25. Fig. 24 shows measured data. Because of defocus of parabolic trough collectors in some sunny days, the energy output of parabolic trough collectors was zero, which is indicated by the green dots in the X axis in Fig. 24. Fig. 25 shows the simulated thermal performance of both collectors, if there was no defocus of the parabolic trough collectors. It can be seen from Fig. 25 that the parabolic trough collector can produce more solar heat than the flat plate collector field when the daily solar radiation is higher than 2 kWh/m^2. The maximum daily global radiation on the horizontal surface was not more than 7 kWh/m^2 for the period September 2015- August 2016. Daily solar heat of parabolic trough collectors can be higher than 7 kWh/m^2, while the daily solar heat of flat plate collectors cannot exceed 5 kWh/m^2 in the studied period.

Further details are given in the attached paper 3.

5 Optimization

Designing solar heating plants is a multivariable optimization task because many design parameters should be varied and optimized on a project-specific basis, especially the area of the collectors and storage size. All the potential benefits of hybrid solar heating plants can only be experienced if the design, size and the whole integrated system are consistently optimized [6]. Due to the oversize of the solar collector field in Taars plant, parabolic trough collectors were therefore often defocused a lot in sunny days during the summer. The defocus of parabolic trough collectors decreased the performance of the hybrid solar heating plant significantly. Cost of energy produced by solar energy systems in district heating networks has been discussed for a long time. The levelized cost of heat (LCOH) has become the most popular and common criteria to identify the most cost-effective energy production technologies on a consistent basis. Configuration of solar collector areas and storage volume of the hybrid solar heating plant based on LCOH was optimized by means of TRNSYS model. Furthermore, orientation of parabolic trough collectors and different scenarios of cost in the future were also investigated. Further details are given in the attached paper 4.

In the validated TRNSYS model, the mass flow control for the solar collector field was developed with the purpose of having a stable outlet temperature of 95℃. The maximum outlet temperature of flat plate collector field can reach 80℃ at midday. Solar radiation data of the Design Reference Year (DRY) for North Jutland was used as input. Half hour time steps was used in the simulations.

5.1 Cost investigation

The heat price from the natural gas boiler system is assumed to be 0.57 DKK/kWh in this study. The assumed cost of the flat plate collector field with collectors without FEP foils is shown by Equation 6. The cost of the flat plate collector field with collectors with FEP foils is assumed to be 7.6% higher than that of the flat plate collector field with collectors without FEP foils. The cost of the parabolic trough collector field and the storage tank is expressed by Equation 7 [56] and 8 [57] respectively. The cost per m^2 collector of the parabolic trough collector field is 40%-70% higher than the cost of flat plate collector field depending on the size. The yearly operation and maintenance cost of the flat plate collector field is assumed as follows: a) 2 DKK/MWh heat produced for maintenance[58]; b) 1.5 kWh electricity/100 kWh heat produced for operation (2.3 DKK/kWh electricity)[57]. The yearly operation and maintenance cost of the parabolic trough collector field is assumed to be 0.8% of the initial cost [42].

$$C_{fpc} = \begin{cases} 2400 \ \text{DKK/m}^2 \ \text{for} \ 500 \ \text{m}^2 < A_{fpc} \leq 1000 \ \text{m}^2 \\ 2300 \ \text{DKK/m}^2 \ \text{for} \ 1000 \ \text{m}^2 < A_{fpc} \leq 3000 \ \text{m}^2 \\ 2180 \ \text{DKK/m}^2 \ \text{for} \ 3000 \ \text{m}^2 < A_{fpc} \leq 10000 \ \text{m}^2 \end{cases} \quad (06)$$

$$C_{ptc} = 13925 \times A_{ptc}{}^{-0.17} \quad (07)$$

$$C_{storage} = \left(11680 \times V_{storage}{}^{-0.5545} + 130\right) \times 7.44 \quad (08)$$

Other detailed assumption can be found in paper 4.

5.2 The influence of storage volume

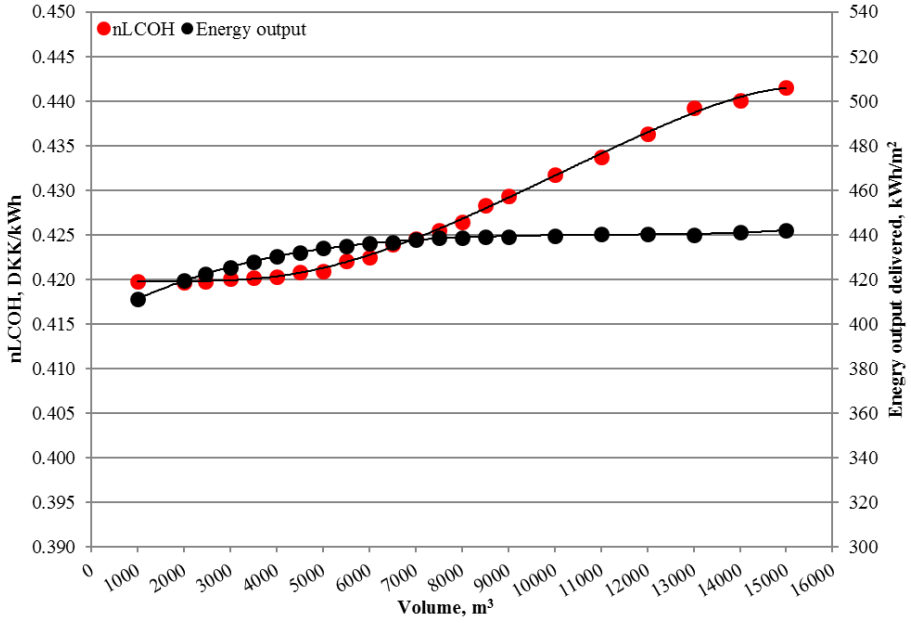

Fig. 26 The influence of storage volume on the nLCOH in the Taars plant.

Areas of both collector fields and volume of the storage tanks are important design parameters for the hybrid solar heating plant. The optimal storage volume and solar collector areas of the solar collector fields depend strongly on each other. The parabolic trough collectors was defocused in some sunny days in the summer period. On the one hand, oversize of the solar collector is the reason. On the other hand, it is because the existing storage volume are too small for solar collector field. Fig. 26 shows the influence of the storage volume on the nLCOH and solar energy output (excluding heat loss) for the reference case. The nLCOH of the Taars plant in the DRY is 0.420 DKK/kWh. The nLCOH almost has the same level of 0.420 DKK/kWh when the storage volume varies between 2430 m^3 and 5000 m^3. The heat output of the plant delivered to the district heating network can increase from 422 kWh/m^2 to 434 kWh/m^2 in the Design Reference Year. When the heat storage volume is 7000 m^3, the heat output delivered to the district heating network almost peaks at 438 kWh/m^2. For further increased storage volumes, the

thermal performance is not much increased. 5000-7000 m^3 could be the reasonable storage volume for the Taars plant.

5.3 Optimal solar collector areas

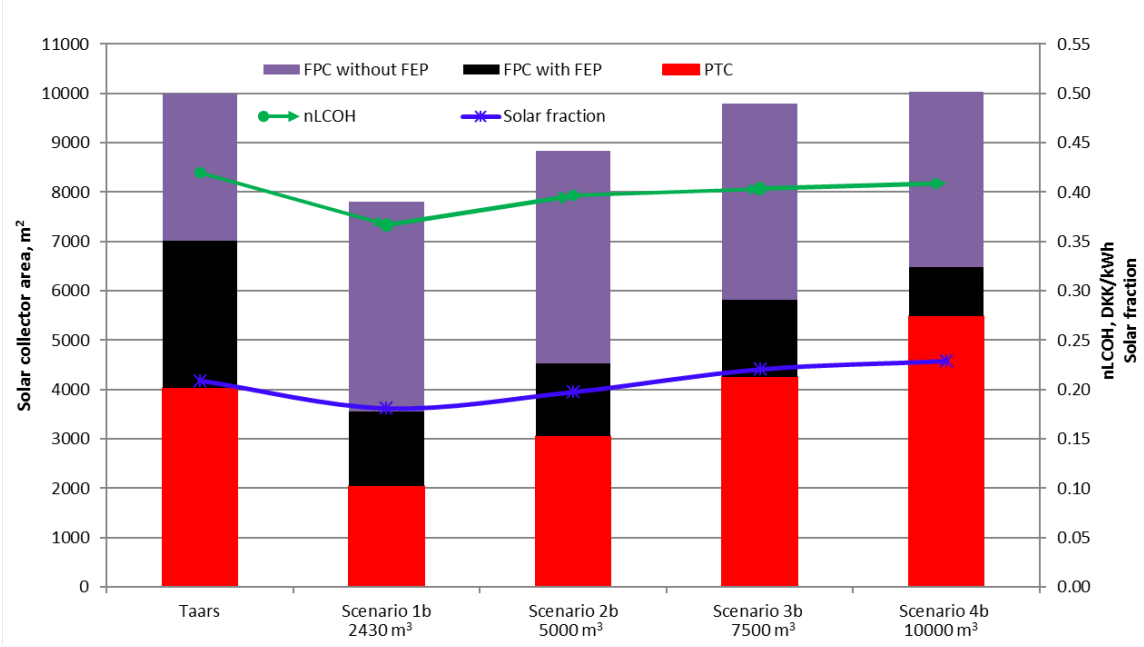

Fig. 27 Optimal solar collector areas for different scenarios of storage volume based on the minimum nLCOH.

Fig. 27 shows the optimal collector areas of different collectors for 4 different scenarios of storage volume based on the aim function of minimum nLCOH. It is suggested that the optimal collector field should integrate flat plate collectors and parabolic trough collectors in series to reach minimum nLCOH points with the range 0.367 - 0.400 DKK/kWh in the studied scenarios. The yearly solar fraction of the Taars plant in the DRY is 21.6%. The yearly solar fractions of the investigated four scenarios 1-4 in Fig. 27 are placed in the interval from 18% to 23%. The same storage volume of the Taars plant was used in scenarios 1 in order to determine the optimal solar collector areas for the studied plant. The comparison of the reference Taars plant and scenario 1 in Fig. 27 shows that the solar collector fields was oversized by at least 20% during the design phase, which causes that the net LCOH of the Taars plant is higher than that of scenario 1. The results show that the lowest net LCOH is found with a flat plate collector field of 5750 m^2 and a parabolic trough collector field of 2050 m^2 in scenario 1. But the net LCOH of Taars plant is still lower than the price for natural gas boiler systems (0.57 DKK/kWh). In addition, the comparison of Taars plant and scenario 4 in Fig. 27 shows that if there was a 10000 m^3 large storage volume, the yearly solar fraction could have increased to 23% with lower heat price, then the cost-effectiveness of such large-scale solar heating plants should have increased a lot.

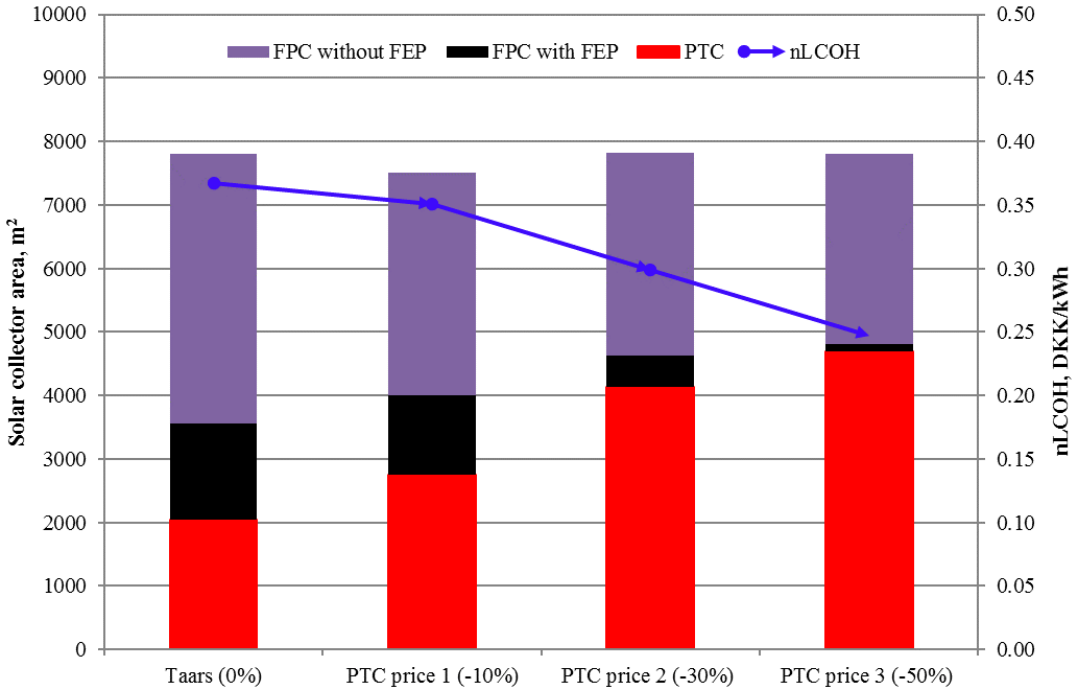

Fig. 28 Optimal solar collector areas for different scenarios of PTC price based on the minimum nLCOH.

The high price is the main barrier for the parabolic trough collectors to be applied widely in the market compared to the flat plate collectors. With the commercial development of PTC just started in 1970s [59], there is huge decrease potential of the cost of PTC in the near future. So four PTC price scenarios varying from 0% to -50% reduction in the current price level were investigated to obtain an overview of the development for PTC technology in district heating networks in the future. Areas of the collectors, tilt of the FPC and orientation of the PTC were optimized simultaneously to reach minimum *nLCOH*. Fig. 28 shows the optimal design points for all the PTC price scenarios. The optimal tilt of flat plate collectors is 35°. The optimal orientation of parabolic trough collectors is E – W orientation. The weighted average operation temperature for FPC without FEP foils, FPC with FEP foils, PTC of these 4 scenarios are 60℃, 70-80℃, 80-85℃, respectively. All the other variables are kept as in the Taars plant. When the price of PTC decreases by 50%, the optimal *nLCOH* of the plant can be reduced from 0.367 DKK/kWh to 0.247 DKK/kWh. It can be found that the design strategy of using both flat plate collectors and parabolic trough collectors in series is feasible and optimal in order to reach minimum net LCOH in all the investigated scenarios. It can also be seen that the use of flat plate collector with FEP foils has less and less proportion in the future scenarios, which is because the parabolic trough collectors can gradually replace the flat plate collectors with FEP foils if the parabolic trough collectors can be cheaper in the near future.

6 Discussion

The studied plant is the first pilot large-scale solar heating plant with flat plate collectors and parabolic trough collectors in series for district heating networks in Europe, even worldwide. The boiling problem for solar district heating plants in the summer is one of the main factors to limit the size of plants, if there is no seasonal storage. On the one hand, the application of parabolic trough collectors can easily be defocused to avoid overheat production, which can increase the flexibility of solar heating plants in the whole energy system, compared to evacuated tube collectors and compound parabolic collectors. On the other hand, too much defocus of the parabolic trough collector reduces the cost-effective competitiveness of the hybrid solar heating plants. The integration of parabolic trough collectors can also guarantee that flat plate collectors work at relatively low operation temperature and produce more than the normal solar heating plants. A large fraction of cheaper flat plate collector without FEP foil can also be used. The investigations in this study figure out the optimal solar collector areas for all the three types for the Taars plant.

In addition, Fresnel collectors is another line-focusing collector with increasing interests in the last decade. Fresnel collectors have a potential cheaper price and higher land use efficiency than parabolic trough collectors, while it has lower efficiency compared to parabolic trough collectors. Maybe Fresnel collectors can be developed to be more attractive than parabolic trough collectors for hybrid solar district heating plants. All in all, the integration of evacuated tube collectors, compound parabolic collectors, or Fresnel collectors with flat plate collectors could also be interesting design concepts to investigate for large-scale hybrid solar district heating plants.

7 Conclusions

A hybrid solar heating plant with flat plate collectors and parabolic trough collectors was investigated in detail. The feasibility of parabolic trough collectors in large solar heating plants was determined in this study. Both measured and simulated annual solar radiation and thermal performances of the studied plant were presented.

Optimization of the hybrid solar heating field based on LCOH was also carried out. The advantages of such hybrid solar district heating plants are summarized as follows: 1. Flat plate collector field in the hybrid solar heating plant can produce more than the normal existing plants with only flat plate collectors; 2, The plant can provide a constant high outlet temperature for the district heating networks, which is very important for the hydraulic and thermal balance of the district heating networks. 3, The defocusing of the PTC field can increase the safety of the solar district heating field in the whole energy supply system.

The main objective of this study is to analyze the thermal performance of the hybrid solar heating plant and determine the feasibility of parabolic trough collectors in the solar district heating plants, particularly under Danish climate conditions. The main conclusions can be drawn as followed:

(1) DTU diffuse solar radiation model can be used to split global radiation into diffuse radiation and beam radiation under Danish conditions. The hybrid DTU model & Perez models can be used to calculate total solar radiation on tilted surfaces accurately.
(2) The yearly measured performance of the flat plate collector field in this study for Danish conditions is as expected about 450 kWh/m^2 with a weighted average operation temperature range of 50-60 ℃. Parabolic trough collector field could have produced much more solar heat if there was no defocus in the sunny days in the summer. Parabolic trough collectors with E-W orientation are more attractive than that with N-S orientation for district heating if the system has limited heat storage volume and low heat demand in the summer.
(3) Even though Denmark is located at high latitudes, parabolic trough collector can work effectively if the DNI resource is utilized fully with a precise enough parabolic trough collector design and accurate solar tracking.
(4) Hybrid solar district heating plants can be technical-economically attractive in Denmark compared to conventional natural gas boiler systems.
(5) Expert design for large-scale hybrid solar heating plants is needed during the design and planning phase to avoid oversizing of the collector fields. The optimization of solar collector area and storage volume to minimize LCOH should be addressed carefully in the planning and designing phase.

8 Future work

The main barrier of parabolic trough collectors for application in district heating networks is its relatively high initial investment cost compared to flat plate collectors. Parabolic trough collectors with vacuum tubes are normally for high temperature levels in solar thermal power systems. In hybrid solar district heating plants, cheaper parabolic trough collectors without vacuum conditions for the absorber could be cost-effective. Such small sized mass produced parabolic trough collectors might be attractive for district heating purpose.

Solar heating plants connected to district heating networks are typically designed to cover about 20% of the total district heating consumption on an annual basis in Denmark, if there is no seasonal storage. Heat demand for district heating networks is low and solar radiation is high in the summer. To harvest the thermal performance of parabolic trough collectors in the summer and achieve high solar fraction on a yearly basis, seasonal storage for hybrid solar district heating plants should be investigated. Furthermore, parabolic trough collector fields are especially suitable for large cities with high heat demands. The larger the parabolic trough collector field is, the lower the LCOH will be, assuming a high heat demand. Professional and skilled operators and technicians normally are employed in large energy systems, which also is very important in order to achieve a high system performance. Hybrid solar heating plants could also be an interesting solution to cover heat demand of industry processes.

Deep research about such hybrid solar district heating plants in high solar radiation areas should be done. Integrating solar energy with other renewable energy resources to achieve high fraction of renewable energy in the whole energy system should be determined. Focus and defocus of parabolic trough collectors with flexible and accurate control in hybrid solar heating plants can allow solar heating plants to work as “back up boilers” in future smart energy systems.

Nomenclature

Abbreviations

CHP	combined heating and power
CSP	concentrating solar power
DTU	Technical University of Denmark
DNI	direct normal irradiance
DH	district heating
DHC	district heating and cooling
DKK	Danish Krone
DRY	Design Reference Year
EU	European Union
E-W	East-West
FEP	Fluorinated ethylene propylene
FPC	flat plate collectors
HE	heat exchanger
HD model	Hay and Davies model
HDKR model	Hay, Davies, Klucher and Reindl model
N-S	North-Sourth
ORC	Organic Rankin Cycle
PTC	parabolic trough collectors
IEA	International Energy Agency
SHC	Solar Heating and Cooling Program
SDH	solar district heating
LCOH	Levelized Cost of Heat, DKK/kWh
LCOE	Levelized Cost of Energy, DKK/kWh

nLCOH Levelized Cost of Solar Heat, DKK/kWh

Latin symbols

Q useful output power, W

A collector aperture area, m^2

A_{fpc} aperture area of flat plate collector field, m^2

A_{ptc} aperture area of parabolic trough collector field, m^2

$V_{storage}$ volume of tank storage, m^3

C_{fpc} cost of flat plate collector field, DKK/m^2

C_{ptc} cost of parabolic trough collector field, DKK/m^2

$C_{storage}$ cost of diurnal tank storage, DKK/m^3

c_1 collector heat loss coefficient at (Tm-Ta)=0, W/(m^2·K)

c_2 temperature dependence of collector heat loss coefficient, W/(m^2·K^2)

c_3 effective thermal capacity of collector, kJ/(m^2·K)

G_b beam irradiance, W/m^2

G_d diffuse irradiance, W/m^2

$K_{\theta b}$ incidence angle modifier for beam radiation,-

$K_{\theta d}$ incidence angle modifier for diffuse radiation,-

T_m mean solar collector fluid temperature, °C

T_a ambient temperature, °C

dTm/dt time derivative of the mean solar collector fluid temperature, K/s

b_0 first IAM coefficient(beam radiation),-

C_t operation and maintenance costs (year t), DKK

$C_{storage}$ specific costs of the tanks incl. installation (excl. VAT and subsidies), DKK/m^3

DEP_t asset depreciation (year t), DKK

E_t energy generated (year t), kWh

SE specific useful energy delivered by the solar thermal system in the year t (thermal losses in pipe loop and thermal storage considered), kWh

r discount rate , %

I_s	specific solar thermal system costs incl. installation (excl. VAT and subsidies), DKK/m²
I_b	specific boiler system costs incl. installation (excl. VAT and subsidies), DKK
NE	heat from the natural gas boiler system, kWh
P_s	operation & maintenance expenditures of the solar plant in the year t, DKK
P_b	operation & maintenance expenditures of the natural gas boiler system in the year t, DKK
RV	residual value, DKK
S_0	subsidies and incentives, DKK
T_a	ambient temperture, ℃
I_0	initial investment, DKK
TR	corporate tax rate, %
T	period of use (solar thermal system life time in years), a
t	year within the period of use (1,2,… T)

Greek symbols

η_0	peak collector efficiency, -
θ	incident angle of the beam radiation, °

References

[1] COP21, “2015 Paris Climate Conference,” *Http://www.cop21paris.org/about/cop21*, 2015. [Online]. Available: Sep.2017.

[2] European Commission, “Buildings - European Commission,” *https://ec.europa.eu/energy/en/topics/energy-efficiency/buildings*, 2018. [Online]. Available: https://ec.europa.eu/energy/en/topics/energy-efficiency/buildings. [Accessed: 23-Apr-2018].

[3] European Commission, “Heating and cooling - European Commission,” 2016. [Online]. Available: https://ec.europa.eu/energy/en/topics/energy-efficiency/heating-and-cooling. [Accessed: 25-May-2018].

[4] M. G. Fernández, C. Roger-Lacan, U. Gährs, and V. Aumaitre, *Efficient district heating and cooling systems in the EU*, no. December. 2016.

[5] European Solar Thermal Industry Federation, “Solar Heat Europe,” *http://solarheateurope.eu/welcome-to-solar-heat-europe/*, 2017. [Online]. Available: Nov.2017.

[6] D. Buoro, P. Pinamonti, and M. Reini, “Optimization of a distributed cogeneration system with solar district heating,” *Appl. Energy*, vol. 124, pp. 298–308, 2014.

[7] International Energy Agency, “IEA Solar Heating & Cooling Programme,” *https://www.iea-shc.org/*, 2017. [Online]. Available: Mar.2017.

[8] M. De Guadalfajara, M. A. Lozano, and L. M. Serra, “Evaluation of the potential of large solar heating plants in Spain,” *Energy Procedia*, vol. 30, pp. 839–848, 2012.

[9] A. Carotenuto, R. D. Figaj, and L. Vanoli, “A novel solar-geothermal district heating, cooling and domestic hot water system: Dynamic simulation and energy-economic analysis,” 2017.

[10] T. Urbaneck, T. Oppelt, B. Platzer, H. Frey, U. Uhlig, T. Goschel, D. Zimmermann, and D. Rabe, “Solar district heating in East Germany - transformation in a cogeneration dominated city,” *Energy Procedia*, vol. 70, pp. 587–594, 2015.

[11] P. Reiter, H. Poier, and C. Holter, “BIG solar graz: solar district heating in Graz – 500,000 m2 for 20% solar fraction,” *Energy Procedia*, vol. 91, pp. 578–584, 2016.

[12] H. ur Rehman, J. Hirvonen, and K. Sirén, “A long-term performance analysis of three different configurations for community-sized solar heating systems in high latitudes,” *Renew. Energy*, vol. 113, pp. 479–493, Dec. 2017.

[13] J. Hirvonen, H. Ur Rehman, and K. Sirén, “Techno-economic optimization and analysis of a high latitude solar district heating system with seasonal storage, considering different community sizes,” *Sol. Energy*, vol. 162, pp. 472–488, 2018.

[14] H. ur Rehman, J. Hirvonen, and K. Sirén, “Influence of technical failures on the performance of an optimized community-size solar heating system in Nordic conditions,” *J. Clean. Prod.*, vol. 175, pp. 624–640, Feb. 2018.

[15] R. Soloha, I. Pakere, and D. Blumberga, “Solar energy use in district heating systems. A case study in Latvia,” *Energy*, vol. 137, pp. 586–594, 2017.

[16] C. Flynn and K. Siren, “Influence of location and design on the performance of a solar district heating system equipped with borehole seasonal storage,” *Renew. Energy*, vol. 81, pp. 377–388, 2015.

[17] F. M. Rad, A. S. Fung, and M. A. Rosen, “An integrated model for designing a solar community heating system with borehole thermal storage,” 2017.

[18] Drake landing solar community, “Drake landing solar community,” *http://www.dlsc.ca/*, 2017. [Online]. Available: July.2017.

[19] A. L. Reed, A. P. Novelli, K. L. Doran, S. Ge, N. Lu, and J. S. Mccartney, “Solar district heating with underground thermal energy storage: Pathways to commercial viability in North America *,” *Renew. Energy*, vol. 126, pp. 1–13, 2018.

[20] “District heating and cooling as part of Danish energy and climate policy.” [Online]. Available: http://www.danskfjernvarme.dk/english/climate-policy. [Accessed: 25-May-2018].

[21] Danish Energy Agency, *Denmark’s Energy and Climate Outlook 2017*. 2017.

[22] Danish District Heating Association, “Danish District Heating Association in the EU and globally,” *http://www.danskfjernvarme.dk/english/eu-and-globally*, 2017. [Online]. Available: Sep.2017.

[23] M. Noussan, M. Jarre, L. Degiorgis, and A. Poggio, “Data Analysis of the Energy Performance of Large Scale Solar Collectors for District Heating,” *Energy Procedia*, vol. 134, pp. 61–68, 2017.

[24] Danish Energy Agency, “Regulation and planning of district heating in

Denmark,” *https://ens.dk/sites/ens.dk/files/Globalcooperation/regulation_and_planning_of_district_heating_in_denmark.pdf*. [Online]. Available: Sep.2017.

[25] “District Heating -Danish experiences.” [Online]. Available: https://stateofgreen.com/files/download/1674. [Accessed: 25-May-2018].

[26] Danish Energy Agency, “District Heating-Danish and Chinese experience,” 2017.

[27] IEA, “IEA Policies and Measures: Denmark Heat Supply Act,” *https://www.iea.org/policiesandmeasures/pams/denmark/name-21778-en.php*, 2014. [Online]. Available: https://www.iea.org/policiesandmeasures/pams/denmark/name-21778-en.php. [Accessed: 26-Jun-2018].

[28] “District Energy - Energy Efficiency for Urban Areas,” 2011. [Online]. Available: https://ens.dk/sites/ens.dk/files/Globalcooperation/district_energy.pdf. [Accessed: 25-May-2018].

[29] Jan-Olof Dalenbäck, “IEA SHC Task 7 CENTRAL SOLAR HEATING PLANTS WITH SEASONAL STORAGE – CSHPSS 1981-1990,” in *Edited Status Report*.

[30] D. Bauer, R. Marx, J. Nußbicker-Lux, F. Ochs, W. Heidemann, and H. Müller-Steinhagen, “German central solar heating plants with seasonal heat storage,” *Sol. Energy*, vol. 84, no. 4, pp. 612–623, 2010.

[31] F. M. Werner Weiss, Monika Spörk-Dür, “Solar Heat Worldwide-Global Market Development and Trends in 2016-Detailed Market Figures 2015 (2017 version),” http://www.iea-shc.org/solar-heat-worldwide, 2017.

[32] PlanEnergi, “Solar District Heating in Denmark 1988-2018,” *http://planenergi.eu/activities/district-heating/solar-district-heating/sdh-in-dk-1988-2018/*, 2018. [Online]. Available: http://planenergi.eu/activities/district-heating/solar-district-heating/sdh-in-dk-1988-2018/. [Accessed: 27-Feb-2018].

[33] Arcon-Sunmark, “Arcon-Sunmark A/S,” *http://arcon-sunmark.com/products*. [Online]. Available: Mar.2018.

[34] T. Daniel, K. S. Christian, and S. S. Simon, “POTENTIALS FOR GROUND-MOUNTED SDH IN EUROPE,” in *2018 International Solar Heating Conference Proceeding*, 2018.

[35] S. Furbo, J. Dragsted, B. Perers, E. Andersen, F. Bava, and K. P. Nielsen, “Yearly thermal performances of solar heating plants in Denmark – Measured and calculated,” *Sol. Energy*, vol. 159, pp. 186–196, Jan. 2018.

[36] IEA, “IEA-SHC Task 49,” *http://task49.iea-shc.org/publications*, 2016. [Online]. Available: August 2017.

[37] E. Frank, H. Marty, L. Hangartner, and S. Minder, “Evaluation of measurements on parabolic trough collector fields for process heat integration in Swiss dairies,” *Energy Procedia*, vol. 57, pp. 2743–2751, 2014.

[38] R. Silva, M. Perez, and A. Fernandez-Garcia, “Modeling and co-simulation of a parabolic trough solar plant for industrial process heat,” *Appl. Energy*, vol. 106, pp. 287–300, 2013.

[39] R. Silva, M. Berenguel, M. Perez, and A. Fernandez-Garcia, “Thermo-economic design optimization of parabolic trough solar plants for industrial process heat applications with memetic algorithms,” *Appl. Energy*, vol. 113, pp. 603–614, 2014.

[40] O. Kizilkan, A. Kabul, and I. Dincer, “Development and performance assessment of a parabolic trough solar collector-based integrated system for an ice-cream factory,” *Energy*, vol. 100, pp. 167–176, 2016.

[41] D. Krueger, A. Heller, K. Hennecke, K. Duer, S. Energietechnik, D. Zentrum, and L. Höhe, “Parabolic trough collectors for district heating systems at high latitudes,” in *Proceedings of Eurosun*, 2000.

[42] Aalborg CSP A/S, “Aalborg CSP,” *http://www.aalborgcsp.com/*, 2018. [Online]. Available: Mar.2018.

[43] B. Perers, S. Furbo, and J. Dragsted, “Thermal performance of concentrating tracking solar collectors,” *DTU.Report*, vol. 292, no. August, 2013.

[44] Z. Tian, B. Perers, S. Furbo, and J. Fan, “Annual measured and simulated thermal performance analysis of a hybrid solar district heating plant with flat plate collectors and parabolic trough collectors in series,” *Appl. Energy*, vol. 205, pp. 417–427, 2017.

[45] V. Quaschning, “Technology Fundamentals: Solar Thermal Power Plants,” *Renew. Energy World*, vol. 06, pp. 109–113, 2003.

[46] DMI, “Danish Meteorological Institute,” *http://www.dmi.dk/fileadmin/user_upload/Rapporter/TR/2013/TR13-19.pdf*, 2013.

[47] J. Dragsted and S. Furbo, “Solar radiation and thermal performance of solar collectors for Denmark,” *DTU Rep.*, vol. 275, 2012.

[48] TRNSYS website, “TRNSYS 17-a TRaNsient SYstem Simulation program-Standard Component Library Overview and Mathematical Reference,” *http://sel.me.wisc.edu/trnsys*, 2017. [Online]. Available: Mar.2017.

[49] B. Y. H. Liu and R. C. Jordan, “The interrelationship and characteristic distribution of direct, diffuse and total solar radiation,” *Sol. Energy*, vol. 4, no. 3, pp. 1–19, Jul. 1960.

[50] B. W. A. Duffie Jone A, “Solar engineering of thermal process,” 2013.

[51] E. Andersen, L. Hans, and S. Furbo, “The influence of the solar radiation model on the calculated solar radiation from a horizontal surface to a tilted surface,” in *EuroSun 2004 Congress*, 2014.

[52] SolarKeyMark, “Solar Keymark Certification,” *http://www.solarkeymark.dk/*, 2017. [Online]. Available: October 2017.

[53] Y. Louvet, S. Fischer, S. Furbo, F. Giovanetti, F. Mauthner, D. Mugnier, and D. Philippen, “LCOH for Solar Thermal Applications LCOH for Solar Thermal Applications Conventional reference system,” *http://task54.iea-shc.org/*, 2017. [Online]. Available: July.2017.

[54] TRNSYS, “Trnsys 17,” *http://www.trnsys.com/*. [Online]. Available: Mar. 2018.

[55] F. Cao, H. Li, T. Yang, Y. Li, T. Zhu, and L. Zhao, “Evaluation of diffuse solar radiation models in Northern China: New model establishment and radiation sources comparison,” *Renew. Energy*, vol. 103, pp. 708–720, Apr. 2017.

[56] J. Egelwisse, “Solar heating plants based on CSP and FP collectors,” *DTU Master Thesis*, no. July, 2015.

[57] F. Mauthner and S. Herkel, “Classification and benchmarking of solar thermal systems in urban environments.TECHNOLOGY AND DEMONSTRATORS: Technical Report Subtask C – Part C1,” *http://task52.iea-shc.org/publications*, 2016. [Online]. Available: Mar.2017.

[58] F. Bava, S. Furbo, and B. Perers, “Simulation of a Solar Collector Array Consisting of two Types of Solar Collectors, with and Without Convection Barrier,” *Energy Procedia*, vol. 70, pp. 4–12, May 2015.

[59] A. Fernández-García, E. Zarza, L. Valenzuela, and M. Pérez, “Parabolic-trough solar collectors and their applications,” *Renew. Sustain. Energy Rev.*, vol. 14, no. 7, pp. 1695–1721, Sep. 2010.

This page is intentionally left blank.

Part II Papers

[1] **Zhiyong Tian**, Bengt Perers, Simon Furbo, Jianhua Fan, Jie Deng and Janne Dragsted. A Comprehensive Approach for Modelling Horizontal Diffuse Radiation, Direct Normal Irradiance and Total Tilted Solar Radiation Based on Global Radiation under Danish Climate Conditions, **Energies**. vol. 11, no. 5, May 2018.

[2] **Zhiyong Tian**, Bengt Perers, Simon Furbo and Jianhua Fan, Analysis and validation of a quasi-dynamic model for a solar collector field with flat plate collectors and parabolic trough collectors in series for district heating**, Energy**, vol. 142, pp. 130–138, 2018.

[3] **Zhiyong Tian**, Bengt Perers, Simon Furbo and Jianhua Fan, Annual measured and simulated thermal performance analysis of a hybrid solar district heating plant with flat plate collectors and parabolic trough collectors in series, **Applied Energy**, vol. 205, pp. 417–427, 2017.

[4] **Zhiyong Tian**, Bengt Perers, Simon Furbo and Jianhua Fan, Thermo-economic optimization of a hybrid solar district heating plant with flat plate collectors and parabolic trough collectors in series. **Energy Conversion and Management**, vol. 165, pp. 92–101, 2018.

[5] Fabienne Sallaberry, **Zhiyong Tian**, Odei Goñi Jauregi, Simon Furbo, Bengt Perers, Andreas Zourellis and Jan Holst Rothmann, Evaluation of the Tracking Accuracy of Parabolic-Trough Collectors in a Solar Plant for District Heating, **Proceedings of SolarPACES 2017 conference**.

[6] Benjamin Ahlgren, **Zhiyong Tian**, Bengt Perers, Janne Dragsted, Emma Johansson, Kajsa Lundberg, Jonatan Mossegård, Joakim Byström, Olle Olsson. A simplified model for linear correlation between annual yield and DNI for parabolic trough collectors. **Energy Conversion and Management**, vol. 174, pp. 295–308, 2018.

This page is intentionally left blank.

Paper I

Zhiyong Tian, Bengt Perers, Simon Furbo, Jianhua Fan, Jie Deng and Janne Dragsted.

A Comprehensive Approach for Modelling Horizontal Diffuse Radiation, Direct Normal Irradiance and Total Tilted Solar Radiation Based on Global Radiation under Danish Climate Conditions

Energies. vol. 11, no. 5, May 2018.

This page is intentionally left blank.

energies

MDPI

Article

A Comprehensive Approach for Modelling Horizontal Diffuse Radiation, Direct Normal Irradiance and Total Tilted Solar Radiation Based on Global Radiation under Danish Climate Conditions

Zhiyong Tian, Bengt Perers, Simon Furbo, Jianhua Fan, Jie Deng * and Janne Dragsted

Department of Civil Engineering, Technical University of Denmark, 2800 Kgs. Lyngby, Denmark; zhiytia@byg.dtu.dk or tianzy0913@163.com (Z.T.); beper@byg.dtu.dk (B.P.); sf@byg.dtu.dk (S.F.); jif@byg.dtu.dk (J.F.); jaa@byg.dtu.dk (J.D.)

* Correspondence: deng-jie2@163.com; Tel.: +45-45251889

Received: 17 April 2018; Accepted: 5 May 2018; Published: 22 May 2018

Abstract: A novel combined solar heating plant with flat plate collectors (FPC) and parabolic trough collectors (PTC) was constructed and put into operation in Taars, 30 km north of Aalborg, Denmark in August 2015. To assess the thermal performance of the solar heating plant, global radiation, direct normal irradiance (DNI) and total radiation on the tilted collector plane of the flat plate collector field were measured. To determine the accuracy of the measurements, the calculated solar radiations, including horizontal diffuse radiation, DNI and total tilted solar radiation with seven empirical models, were compared each month based on an hourly time step. In addition, the split of measured global radiation into diffuse and beam radiation based on a model developed by DTU (Technical University of Denmark) and the Reduced Reindl correlation model was investigated. A new method of combining empirical models, only based on measured global radiation, was proposed for estimating hourly total radiation on tilted surfaces. The results showed that the DTU model could be used to calculate diffuse radiation on the horizontal surface, and that the anisotropic models (Perez I and Perez II) were the most accurate for calculation of total radiation on tilted collector surfaces based only on global radiation under Danish climate conditions. The proposed method was used to determine reliable horizontal diffuse radiation, DNI and total tilted radiation with only the measurement of global radiation. Only a small difference compared to measured data, was found. The proposed method was cost-effective and needed fewer measurements to obtain reliable DNI and total radiation on the tilted plane. This method may be extended to other Nordic areas that have similar weather.

Keywords: Danish climate conditions; solar radiation models; horizontal diffuse radiation; direct normal irradiance (DNI); total radiation on the tilted surface

1. Introduction

Energy consumption in the building sector accounts for about 40% of society's energy consumption in developed countries. Using renewable energy, especially solar energy, for heating and cooling in the building sector is a promising way to reduce the fossil energy consumption of buildings [1,2]. Solar thermal energy is one of the most commercial renewable energies in the building sector [3,4]. Large solar heating plants connected to district heating networks have been of great success in Europe, especially in Denmark. Most large scale solar heating plants in Europe, even worldwide, are constructed in Denmark. Denmark is the first and the only country with a mature commercial market for solar district heating plants. By the end of 2016, more than 1.3 million m^2 solar heating

plants were in operation in Denmark [5]. Real-time solar radiation data is widely used as a basic input to control large-scale solar collector fields across thousands of square meters during their lifetime. Furthermore, accurate solar radiation data are very important for designing solar heating systems and estimating the thermal performance of solar district heating plants. Compared to global irradiance, the direct beam component shows much more variability in space and time. Global radiation split into beams and diffuse radiation on the collector plane is important for evaluation of the performance of different collector types and collector field designs as well. In the past, in most cases, inexpensive and inaccurate solar radiation sensors have been used to measure solar radiation on collector planes in solar district heating plants in Denmark. Few technicians onsite in solar heating plants have paid much attention to the accuracy of measurements about solar radiation. Poor solar radiation may result in the wrong control strategies for such large-scale solar collector fields, which can influence the cost-performance of solar heating plants significantly. A simple model for accurately modelling solar radiation is needed to double-check solar radiation measurements onsite, in a cost-effective and fast way.

1.1. State of the Art

Generally, climate stations measure global radiation and, only in rare cases, accurate DNI or diffuse solar radiation on the horizontal surface. Therefore, total irradiation on tilted surfaces and DNI in most cases is calculated using measured global irradiation by means of empirical models for general use. Shukla et al. [6] carried out a comparative study of isotropic and anisotropic sky models to estimate solar radiation incidence on tilted surfaces in India. Demain et al. [7] evaluated 14 empirical models to predict global radiation on inclined surfaces. A hybrid model from the coupling of three models under different sky conditions have been developed for Belgium. Khorasanizadeh et al. set up a new diffuse solar radiation model to determine the optimum tilt angle of surfaces in Tabass, Iran [8]. Marques Filho et al. carried out observational charaterisation and empirical modelling of global radiation, diffuse and direct solar radiation on surfaces in the city of Rio de Janeiro [9]. El Mghouchi et al. evaluated four empirical models to predict daily direct diffuse and global radiation in Tutuan city, north of Morocco [10]. Jakhrani et al. investigated the accuracy of different empirical models for calculating total solar radiation on tilted surfaces [11]. It was found that the isotopic model (Liu and Jordan model) was better for the prediction of solar energy radiation in cloudy weather conditions and could be used to calculate available solar radiation on tilted surfaces in overcast skies under Malaysian climate conditions. El-Sebaii et al. also calculated diffuse radiation on horizontal surfaces and total solar radiation on tilted surfaces using empirical models [12]. They [12] also found that the isotropic model (Liu and Jordan model) could be used to calculate total radiation on tilted surfaces with good accuracy in Jeddah, Saudi Arabia. Gopinathan investigated solar radiation on variously oriented sloping surfaces in Lesotho, South Africa, with the isotropic model [13]. Li et al. carried out estimation of daily global solar radiation in China [14]. Alyahya et al. analysed the new solar radiation Atlas for Saudi Arabia [15]. Bird et al. developed a simple solar spectral model for direct and diffuse irradiance on horizontal and tilted planes on the earth's surface for cloudless atmospheres [16]. There have also been several studies on the prediction of solar radiation using machine learning and multivariable regression methods [17,18]. Despotovic et al. [19] investigated the accuracy of different empirical models in predicting total tilted solar radiation and diffuse horizontal solar radiation, respectively. Ineichen concluded that the Perez model is slightly better (in terms of RMSD) than other models in any case, even with synthetic data [20]. Gueymard et al. [21] carried out a comprehensive evaluation study of the performance of 140 separation models selected from the literature to predict direct normal irradiance from global horizontal irradiance. The evaluation was based on measured, high-quality, 1-min data of global horizontal irradiance and DNI at 54 research-class stations from seven continents. Only two models consistently delivered the best predictions over the arid, temperate and tropical zones and no model performed consistently well over the high-albedo zone. A comparative study of the impact of horizontal-to-tilted solar irradiance

conversion in modelling small PV array performance was presented in [22]. A neural network model was employed to predict daily direct solar radiation in [23]. Frydrychowicz-Jastrzębska et al. compared selected isotropic and anisotropic mathematical models to calculate the distribution of solar radiation on the photovoltaic module plane with any spatial orientation for Poland [24].

Mubarak et al. [25] compared five empirical models for PV applications. The authors concluded that the models of Hay and Davies and Reindl are recommended to estimate tilted irradiance for south-facing modules in regions with mainly cloudy conditions and when albedo measurements are not available. The Hay and Davies model is useful for vertical surfaces (e.g., facades and glazing), whereas the Perez model is recommended for sunny sites and when albedo measurements are available. Lee et al. [26] investigated solar radiation models to estimate direct normal irradiance for Korea. The Reindl-2 model was selected as the best among the evaluated ten existing models for Korea. Different conclusions can be drawn for different locations. Using previous empirical models to convert global solar radiation data for general use in high latitude areas, such as Denmark, may not give highly accurate results. Furthermore, limited literature was found on the analysis and prediction of total tilted solar radiation and DNI at high latitudes. A novel combined solar heating plant with a 4039 m^2 parabolic trough collector field and a 5960 m^2 flat plate collector field in Taars was put into operation in August 2015 [27]. To evaluate the thermal performance of the plant and the accuracy of the calculated solar radiation, total tilted and horizontal solar radiation was measured in the collector field. In addition, a weather station was in operation close to the solar collector fields to ensure that the pyranometers in the plant had correct values to reduce systemic errors and to measure direct normal irradiance (DNI).

Diffuse radiation influences the thermal performance of the flat plate collector field. In this study, diffuse horizontal radiation was estimated using the RR model (Reduced Reindl correlation model) [28] and the DTU (Technical University of Denmark) model [29]. The DTU model was developed based on measurements from 2006–2010 at a climate station at DTU [29] and was used in this paper to calculate diffuse radiation on the horizontal surface with only global radiation as an input. The RR model was developed by Reindl in 1990 for general use to calculate diffuse radiation on the horizontal surface with only global radiation as an input [30]. These two models were compared to the measured data from the Taars plant.

When diffuse radiation on the horizontal surface has been calculated, direct radiation on the same surface can be derived by the subtraction of beam radiation from global radiation. DNI can then be determined by dividing by the cosine of the zenith angle indirectly. The last two steps for direct radiation are exact numerical conversions without calculation error.

1.2. Scope and Objective

The novel contributions of this paper are as follows: (1) A solar radiation model developed for the Danish climate conditions in the Nordic area was validated; (2) The measured data were from a pilot solar heating plant, not a laboratory, which is more practical and the whole chain of calculations, up to the long term performance of the solar collectors, can be validated; and (3) DNI, diffuse radiation on the horizontal surface and total radiation on the tilted surface during the whole year were analysed.

This paper validated the performance of the DTU model for the derivation of horizontal diffuse irradiance and beam radiation based on more widely available global horizontal irradiance data under Danish climate conditions. One isotropic model and four anisotropic models for the calculation of total titled radiation were also investigated. The difference between measured solar radiation and modelled solar radiation estimated by the empirical formulas under Danish climate conditions, including DNI, diffuse horizontal radiation and total titled solar radiation, were shown. MBE, RMSE, MAPE and RPE were used to assess the feasibility of the investigated empirical models under Danish climate conditions. Calculated total tilted radiation only based on global horizontal radiation and on both global horizontal radiation and beam radiation were discussed, which could provide a new method to calculate total tilted radiation with less measurements under Danish climate conditions and may be

extended to other Nordic areas that have similar weather. The combined method to calculate total tilted solar radiation could be a useful tool for design large-scale solar district heating plants, which have been of great success in Denmark.

The aim of this article was to develop a solar radiation model to predict DNI and total tilted solar radiation accurately for solar thermal systems under Danish climate conditions.

The structure of the article is summarised as follows: Section 1 is the introduction; Section 2 is the introduction of the measurements; Sections 3 and 4 present the method and detailed empirical models used in this study; Section 5 shows the validation of the empirical models; Section 6 shows the predicted DNI and total tilted solar radiation of the selected models; Section 7 is the discussion; and Section 8 is the conclusion.

2. Data Collection and Location Description

As is shown in Figure 1, Denmark has six solar radiation zones with different yearly global radiation, around 1000–1200 kWh/m^2. The Taars plant is located in the first solar radiation zone, in the northern part of Denmark [31–33]. Figure 2 illustrates the locations of the weather station and the pyranometers in the flat plate collector field. The weather station is next to a solar heating plant. There are several pyranometers to measure global solar radiation and total radiation on the tilted plane of the flat plate collectors in the middle of flat plate collector field (Figure 1). The latitude of Taars is 57.39°N and the longitude is 10.11°E.

As is shown in Figures 2 and 3, four south facing pyranometers with a tilt 50° were installed on the top of a flat plate collector plane in the middle of the flat plate collector field [35]. Three Apogee Pyranometer SP-110 are used as backup sensors to double check the measured total radiation, as is shown in the Figure 3 left. Two of the pyranometers to measure solar radiation on the horizontal surface and solar radiation on the titled collector plane were Kipp & Zonen SMP11 (see Figure 3), which are used in this study. DNI was measured with a PMO6-CC pyrheliometer with the sun tracking platform Sunscanner SC1 in the weather station next to the solar heating plant (see Figures 2 and 4). Tables 1 and 2 show the technical specifications of the Kipp & Zonen SMP11 pyranometer and PMO6-CC pyrheliometer [36,37]. The measurements, including global radiation, total tilted solar radiation and DNI, were recorded in 2 minutes intervals from the middle of August 2015.

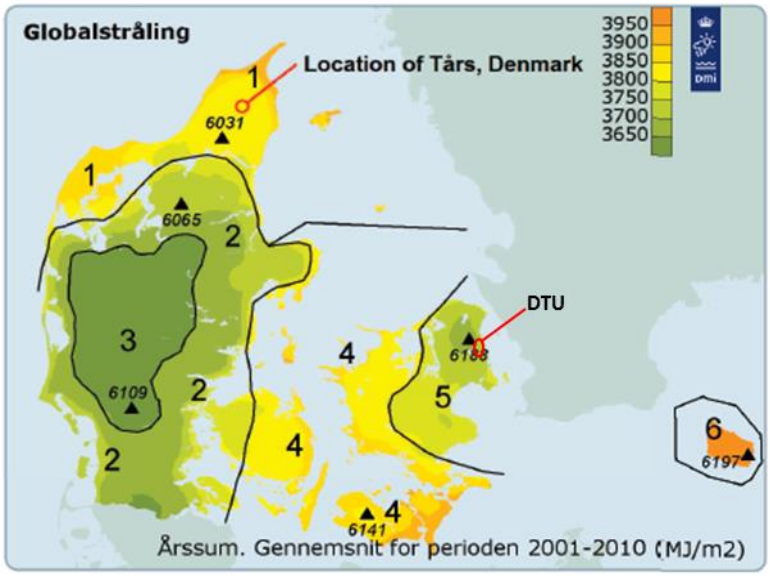

Figure 1. Location of Taars in Denmark [34].

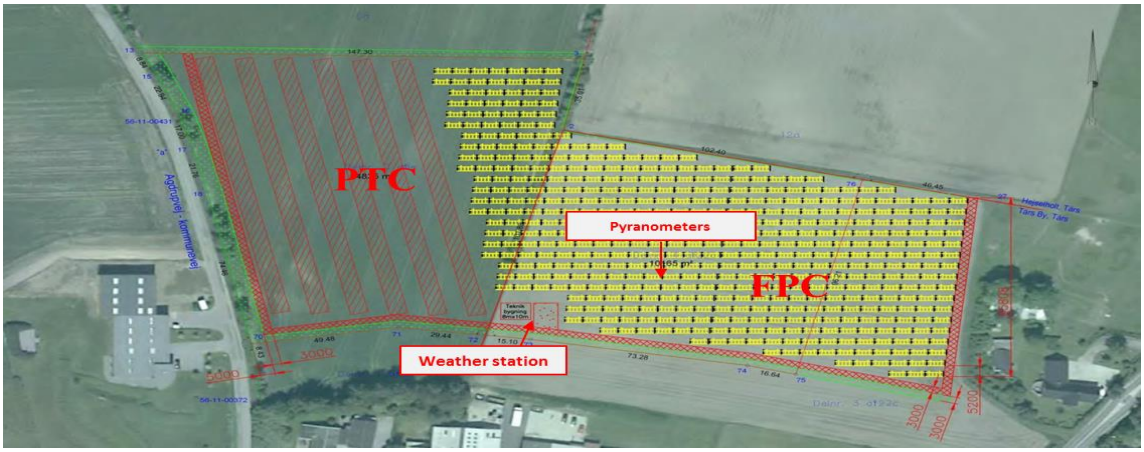

Figure 2. Location of the weather station and pyranometers (PTC: parabolic trough collector, FPC: flat plate collector) [27].

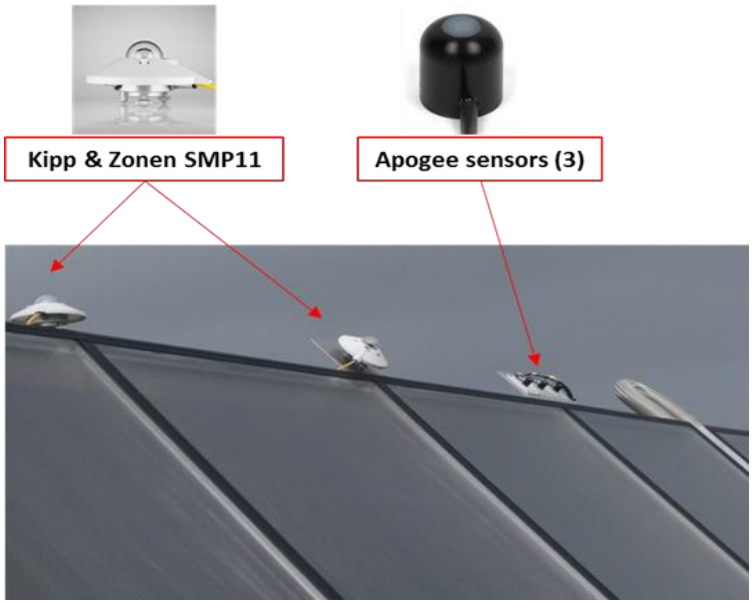

Figure 3. The pyranometers in the middle of the flat plate collector field.

Table 1. Specifications of Kipp & Zonen SMP11 pyranometer.

Parameter	Values
Spectral range (50% points)	285 to 2800 nm
Response time (63%)	<0.7 s
Response time (95%)	<2 s
Zero offset A	<7 W/m^2
Zero offset B	<2 W/m^2
Directional response (up to 80° with 1000 W/m^2 beam)	<10 W/m^2
Temperature dependence of sensitivity (−20 °C to +50 °C)	<1%
Analogue output (−V version)	0 to 1 V
Analogue output (−A version)	4 to 20 mA

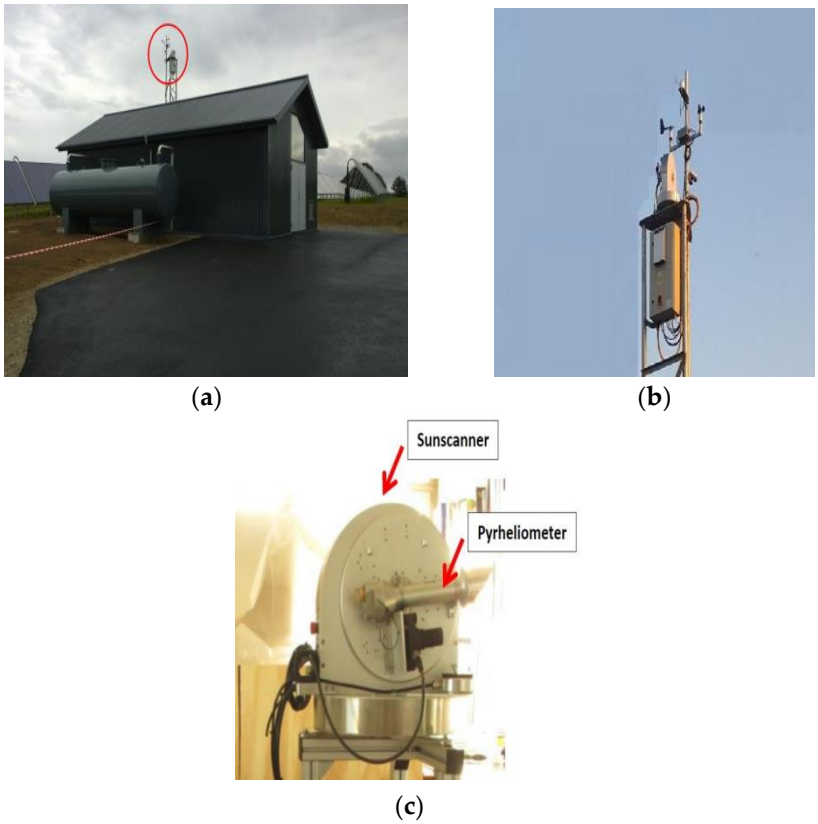

Figure 4. Weather station used and the pyrheliometer of the Taars solar heating plant. (**a**) Weather station; (**b**) the weather sensors including pyrheliometer; and (**c**) used pyrhelionmeter and sunscanner.

Table 2. Specifications of PMO6-CC pyrheliometer.

Parameter	Values
Dimension	80 × 80 × 230 mm
Mass	2.15 kg
Field of view (full angle)	5°
Slope angle	1°
Range	up to 1400 W/m^2 (or custom design available)
Traceability to WRR	<0.1%
Operating temperature range	−25 °C to +50 °C

3. Methodology

Figure 5a gives a schematic illustration of this study. Firstly, the DTU model and RR models were used to calculate horizontal diffuse radiation based on measured global radiation. Five calculation models for total radiation on tilted surfaces for general use were investigated: one isotropic model and four anisotropic models. Circumsolar diffuse and horizon-brightening components on the tilted surfaces were taken into consideration in the anisotropic models, but not in the isotropic model. Calculated total tilted solar radiation of the empirical models based on measured global radiation and DNI was derived. Measured total tilted radiation was used to evaluate the suitability of the empirical models for measuring total tilted radiation in Danish conditions (see the validation cycle in Figure 5a), as elaborated on in Section 5.

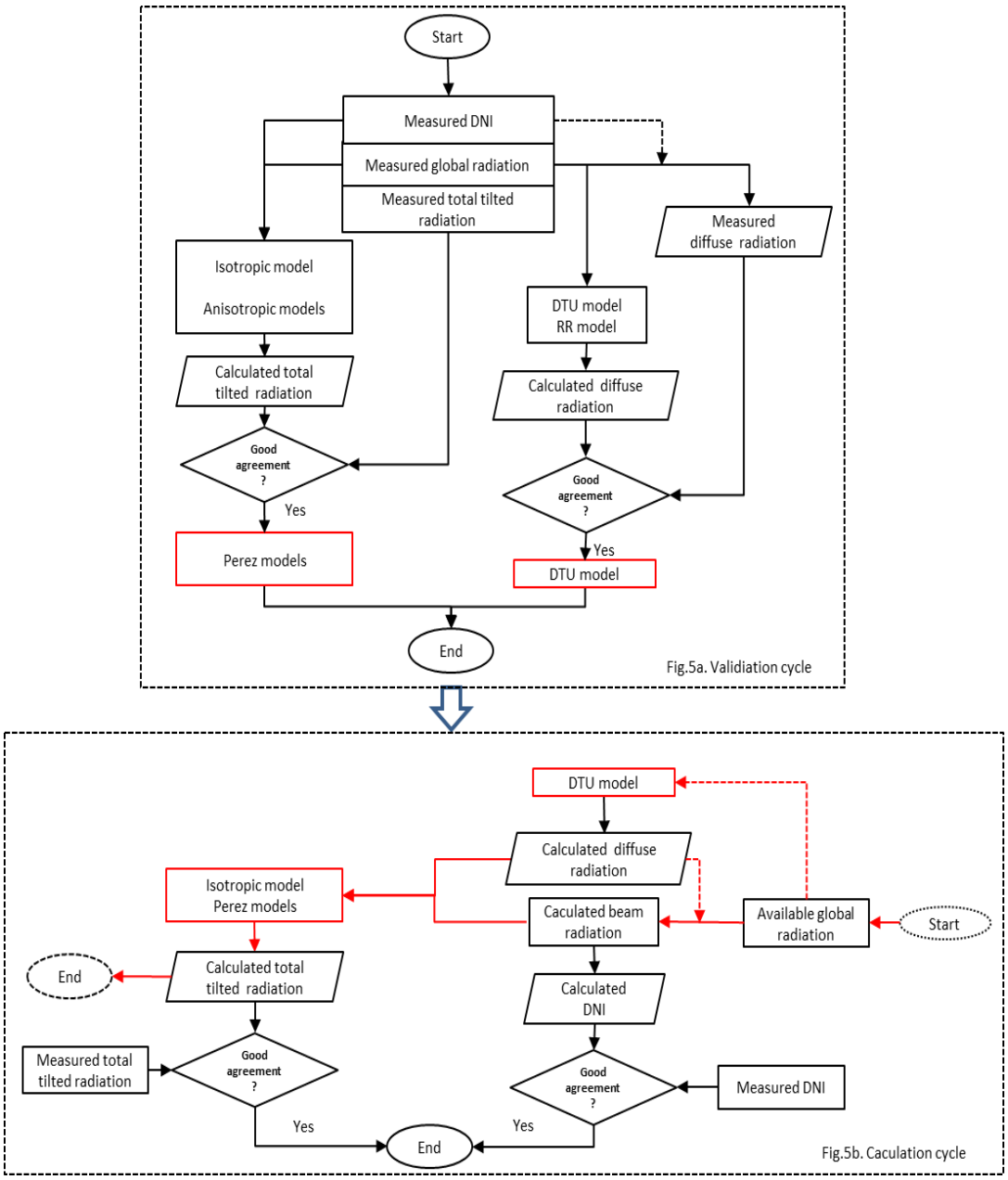

Figure 5. Schematic illustration of the methodology. (**a**) Validation cycle; (**b**) Calculation cycle.

Then, the selected empirical models based on calculated diffuse radiation and beam radiation were employed to calculate total tilted radiation (Figure 5b), as described further in Section 6. Calculated total tilted radiation using the DTU model and the investigated empirical models (Perez models) only based on global radiation showed good agreement with the measured values from September 2015 to August 2016 (Figure 5b). DNI calculated by the DTU model also had good agreement with measured DNI. In summary, the proposed method to calculate total tilted solar radiation only based on measured global horizontal radiation (red flow chart) is a new, simple and cost-effective approach to obtain accurate total tilted solar radiation for Danish conditions, as measuredglobal radiation data is always available from climate stations. Furthermore, DNI and diffuse radiation measurements are relatively costly both in terms of equipment and manpower. Accurate long-term data for these variables are seldom available in most cases. Therefore, accurate calculated DNI, diffuse radiation and total

tilted radiation based only on measured global radiation using the method proposed in this paper is very valuable.

4. Empirical Models

DNI, global radiation and total tilted solar radiation on the top of a 50° tilted, south facing collector were measured with a high time resolution of 2 min. Hourly mean values were calculated based on the measured values. Calculated solar radiation in this study was based on the mean data of a 1 h time step. Both the DTU model and the RR model were used to calculate diffuse radiation on the horizontal surface. Five other empirical models (one isotropic model and four anisotropic models) were used to calculate total solar radiation on the tilted surface. Ground reflectance or albedo was assumed to be 0.1. This value was a reasonable estimation of ground reflectance when shadows between collector rows in the solar heating plant were considered.

4.1. Measured Horizontal Diffuse Radiation

Diffuse radiation on the horizontal surface was not measured directly in the Taars plant. However, diffuse radiation can be derived accurately as the difference between total radiation and beam radiation. Measured beam radiation was calculated by measured DNI and solar zenith angle using Equation (1). Measured diffuse radiation on the horizontal surface was determined as the difference between the measured global radiation and beam radiation components, indirectly, using Equation (2).

$$G_b = \text{DNI} \times \cos\theta_z \tag{1}$$

$$G_d = G - G_b \tag{2}$$

4.2. Modelled Horizontal Diffuse Radiation

(1) DTU model

Dragsted et al. measured and analysed solar radiation from a climate station at the Technical University of Denmark from 2006 to 2010, and developed an empirical model to calculate horizontal diffuse radiation from global radiation on the horizontal surface for Danish climate conditions [29]. The empirical model is as follows in Equations (3)–(7):

$$K_T = G/G_0 \tag{3}$$

$$G_d/G = -0.60921{K_T}^3 + 1.9982{K_T}^2 - 0.2787K_T + 1, 0.00 \le K_T < 0.29 \tag{4}$$

$$G_d/G = 3.99{K_T}^3 - 7.1469{K_T}^2 + 2.3996K_T + 0.746, 0.29 \le K_T < 0.72 \tag{5}$$

$$G_d/G = 288.63{K_T}^4 - 625.26{K_T}^3 + 448.06{K_T}^2 - 105.84K_T, 0.72 \le K_T < 0.80 \tag{6}$$

$$G_d/G = 65.89{K_T}^4 - 210.69{K_T}^3 + 222.91{K_T}^2 - 77.203K_T, 0.80 \le K_T < 1.20 \tag{7}$$

(2) Reduced Reindl correlation model

The Reduced Reindl correlation model is based on the relationships developed by Reindl et al. [30]. The Reduced Reindl model uses clearness index and solar altitude angle to estimate diffuse radiation on the horizontal surface. The correlation is given by Equations (8)–(10):

$$G_d/G = 1.020 - 0.254K_T + 0.0123\sin\alpha, 0 \le K_T \le 0.3, G_d/G \le 1.0 \tag{8}$$

$$G_d/G = 1.400 - 1.794K_T + 0.177\sin\alpha, 0.3 < K_T < 0.78, 0.1 \le G_d/G \le 0.97 \tag{9}$$

$$G_d/G = 0.486K_T - 0.182\sin\alpha, 0.78 \le K_T, 0.1 \le G_d/G \tag{10}$$

4.3. Modelled Total Tilted Solar Radiation

(1) Isotropic model

The typical isotropic model was developed by Liu and Jordan (Liu–Jordan model; Equations (11) and (12)) [38] and has been used widely in recent decades. The isotropic model assumes that diffuse radiation is uniformly distributed over the complete sky dome and that reflection on the ground is diffuse.

$$R_b = \frac{\cos\theta}{\cos\theta_z} \tag{11}$$

$$G_T = G_b R_b + G_d\left(\frac{1+\cos\beta}{2}\right) + G\rho_g\left(\frac{1-\cos\beta}{2}\right) \tag{12}$$

(2) Anisotropic model

(a) Hay and Davies model (HD model)

The Hay and Davies model (Equations (13) and (14)) accounts for both circumsolar and isotropic diffuse radiation [39,40]. Horizon brightening is not taken into account. There is an increased intensity of diffuse radiation in the area around the sun (circumsolar diffuse radiation). An anisotropy index A_i is introduced in the HD model to weight the amount of circumsolar diffuse radiation. The anisotropy index is used to quantify a portion of the diffuse radiation treated as circumsolar, with the remaining portion of diffuse radiation assumed isotropic. The circumsolar component is assumed to be from the sun's position.

$$A_i = G_b/G_0 \tag{13}$$

$$G_T = (G_b + G_d A_i)R_b + G_d(1-A_i)\left(\frac{1+\cos\beta}{2}\right) + G\rho_g\left(\frac{1-\cos\beta}{2}\right) \tag{14}$$

(b) Hay, Davies, Klucher and Reindl model (HDKR model)

A horizon brightening diffuse term was added to the HD model by Reindl et al. in the HDKR model [39]. Horizon brightening is combined with the isotropic diffuse term and the magnitude is named by a modulating factor $\sqrt{G_b/G}$, as is shown in the Equation (15).

$$G_T = (G_b + G_d A_i)R_b + G_d(1-A_i)\left(\frac{1+\cos\beta}{2}\right)\left(1+\sqrt{\frac{G_b}{G}}\sin^3\left(\frac{\beta}{2}\right)\right) + G\rho_g\left(\frac{1-\cos\beta}{2}\right) \tag{15}$$

(c) Perez I model

Compared to the other models described, the Perez model is more computationally intensive and represents a more detailed analysis of isotropic diffuse, circumsolar and horizon brightening radiation by using empirically derived coefficients [41]. Perez et al. developed the model accounting for circumsolar, horizon brightening and isotropic diffuse radiation with an empirically derived "reduced brightness coefficient" [42] in 1988. This is called the Perez I model, and is given by Equations (16)–(21). The coefficients of the Perez I model are listed in Table 3.

$$G_T = G_b R_b + G_d\left[(1-F_1)\left(\frac{1+\cos\beta}{2}\right) + F_1\left(\frac{a}{c}\right) + F_2\sin\beta\right] + G\rho_g\left(\frac{1-\cos\beta}{2}\right) \tag{16}$$

$$a/c = \frac{\mathrm{Max}[0,\cos\theta]}{\mathrm{Max}[\cos 85, \cos\theta_z]} \tag{17}$$

$$\varepsilon = \frac{\left[1+\frac{G_N}{G_d}+1.041{\theta_z}^3\right]}{[1+1.041{\theta_z}^3]} \tag{18}$$

$$\Delta = \frac{G_d}{G_0} \tag{19}$$

$$F_1 = f_{11}(\varepsilon) + f_{12}(\varepsilon) \cdot \Delta + f_{13}(\varepsilon) \cdot \theta_z \quad (20)$$

$$F_2 = f_{21}(\varepsilon) + f_{22}(\varepsilon) \cdot \Delta + f_{23}(\varepsilon) \cdot \theta_z \quad (21)$$

Table 3. The coefficients of the Perez I model

ε Bin	Upper Limit for ε	Cases (%)	f_{11}	f_{12}	f_{13}	f_{21}	f_{22}	f_{23}
1	1.065	13.6	−0.196	1.084	−0.006	−0.114	0.18	−0.019
2	1.23	5.6	0.236	0.519	−0.18	−0.011	0.2	−0.038
3	1.5	7.52	0.454	0.321	−0.255	0.072	−0.098	−0.046
4	1.95	8.87	0.866	−0.381	−0.375	0.203	−0.403	−0.049
5	2.8	13.17	1.026	−0.711	−0.426	0.273	−0.602	−0.061
6	4.5	21.45	0.978	−0.986	−0.35	0.28	−0.915	−0.024
7	6.2	16.06	0.748	−0.913	−0.236	0.173	−1.045	0.065
8	-	13.73	0.318	−0.757	0.103	0.062	−1.698	0.236

(d) Perez II model

The Perez II model has the same formulation as the Perez I model [43]. Both models differ only in the F_1 and F_2 coefficients. The method for calculating the detailed parameters a, c, F_1 and F_2 in the Perez I and Perez II models can be found in Equations (17)–(21). The coefficients of the Perez II model are shown in Table 4.

Table 4. The coefficients of the Perez II model.

ε Bin	f_{11}	f_{12}	f_{13}	f_{21}	f_{22}	f_{23}
1	−0.00831	0.58773	−0.06206	−0.05960	0.07212	−0.02202
2	0.12999	0.68260	−0.15138	−0.01893	0.06597	−0.02887
3	0.32970	0.48687	−0.22110	−0.055414	−0.06396	−0.02605
4	0.56821	0.18745	−0.29513	−0.10886	−0.15192	−0.01398
5	0.87303	−0.39204	−0.36162	0.22556	−0.46204	−0.00124
6	1.13261	−1.23673	−0.41185	0.28778	−0.82304	0.05587
7	1.06016	−1.59999	−0.35892	0.26421	−1.12723	0.13107
8	0.67775	−0.32726	−0.25043	0.26421	−1.37650	0.25062

5. Diffuse Radiation and Total Tilted Radiation

5.1. Diffuse Radiation on the Horizontal Surface

Measured diffuse radiation and calculated diffuse radiation based on the DTU and RR models only using measured global radiation is shown in Figure 6. Yearly measured diffuse radiation and calculated diffuse radiation according to the DTU model was 524 and 510 kWh/m^2, respectively. Yearly calculated diffuse radiation according to the RR model was 494 kWh/m^2. Monthly calculated results according to the RR model were 6% lower than the measured values on average in Taars. Diffuse radiation calculated by the DTU model was closer to the measured values than the RR model. The difference between measured and simulated diffuse radiation according to the DTU model was about 3% on average. It may be concluded that the DTU model is more suitable for Danish climate conditions compared to the other universal and classic empirical model.

5.2. Total Radiation on the Tilted Surface Based on Global Radiation and Beam Radiation

Calculated total radiation on the tilted surface by use of the isotropic and anisotropic models based on measured total horizontal radiation and measured beam radiation from September 2015 to August 2016 is shown in Figure 7 together with measured values. The surface is facing south with a tilt of 50°.

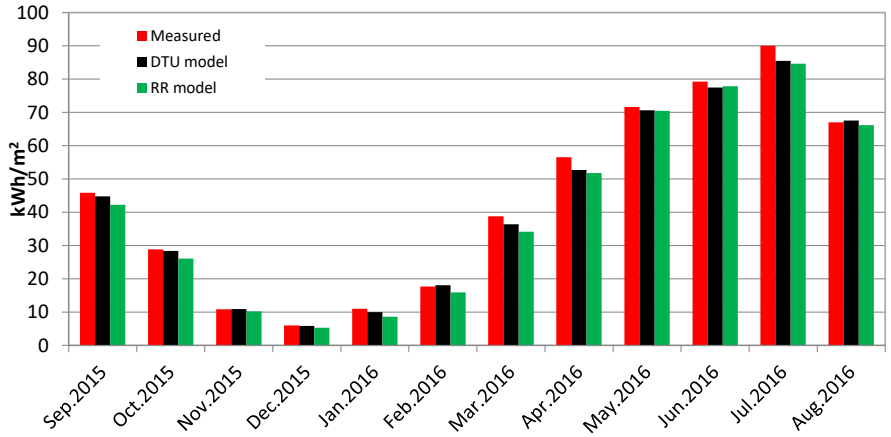

Figure 6. Calculated and measured diffuse radiation on the horizontal surface (September 2015–August 2016).

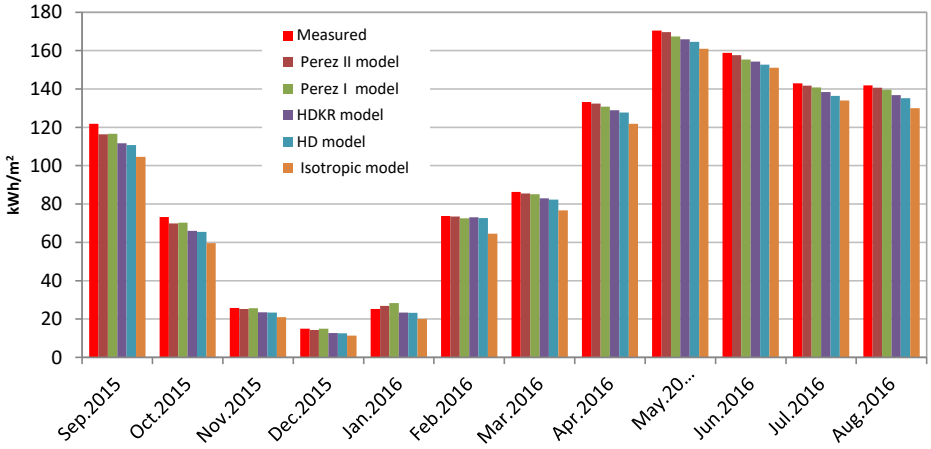

Figure 7. Calculated and measured total radiation on the 50° tilted south facing surface (September 2015–August 2016).

The calculated monthly total tilted radiation levels according to the isotropic model were much lower than the measured values in Figure 7 compared to the anisotropic models. The measured yearly total radiation was 1170 kWh/m^2. The monthly total tilted solar radiation in November 2015, December 2015 and January 2016, was around 20 kWh/m^2. Contrary to the conclusions derived under Saudi Arabian and Malaysian weather conditions in past studies [11,12], in the present study, the anisotropic models were better than the isotropic model under Danish climate conditions. For the four anisotropic models, the calculated total tilted radiation according to the Perez II model and the Perez I model gave results closest to the sum of measured values, with only average differences of 1–2%, which is similar to the results reported by Andersen et al. [44].

5.3. Comparison of the Different Models

Measured data from the Taars solar heating plant were used to evaluate the models. Four statistical error parameters were introduced to evaluate the monthly results from September 2015 to August 2016 in Figures 6 and 7 to determine the accuracy of the models for Danish climate conditions.

(1) MBE, mean bias error

$$\mathrm{MBE} = \frac{1}{k}\sum_{1}^{k}\left(G^{i}_{Calculated} - G^{i}_{Measureed}\right) \quad (22)$$

(2) RMSE, root mean square error

$$\mathrm{RMSE} = \left(\frac{1}{k} \sum_{1}^{k} \left(G^{i}_{Calculated} - G^{i}_{Measureed} \right)^{2} \right)^{1/2} \tag{23}$$

(3) MAPE, mean absolute percentage error

$$\mathrm{MAPE} = \frac{1}{k} \sum_{1}^{k} \left| \frac{G^{i}_{Calculated} - G^{i}_{Measureed}}{G^{i}_{Measureed}} \right| \tag{24}$$

(4) RPE, relative percentage error

$$\mathrm{RPE} = \frac{\sum_{1}^{k} \left(G^{i}_{Calculated} - G^{i}_{Measureed} \right)}{\sum_{1}^{k} G^{i}_{Measureed}} \tag{25}$$

Comparisons between measured values and calculated values of diffuse radiation on the horizontal surface and total radiation on the tilted surface are shown in Tables 5 and 6, respectively. The lower the MBE and RMSE are, the better the agreement between the measured and calculated values. For MBE, a positive value means an overestimation of the calculated values and a negative value means an underestimation of the calculated values. A drawback of MBE is that one positive value in one calculation step may cancel a negative value in another calculation step. RMSE is always positive. MAPE is positive and a low MAPE means the model is accurate. A negative RPE means the proposed model slightly underestimates radiation. Table 5 shows that the DTU model is more accurate than the RR model for Danish conditions based on the four investigated criteria. The RMSE of the DTU model and the RR model were 2 and 3 kWh/m^2, respectively. The RMSE and MAPE of the Perez models were much lower than other models, as shown in Table 6. It can be concluded that the anisotropic models (Perez II model and Perez I model) were the most accurate among the investigated empirical models and the most suitable for calculations of total tilted radiation under Danish climate conditions.

Table 5. Measured and calculated MBE (kWh/m^2), RMSE (kWh/m^2), MAPE (%) and RPE (%) for diffuse horizontal radiation.

Items	DTU Model	RR Model
MBE	−1.3	−2.5
RMSE	2.0	3.0
MAPE	3.5%	8.1%
RPE	−2.9%	−5.7%

Table 6. Measured and calculated MBE (kWh/m^2), RMSE (kWh/m^2), MAPE (%) and RPE (%) for monthly total tilted radiation.

Items	Perez II Model	Perez I Model	HDKR Model	HD Model	Isotropic Model
MBE	−2.4	−3.4	−8.4	−10.0	−18.6
RMSE	2.0	2.6	4.9	5.8	10.0
MAPE	2.1%	2.8%	5.7%	5.9%	12.0%
RPE	−1.2%	−1.8%	−4.3%	−5.2%	−9.7%

6. DNI and Total Tilted Radiation Only Based on Global Radiation

6.1. Measured and Calculated DNI Only Based on Global Radiation

Global radiation data is available from climate stations at the Danish Meteorological Institute (DMI). DNI is not measured at climate stations and only seldom in solar heating plants in Denmark. Moreover, DNI is a very important design parameter for concentrating solar collectors, such as the parabolic trough collectors in Taars. As was shown in Sections 5.1 and 5.3, diffuse radiation calculated by the DTU model was more accurate than the RR empirical model under Danish conditions. Using Equations (1) and (2), diffuse radiation calculated by the DTU model was used to calculate DNI or beam radiation. Therefore, the DTU model was used as the optimal model in this section to predict DNI. Figure 8 shows monthly calculated DNI (DTU) and measured DNI from September 2015 to August 2016. The calculated yearly DNI (997 kWh/m^2) was about 1% larger than measured yearly DNI (990 kWh/m^2) for the period from September 2015 to August 2016, which was within measuring accuracy. Monthly DNI can be higher than 100 kWh/m^2 in the summer season, as is shown in Figure 8.

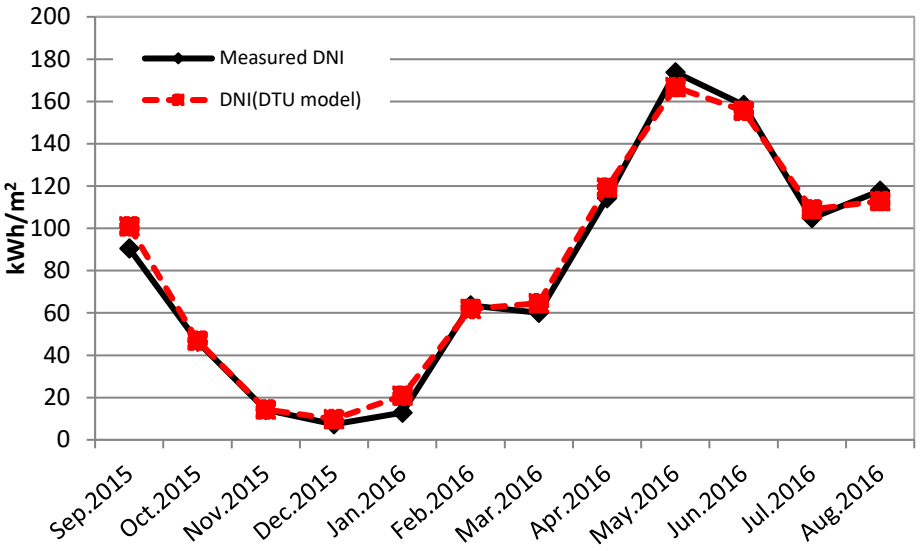

Figure 8. Calculated DNI (DTU) and measured DNI in the Taars solar heating plant.

6.2. Measured and Calculated Total Tilted Radiation Only Based on Global Radiation

As mentioned, normally global radiation from the Danish Meteorological Institute is available. Total radiation on collector surfaces is measured at most solar heating plants but with a poor accuracy in Denmark. Using the DTU model and Equations (1) and (2), calculated diffuse radiation and beam radiation could be obtained based on measured global radiation on the horizontal surface. In addition, because the isotropic model could be used easily and widely and the anisotropic models (Perez II model and Perez I model) were closest to the measured values, as described in Sections 5.2 and 5.3, the isotropic model and the anisotropic models (Perez II and Perez I) were selected to calculate total radiation on the tilted surface based on calculated diffuse radiation and calculated beam radiation from the DTU model, which was calculated only from measured global radiation. The calculated total radiation on the tilted surface using the isotropic model (1070 kWh/m^2) was 8% lower than the measured one (1170 kWh/m^2) from September 2015 to August 2016 (Figure 9a). The calculated total tilted radiation by the Perez I model (1160 kWh/m^2) and Perez II model (1169 kWh/m^2) was less than 1% different than the yearly measured total radiation (Figure 9b,c). Both of the Perez models had the best agreement with the measurements of the investigated three empirical models.

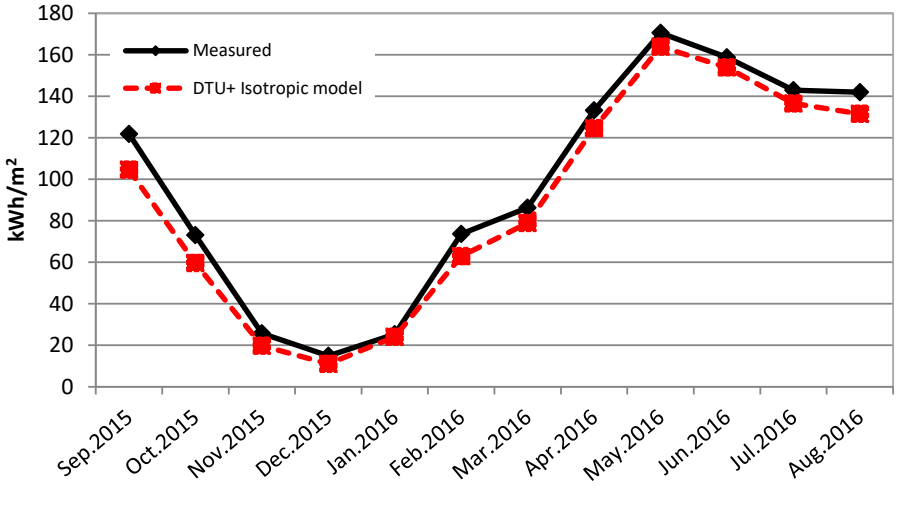

(**a**)

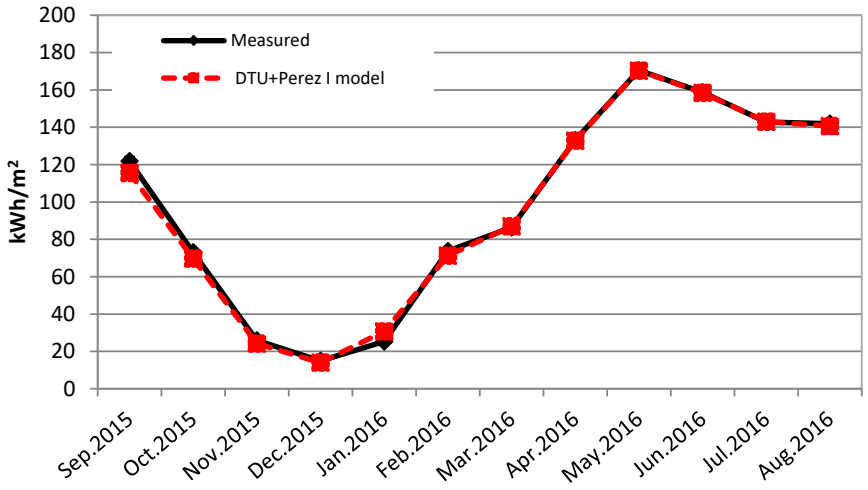

(**b**)

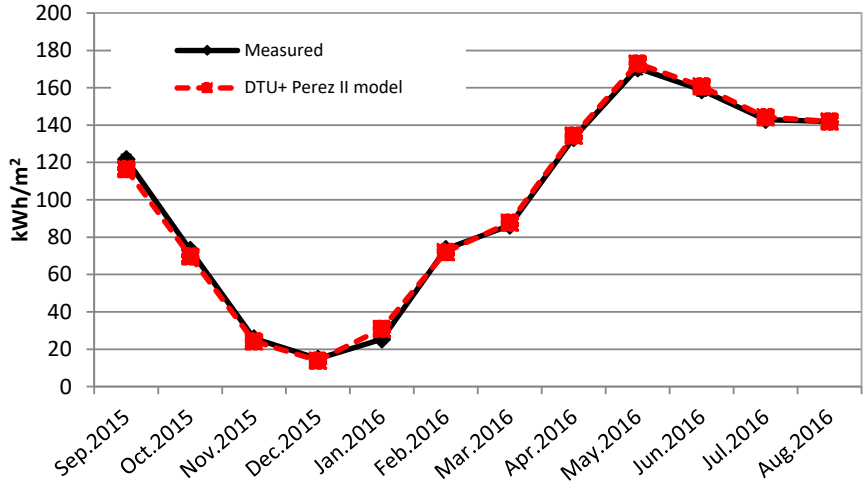

(**c**)

Figure 9. Measured monthly tilted total radiation and calculated tilted total radiation based on calculated diffuse radiation and beam radiation (September 2015–August 2016: (**a**) DTU and Isotropic model; (**b**) DTU and Perez I model; (**c**) DTU and Perez II model).

Figure 10 shows the daily measured total tilted solar radiation as a function of the modelled total tilted solar radiation from the DTU and Perez II model. The trend in Figure 10 demonstrates good agreement between the daily measured and modelled data. It was also found that maximum daily total tilted solar radiation could be higher than 8 kWh/m^2. These results are in good agreement with conclusions presented elsewhere [44]. From the above results, it was found that the DTU model together with the Perez II and I models could be used to predict total radiation on tilted surfaces based only on measured global radiation under Danish conditions very accurately. Furthermore, the proposed models could be employed to check measured total radiation on tilted flat plate collector planes in solar district heating plants in Denmark. The proposed method could also be used to derive solar radiation data for planning solar collector fields based on available horizontal global radiation measurements.

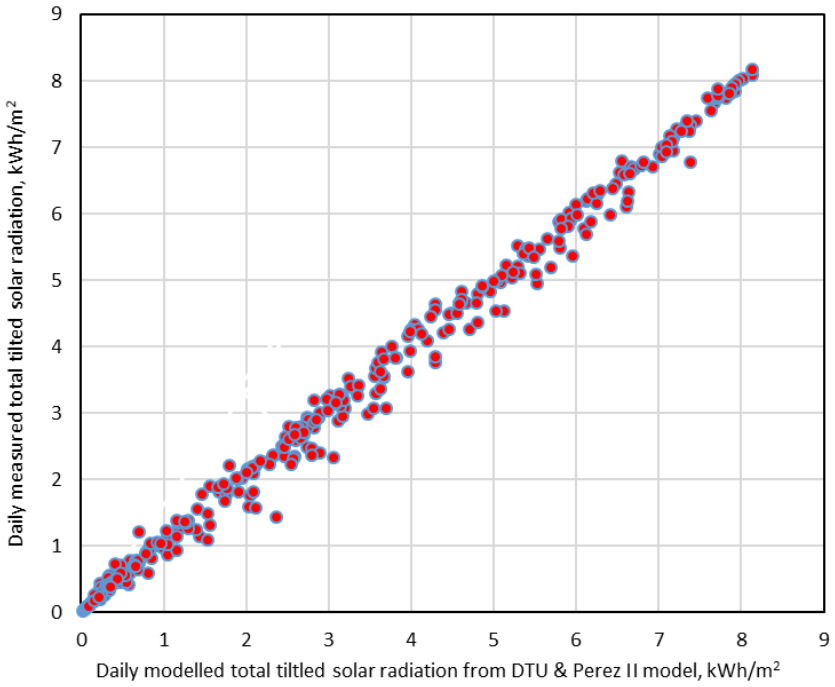

Figure 10. Daily measured total tilted solar radiation as a function of modelled total tilted solar radiation from the DTU and Perez II model.

7. Discussion

In general, the anisotropic sky models (Hay and Davies, Reindl, and Perez) provide comparable estimates of the total radiation on a tilted surface and are recommended for general use [43]. The Hay and Davies and the Reindl models are computationally simple when compared to the Perez model. The isotropic sky model under-predicts total radiation on a tilted surface and is not recommended for general use. The HD and Reindl models were recommended in the mentioned references [25,26]. The HD model has also been selected to predict total tilted solar radiation in Greece [45]. The Perez models were the best models under Danish climate conditions in this study, which aligns with other past research [46,47].

8. Conclusions

Measured and calculated monthly horizontal diffuse solar radiation and total tilted solar radiation from September 2015 to August 2016 (a full year) in a demonstration solar district heating plant in Denmark were analysed in this study using an hourly time step. The DTU model, developed for the calculation of horizontal diffuse radiation in Danish climate conditions, was evaluated and validated

using the measured data. Calculated monthly DNI based on the DTU model with only measured global radiation as an input was also investigated with good agreement with measurements. Furthermore, one isotropic model and four anisotropic models for general use were investigated for the calculation of total monthly radiation on the tilted surface under Danish climate conditions. From these results, the following conclusions can be drawn:

(1) It was found that the DTU model could be used for the calculation of diffuse radiation on the horizontal surface or DNI in Denmark with better accuracy than the other classic empirical model.
(2) Anisotropic models could be used to calculate total radiation on tilted surfaces with better accuracy than the isotropic model under Danish conditions.
(3) The Perez models together with the DTU model could be a suitable new method to determine total radiation on tilted surfaces and double-check real-time measured solar radiation for Danish solar heating plants. The only input for this method was global radiation measurement.
(4) Yearly global radiation and DNI was around 1000 kWh/m^2 and total tilted solar radiation was around 1200 kWh/m^2 in this study.

The proposed method was simple, cost-effective and gave relatively accurate measurements of total tilted radiation under Danish conditions.

Author Contributions: Zhiyong Tian set up the model, carried out the calculations and wrote the original article; Bengt Perers has contribution on the literature search and data collection. Simon Furbo has contribution to the writing and data collection; Jianhua Fan has contribution to the writing and data collection; Jie Deng provided assistance to set up the model; Janne Dragsted contributed to the modelling

Acknowledgments: Special thanks are expressed to AalborgCSP A/S (Andreas Zourellis, Jan Holst Rothman, Steffen Rovsing Møller and Per Aasted) for the information provided. The first author acknowledges financial support from the China Scholarship Council for PhD study at the Technical University of Denmark (No.201506120074). This work was also a part of an EUDP project financed by the Danish Energy Agency and the IEA-SHC Task 55 "Towards the Integration of Large SHC Systems into DHC Networks".

Conflicts of Interest: The authors declare no conflict of interest.

Abbreviations

DNI	Direct normal irradiance, W/m^2
MBE	Mean bias error, kWh/m^2
RMSE	Root mean square error, kWh/m^2
MAPE	Mean absolute percentage error
RPE	Relative percentage error
DTU	Technical University of Denmark
RR model	Reduced Reindl correlation model
PTC	parabolic trough collector
FPC	flat plate collector

Nomenclature

R_b	The ratio of beam radiation on the tilted surface to that on a horizontal surface at any time
A_i	Anisotropy index
k	Number of calculated values
i	Every calculated value
G	Mean total radiation on the horizontal surface, W/m^2
G_d	Mean diffuse radiation on the horizontal surface, W/m^2
G_0	Mean extraterrestrial radiation on the horizontal surface, W/m^2
G_T	Mean total radiation on the tilted surface, W/m^2
G_b	Mean beam radiation on the horizontal surface, W/m^2
G_N	Mean direct normal beam radiation, W/m^2
K_T	Clearness index
a/c	Weighted circumsolar solid angle

$G_{Calculated}$	Calculated solar radiation, kWh/m^2
$G_{Measured}$	Measured solar radiation, kWh/m^2
F_1	Reduced brightness coefficient (circumsolar)
F_2	Reduced brightness coefficient (horizon brightening)
Greek Letters	
β	Slope
θ_z	Zenith angle
θ	Incident angle
α	Solar altitude angle
ρ_g	Diffuse reflectance for the total solar radiation
ε	Sky clearness parameter
Δ	Sky brightness parameter

References

1. Liu, Z.; Wu, D.; Yu, H.; Ma, W.; Jin, G. Field measurement and numerical simulation of combined solar heating operation modes for domestic buildings based on the Qinghai–Tibetan plateau case. *Energy Build.* **2018**, *167*, 312–321. [CrossRef]
2. Yu, B.; Jiang, Q.; He, W.; Liu, S.; Zhou, F.; Ji, J.; Xu, G.; Chen, H. Performance study on a novel hybrid solar gradient utilization system for combined photocatalytic oxidation technology and photovoltaic/thermal technology. *Appl. Energy* **2018**, *215*, 699–716. [CrossRef]
3. Liu, Z.; Li, H.; Liu, K.; Yu, H.; Cheng, K. Design of high-performance water-in-glass evacuated tube solar water heaters by a high-throughput screening based on machine learning: A combined modeling and experimental study. *Sol. Energy* **2017**, *142*, 61–67. [CrossRef]
4. Li, H.; Liu, Z.; Liu, K.; Zhang, Z. Predictive Power of Machine Learning for Optimizing Solar Water Heater Performance: The Potential Application of High-Throughput Screening. *Int. J. Photoenergy* **2017**, *2017*, 1–10. [CrossRef]
5. Weiss, W.; Monika Spörk-Dür, F.M. Solar Heat Worldwide-Global Market Development and Trends in 2016-Detailed Market Figures 2015 (2017 Version). 2017. Available online: http://www.iea-shc.org/solar-heat-worldwide (accessed on 7 May 2018).
6. Shukla, K.N.; Rangnekar, S.; Sudhakar, K. Comparative study of isotropic and anisotropic sky models to estimate solar radiation incident on tilted surface: A case study for Bhopal, India. *Energy Rep.* **2015**, *1*, 96–103. [CrossRef]
7. Demain, C.; Journée, M.; Bertrand, C. Evaluation of different models to estimate the global solar radiation on inclined surfaces. *Renew. Energy* **2013**, *50*, 710–721. [CrossRef]
8. Khorasanizadeh, H.; Mohammadi, K.; Mostafaeipour, A. Establishing a diffuse solar radiation model for determining the optimum tilt angle of solar surfaces in Tabass, Iran. *Energy Convers. Manag.* **2014**, *78*, 805–814. [CrossRef]
9. Marques Filho, E.P.; Oliveira, A.P.; Vita, W.A.; Mesquita, F.L.L.; Codato, G.; Escobedo, J.F.; Cassol, M.; França, J.R.A. Global, diffuse and direct solar radiation at the surface in the city of Rio de Janeiro: Observational characterization and empirical modeling. *Renew. Energy* **2016**, *91*, 64–74. [CrossRef]
10. El Mghouchi, Y.; El Bouardi, A.; Choulli, Z.; Ajzoul, T. Models for obtaining the daily direct, diffuse and global solar radiations. *Renew. Sustain. Energy Rev.* **2016**, *56*, 87–99. [CrossRef]
11. Jakhrani, A.Q.; Othman, A.; Rigit, A.R.H.; Samo, S.R.; Ahmed, S. Estimation of Incident Solar Radiation on Tilted Surface by Different Empirical Models. *Int. J. Sci. Res. Publ.* **2012**, *2*, 15–20.
12. El-Sebaii, A.A.; Al-Hazmi, F.S.; Al-Ghamdi, A.A.; Yaghmour, S.J. Global, direct and diffuse solar radiation on horizontal and tilted surfaces in Jeddah, Saudi Arabia. *Appl. Energy* **2010**, *87*, 568–576. [CrossRef]
13. Gopinathan, K.K. Solar radiation on variously oriented sloping surfaces. *Sol. Energy* **1991**, *47*, 173–179. [CrossRef]
14. Li, H.; Ma, W.; Lian, Y.; Wang, X. Estimating daily global solar radiation by day of year in China. *Appl. Energy* **2010**, *87*, 3011–3017. [CrossRef]
15. AlYahya, S.; Irfan, M.A. Analysis from the new solar radiation Atlas for Saudi Arabia. *Sol. Energy* **2016**, *130*, 116–127. [CrossRef]

16. Bird, R.E.; Riordan, C. Simple Solar Spectral Model for Direct and Diffuse Irradiance on Horizontal and Tilted Planes at the Earth's Surface for Cloudless Atmospheres. *J. Clim. Appl. Meteorol.* **1986**, *25*, 87–97. [CrossRef]
17. Lou, S.; Li, D.H.W.; Lam, J.C.; Chan, W.W.H. Prediction of diffuse solar irradiance using machine learning and multivariable regression. *Appl. Energy* **2016**, *181*, 367–374. [CrossRef]
18. Kashyap, Y.; Bansal, A.; Sao, A.K. Solar radiation forecasting with multiple parameters neural networks. *Renew. Sustain. Energy Rev.* **2015**, *49*, 825–835. [CrossRef]
19. Despotovic, M.; Nedic, V.; Despotovic, D.; Cvetanovic, S. Evaluation of empirical models for predicting monthly mean horizontal diffuse solar radiation. *Renew. Sustain. Energy Rev.* **2016**, *56*, 246–260. [CrossRef]
20. Ineichen, P. *Global Irradiance on Tilted and Oriented Planes: Model Validations*; Technical Report; University Geneva: Geneva, Switzerland, October 2011.
21. Gueymard, C.A.; Ruiz-Arias, J.A. Extensive worldwide validation and climate sensitivity analysis of direct irradiance predictions from 1-min global irradiance. *Sol. Energy* **2016**, *128*, 1–30. [CrossRef]
22. Polo, J.; Garcia-Bouhaben, S.; Alonso-García, M.C. A comparative study of the impact of horizontal-to-tilted solar irradiance conversion in modelling small PV array performance. *J. Renew. Sustain. Energy* **2016**, *8*. [CrossRef]
23. Boussaada, Z.; Curea, O.; Remaci, A.; Camblong, H.; Mrabet Bellaaj, N. A Nonlinear Autoregressive Exogenous (NARX) Neural Network Model for the Prediction of the Daily Direct Solar Radiation. *Energies* **2018**, *11*, 620. [CrossRef]
24. Frydrychowicz-Jastrzębska, G.; Bugała, A. Modeling the Distribution of Solar Radiation on a Two-Axis Tracking Plane for Photovoltaic Conversion. *Energies* **2015**, *8*, 1025–1041. [CrossRef]
25. Mubarak, R.; Hofmann, M.; Riechelmann, S.; Seckmeyer, G. Comparison of modelled and measured tilted solar irradiance for photovoltaic applications. *Energies* **2017**, *10*, 1688. [CrossRef]
26. Lee, H.J.; Kim, S.Y.; Yun, C.Y. Comparison of solar radiation models to estimate direct normal irradiance for Korea. *Energies* **2017**, *10*, 594. [CrossRef]
27. Aalborg CSP A/S. Available online: http://www.aalborgcsp.com/ (accessed on 7 May 2018).
28. TRNSYS Website TRNSYS 17—A TRaNsient System Simulation program-Standard Component Library Overview and Mathematical Reference. Available online: http://www.trnsys.com/assets/docs/03-ComponentLibraryOverview.pdf (accessed on 28 March 2017).
29. Dragsted, J.; Furbo, S. *Solar Radiation and Thermal Performance of Solar Collectors for Denmark*; DTU Civil Engineering Reports, No. R-275; Department of Civil Engineering, Technical University of Denmark: Copenhagen, Denmark, 2012.
30. Reindl, D.T.; Beckman, W.A.; Duffie, J.A. Diffuse fraction correlations. *Sol. Energy* **1990**, *45*, 1–7. [CrossRef]
31. Tian, Z.; Perers, B.; Furbo, S.; Fan, J. Analysis and validation of a quasi-dynamic model for a solar collector field with flat plate collectors and parabolic trough collectors in series for district heating. *Energy* **2018**, *142*, 130–138. [CrossRef]
32. Tian, Z.; Perers, B.; Furbo, S.; Fan, J. Thermo-economic optimization of a hybrid solar district heating plant with flat plate collectors and parabolic trough collectors in series. *Energy Convers. Manag.* **2018**, *165*, 92–101. [CrossRef]
33. Tian, Z.; Perers, B.; Furbo, S.; Fan, J. Annual measured and simulated thermal performance analysis of a hybrid solar district heating plant with flat plate collectors and parabolic trough collectors in series. *Appl. Energy* **2017**, *205*, 417–427. [CrossRef]
34. DMI Danish Meteorological Institute. 2013. Available online: http://www.dmi.dk/fileadmin/user_upload/Rapporter/TR/2013/TR13-19.pdf (accessed on 7 May 2018).
35. Tian, Z.; Perers, B.; Furbo, S.; Fan, J. Analysis of measured and modeled solar radiation at the taars solar heating plant in denmark. In Proceeding of the 11th Ises Eurosun 2016 confrenence, Palma de Mallorca, Spain, 11–14 October 2016.
36. SMP11, K. Kipp&Zonen SMP11. 2017. Available online: http://www.kippzonen.com/Product/202/SMP11Pyranometer#.V35QMvl95mM (accessed on 7 May 2018).
37. PMO6-CC PMO6-CC Pyrheliometer. 2016. Available online: https://www.pmodwrc.ch/pmod.php?topic=pmo6 (accessed on 7 May 2018).
38. Liu, B.Y.H.; Jordan, R.C. The interrelationship and characteristic distribution of direct, diffuse and total solar radiation. *Sol. Energy* **1960**, *4*, 1–19. [CrossRef]

39. Duffie, J.A.; Beckman, W.A. *Solar Engineering of Thermal Process*; John Wiley & Sons Inc.: Hoboken, NJ, USA, 2013.
40. Hay, J.E. Calculations of the solar radiation incident on an inclined surface. In Proceedings of the First Canadian Solar Radiation Data Workshop, Toronto, ON, Canada, 17–19 April 1978; pp. 59–72.
41. Loutzenhiser, P.G.; Manz, H.; Felsmann, C.; Strachan, P.A.; Frank, T.; Maxwell, G.M. Empirical validation of models to compute solar irradiance on inclined surfaces for building energy simulation. *Sol. Energy* **2007**, *81*, 254–267. [CrossRef]
42. Perez, R.; Stewart, R.; Seals, R.; Guertin, T. *The Development and Verification of the Perez Diffuse Radiation Model*; Atmospheric SciencesResearch Center: Albany, NY, USA, 1988.
43. Thermal Energy System Specialists (TRNSYS). *TRNSYS 17—Volume 7 Programmer's Guide*; TRNSYS: Madison, WI, USA, 2014.
44. Andersen, E.; Hans, L.; Furbo, S. The influence of the solar radiation model on the calculated solar radiation from a horizontal surface to a tilted surface. In Proceedings of the EuroSun Congress, Freiburg, Germany, 20–23 June 2014.
45. Raptis, P.I.; Kazadzis, S.; Psiloglou, B.; Kouremeti, N.; Kosmopoulos, P.; Kazantzidis, A. Measurements and model simulations of solar radiation at tilted planes, towards the maximization of energy capture. *Energy* **2017**, *130*, 570–580. [CrossRef]
46. De Simón-Martín, M.; Alonso-Tristán, C.; Díez-Mediavilla, M. Diffuse solar irradiance estimation on building's façades: Review, classification and benchmarking of 30 models under all sky conditions. *Renew. Sustain. Energy Rev.* **2017**, *77*, 783–802. [CrossRef]
47. Yang, D. Solar radiation on inclined surfaces: Corrections and benchmarks. *Sol. Energy* **2016**, *136*, 288–302. [CrossRef]

This page is intentionally left blank.

Paper II

Zhiyong Tian, Bengt Perers, Simon Furbo and Jianhua Fan.

Analysis and validation of a quasi-dynamic model for a solar collector field with flat plate collectors and parabolic trough collectors in series for district heating

Energy, vol. 142, pp. 130–138, 2018.

This page is intentionally left blank.

Energy 142 (2018) 130–138

Contents lists available at ScienceDirect

Energy

journal homepage: www.elsevier.com/locate/energy

Analysis and validation of a quasi-dynamic model for a solar collector field with flat plate collectors and parabolic trough collectors in series for district heating

Zhiyong Tian*, Bengt Perers, Simon Furbo, Jianhua Fan

Department of Civil Engineering, Technical University of Denmark, Kgs. Lyngby, Denmark

ARTICLE INFO

Article history:
Received 10 May 2017
Received in revised form
26 September 2017
Accepted 27 September 2017
Available online 28 September 2017

Keywords:
Hybrid solar district heating plants
Quasi-dynamic model
Validation
In-situ measurements

ABSTRACT

A quasi-dynamic TRNSYS simulation model for a solar collector field with flat plate collectors and parabolic trough collectors in series was described and validated. A simplified method was implemented in TRNSYS in order to carry out long-term energy production analyses of the whole solar heating plant. The advantages of the model include faster computation with fewer resources, flexibility of different collector types in solar heating plant configuration and satisfactory accuracy in both dynamic and long-term analyses. In situ measurements were taken from a pilot solar heating plant with 5960 m^2 flat plate collectors and 4039 m^2 parabolic trough collectors in series in Taars, Denmark from Sep.2015 to Aug.2016. The simulated thermal performances of both the parabolic trough collector field and the flat plate collector field have a good agreement with the measured performances. The thermal performance of the hybrid solar district heating plant is also presented. The measured and simulated results show that the integration of parabolic trough collectors in solar district heating plants can guarantee that the system produces hot water with relatively constant outlet temperature. The daily energy output of the parabolic trough collector field can be more than 5 kWh/m^2, while the daily energy output of the flat plate collector field is less than 5 kWh/m^2 under Danish climate conditions. The simplified and validated TRNSYS model can be a useful tool to simulate and optimize thermal performance of solar heating plants with both flat plate and parabolic trough collectors.

1. Introduction

The number of large scale solar heating plants for district heating increased very fast in Europe during the last couple of years, especially in Denmark [1], [2]. More than 70% of large scale solar heating plants for district heating around the world are constructed in Denmark so far [3]. Most of the collectors in the existing plants are flat plate collectors. Due to collector heat losses, the efficiency of flat plate solar collectors is significantly lower at operation temperatures of 85°C–95 °C compared to the efficiency at temperatures of 40°C–60 °C. Parabolic trough collectors typically have a low heat loss coefficient and are therefore less affected by the operation temperature level of the collectors. Parabolic trough collector is the most used technology currently among solar concentrating power collector technologies [4]. Parabolic trough collectors are mainly used for electricity production at temperatures of 200–400 °C so far [5], [6]. Industry process temperatures found in industrial processes are manifold, ranging from low (T < 100 °C), medium (100 °C < T < 250 °C) to high (T > 250 °C) operating temperatures [7]. Parabolic trough collector is also suitable for these temperature ranges [7]. More and more parabolic trough collectors have been employed in the industry process heat production in the recent years [6,8–11]. Most small scale parabolic trough heating plants are applied for industry processes using glycol/water as heat transfer fluid in recent years [7]. Parabolic trough collector also can be used with advantage operated at temperature range 85–95 °C in solar district heating plants. The feasibility of parabolic trough collectors in large scale solar heating plants for district heating has been validated in the pilot Thisted plant in Denmark in 2013 [12]. A pilot solar collector system with flat plate collector and parabolic trough collector fields for district heating networks in series can harvest the advantages of the flat plate collectors at low temperature levels and the parabolic trough collectors at high temperature levels. A combined solar heating

* Corresponding author.
E-mail addresses: tianzy0913@163.com, zhiytia@byg.dtu.dk (Z. Tian).

https://doi.org/10.1016/j.energy.2017.09.135
0360-5442/

plant with 5960 m^2 flat plate collectors and 4039 m^2 parabolic trough collectors in series for a district heating network was constructed in Taars, Denmark in 2015 [13–15]. A general solar collector field model for both flat plate and parabolic trough collectors would be essential for the evaluation of the combined system.

1.1. Single solar collector model

Many test methods for single solar collectors have been developed [16–28]. The test methods can be divided into the steady-state method, quasi-dynamic method and dynamic method. The quasi-dynamic method is used in the model in this paper. The quasi-dynamic test (QDT) method described in most of the common standards such as EN 12975-2 [16], ISO 9806:2013 [17] and ASHRAE 93 [18] is an efficient model applicable to both concentrating and non-concentrating collector designs, which is firstly developed by Bengt Perers in 1990s [19–21]. Fischer, S., et al. [22] also showed that the QDT method can be used to predict the performance of single parabolic trough collector. Some improved dynamic methods were developed by Deng J. and Kong W. et al. [23–28].

1.2. Solar collector field model

B. Perers [29] had introduced several solar collector models to MINSUN simulation program, which can simulate the thermal performance of different collector fields in 1990. The results had shown that parabolic trough collectors with good optical performance had thermal performance comparable to flat plate or evacuated tube collectors at high latitudes. B. Perers. et al. also investigated the application of parabolic trough collectors in a small scale pilot plant in Thisted, Denmark [12]. This was the earliest research about the practical application of parabolic trough collectors at high latitudes. Guadalfajara M. et al. developed a simple method to simulate the performance of central solar heating plants with seasonal storage [30]. The simple method could give an overview of the thermal performance of solar heating plant which can be helpful for pre-design of the large solar heating plants. The disadvantage of the simple method is that the control strategy is not taken into consideration. Marco. et al. [31] investigated a 1070 m^2 flat plate collector field for the industry process heat, which focused on thermal performance of the solar collector field by comparing the measured field efficiency with the nominal collector efficiency. Hassine I B. et al. [32] also investigated two about 1000 m^2 solar heating plants. Control strategy in the primary and second loop was optimized to have a constant outlet temperature. Frank E. et al. [33] evaluated the operation performance of two around 1000 m^2 parabolic trough collector fields in Switzerland. A quasi-dynamic simulation model for direct steam generation in parabolic trough collector loops using TRNSYS was introduced [34].

1.3. Scope

The previous studies [16–28] mainly focus on simulation or test on a single collector in the laboratory, direct steam generation [34] and thermal performance of relatively small scale solar collector fields (1000 m^2) [30–34]. A collector array field may consist of collectors connected in series and in parallel. Thermal performance of the total collector array should be determined by both the number of modules in series and the characteristics of each module. Most studies were on the flat plate collector. Currently, the performances of large scale solar collector fields under real operation conditions have not yet been widely documented and standardized. Evaluating thermal performance of large-scale solar collector fields with good accuracy is still an important topic in the large scale solar heating industry. Technical parameters from a standard efficiency test of single collector can be used to simulate the thermal performance of total solar collector arrays. Compared to solar collector models, solar collector field model also should consider row shading, axis orientation, heat losses in pipes. etc. A simple and practical method to predict thermal performance of different solar collector fields for general use can increase confidence of large solar heating plants technology in the market. The quasi-dynamic collector model is applied to simulate thermal performance of a nearly 10000 m^2 hybrid solar collector field in Denmark. The quasi-dynamic collector field model was validated by the almost annual in-situ measurements of both flat plate and parabolic trough collector field. The validated quasi-dynamic collector field model could be a very useful tool to optimize the combined solar heating plant to determine the optimal design parameters. The novelty of this study is summarized as follows: 1, The objective is a novel large-scale solar district heating plant with flat plate collectors and parabolic trough collector in series. 2, Validation of the quasi-dynamic model for both large-scale flat plate collector and parabolic trough collector fields was shown; 3, Both simulated and measured dynamic performances of the novel hybrid solar collector field were presented; 4, The advantages of the hybrid solar heating plant were shown, which can introduce a new design concept of large-scale solar district heating plants to other places.

2. Taars solar heating plant

The Taars solar heating plant is located in Taars, 30 km north of Aalborg, Denmark. The solar heating plant is the first demonstration project with parabolic trough collectors for district heating in Europe. The plant was put into operation in August.2015, as shown in Fig. 1. Fig. 2 illustrates the layout of the solar collector field. The PTC collector field consists of six rows of PTC collectors with 4039 m^2 aperture area and the orientation of the PTC collectors is 13.4° towards west from south. The flat plate collector field in the right of Fig. 1 consists of 5960 m^2 aperture area and the orientation is south. The tilt of the flat plate collector field is 50°. The row distances for the parabolic trough collector field and the flat plate collector field are 12.6 m and 5.67 m respectively. The solar collector fluid of the parabolic trough collector field and the flat plate collector field is water and mixture of glycol/water (35%) respectively. The FPC field preheats the return water from the district heating networks to about 75 °C. Then the preheated water from the FPC field is heated by the PTC field to 95 °C. The system was measured over a year (Sep.2015–Aug.2016). Two heat storage tanks (2430 m^3 in total) were used for the heat storage of several summer days. Tables 1 and 2 show the geometrical parameters of FPC and PTC separately [13] [35].

3. TRNSYS model based on quasi-dynamic method

A flat plate collector field and a parabolic trough collector field model were established in TRNSYS [36]. In the flat plate collector field, heat exchanger unit, shadows and pipes are included. The collector arrays consist of collectors connected in series and in parallel. There are two kinds of flat plate collector with/without FEP foil between absorber and cover glass used in the flat plate collector field. The flat plate collector field has 39 rows in parallel. 6 FPC collectors without foil in series and other 6 FPC collectors with foil in series in average were used in most rows. In the parabolic trough collector loop, shadows, supply pipes and return pipes of the solar collector field are taken into consideration. The thermal performance of the total collector array is determined by the number of modules in series and the characteristics of each module. The

Fig. 1. Solar collector fields in the Taars solar heating plant [13].

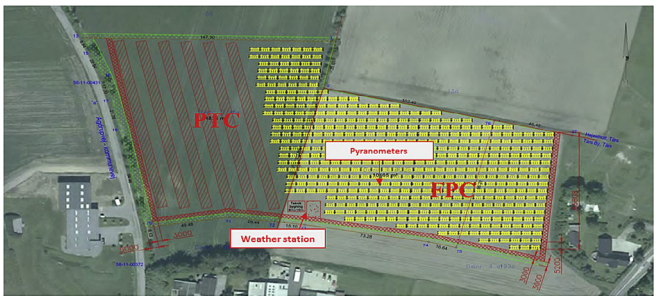

Fig. 2. Layout of the parabolic trough collector and flat plate collector fields [15].

Table 1
Geometrical parameters of the FPC in the Taars plant.

Geometrical parameters for the FPC		
Length, m	5.96	
Width, m	2.27	
Thickness, m	0.14	
Gross area, m^2	13.57	
Aperture area, m^2	12.60	
Solar collector volume, L	10.6	
Absorber	Material	Cu pipe/Al plate
	Absorption	0.95
	Emission	0.05
Insulation	Backside	75 mm mineral wool
	Side	30 mm mineral wool
Cover(s)	Antireflex glass (AR:3.2 mm)-with/without FEP foil	

Table 2
Geometrical parameters of the PTC in the Taars plant.

Geometrical parameters for the PTC	
Absorber tube outer diameter (m)	0.070
Absorber tube inner diameter (m)	0.066
Glass envelope outer diameter (m)	0.125
Glass envelope inner diameter (m)	0.119
Parabola width (m)	5.77
Numbers of modules per row	10
Mirror length in each module (m)	12
Geometric concentration ratio	26.2

numbers of modules per row of both FPC and PTC are 12 and 10, respectively. The discretization in the modelling is done inside the collector and pipe models used. Each collector array is discretized with nodes. The solar collector field model can simulate an array of identical solar collectors hooked up in series. The number of nodes is used to specify how many collectors are hooked up in a series arrangement (outlet of first collector = inlet of second collector, etc.) for each parallel flow loop [37].

The type 1290 is used to simulate thermal performance of both parabolic trough collector and flat plate collector field. The Type 1290 is based on EN12975-2 Dynamic Efficiency Approach (ASHRAE IAMs) [37].

The solar collector model equation is given as follows,

$$\frac{Q}{A} = \eta_0 K_{\theta b}(\theta) G_b + \eta_0 K_{\theta d}(\theta) G_d - c_1(T_m - T_a) - c_2(T_m - T_a)^2 - c_3\frac{dT_m}{dt} \quad (1)$$

$$K_{\theta b}(\theta) = 1 - b_0\left(\frac{1}{COS\theta} - 1\right) - b_1\left(\frac{1}{COS\theta} - 1\right)^2, \theta \le 60^\circ \quad (2)$$

When $\theta > 60^\circ$, the IAM is linearized from the value at 60° to a value of zero at 90°.

Total radiation G is divided into the beam G_b and diffuse G_d parts in this collector model. Incident angle modifiers are used for beam radiation and diffuse radiation. $K_{\theta b}(\theta)$ is a function of the angle of incidence of the direct radiation and the constant $K_{\theta d}$ for the diffuse radiation. Thus the collector model can be used to predict the thermal performance of both the parabolic trough collectors and the flat plate collectors.

Type 30 was employed to simulate shadows from the solar collectors for both collector subfields. This component determines incident radiation upon an array of collectors with shadows from the row in front of the row in question. There are two possible modes. Model 1 considers shadows from fixed flat plate collectors with a tilt. Total, beam, and diffuse radiation are output. Model 2 is for single axis tracking parabolic trough collectors that utilize beam radiation only. Type 5 was used to simulate the heat exchanger connected to the FPC field. Type 31 was used to simulate the pipes. Measured DNI and global horizontal solar radiation and inlet temperature etc. are inputs used for model validation. Measurements and uncertainties can be found in section 4. Mathematical descriptions on the components can be found in Ref. [37].

(1) Flat plate collectors

The flat plate collectors, HTHEATboost 35/10 without FEP foil and HTHEATstore 35/10 with FEP foil, are produced by Arcon-Sunmark A/S [35]. Standard parameters for the collectors based on gross areas can be found in Table 3 [38]. Total radiation on the flat plate collector is the main input for the flat plate collector field model. Two separate 1290 type components in series are used to simulate the thermal performance of the flat plate collector without and with FEP foil in series.

Table 3
Efficiency parameters of flat plate collectors.

η_0	b_0	b_1	$K_{\theta d}$	c_1, [W/(m^2·K)]	c_2, [W/(m^2·K^2)]	c_3, [kJ/(m^2·K)]	
0.779	0.1	0	0.98	2.410	0.015	6.798	HEATboost 35/10
0.745	0.1	0	0.93	2.067	0.009	7.313	HEATstore 35/10

Table 4
Efficiency parameters of parabolic trough collectors.

η_0	b_0	b_1	$K_{\theta d}$	c_1, [W/(m^2·K)]	c_2, [W/(m^2·K^2)]	c_3, [kJ/(m^2·K)]
0.75	0.27	0	0.038	0.04	0	4

(2) Parabolic trough collectors

Peak collector efficiency η_0 and the heat loss coefficients c_1 and c_2 for the parabolic trough collectors based on aperture area were assumed to be equal to the values of the pilot plant in Thisted, Denmark [14], as shown in Table 4. Beam radiation on the PTC plane is the main input for the parabolic trough collector field model.

4. Measurements and uncertainties

4.1. Measurements

The solar heating plant system is well equipped with different accurate sensors. Total solar radiation on the collector's surface and global radiation, ambient temperature and wind speed data were measured. It also had temperature sensor inputs onto which SIEMENS TS500 thermometer with drilled thermoswell temperature sensors [39] were connected to measure inlet and outlet temperatures of both flat plate collector field and parabolic trough collector field. The volume flow rate of the solar fluid was measured using Sitrans FM MAG3100 P flow meters from SIEMENS. The TS500 temperature sensors (PT100) have an uncertainty of ±0.30 K + 0.0050*|T [K]| [39]. Sitrans FM MAG3100 P flow meters had an uncertainty of 1% (maximum).

Two pyranometers (Kipp&Zonen SMP11) are used to measure the global radiation on the horizontal surface and total radiation on the tilted flat plate collector [40]. DNI is measured by the PMO6-CC pyrheliometer [41] with the sun tracking platform Sunscanner SC1 [42], which has high accuracy and automatically cleaning function. The solar radiation sensors had an good accuracy. All the raw measurement data was logged at 2 min interval.

4.2. Uncertainties

Measured power output is calculated by eq. (3). Separate uncertainty of each parameter causes uncertainty of the measured power. As shown in section 4.1, uncertainty of the flow rate sensor is 1%. Uncertainties of density and specific heat of water or glycol/water mixture are estimated as 0.5%. By equation (4), typical uncertainties of the measured power output of the FPC field and the PTC field can be calculated. Details can be found in Figs. 5, 7, 10 and 12 in section 5.

$$Q = V \times \rho \times C_P \times (T_{out} - T_{in}) \tag{3}$$

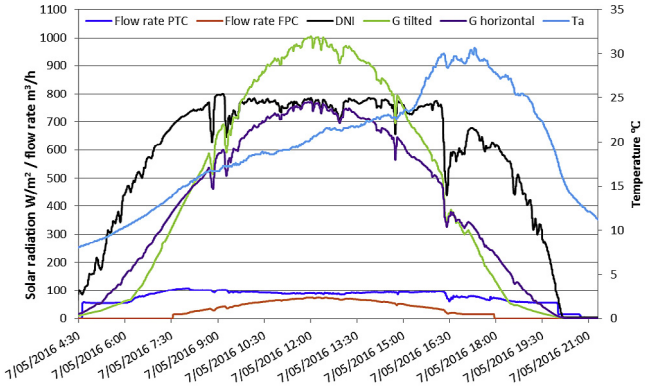

Fig. 3. Global solar radiation, total tilted radiation, DNI, ambient temperature and flow rates on the sunny day (May 7, 2016).

5. Validation

Section 5.1 shows dynamic comparisons of measured and modelled performances of the flat plate collector field and the parabolic trough collector field on a cloudy and a sunny day. Section 5.2 illustrates daily and monthly comparisons of measured and modelled performances based on the quasi-dynamic model. The time step of all the calculations is 1 min. All the performances per m^2 are based on aperture area. Inlet temperature and volume flow rate of both the FPC and the PTC field in simulation are taken from the measurements from the Taars plant.

5.1. Dynamic performance in typical days

One typical sunny day (May 7, 2016) and one typical cloudy day (August 14, 2016) were selected to analyze the thermal performance and validate the developed model. Figs. 3 and 8 show that weather conditions, such as ambient temperature, DNI, global radiation and total radiation on the south-oriented tilted collector plate (50°) and flow rates on both days, respectively. The measured and simulated outlet temperature and power output of the FPC field shown in this section are the values of the secondary water loop of the FPC field including the heat exchanger.

5.1.1. Sunny day (may 7 of 2016)

As shown in Fig. 3, May 7 in 2016 was a typical sunny day. The maximum of global radiation on the tilted surface was about 1000 W/m^2 and the max DNI was about 800 W/m^2. The ambient temperature peaks at around 30 °C. Measured volume flow rates of both the FPC and the PTC fields are shown in Fig. 3. Since the PTC field tracked the sun from sunrise to sunset during the daytime, the operation period of the PTC field is longer than that of the FPC field.

$$S(Q) = \sqrt{\left(\frac{\partial Q}{\partial V}\cdot S_v\right)^2 + \left(\frac{\partial Q}{\partial \rho}\cdot S_\rho\right)^2 + \left(\frac{\partial Q}{\partial C_p}\cdot S_{C_p}\right)^2 + \left(\frac{\partial Q}{\partial T_{out}}\cdot S_{t_{out}}\right)^2 + \left(\frac{\partial Q}{\partial T_{in}}\cdot S_{t_{in}}\right)^2} \tag{4}$$

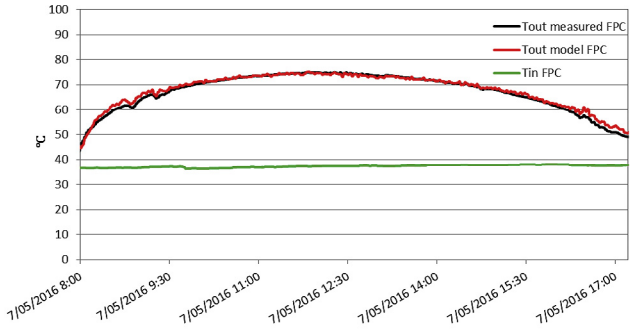

Fig. 4. Inlet temperature, measured and modelled outlet temperature of the FPC field on the sunny day.

On the sunny day, the flow rate of PTC field was almost constant. The volume flow rate of the FPC field varied with the solar radiation and was largest at noon.

1) FPC field on the sunny day

Fig. 4 shows measured inlet and outlet temperature and simulated outlet temperature of the FPC field in May 7, 2016. Fig. 5 shows measured and modelled power output of the FPC field in May 7, 2016. The maximum power output of the flat plate collector field is close to 600 W/m^2 at noon in May 7, 2016. The modelled and measured outlet temperature, the modelled and measured power output have good agreements in Figs. 4 and 5.

2) PTC field on the sunny day

Fig. 6 shows measured inlet and outlet temperature and simulated outlet temperature of the PTC field in May 7, 2016. Fig. 7 illustrates the comparison between measured and modelled power output of the parabolic trough collector field in May 7, 2016. The modelled results have similar fluctuations as the measured results. As shown in Fig. 7, the measured and modelled thermal performances of the PTC field had a good agreement. Compared to the thermal performance of the FPC field at noon, the thermal performance of the PTC field was a bit higher before and after noon. That was because of tracking the sun. It also can be seen in Fig. 7 that there was an increase of power output after sunset. That was due to discharge of the heat stored in the receiver. The low heat losses of the parabolic trough collectors means that this can be done even after sunset. It is also found that the outlet temperature of the PTC field is relatively constant, which is very important for the hydraulic balance of the district heating network.

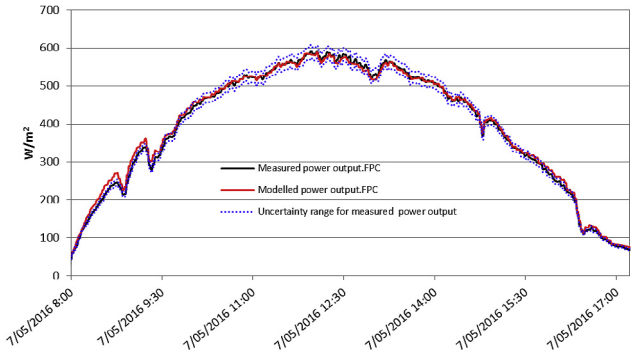

Fig. 5. Measured and modelled power output of the FPC field on the sunny day.

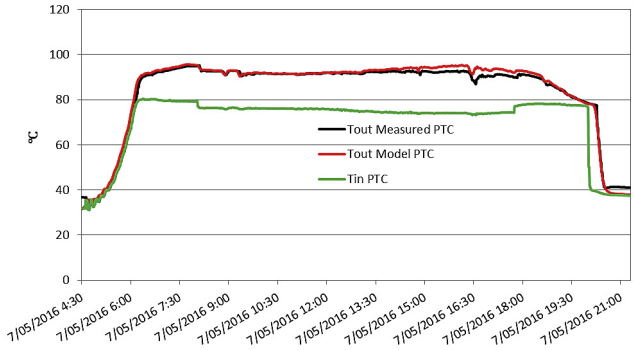

Fig. 6. Inlet temperature, measured and modelled outlet temperature of the PTC field on the sunny day.

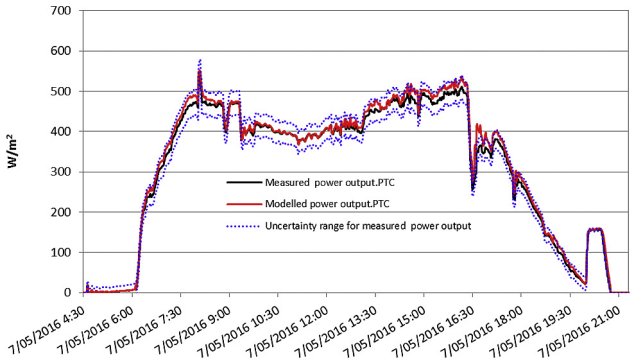

Fig. 7. Measured and modelled power output of the PTC field on the sunny day.

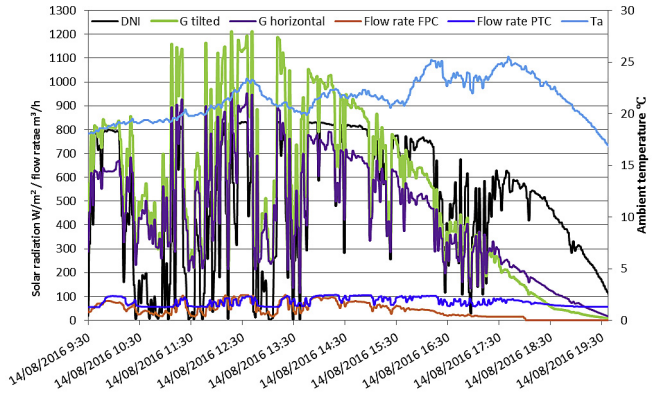

Fig. 8. Global solar radiation, total tilted radiation, DNI, ambient temperature and flow rates on the cloudy day.

5.1.2. Cloudy day (August 14 of 2016)

August 14 in 2016 was a cloudy day. As shown in Fig. 8, the maximum of DNI and global solar radiation was larger than 800 W/m^2. Fig. 8 shows the fluctuation of weather from 9:30 a.m. to 19:30 p.m. in August 14, 2016. Both the DNI and the global solar radiation fluctuated dramatically during the daytime. The total solar radiation on the tilted flat plate collector was larger than that on the horizontal surface. The largest total radiation on the tilted solar collector in short periods exceeded 1200 W/m^2. On the cloudy day, the flow rates of both collector fields fluctuated along with the solar radiation.

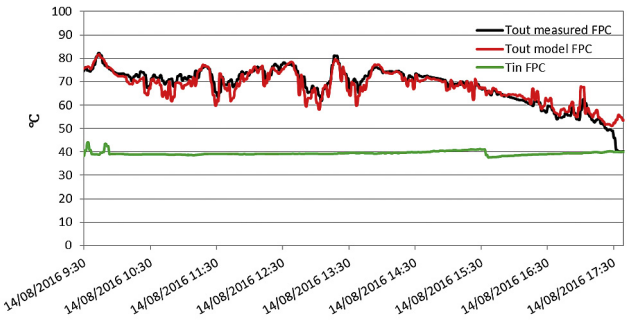

Fig. 9. Inlet temperature, measured and modelled outlet temperature of the FPC field on the cloudy day.

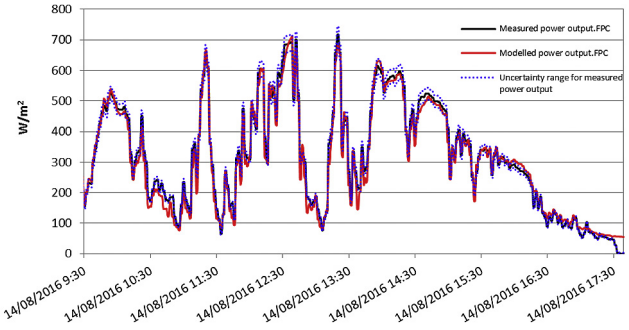

Fig. 10. Measured and modelled power output of the FPC field on the cloudy day.

1) FPC field on the cloudy day

Fig. 9 shows measured inlet and outlet temperature and simulated outlet temperature of the FPC field in August 14, 2016. Fig. 10 shows measured and modelled power output of the FPC field in August 14, 2016. The modelled and measured power outputs had very similar fluctuation trends.

2) PTC field on the cloudy day

Fig. 11 shows measured inlet and outlet temperature and simulated outlet temperature of the PTC field in August 14, 2016. Fig. 12 shows the measured and modelled power output of the PTC field on a cloudy day (August 14, 2016). The maximum of power output in August 14, 2016 was higher than 500 W/m^2. The

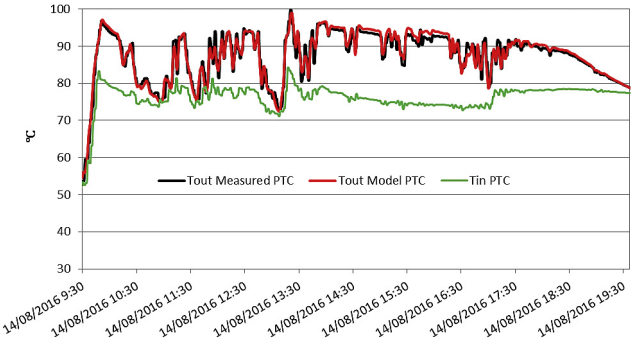

Fig. 11. Inlet temperature, measured and modelled outlet temperature of the PTC field on the cloudy day.

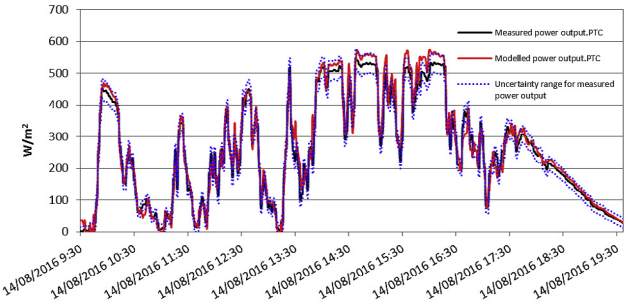

Fig. 12. Measured and modelled power output of the PTC field on the cloudy day.

modelled power output has almost the same fluctuating change as the measured power output.

The daily energy output of the FPC and PTC fields are shown in Table 5. The modelled and measured energy outputs present a good agreement on both cloudy and sunny days. The measured energy output of the PTC field is a bit lower than the modelled values on both the cloudy and the sunny days. That may be due to dirt on the mirror of the parabolic trough collectors because the mirrors have not been washed yet since August 2015. Furthermore, compared to the energy output of the FPC field, the PTC field produced about 40% more solar heat than the FPC field on the sunny day.

5.2. Daily and monthly performance

Calculations of daily and monthly performances of both solar collector fields are based on 1 min time step. The daily and monthly thermal performances of the parabolic trough collector field and the flat plate collector field during year-around operation are presented in Figs. 13–16.

1) Flat plate collector field

Fig. 13 shows that the measured and the modelled thermal performances are strongly linear related. Overall, the modelled results have a fine match with the measured data. The max daily solar heat production of the flat plate collector field was below 5 kWh/m^2/day.

As shown in Fig. 14, the flat plate collector field produced small heat quantities in November–January. The FPC field produced more and more heat from January to April. The FPC field produced more than 50 kWh/m^2 in April. The measured and simulated monthly solar heat productions show a good agreement from Sep.2015 to Aug.2016.

2) Parabolic trough collector field

Daily and monthly measured and modelled energy outputs of the PTC field (Sep.2015–Apr.2016) are shown in Figs. 15 and 16. In Fig. 15, a single point represents a daily result (September.2015–April.2016). There is a strong linear correlation between the measured daily thermal performance and the modelled daily thermal performance in Fig. 15, which shows the modelled values have good agreement with the measured values. Due to the oversized flat plate collector field and low heat load in the summer, the parabolic trough collector field was defocused on several sunny days in the summer. Therefore, only thermal performances of the parabolic trough collector field without defocusing during the period from Sep.2015 to Apr.2016 was presented in this section to verify the TRNSYS model. The maximum daily thermal performance of the parabolic trough collector field can be higher than

Table 5
Sum of daily solar radiation, and daily solar energy outputs of the FPC and PTC fields, May 7 and August 14 of 2016.

	$H_{Beam\ (PTC)}$, kWh/m^2	$H_{Tilted\ (FPC)}$, kWh/m^2	Measured, kWh/m^2	Modelled, kWh/m^2	Difference, kWh/m^2	Deviation	
Sunny day (May 7, 2016)	8.59	7.67	3.65	3.69	0.04	1.10%	FPC
			5.19	5.34	0.15	3.00%	PTC
Cloudy day (Aug. 14, 2016)	5.37	5.90	2.63	2.59	−0.04	−1.70%	FPC
			2.72	2.82	0.1	3.90%	PTC

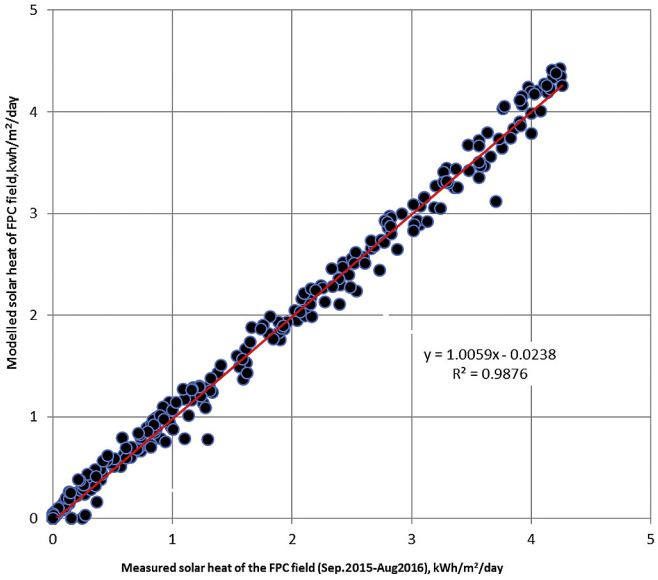

Fig. 13. Daily modelled solar energy output as a function of daily measured solar energy output of the FPC field.

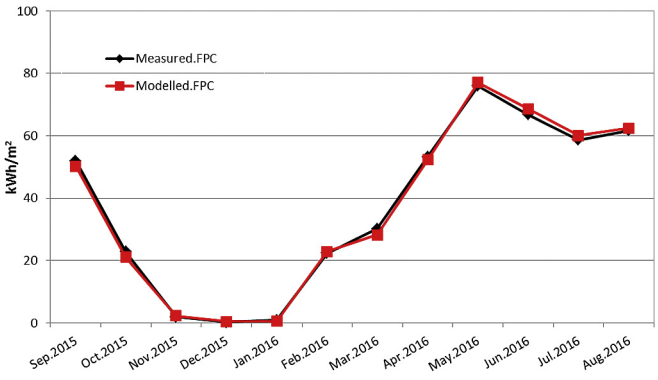

Fig. 14. Monthly measured and modelled energy output of the FPC field (Sep.2015–Aug.2016).

5 kWh/m^2/day, while the max daily thermal performance of the flat plate collector field is below 5 kWh/m^2/day. The thermal energy output of both the flat plate collector field and parabolic trough collector field in November, December, January is quite low because of the low solar radiation in winter. From February, the thermal energy output of the parabolic trough collector array increased dramatically because of more sunny days and the PTC field produced more solar heat than the FPC field.

6. Discussions

The flat plate collector field preheats return water from 45 °C up to about 75 °C, and then the preheated water is heated to 95 °C by

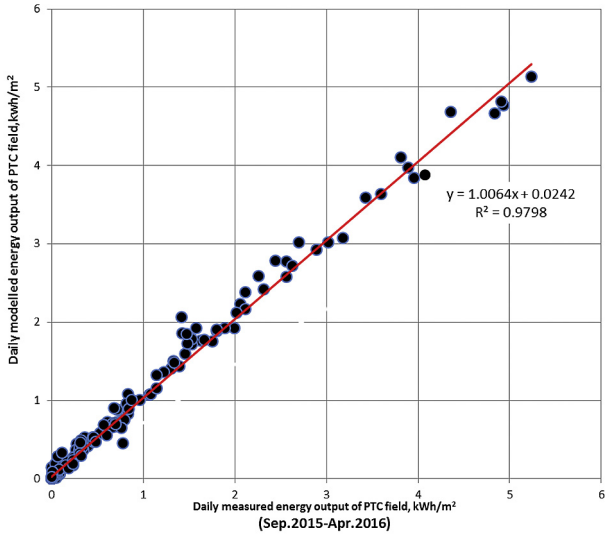

Fig. 15. Daily modelled solar energy output as a function of measured solar energy output of the PTC field.

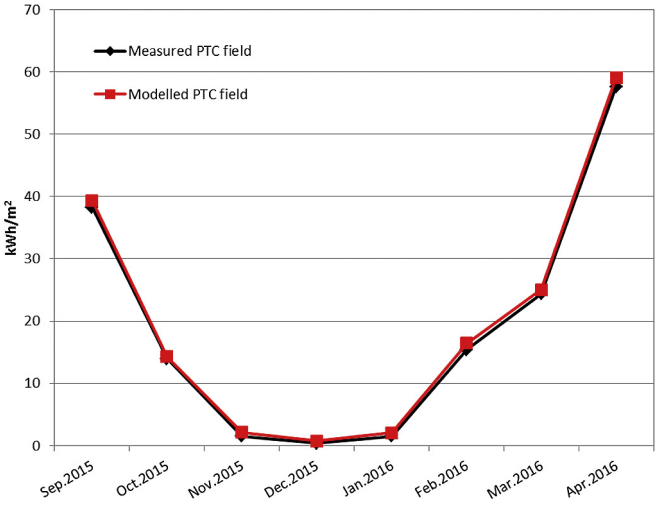

Fig. 16. Monthly measured and modelled energy output of the PTC field.

the parabolic trough collector field in the Taars plant. The design strategy that the PTC field produces the high temperature water also guarantees that the FPC field has better performance and higher efficiency due to relatively low operation temperature compared to normal flat plate collector fields. In addition, section 5 shows that the TRNSYS models of the FPC field and the PTC field have quite good agreement with measurements. The PTC field was defocused sometimes in the quite sunny days in summer (May–August) because the flat plate collector field was oversized and the heat load of the district heating networks in summer was low.

So Figs. 15 and 16 only show the measured results from Sep.2015–Apr.2016. The PTC field would have higher energy output than the measured values, if the parabolic trough collectors were not defocused on sunny days in the summer. On the other hand, the defocusing of the PTC field can avoid boiling problems of the solar collector field in the summer season.

7. Conclusions and future work

The quasi-dynamic simulation model of both large parabolic trough collector field and flat plate collector field was validated by the measured thermal performance of the Taars solar heating plant in Denmark. Dynamic performance on two typical days was selected for the detailed validation. The simulated and the measured daily and monthly performances of the solar heating plant were also compared. The following conclusions can be drawn:

(1) The quasi-dynamic method with the technical parameters from the standard test report based on single collector can be used to predict the thermal performance of both parabolic trough collector and flat plate collector fields.
(2) The daily energy output of the parabolic trough collector field can be more than 5 kWh/m^2, while the daily energy output of the flat plate collector field is less than 5 kWh/m^2 under Danish climate conditions in this study.
(3) The integration of parabolic trough collectors can increase the flexibility of solar district heating plants. The parabolic trough collectors can be easily defocused in the summer to avoid the overheat production. The flat plate collectors only work at low temperature range in the hybrid solar heating plant in order to increase the thermal performance of the flat plate collectors, compared to normal existing solar heating plants. A relatively constant and high outlet temperature of the hot water is easily achieved in the hybrid solar district heating plants.

In summary, the validated solar collector field model in this study is able to model reliable dynamic performances with a time step of 1 min. The proposed model is cost-effective, reasonable accurate and requires low computational time. The validated model may be a useful tool to analyze long-term performance, optimize design parameters and evaluate control strategy of large solar heating plants for district heating.

Acknowledgements

The first author really appreciates the China Scholarship Council (No. 201506120074) for the financial support for the Ph.D. study at the Technical University of Denmark. Special thanks are expressed to Aalborg CSP A/S for the information provided and maintaining the high accuracy and reliablility of the measurement system (Andreas Zourellis, Jan Holst Rothman, Steffen Rovsing Møller and Per Aasted). This work is also a part of an EUDP (Energy Technology Development and Demonstration Program) project financed by the Danish Energy Agency and the IEA-SHC Task 55 “Towards the Integration of Large SHC Systems into DHC Networks”.

Symbols

Q	Useful output power, W
A	Collector array area, m^2
c_1	Heat loss coefficient at (Tm-Ta) = 0, W/(m^2·K)
c_2	Temperature dependence of the heat loss coefficient, W/(m^2·K^2)
c_3	Effective thermal capacity, kJ/(m^2·K)
G_b	Beam radiation, W/m^2
G_d	Diffuse radiation, W/m^2
$K_{\theta b}$	Incidence angle modifier for beam radiation, -
$K_{\theta d}$	Incidence angle modifier for diffuse radiation, -
T_m	Mean fluid temperature, °C
T_a	Ambient temperature, °C
η_0	Peak collector efficiency, -
dTm/dt	Time derivative of the mean fluid temperature, K/s
θ	Incident angle of the beam radiation, °
b_0	IAM coefficient(beam radiation), -
b_1	IAM coefficient(beam radiation), -
G_{tilted}	Total solar radiation on the tilted plate, W/m^2
G_h	Global solar radiation on the horizontal surface, W/m^2
$H_{Beam\ (PTC)}$	Daily beam radiation on the parabolic trough collector aperture, kWh/m^2
$H_{Tilted\ (FPC)}$	Daily total radiation on the flat plate collector aperture, kWh/m^2
T_{out}	Outlet temperature, °C
T_{in}	Inlet temperature, °C
ρ	Density, kg/m^3
C_P	Specific Heat Capacity, J/(kg·°C)
V	Volume flow rate, m^3/s
S	Uncertainty of specific parameters

Abbreviation

Parabolic trough collector PTC
Flat plate collector FPC
Heat transfer fluid HTF
Incidence angle modifier IAM
Direct normal irradiance DNI
Heat transfer fluid HTF
Concentrating solar power CSP
Quasi-dynamic test QDT
Fluorinated ethylene propylene FEP

References

[1] Furbo S, Fan J, Perers B, Kong W, Trier D, From N. Testing, development and demonstration of large scale solar district heating systems. Energy Procedia 2015;70:568–73.
[2] Weiss Werner, Spörk-Dür Monika, Mauthner Franz. Solar heat worldwide-global market development and trends in 2016-detailed market figures 2015 (2017 version). 2017. http://www.iea-shc.org/solar-heat-worldwide.
[3] Mauthner F, Weiss W. Solar heat worldwide: markets and contribution to the energy supply 2014. Int Energy Agency Solar Heat Cool Progr 2016:38–9.
[4] Morin G, Dersch J, Platzer W, Eck M, Häberle A. Comparison of linear fresnel and parabolic trough collector power plants. Sol Energy 2012;86(1):1–12.
[5] Jebasingh VK, Herbert GMJ. A review of solar parabolic trough collector. Renew Sustain Energy Rev Feb. 2016;54:1085–91.
[6] Fernández-García A, Zarza E, Valenzuela L, Pérez M. Parabolic-trough solar collectors and their applications. Renew Sustain Energy Rev Sep. 2010;14(7):1695–721.
[7] IEA. IEA-shc Task 49. 2016 [Online]. Available: August 2017, http://task49.iea-shc.org/publications.
[8] Kizilkan O, Kabul A, Dincer I. Development and performance assessment of a parabolic trough solar collector-based integrated system for an ice-cream factory. Energy Apr. 2016;100:167–76.
[9] Silva R, Cabrera FJ, Pérez-García M. Process heat generation with parabolic trough collectors for a vegetables preservation industry in southern Spain. Energy Procedia 2014;48:1210–6.
[10] El Ghazzani B, Martinez Plaza D, Ait El Cadi R, Ihlal A, Abnay B, Bouabid K. Thermal plant based on parabolic trough collectors for industrial process heat generation in Morocco. Renew Energy Dec. 2017;113:1261–75.
[11] Larcher M, Rommel M, Bohren A, Frank E, Minder S. Characterization of a parabolic trough collector for process heat applications. Energy Procedia 2014;57:2804–11.
[12] Perers B, Furbo S, Dragsted J. Thermal performance of concen- trating tracking solar collectors. DTURep August, 2013;292.
[13] CSP A. Aalborg CSP. 2017 [Online]. Available: July.2017, http://www.aalborgcsp.com.
[14] Perers B, Furbo S, Tian Z, Egelwisse J, Bava F, Fan J. Tårs 10000 m2 CSP + flat plate solar collector plant - cost-performance optimization of the design. Energy Procedia 2016;91:312–6.

[15] Tian Z, Perers B, Furbo S, Fan J. Annual measured and simulated thermal performance analysis of a hybrid solar district heating plant with flat plate collectors and parabolic trough collectors in series. Appl Energy 2017;205:417–27.
[16] CEN. EN 12975–2. Thermal solar systems and components – Solar collectors –Part 2: test methods. European Committee for Standardisation. 2006.
[17] Volejnik-technicke. International Standard Solar energy — Solar thermal collectors — test methods. 2013.
[18] ANSI/ASHRAE. ASHRAE Standard 93 methods of testing to determine thermal performance of solar collectors. 2003.
[19] Perers B. An improved dynamic solar collector test method for determination of non-linear optical and thermal characteristics with multiple regression. Sol Energy 1997;59:163–78.
[20] Perers Bengt. Optical modelling of Solar collectors and booster reflectors under non stationary conditions. 1995.
[21] Perers B. In: Dynamic method for solar collector array Testing a N D evaluation with standard, vol. 50; 1993. p. 517–26. no. 6.
[22] Fischer S. Efficiency Testing of Parabolic trough Collectors Using the Quasi-Dynamic Test Procedure According to the European Standard en 12975. In: SolarPACES 13th symposium on concentrating solar power and chemical energy technologies; 2006. no. June 2006.
[23] Deng J, Yang X, Wang P. Study on the second-order transfer function models for dynamic tests of flat-plate solar collectors Part I: a proposed new model and a fitting methodology. Sol Energy Apr. 2015;114:418–26.
[24] Deng J, Xu Y, Yang X. A dynamic thermal performance model for fl at-plate solar collectors based on the thermal inertia correction of the steady-state test method. Sol Energy 2015;76:679–86.
[25] Deng J, Yang X, Wang P. Study on the second-order transfer function models for dynamic tests of flat-plate solar collectors Part II: experimental validation. Sol Energy 2017;141:334–46.
[26] Kong W, Wang Z, Fan J, Bacher P, Perers B, Chen Z, et al. An improved dynamic test method for solar collectors. Sol Energy 2012;86(6):1838–48.
[27] Kong W, Wang Z, Li X, Li X, Xiao N. Theoretical analysis and experimental verification of a new dynamic test method for solar collectors. Sol Energy 2012;86(1):398–406.
[28] Sun C, Liu Y, Duan C, Zheng Y, Chang H, Shu S. A mathematical model to investigate on the thermal performance of a flat plate solar air collector and its experimental verification. Energy Convers Manag 2016;115:43–51.
[29] Perers B. Simulation and evaluation methods for solar energy systems. 1990.
[30] Guadalfajara M, Lozano MA, Serra LM. A simple method to calculate central solar heating plants with seasonal storage. Energy Procedia 2014;48:1096–109.
[31] Cozzini M, Pipiciello M, Fedrizzi R, Ben Hassine I, Pietruschka D, Söll R. Performance analysis of a flat plate solar field for process heat. Energy Procedia 2016;91:11–9.
[32] Ben Hassine I, Sehgelmeble MC, Soll R, Pietruschka D. Control optimization through simulations of large scale solar plants for industrial heat applications. Energy Procedia 2015;70(0):595–604.
[33] Frank E, Marty H, Hangartner L, Minder S. Evaluation of measurements on parabolic trough collector fields for process heat integration in Swiss dairies. Energy Procedia 2014;57:2743–51.
[34] Biencinto M, Gonzålez L, Valenzuela L. A quasi-dynamic simulation model for direct steam generation in parabolic troughs using TRNSYS. Appl Energy 2016;161:133–42.
[35] Arcon-Sunmark, "Arcon-Sunmark," http://arcon-sunmark.com/products. [Online]. Available: Mar.2017.
[36] TRNSYS, "Trnsys 17," http://www.trnsys.com. [Online]. Available: August 2017.
[37] TRNSYS website, "TRNSYS 17-a TRaNsient SYstem Simulation program-Standard Component Library Overview and Mathematical Reference," http://sel.me.wisc.edu/trnsys. [Online]. Available: Mar.2017.
[38] SP. Technical research institute of Sweden. 2016. https://www.sp.se/en/Sidor/default.aspx.
[39] Simens. Simens. 2016. https://www.siemens.com/global/en/home.html.
[40] SMP11 K. Kipp&Zonen SMP11. 2017. http://www.kippzonen.com/Product/202/SMP11Pyranometer#.V35QMvl95mM.
[41] PMO6-CC. PMO6-CC pyrheliometer. 2016. https://www.pmodwrc.ch/pmod.php?topic=pmo6.
[42] Sunscanner SC1. Sunscanner SC1. 2016. http//www.black-photon.de/products/sunscanner-sc1.html.

This page is intentionally left blank.

Paper III

Zhiyong Tian, Bengt Perers, Simon Furbo and Jianhua Fan.

Annual measured and simulated thermal performance analysis of a hybrid solar district heating plant with flat plate collectors and parabolic trough collectors in series,

Applied Energy, vol. 205, pp. 417–427, 2017.

This page is intentionally left blank.

Applied Energy 205 (2017) 417–427

Contents lists available at ScienceDirect

Applied Energy

journal homepage: www.elsevier.com/locate/apenergy

Annual measured and simulated thermal performance analysis of a hybrid solar district heating plant with flat plate collectors and parabolic trough collectors in series

Zhiyong Tian*, Bengt Perers, Simon Furbo, Jianhua Fan

Department of Civil Engineering, Technical University of Denmark, Brovej Building 118, Lyngby, 2800, Denmark

HIGHLIGHTS

- A novel hybrid large-scale solar district heating plant was introduced.
- Annual thermal performance of the hybrid solar heating plant was investigated.
- Potential of parabolic trough collectors at high latitudes was shown.
- The novel design concept provides a design basis for solar heating plants.

ARTICLE INFO

Keywords:
Solar district heating plants
Parabolic trough collectors
Flat plate collectors
Thermal performance

ABSTRACT

Flat plate collectors have relatively low efficiency at the typical supply temperatures of district heating networks (70–95 °C). Parabolic trough collectors retain their high efficiency at these temperatures. To maximize the advantages of flat plate collectors and parabolic trough collectors in large solar heating plants for a district heating network, a hybrid solar collector field with 5960 m^2 flat plate collectors and 4039 m^2 parabolic trough collectors in series was constructed in Taars, Denmark. The design principle is that the flat plate collectors preheat the return water from the district heating network to about 70 °C and then the parabolic trough collectors would heat the preheated water to the required supply temperature of the district heating network. Annual measured and simulated thermal performances of both the parabolic trough collector field and the flat plate collector field are presented in this paper. The thermal performance of both collector fields with weather data of a Design Reference Year was simulated to have a whole understanding of the application of both collectors under Danish climate conditions as well. These results not only can provide a design basis for this type of hybrid solar district heating plants with flat plate collectors and parabolic trough collectors in the Nordic region, but also introduce a novel design concept of solar district heating plants to other high solar radiation areas.

1. Introduction

Building energy consumption currently accounts for about 40% of the total society energy consumption in developed countries [1–4]. Different energy system configurations were optimized and the results showed that solar collector fields should be included in the energy supply system to achieve both the economic and environmental optimization [5]. Multi-objective optimizations on central solar heating plants with seasonal storage were carried out [6]. The results showed that the central solar heating plant led to significant environmental and economic improvements compared to the use of a conventional natural gas heating system. Overall, solar heating plants for district heating can reduce the fossil energy consumption in the building sector [7].

1.1. State of the art

In the early 1980s, the first several large solar collector arrays was built to connected to the district heating networks in Sweden. Then the market of large solar heating plants has increased fast in Denmark [8], Germany [9], Austria [10], Spain and Greece [11]. In 2016, 37 large-scale solar thermal systems were installed compared to 21 new installations in 2015 in Europe. Within these installations, 31 systems were installed in Denmark, 1 system in Sweden, 1 system in France and 4 systems in Germany [11]. Moreover the collector area of 5 existing Danish plants was extended in 2016. An online platform was established for almost all the solar heating plants in Denmark [12]. More than 1.3 million m^2 solar heating plants were in operation in Denmark

* Corresponding author.
E-mail addresses: tianzy0913@163.com, zhiytia@byg.dtu.dk (Z. Tian).

http://dx.doi.org/10.1016/j.apenergy.2017.07.139
Received 10 May 2017; Received in revised form 28 July 2017; Accepted 31 July 2017
Available online 07 August 2017

Nomenclature

Q	useful output power, W
A	collector aperture array area, m^2
c_1	heat loss coefficient at (Tm-Ta) = 0, $W/(m^2 \cdot K)$
c_2	temperature dependence of the heat loss coefficient, $W/(m^2 \cdot K^2)$
c_3	effective thermal capacity, $kJ/(m^2 \cdot K)$
G_b	beam radiation, W/m^2
G_d	diffuse radiation, W/m^2
$K_{\theta b}$	incidence angle modifier for beam radiation, –
$K_{\theta d}$	incidence angle modifier for diffuse radiation, –
T_m	mean fluid temperature, °C
T_a	ambient temperature, °C
η_0	maximum efficiency, –
dTm/dt	time derivative of the mean solar collector fluid temperature, K/s
θ	incident angle of the beam radiation, °
b_0	first IAM coefficient (beam radiation), –
b_1	second IAM coefficient(beam radiation), –
PTC	parabolic trough collector
FPC	flat plate collector
DNI	direct normal irradiance
DTU	Technical University of Denmark
DRY	Design Reference Year
IAM	incidence angle modifier
HE	heat exchanger
DH	district heating networks
IEA	International Energy Agency
SHC	Solar Heating and Cooling Programme
SF	solar fraction

by the end of 2016 and 270 thousand m^2 solar heating plants are being planned, as shown in Fig. 1. Several large solar heating plants have been constructed in Denmark [13], such as in Vojens (70,000 m^2), Marstal (33,360 m^2), Gram (44,000 m^2), Silkeborg (156,694 m^2), etc. Denmark is the frontrunner not only in Europe but also worldwide for both large-scale systems installed as well as capacity installed in solar district heating sector. Denmark is also the only example of a mature and commercial solar district heating market around the world, which can provide references for other places. Solar collectors are the most important components for the large solar district heating plants. Most solar collectors used in the normal solar heating plants are ground mounted flat plate collectors (FPC).

1.2. Parabolic trough collectors

Most parabolic trough collectors (PTC) have previously been used to produce electricity. With the requirements of energy conservation in industry, more and more parabolic trough solar collectors have been employed to provide heat for industrial processes in recent years. IEA-SHC TASK 49 [15] has focused on the application of solar collectors in the industry sector. Frank et al. [16] investigated the thermal performances of parabolic trough collectors in two solar heating plants in Swiss dairies and found that the thermal performance of both the solar collector fields could be high under Swiss climate conditions. Silva et al. [17, 18] did simulations and thermo-economic design optimization on

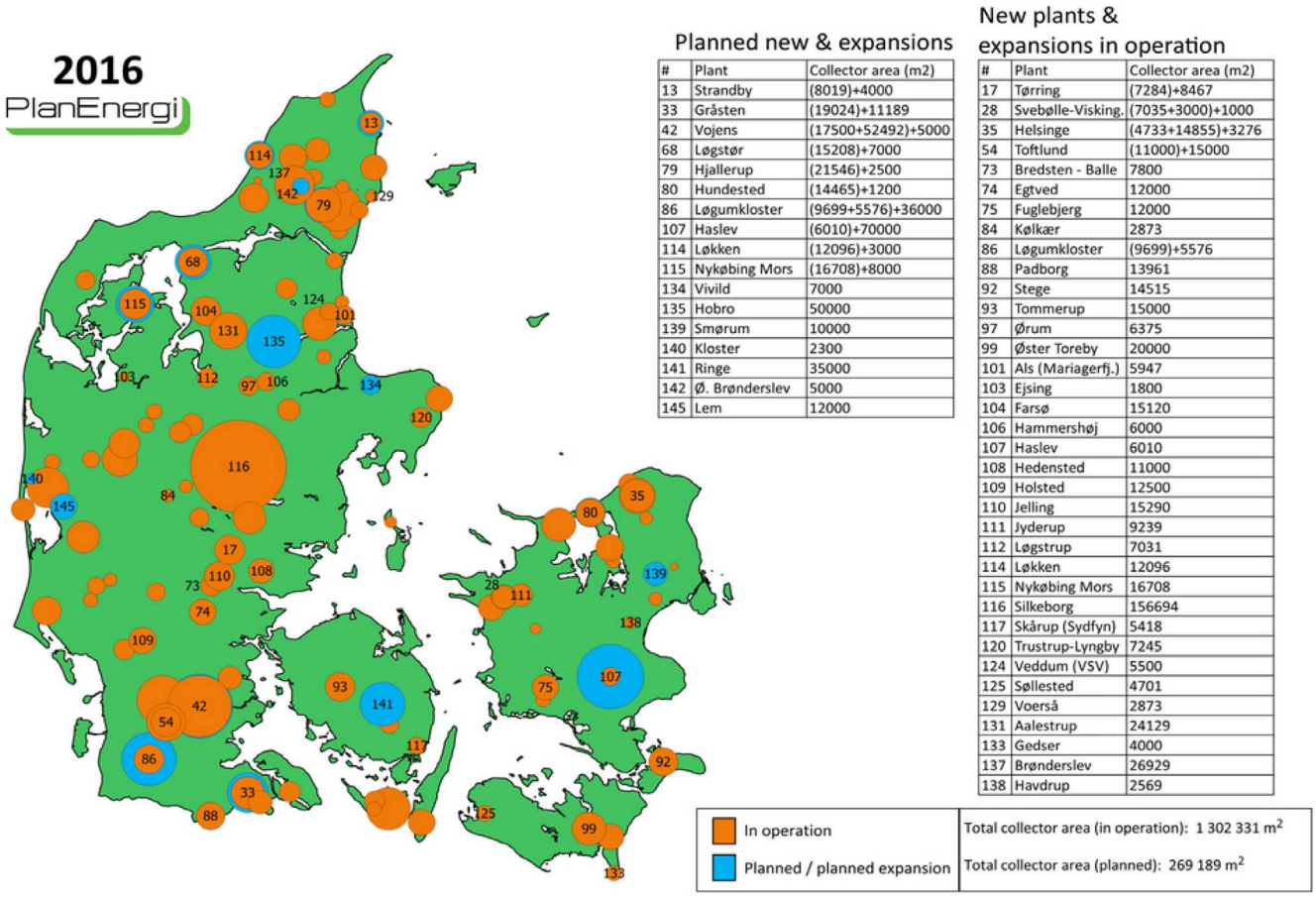

Fig. 1. Solar heating plants in Denmark [14].

parabolic trough collectors for heat production for industrial processes. LCOE (Levelized Cost Of Energy) of 5 c€/kWh and a PBT (payback time) of 8 years could be achieved at the base scenario conditions considered. Hassine et al. [19] investigated the control strategy of two 1000 m^2 solar heating plants (in Austria and Italy). Some design faults of the collector loop controller were found in the first operation period. Based on measurements and simulations with dynamic models, the potential improvements of low-level control algorithms were suggested for the two solar heating plants.

Larcher et al. [20] presented experimental investigations on a parabolic trough collector under development for process heat applications. Results of quasi steady state efficiency measurements on parabolic trough collectors were shown. Kizilkan et al. [21] proposed a parabolic trough solar collector-based integrated system for an ice-cream factory in Turkey and discussed the thermal performance. The payback period of the proposed integrated system was found to be 8.5 years. The payback period was almost the same as reported by Silva [17, 18]. An experimental investigation on a small-sized parabolic trough solar collector for hot water in cold areas was carried out and showed great anti-freezing property of the proposed collector [22]. These investigations show that the application of parabolic trough collectors for high temperature heat production can be economical and feasible if the systems are designed reasonably.

A preliminary case study of parabolic trough collectors for district heating at high latitudes with low solar radiation resources was carried out in 2000 [23]. The economic comparison indicated that parabolic trough systems could be competitive with flat plate collectors, but few practical projects with parabolic trough collectors for district heating were undertaken in the following decades. On the other hand, it is found that most present research of parabolic trough collectors has been on applications with 500–1500 m^2 collectors for industrial processes [16–21] or steam and electricity production [24–33]. Limited reports with detailed measurements of the in situ annual thermal performance of large-scale solar heating fields with flat plate collector and parabolic trough collectors for district heating networks are available.

The operation temperature of solar collectors in solar heating plants in Denmark is in the range from about 40 °C to 95 °C. The efficiency of flat plate collectors decreases significantly in the range 70–95 °C, while parabolic trough collectors maintain relatively high efficiency in this range. To exploit the advantages of both flat plate collectors and parabolic trough collectors in large solar heating plants for district heating networks, a new concept for a hybrid solar heating plant consisting of flat plate collectors and parabolic trough collectors in series has been proposed. The basic principle is that the flat plate collector field preheats the return water from the district heating network from 40 °C to 70 °C and then the parabolic trough collector field heats the preheated water from 70 °C to 95 °C. Feasibility of application of the parabolic trough collector technology in Denmark has been primarily investigated by Aalborg CSP A/S [34] and Technical University of Denmark (DTU) [35] since 2013.

1.3. Scope

A demonstration hybrid solar district heating plant based on the mentioned principle was constructed in Taars of Denmark and put into operation in August 2015. The hybrid solar heating plant consists of 5960 m^2 flat plate collectors and 4039 m^2 parabolic trough collector in series. The aim of this work is to demonstrate the application of the hybrid solar heating pant with parabolic trough collectors and introduce a novel design concept for the new solar heating plants. The novelty of this paper is stressed as follows: (1) The studied solar heating plant is the first hybrid large scale solar heating plant (9999 m^2) developed for the domestic district heating network in the Nordic area, or even around the world, which integrates the PTC and FPC technologies; (2) Parabolic trough collectors with water as the heat transfer fluid in the novel combined solar heating plant are used to provide hot water for the district heating network, while parabolic trough collectors with oil as the heat transfer fluid are normally used for electricity production; (3) The idea of the hybrid solar heating plant is that the flat plate collectors only work at the low operation temperature level and the parabolic trough collectors work at relatively high temperature level; (4) The integration of parabolic trough collectors can increase the flexibility of the solar heating plants significantly in the whole district heating networks due to the possibility of defocusing; (5) Potential and feasibility of the PTC technology in the hybrid solar heating plant under the Danish climate conditions with low solar radiation resource was shown, which can provide a design basis for the development of concentrating solar power technologies in the Nordic area in the near future.

Annual measured and simulated thermal performances with a validated TRNSYS model of the hybrid solar heating plant during its first operation year from September 2015 to August 2016 are shown in this paper. The rest of the paper is organized as follows: the 2nd section introduces the Taars solar heating plant briefly, The 3rd section shows the methods, including measurements and validated TRNSYS in this study. The 4th section presents meteorological data and heat demand. The 5th section presents annual thermal performance of Taars solar heating plant, including both measured and modelled energy output, solar fraction and utilized efficiency. The 6th section shows the typical performance of the Taars plant in Design Reference Year and illustrates the potential of the hybrid plant under Danish climate conditions. Finally, the 7th section is the conclusions and future work.

2. Taars solar heating plant

2.1. Overview

Figs. 2 and 3 show the hybrid solar heating plant with a 5960 m^2 flat plate collector field and a 4039 m^2 parabolic trough collector field in series in Taars, Denmark (latitude: 57.39 °N, longitude: 10.11 °E, altitute:48 m). The plant was put into operation in August 2015 [34, 35]. Technical data on the solar collector field can be found in Tables 1 and 2. Fig. 4 briefly illustrates the basic principle of the solar heating

Fig. 2. Picture of the Taars solar heating plant.

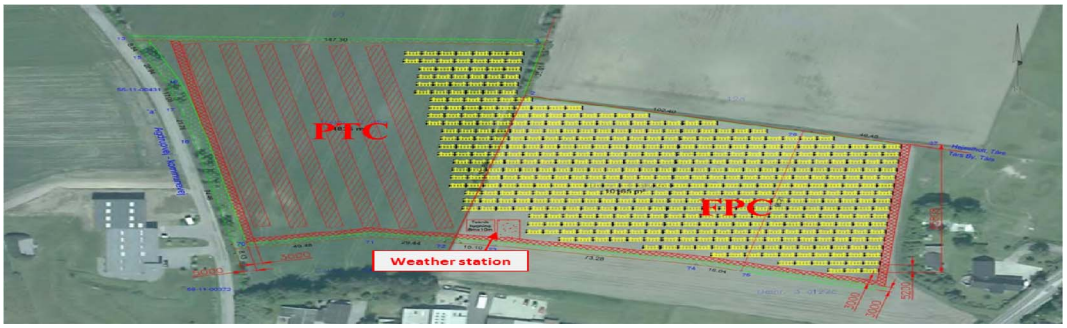

Fig. 3. Layout of the solar collector field.

Table 1
Parameters of the PTC collector in the Taars plant.

Geometrical parameters for the PTC collector	
Absorber tube outer diameter (m)	0.070
Absorber tube inner diameter (m)	0.066
Glass envelope outer diameter (m)	0.125
Glass envelope inner diameter (m)	0.119
Parabola width (m)	5.77
Numbers of modules per row	10
Mirror length in each module (m)	12
Geometric concentration ratio	26.2

Table 2
Parameters of the FPC collectors in the Taars plant.

Geometrical parameters for the FP collector		
Length, m	5.96	
Width, m	2.27	
Thickness, m	0.14	
Gross area, m^2	13.57	
Aperture area, m^2	12.60	
Solar collector volume, L	10.6	
Absorber	Material	Cu pipe /Al plate
	Absorption	0.95
	Emission	0.05
Insulation	Backside	75 mm mineral wool
	Side	30 mm mineral wool
Cover(s)	Atireflex glass(AR:3.2 mm)-with/without FEP	

Table 3
Parameters of the investigated solar collectors.

η_0	b_0	b_1	$K_{\theta d}$	c_1 [W/(m^2·K)]	c_2 [W/(m^2·K^2)]	c_3 [kJ/(m^2·K)]	
0.779	0.1	0	0.98	2.410	0.015	6.798	HEATboost 35/10
0.745	0.1	0	0.93	2.067	0.009	7.313	HEATstore 35/10
0.75	0.27	0	0.038	0.04	0	4	PTC collector

plant. The solar collector fluid of the parabolic trough collectors is water, while that of FPC is a glycol/water mixture (35%). The return water from the district heating network is heated up to 65–75 °C by the heat exchanger connected to the flat plate collector field. Then the preheated water from the flat plate collector field is heated to the required temperature by going through the parabolic trough collector field. The orientation of parabolic trough collectors was 13.4° towards west from south. The parabolic trough collectors track the sun from east to west when the collectors work during the whole day. There are six rows of parabolic trough collectors and the row distance is 12.6 m. The length of each row parabolic trough collector loop is about 125 m. The orientation of flat plate collectors is south and the collector row distance is 5.67 m. The tilt of the flat plate collectors is 50°. The parabolic trough collectors are delivered by Aalborg CSP A/S. The flat plate collectors consist of two types of the flat plate collectors, namely HTHEATboost 35/10 and HTHEATstore 35/10, manufactured by Arcon-Sunmark A/S [36]. Half of the flat plate collector field is made of HTHEATboost 35/10, while the other half is HTHEATstore 35/10. The backup heat resource consists of two natural gas boilers (9.1 MW in

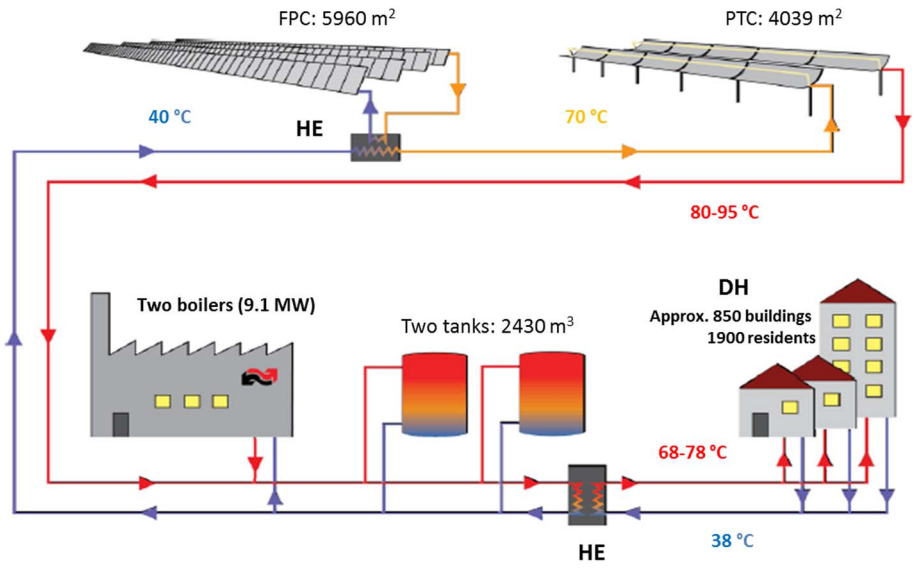

Fig. 4. Schematic illustration of the Taars solar heating plant.

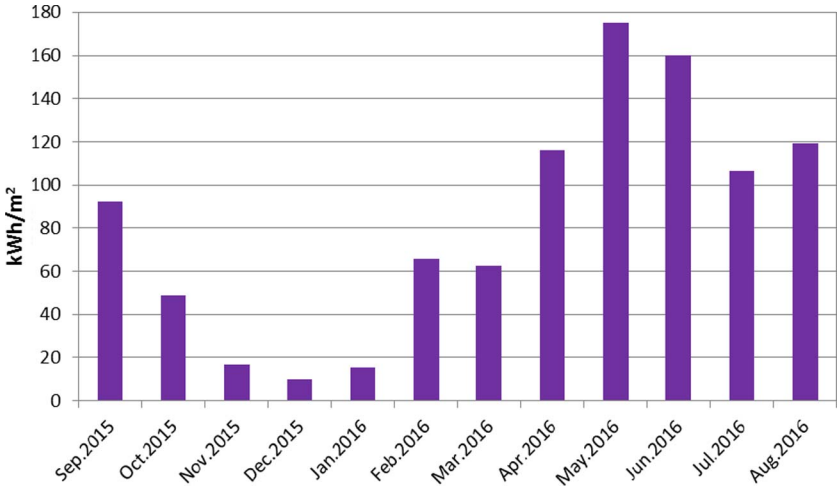

Fig. 5. DNI in the Taars solar heating plant (Sep. 2015-Aug. 2016).

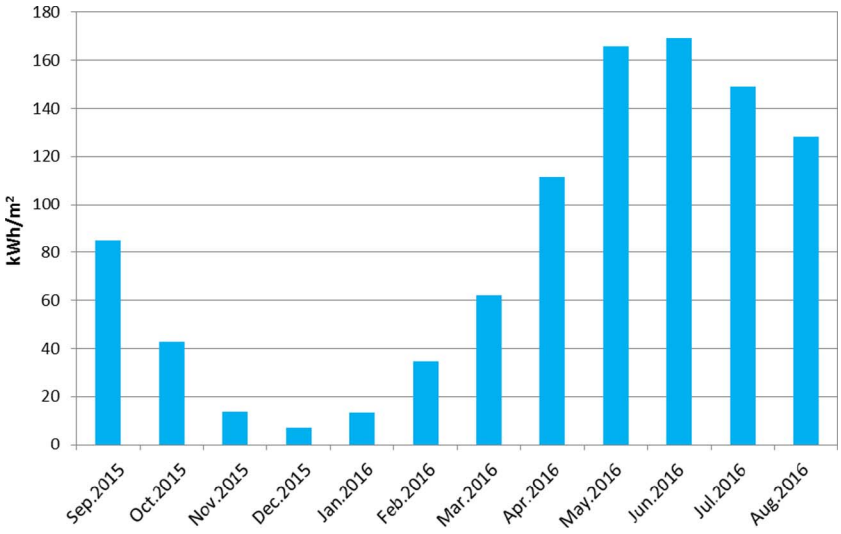

Fig. 6. Global radiation on the horizontal surface in the Taars solar heating plant (Sep. 2015-Aug. 2016).

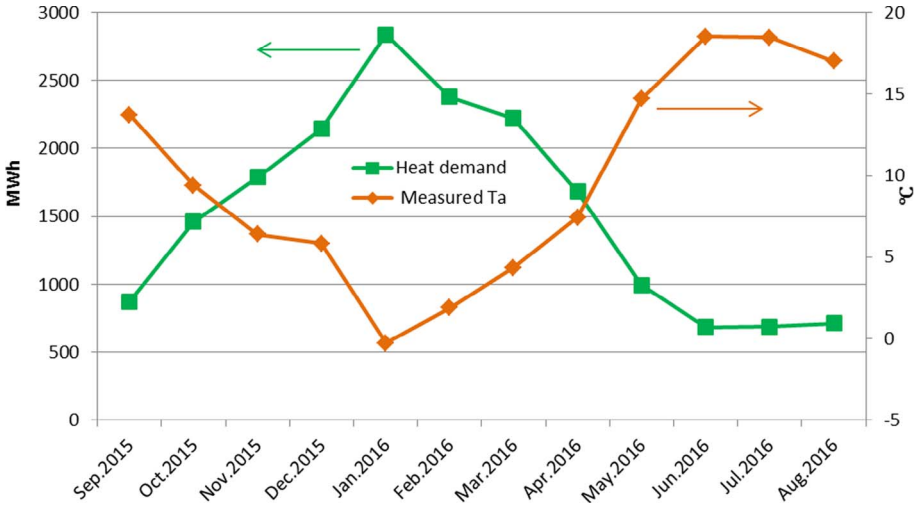

Fig. 7. Monthly heat demand and average ambient temperature in the Taars solar heating plant (Sep. 2015-Aug. 2016).

total). Two tanks with a total volume of 2430 m^3 are used as heat storage for several days in the summer.

2.2. Control strategy

The plant is oversized for the heat demand in the summer months. To avoid overheating issues in the summer, the parabolic trough collectors are sometimes put out of focus. Feed forward control is used to keep a constant outlet temperature by the flow control in the parabolic trough collector field.

Table 4
Sums of DNI, global radiation and heat demand of the Taars solar heating plant (Sep. 2015-Aug. 2016).

Items	Values
DNI, kWh/m^2	990
Global radiation on the horizontal surface, kWh/m^2	980
Heat demand, MWh	18460

3. Methods

The efficiency expressions and the incidence angle modifier of the investigated solar collectors are given by Eqs. (1) and (2). The parameters of the parabolic trough collectors based on the aperture area were determined by the Technical University of Denmark [37]. The technical parameters of flat plate collectors based on the gross area were determined by SP Technical Research Institute of Sweden [38], which are available in the reference [39]. The parameters of the investigated solar collectors can be found in Table 3.

$$\frac{Q}{A} = \eta_0 K_{\theta b}(\theta) G_b + \eta_0 K_{\theta d}(\theta) G_d - c_1(T_m - T_a) - c_2(T_m - T_a)^2 - c_3 \frac{dT_m}{dt} \quad (1)$$

$$K_{\theta b}(\theta) = 1 - b_0\left(\frac{1}{\cos\theta} - 1\right) - b_1\left(\frac{1}{\cos\theta} - 1\right)^2, \theta \leqslant 60° \quad (2)$$

when $\theta > 60°$, the IAM is linearized from the value at 60° to a value of zero at 90°.

3.1. Measurements

The system is well equipped with different accurate sensors and the monitoring data are automatically transferred to the computers. Global solar radiation on the horizontal surface and total radiation on the tilted flat plate collectors are measured with Kipp & Zonen SMP11. DNI is measured with a PMO6-CC pyrheliometer with the sun tracking platform Sunscanner SC1. The inlet and outlet temperatures of the collector fields are measured with SIEMENS TS500 temperature sensors, flow rates of both the FPC field and the PTC field are measured with Sitrans FM MAG3100P flow meters - SIEMENS. Measured thermal performance is calculated based on the measured parameters.

3.2. Trnsys model

A Trnsys model was set up to simulate the thermal performance of both the flat plate collector and the parabolic trough collector field. The TRNSYS model was based on the quasi dynamic method. TRNSYS type 1290 was used to simulate the thermal performance of the collector fields. Type 3b was used as the pump unit in the collector fields. Type 5b was the heat exchanger unit in the FPC field. Type 30 simulated the shadows between the collector rows. Type 4 was used to simulate the tanks. The TRNSYS model was validated by the measurements and was accurate enough to predict the thermal performances of both solar collector fields. Detailed information and validation of the TRNSYS model and uncertainties of measurements are given in [40, 41].

4. Meteorological data and heat demand

Figs. 5 and 6 show measured monthly DNI and global solar radiation in the Taars heating plant. Obviously, solar radiation from November 1 to January 31 was low in Denmark. Fig. 7 shows monthly average ambient temperature from Sep. 2015 to Aug. 2016 and the heat demand of the Taars district heating network. The average ambient temperature in Jan. 2016 was −0.3 °C, which was the lowest during the studied operation period. The average monthly ambient temperature in both June and July of 2016 was about 18 °C, which was the highest. Table 4 shows the sums of DNI, global radiation on the horizontal surface and heat demand from Sep. 2015 to Aug. 2016. DNI and global radiation were 990 and 980 kWh/m^2 respectively. Heat demand of the Taars district heating network from Sep. 2015 to Aug. 2016 was 18,460 MWh.

5. Annual thermal performance

All the measured and modelled thermal performances given per square meter solar collector field are based on the aperture area of the solar collectors. The time step was 1 min in the calculations. The inlet temperature and volume flow rate of both the FPC and the PTC collector field in simulation were taken from the measurements.

5.1. Thermal performance of FPC collectors

Fig. 8 shows monthly measured and modelled thermal performances of the flat plate collector field from Sep. 2015 to Aug. 2016. The thermal performance of the flat plate collector field was low during the winter because of the low solar radiation. The max monthly thermal performance of the flat plate collector field was higher than 70 kWh/m^2 in May 2016. Both measured and modelled yearly total thermal performances of the flat plate collector field were 2670 MWh for the period Sep. 2015 -Aug. 2016.

5.2. Thermal performance of PTC collectors

As shown in Fig. 9, the parabolic trough collector field did not produce much heat during the winter because of low DNI. But in the spring and summer, the parabolic trough collector field performed very well. The parabolic trough collector field should have worked best in

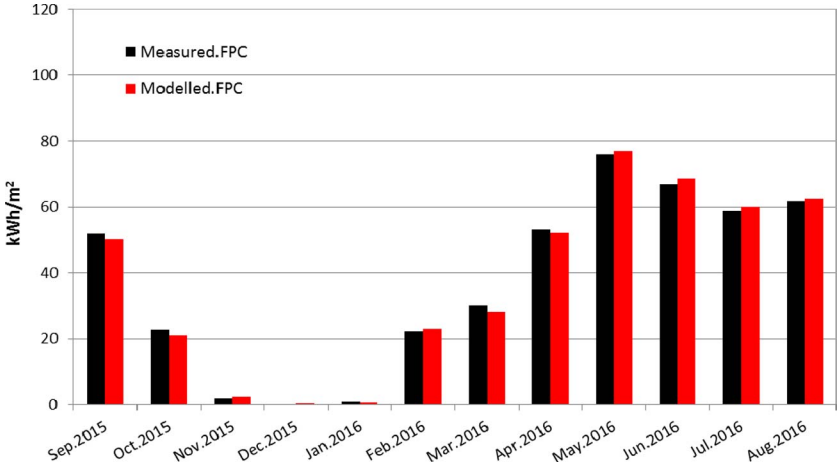

Fig. 8. Monthly thermal performance of FPC field (Sep. 2015-Aug. 2016).

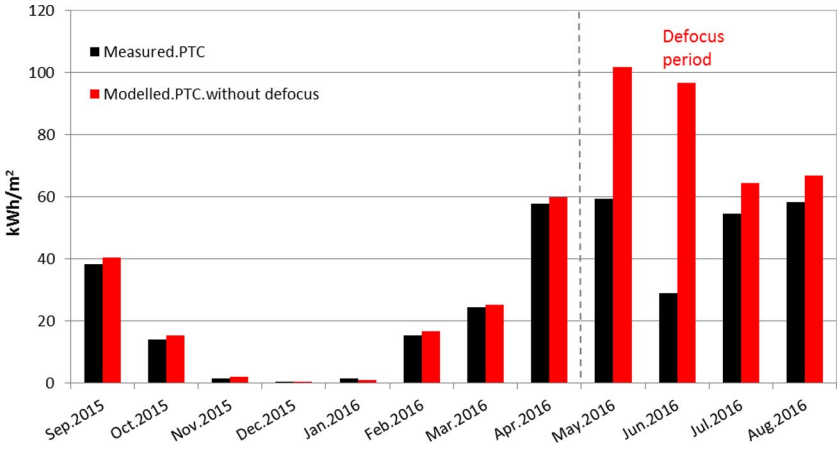

Fig. 9. Monthly thermal performance of PTC field.

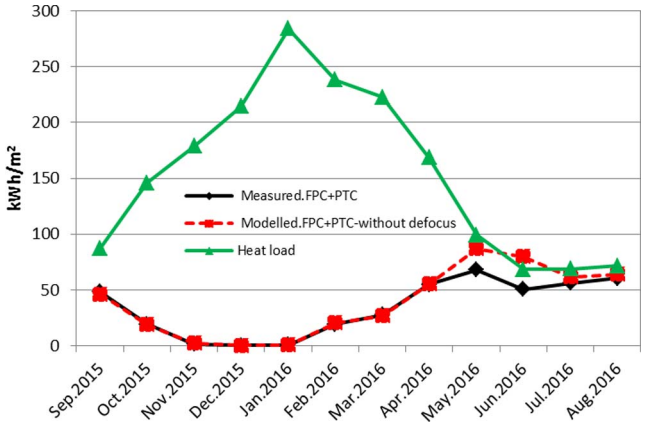

Fig. 10. Heat demand and thermal performance of Taars solar heating plant per m^2 solar collector aperture area, Sep. 2015-Aug. 2016.

Table 5
Annual thermal performance of the Taars plant (Sep. 2015-Aug. 2016).

Items	Value	Unit
Heat demand,	18460	MWh
Measured solar heat. FPC field	448	kWh/m^2
	2672	MWh
Modelled solar heat. FPC field	448	kWh/m^2
	2671	MWh
Measured solar heat. PTC field	354	kWh/m^2
	1431	MWh
Modelled solar heat. PTC field with defocus	359	kWh/m^2
	1450	MWh
Modelled solar heat. PTC field without defocus	490	kWh/m^2
	1981	MWh
Measured solar heat. FPC + PTC	410	kWh/m^2
Modelled solar heat. FPC + PTC with defocus	412	kWh/m^2
Modelled solar heat. FPC + PTC without defocus	465	kWh/m^2
Measured solar fraction	22.2%	–
Modelled solar fraction (PTC with defocus)	22.3%	–
Modelled solar fraction (PTC without defocus)	25.2%	–

the summer, when the solar radiation was high. However, the parabolic trough collector field was defocused sometimes on the sunniest days of summer (such as in May-August) because the flat plate collector field was oversized and the heat demand in the summer was low. The simulated thermal performance in Fig. 9 illustrates that the potential monthly thermal performance of the parabolic trough collector field is higher than 90 kWh/m^2/month if the parabolic trough collector field could continue to operate without defocusing. The measured thermal performance of the parabolic trough collector field for the period September 2015-August 2016 was 354 kWh/m^2, while the modelled value with defocus was 359 kWh/m^2. The simulated thermal performance of the parabolic trough collector field without defocus was 490 kWh/m^2 for the period Sep. 2015-Aug. 2016. That is: a reduction of 136 kWh/m^2 was calculated due to defocusing of the parabolic trough collector field.

5.3. Solar fraction

The Taars district heating network consists of approximate 850

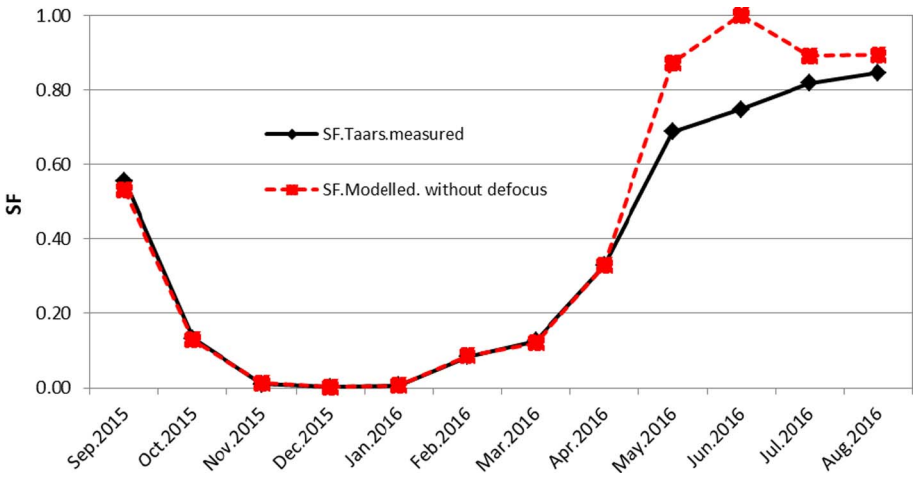

Fig. 11. Solar fraction (SF) of Taars solar heating plant (Sep. 2015-Aug. 2016).

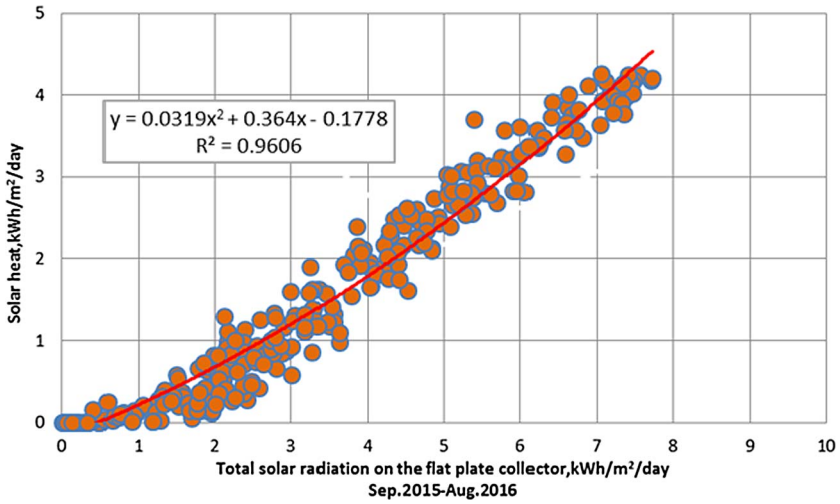

Fig. 12. Measured daily solar heat as a function of total radiation on the flat plate collectors.

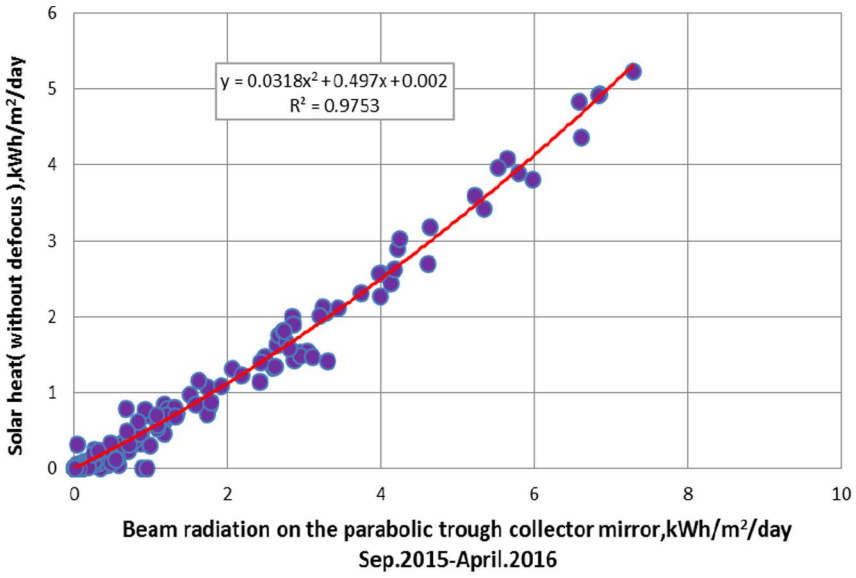

Fig. 13. Measured daily solar heat as a function of daily beam radiation on the parabolic trough collectors.

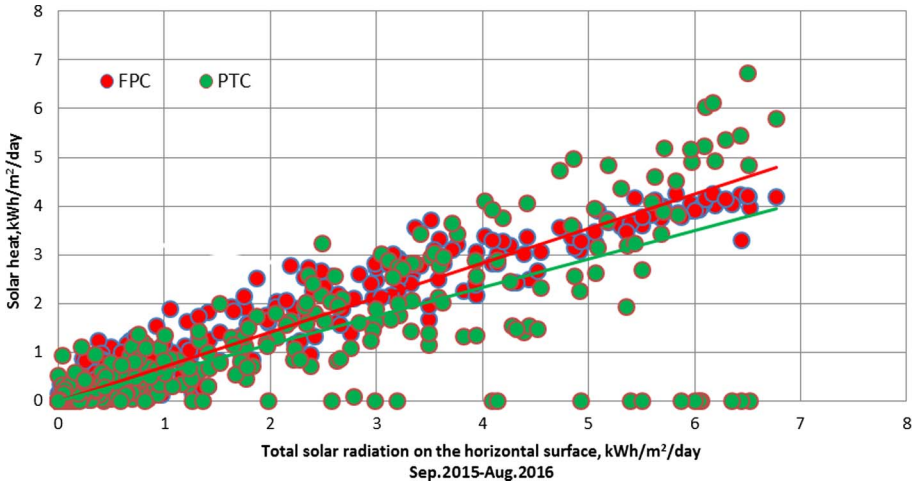

Fig. 14. Measured daily solar heat as a function of daily global radiation for both collector fields.

buildings with about 1900 consumers. Measured heat load and total thermal performance of the solar collector fields per collector area from Aug. 2015 to Sep. 2016 can be found in Fig. 10. The solar fraction, defined as the ratio between the solar heat and the heat demand, was very high in the summer when the heat load was low and the weather was sunny, see Fig. 11. As the solar radiation in the winter was low, both the flat plate collector and the parabolic trough collector field produced low quantities of solar heat and the solar fraction in the winter was close to 0, which is normal for the Nordic area. Table 5 shows a summary of annual thermal performance of the Taars plant.

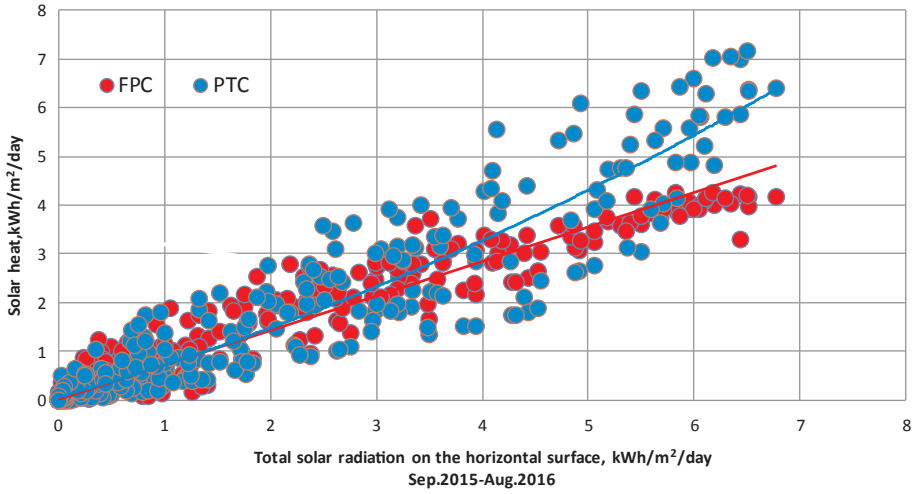

Fig. 15. Modelled daily solar heat as a function of daily global radiation for both collector fields.

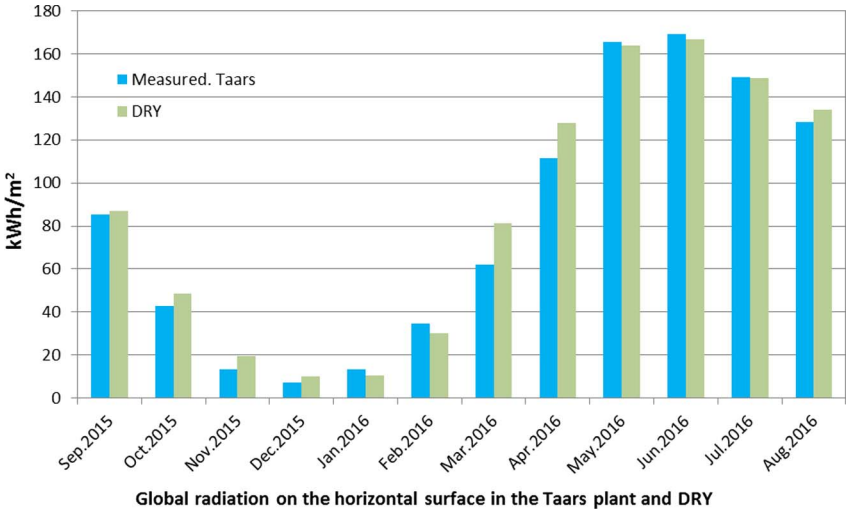

Fig. 16. Monthly global radiation in the Taars plant and in the DRY.

Table 6
Weather parameters measured in Taars (Sep. 2015-Aug. 2016) and in the DRY.

DNI, kWh/m^2	990	Sep. 2015-Aug. 2016
	1150	DRY
Total radiation on tilted FPC plane, kWh/m^2	1170	Sep. 2015-Aug. 2016
	1295	DRY
Global horizontal radiation, kWh/m^2	980	Sep. 2015-Aug. 2016
	1030	DRY
Heat demand, MWh	18460	Sep. 2015-Aug. 2016
	21660	DRY

The measured total energy output of the solar heating plant was 4100 MWh and total heat load was 18,460 MWh during Sep. 2015 to Aug. 2016. The solar fraction of the solar heating plant was 22.2% from Sep. 2015 to Aug. 2016. As shown in Figs. 10 and 11, if the parabolic trough collectors were not defocused, the parabolic trough collectors could have a better thermal performance in the summer. Furthermore, only in June the simulated thermal performance is higher than the heat demand if the parabolic trough collector field was not defocused. By applying large heat storage tanks, the parabolic trough collector field could work normally without defocus in the summer, even in June. In this way solar fraction would have been close to 100% in the months from May to August. The yearly thermal performance of the combined solar collector field without defocusing of parabolic trough collectors in the summer can reach 4650 MWh and the solar fraction would increase from 22.2% to 25.2%. 550 MWh solar heat was lost because of defocusing of parabolic trough collectors in the sunny days in the summer.

5.4. Utilized efficiency

Fig. 12 shows the measured daily solar heat of the flat plate collector field as a function of the total radiation on the tilted flat plate collectors. According to the fitting curve, the average daily efficiency of the flat plate collector field is about 0.48. Max daily solar heat production of flat plate collector field is below 5 kWh/m^2.

The parabolic trough collectors were not put into defocus from Sep. 2015 to Apr. 2016. Fig. 13 shows the measured daily solar heat without defocusing as a function of the beam radiation on the parabolic trough collectors from Sep. 2015 to Apr. 2016. The fitting curve illustrates that the average daily efficiency of the parabolic trough collector field based on the beam radiation on the parabolic trough collectors is about 0.66. If the parabolic trough collectors work without defocusing in the summer, the daily efficiency in the summer would increase to about 0.70 and the parabolic trough collector field would produce more than 5 kWh/m^2 per day in the sunny days.

Both beam radiation and diffuse radiation influence thermal performance of the flat plate collector field, while the thermal performance of the parabolic trough collector field is mainly influenced by the beam radiation. To compare performances of both collector fields in a fair way, global radiation was chosen as a benchmark. Fig. 14. shows

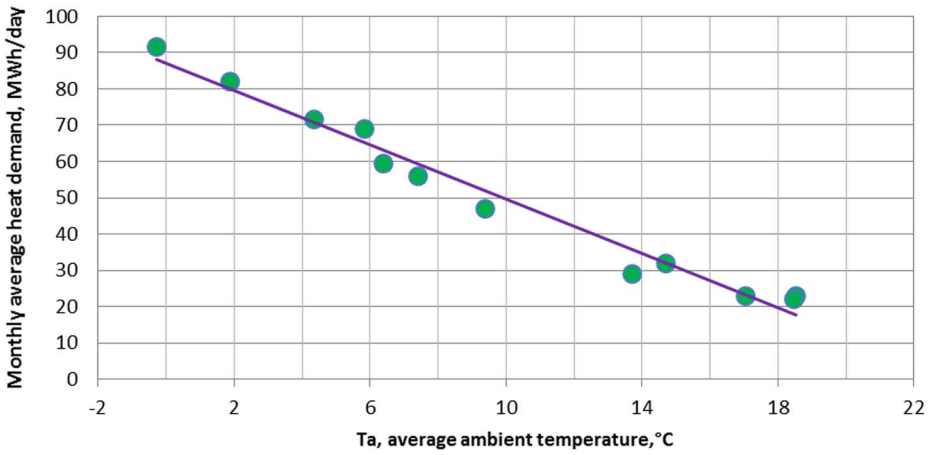

Fig. 17. Measured monthly heat demand (average value per day) as a function of average ambient temperature of Taars solar heating plant (Aug. 2015-Aug. 2016).

Table 7
Calculated annual thermal performance of Taars solar heating plant in the DRY for Northern Jutland.

Item	Value
Solar heat.FPC field	510 kWh/m^2 3040 MWh
Solar heat.PTC field	530 kWh/m^2 2140 MWh
Heat demand Solar fraction	21590 MWh 24%

measured daily solar heat for both collector fields as a function of the global radiation on the horizontal surface. The thermal performance of the parabolic trough collector field without defocus was modelled to investigate the maximum potential of parabolic trough collector field, as shown in Fig. 15. It is seen that the thermal performance of the parabolic trough collector field was zero mainly because of defocus while the weather was sunny in Fig. 14. In Fig. 15, it is found that when the daily global radiation was lower than about 2 kWh/m^2, the parabolic trough collector field did not perform better than the flat plate collector field. Furthermore, the parabolic trough collector field produced more heat than the flat plate collector field, when daily global radiation was higher than about 2 kWh/m^2.

6. Discussions

The Taars solar heating plant is the first large hybrid solar heating plant, which integrates both flat plate collectors and parabolic trough collectors to provide heat for a district heating network. The oversize of the flat plate collector field and low heat demand in the summer were the main reasons why the parabolic trough collectors were defocused in summer periods. Potential of the Taars plant in the DRY (Design Reference Year [42]) is shown in this section.

Fig. 16 shows monthly measured global radiation on horizontal in the Taars plant and global radiation of the DRY of Northern Jutland [42]. Table 6 shows the summary of weather conditions in Taars (Sep. 2015-Aug. 2016) and in the DRY. The measured global radiation in the Taars solar heating plant from Sep. 2015 to Aug. 2016 is 980 kWh/m^2, while that of DRY is 1030 kWh/m^2. It is found that there was less sun shine from Sep. 2015 to Aug. 2016 compared to DRY.

Fig. 17 shows the relation between monthly heat demand (average value per day) and average ambient temperature from Sep. 2015 to Aug. 2016. The heat demand in the DRY in Table 7 is calculated by the fitting curve in Fig. 17 and the average ambient temperatures of the DRY. The heat demand of the Taars solar heating plant in the DRY is a bit higher than measured values from Sep. 2015-Aug. 2016.

Table 7 also shows calculated annual thermal performance of the Taars solar heating plant in the DRY, calculated by DTU Excel tool (Dragsted and Furbo, 2012) [42]. Mean solar collector fluid temperatures of the flat plate collector field and the parabolic trough collector field were assumed to be 55 °C and 80 °C respectively based on the measurements. The parabolic trough collector field is assumed to work without defocus. The potential thermal performance of the Taars solar heating plant in the DRY is 5180 MWh, while the heat demand in the DRY is 21,590 MWh. Furthermore, the solar fraction is 24%. Table 7 also illustrates that the thermal performance of flat plate collectors can be higher than 500 kWh/m^2 under Danish climate conditions when the flat plate collectors work at low operation temperatures like 55 °C in such a combined solar heating plant.

The investigations have shown that it is very important to size the collector areas of both the flat plate collectors and parabolic trough collectors in such a way that oversizing is avoided, so that the parabolic trough collector field is not put out of focus in the summer. An increase of the heat load of the district heating network in the future can increase thermal performance of the plant. Furthermore, a large heat storage could also be helpful to harvest the advantages of parabolic trough collectors in the summer. The advantages of the hybrid solar heating plants are that the flat plate collector field produces about 60 kWh/m^2 one year more than the normal solar heating plants with only flat plate collectors, and the defocus of the parabolic trough collectors increases the flexibility of the solar heating plants in the whole energy supply system. This study not only demonstrates the feasibility and potential of the hybrid solar heating plants at the high latitude with low solar radiation resource, but also introduces a novel design concept of higher efficient solar heating plants for the high solar radiation area

7. Conclusions and future work

Both measured and simulated annual thermal performances of the Taars solar heating plant were analysed for the whole year from September 2015 to August 2016. The thermal performance of the Taars solar heating plant in the DRY for the northern part of Jutland was also investigated. These findings can be used in the design of new large-scale solar district heating plants in the near future. The conclusions are as follows:

The solar fraction of the Taars solar heating plant was 22.2% during the period from Sep. 2015 to Aug. 2016. If the parabolic trough collector field had not been defocused, the total thermal performance would have increased from 4100 MWh to 4650 MWh, that is from 410 kWh/m^2 to 465 kWh/m^2 and the solar fraction would have reached 25.2%.

Potential annual thermal performance of the Taars solar heating plant in the DRY for northern Jutland could reach 5180 MWh (518 kWh/m^2) and a solar fraction of 24% if defocusing of the parabolic

trough collectors is avoided.

Further studies on the optimization of the thermal performance and control strategy of the hybrid solar district heating plant are required to formulate comprehensive design rules for such hybrid solar heating plants.

Acknowledgements

Special thanks are expressed to Aalborg CSP A/S (Andreas Zourellis) for the information provided. The first author also appreciates the financial support of China Scholarship Council for the PhD study (No.201506120074). This work is also a part of an EUDP (Energy Technology Development and Demonstration) project financed by the Danish Energy Agency.

References

[1] Liu Z, Xu W, Qian C, Chen X, Jin G. Investigation on the feasibility and performance of ground source heat pump (GSHP) in three cities in cold climate zone, China. Renew Energy 2015;84:89–96.
[2] Tian Z, Zhang S, Li H, Jiang Y, Dong J, Zhang B, Yi R. Investigations of nearly (net) zero energy residential buildings in Beijing. Procedia Eng 2015;121:1051–7.
[3] Balaras CA, Gaglia AG, Georgopoulou E, Mirasgedis S, Sarafidis Y, Lalas DP. European residential buildings and empirical assessment of the Hellenic building stock, energy consumption, emissions and potential energy savings. Build Environ 2007;42(3):1298–314.
[4] Deng J, Tian Z, Fan J, Yang M, Furbo S, Wang Z. Simulation and optimization study on a solar space heating system combined with a low temperature ASHP for single family rural residential houses in Beijing. Energy Build 2016;126:2–13.
[5] Buoro D, Pinamonti P, Reini M. Optimization of a Distributed Cogeneration System with solar district heating. Appl Energy Jul. 2014;124:298–308.
[6] Tulus V, Boer D, Cabeza LF, Jimenez L, Guillen-Gosalbez G. Enhanced thermal energy supply via central solar heating plants with seasonal storage: a multi-objective optimization approach. Appl Energy 2016;181:549–61.
[7] Persson U, Werner S. Heat distribution and the future competitiveness of district heating. Appl Energy 2011;88(3):568–76.
[8] Furbo S, Fan J, Perers B, Kong W, Trier D, From N. Testing, development and demonstration of large scale solar district heating systems. Energy Procedia 2015;70:568–73.
[9] Fish M, Guigas M, Dalenback J. A review of large-scale solar heating systems in Europe. Sol Energy 1998;63(6):355–66.
[10] Reiter P, Poier H, Holter C. BIG solar graz: solar district heating in graz – 500,000 m2 for 20% solar fraction. Energy Procedia 2016;91:578–84.
[11] Werner Weiss, Monika Spörk-Dür, Franz Mauthner, Solar Heat Worldwide-Global Market Development and Trends in 2016-Detailed Market Figures 2015 (2017 version); 2017. < http://www.iea-shc.org/solar-heat-worldwide > .
[12] Danish District Heating Association. Solvarmedata; 2017, < www.solvarmedata.eu > .
[13] Bava F, Furbo S. A numerical model for pressure drop and flow distribution in a solar collector with horizontal U-connected pipes. Sol Energy 2016;134:264–72.
[14] PlanEnergi. planenergi; 2017. < http://planenergi.eu/activities/fjernvarme/solar-heating/ > . Available: 2017.
[15] IEA. IEA-SHC Task 49; 2016. < http://task49.iea-shc.org/publications > . Available: 2017.
[16] Frank E, Marty H, Hangartner L, Minder S. Evaluation of measurements on parabolic trough collector fields for process heat integration in Swiss dairies. Energy Procedia 2014;57:2743–51.
[17] Silva R, Perez M, Fernandez-Garcia A. Modeling and co-simulation of a parabolic trough solar plant for industrial process heat. Appl Energy 2013;106:287–300.
[18] Silva R, Berenguel M, Perez M, Fernandez-Garcia A. Thermo-economic design optimization of parabolic trough solar plants for industrial process heat applications with memetic algorithms. Appl Energy 2014;113:603–14.
[19] Ben Hassine I, Sehgelmeble MC, Soll R, Pietruschka D. Control optimization through simulations of large scale solar plants for industrial heat applications. Energy Procedia 2015;70(0):595–604.
[20] Larcher M, Rommel M, Bohren A, Frank E, Minder S. Characterization of a parabolic trough collector for process heat applications. Energy Procedia 2014;57:2804–11.
[21] Kizilkan O, Kabul A, Dincer I. Development and performance assessment of a parabolic trough solar collector-based integrated system for an ice-cream factory. Energy 2016;100:167–76.
[22] Zou B, Dong J, Yao Y, Jiang Y. An experimental investigation on a small-sized parabolic trough solar collector for water heating in cold areas. Appl Energy Feb. 2016;163:396–407.
[23] Krueger D, Heller A, Hennecke K, Duer K, Energietechnik S, Zentrum D, et al. Parabolic trough collectors for district heating systems at high latitudes. In: Proceedings of Eurosun; 2000.
[24] Mokheimer EMA, Dabwan YN, Habib MA, Said SAM, Al-Sulaiman FA. Development and assessment of integrating parabolic trough collectors with steam generation side of gas turbine cogeneration systems in Saudi Arabia. Appl Energy 2015;141:131–42.
[25] Eck M, Hirsch T. Dynamics and control of parabolic trough collector loops with direct steam generation. Sol Energy 2007;81(2):268–79.
[26] Boukelia TE, Arslan O, Mecibah MS. ANN-based optimization of a parabolic trough solar thermal power plant. Appl Therm Eng 2016;107:1210–8.
[27] González-Gómez PA, Petrakopoulou F, Briongos JV, Santana D. Cost-based design optimization of the heat exchangers in a parabolic trough power plant. Energy 2017;123:314–25.
[28] Desai NB, Bandyopadhyay S. Optimization of concentrating solar thermal power plant based on parabolic trough collector. J Clean Prod 2015;89:262–71.
[29] Boukelia TE, Arslan O, Mecibah MS. Potential assessment of a parabolic trough solar thermal power plant considering hourly analysis: ANN-based approach. Renew Energy 2017;105:324–33.
[30] Nation DD, Heggs PJ, Dixon-Hardy DW. Modelling and simulation of a novel Electrical Energy Storage (EES) receiver for solar Parabolic Trough Collector (PTC) power plants. Appl Energy 2017;195:950–73.
[31] Bortolato M, Dugaria S, Del Col D. Experimental study of a parabolic trough solar collector with flat bar-and-plate absorber during direct steam generation. Energy 2016;116:1039–50.
[32] Boukelia TE, Mecibah MS, Kumar BN, Reddy KS. Optimization, selection and feasibility study of solar parabolic trough power plants for Algerian conditions. Energy Convers Manag 2015;101:450–9.
[33] Kumar D, Kumar S. Year-round performance assessment of a solar parabolic trough collector under climatic condition of Bhiwani, India: a case study. Energy Convers Manag 2015;106:224–34.
[34] A. CSP, Aalborg CSP; 2016. < http://www.aalborgcsp.com/ > .
[35] Perers B, Furbo S, Tian Z, Egelwisse J, Bava F, Fan J. Tårs 10000 m^2 CSP + Flat plate solar collector plant - cost-performance optimization of the design. Energy Procedia 2016;91:312–6.
[36] Arcon-Sunmark. Arcon-Sunmark. < http://arcon-sunmark.com/products > . Available: Mar. 2017.
[37] Perers B, Furbo S, Dragsted J. Thermal performance of concen- trating tracking solar collectors, DTU.Report, vol. 292, no. August, 2013.
[38] SP. Technical Research Institute of Sweden; 2016. < https://www.sp.se/en/Sidor/default.aspx > .
[39] SolarKeyMark. Solar Keymark Certification; 2017. < http://www.solarkeymark.dk/ > .
[40] Tian Z. Analysis and validation of a quasi-dynamic model for a solar collector field with flat plate collectors and parabolic trough collectors in series for district heating, Manuscript; 2017.
[41] TRNSYS. TRNSYS 17-a TRaNsient SYstem Simulation program -Volume 4 Mathematical Reference. < http://web.mit.edu/parmstr/Public/TRNSYS/04-MathematicalReference.pdf > . Available: June 2017.
[42] Dragsted Janne, Furbo Simon. Solar radiation and thermal performance of solar collectors for Denmark. DTU Rep. 2012;275.

This page is intentionally left blank.

Paper IV

Zhiyong Tian, Bengt Perers, Simon Furbo and Jianhua Fan.

Thermo-economic optimization of a hybrid solar district heating plant with flat plate collectors and parabolic trough collectors in series

Energy Conversion and Management, vol. 165, pp. 92–101, 2018.

This page is intentionally left blank.

Energy Conversion and Management 165 (2018) 92–101

Contents lists available at ScienceDirect

Energy Conversion and Management

journal homepage: www.elsevier.com/locate/enconman

Thermo-economic optimization of a hybrid solar district heating plant with flat plate collectors and parabolic trough collectors in series

Zhiyong Tian, Bengt Perers, Simon Furbo, Jianhua Fan*

Department of Civil Engineering, Technical University of Denmark, Brovej Building 118, Lyngby 2800, Denmark

ARTICLE INFO

Keywords:
Hybrid solar district heating plants
LCOH optimization
Parabolic trough collector
Flat plate collector
TRNSYS-GenOpt

ABSTRACT

Large-scale solar heating plants for district heating networks have gained great success in Europe, particularly in Denmark. A hybrid solar district heating plant with 5960 m^2 flat plate collectors and 4039 m^2 parabolic trough collectors in series was built in Taars, Denmark in 2015. The solar heating plant was used as a reference case in this study. A validated TRNSYS-GenOpt model was set up to optimize the key design parameters of the plant, including areas of both collector types, storage size, orientation of the parabolic trough collectors and so on. This study introduces a generic method to optimize the hybrid solar district heating systems based on levelized cost of heat. It is found that the lowest net levelized cost of heat of hybrid solar heating plants could reach about 0.36 DKK/kWh. The system levelized cost of heat can be reduced by 5–9% by use of solar collectors in the district heating network in this study. The results also show that parabolic trough collectors are economically feasible for district heating networks in Denmark. The generic and multivariable levelized cost of heat method can guide engineers and designers on the design, construction and control of large-scale solar heating plants.

1. Introduction

Solar energy is widely used in the building sector to supply space heating and cooling. Rad et al. [1] reviewed solar community heating and cooling systems with borehole thermal energy storage and gave suggestions about the development of borehole storage. Hazami et al. [2] simulated two domestic hot water systems with flat plate collectors and evacuated tube collectors separately and compared two systems by means of TRNSYS. Deng et al. [3] investigated a solar space heating system coupled with air source heat pump in TRNSYS. Kemal et al. [4] revealed the influence of the size of the storage tank on the performance and usability of solar water heating systems. Kaçan et al. [5] found that the actual optimum values for independent parameters have a vital importance for design engineer with respect to select the proper system component for solar heating system. Li et al. [6] discussed the operational strategy of a combined solar and ground source heat pump system for an office building in TRNSYS. Bellos et al. [7] did energetic and financial evaluation of solar assisted heat pump space heating systems with TRNSYS. Pardo García et al. [8] studied district heating configurations with photovoltaic thermal hybrid solar collectors for a central European multi-family house. Ramos et al. [9] also used TRNSYS to study a combined heating, cooling and power provision in the urban environment. Bava et al. [10] developed a numerical model to investigate the flow distribution in different operation conditions for solar district heating plants in Denmark. Bava et al. [11] also investigated pressure drop and flow distribution in a solar collector with horizontal U-connected pipes with this numerical model. Bava et al. [12] developed a detailed TRNSYS-Matlab model to simulate the thermal performance of large solar collector fields for district heating applications based on developed numerical model. Wang et al. [13] carried out energy, exergy and environmental analysis of a hybrid combined cooling, heating and power system utilizing biomass and solar energy. The vision of the Solar Heating and Cooling Programme of the International Energy Agency is “By 2050 a worldwide capacity of 5 kW_{th} per capita of solar thermal energy systems installed and significant reductions in energy consumption achieved by using passive solar and daylighting: thus solar thermal energy meeting 50% of low temperature heating and cooling demand (heat up to 250 °C)” [14]. Large-scale solar heating plants for district heating networks have developed fast in the last decades, and are one of the most successful applications of solar energy for the building sector.

1.1. Solar district heating plants

In the northern European countries, district heating networks have supplied both space heating and domestic hot water to many residents for many years. In the early 1980s, several large solar heating plants were installed in Sweden, which is the first country to apply large solar

* Corresponding author.
E-mail addresses: tianzy0913@163.com, zhiytia@byg.dtu.dk (Z. Tian), jif@byg.dtu.dk (J. Fan).

https://doi.org/10.1016/j.enconman.2018.03.034
Received 25 October 2017; Received in revised form 7 March 2018; Accepted 13 March 2018
Available online 21 March 2018
0196-8904/

Nomenclature

Abbreviations

DH	district heating
DKK	Danish Krone
DRY	design reference year
DNI	monthly direct normal irradiance, kWh/m^2
E-W	east-west
FEP	fluorinated ethylene propylene
FPC	flat plate collector
HX	heat exchanger
IEA	International Energy Agency
LCOH	levelized cost of heat, DKK/kWh
LCOE	levelized cost of energy, DKK/kWh
nLCOH	net levelized cost of heat, DKK/kWh
N-S	north-south
PTC	parabolic trough collector
SHC	solar heating and cooling
sLCOH	system levelized cost of heat, DKK/kWh
TES	thermal energy storage

Latin symbols

A_{ptc}	aperture area of the parabolic trough collector field, m^2
A_{fpc}	aperture area of the flat plate collector field, m^2
C_{ptc}	cost of the parabolic trough collector field, DKK/m^2
C_{fpc}	cost of the flat plate collector field, DKK/m^2
c_1	heat loss coefficient at (Tm − Ta) = 0, W/(m^2·K)
c_2	temperature dependence of the heat loss coefficient, W/(m^2·K^2)
c_3	effective thermal capacity, J/(m^2·K)
C_t	operation and maintenance costs (year t), DKK
$C_{storage}$	specific costs of the tanks incl. installation (excl. VAT and subsidies), DKK/m^3
DEP_t	asset depreciation (year t), DKK
E_t	energy generated (year t), kWh
G	monthly global radiation, kWh/m^2
I_s	specific solar thermal system costs incl. installation (excl. VAT and subsidies), DKK/m^2
I_b	specific boiler system costs incl. installation (excl. VAT and subsidies), DKK
NE	heat from the natural gas boiler system, kWh
P_s	operation & maintenance expenditures of the solar plant in the year t, DKK
P_b	operation & maintenance expenditures of the natural gas boiler system in the year t, DKK
Q_{ptc}	yearly energy output of the parabolic trough collector field, kWh/m^2
Q_{fpc}	yearly energy output of the flat plate collector field, kWh/m^2
Q_{loss}	yearly heat loss in solar loop pipe and thermal energy storage, kWh
Q_0	yearly energy output of the whole collector field, kWh/m^2
r	discount rate, %
RV	residual value, DKK
SE	specific useful energy delivered by the solar thermal system in the year t (thermal losses in pipe loop and thermal storage considered), kWh
S_0	subsidies and incentives, DKK
T_a	ambient temperature, ˚C
I_0	initial investment, DKK
TR	corporate tax rate,%
T	period of use (solar thermal system life time in years), a
t	year within the period of use (1, 2, … T)

Greek symbol

η_0	optical efficiency, –

Subscript

th	thermal

collector arrays into district heating networks [15]. Recently, the number of large solar district heating plants has increased very fast in Denmark, Germany and Austria [16]. Fisch et al. [17] reviewed all the large-scale solar heating plants in Europe in 1998. IEA-SHC Task 7, 45 and 55 have focused on the application of large solar heating plants in district heating networks [14].

De Guadalfajara et al. [18] evaluated the potential of large solar heating systems with seasonal storage for 10 typical climate conditions in Spain. The system included a 2854 m^2 solar collector field. It was found that the estimated cost of the heat produced in large solar heating systems with seasonal storage with a solar fraction of 50% can be competitive with the heat cost of traditional domestic heat boilers in Spain. Bauer et al. [19] reviewed central solar heating plants with seasonal heat storage in Germany. Experiences from construction and operation of the research and pilot plants has led to technical improvement, higher efficiencies and cost reduction. Olsthoorn et al. [20] reviewed optimization methods on integration of renewable energy into district heating. The optimization method consists of a multi-objective method, sensitivity analysis, thermodynamic-economic analysis, and genetic algorithm. Tulus et al. [21] did multi-objective optimizations on central solar heating plants with seasonal storage in Spain. The results showed that central solar heating plants with seasonal storage led to significant environmental and economic improvements compared to the use of conventional natural gas heating systems. Life cycle assessment for economy and environment was carried out to optimize central solar heating plants. Guerreiro et al. [22] carried out the investigations on efficiency improvement and potential levelized cost of energy reduction with a linear Fresnel concentrator plant with storage. LCOEs showed that there was an enormous potential for the investigated plant. Sartor et al. [23] did simulations and optimizations of a CHP biomass plant and district heating network. The contribution presented a synthetic way to achieve such a task using only simple models on thermodynamic, combustion process, heat transfer and finance. The solar district heating system combined with borehole thermal energy storage (BTES) in Drake Landing Solar Community in Canada has managed to provide 96% of the community's annual space heating demand with solar heat for the period 2012–2016 [24].

Large solar district heating plants have gained great success in Denmark recently [25]. More than 1.3 million m^2 collectors are in operation in solar heating plants in Denmark by the end of 2016 [26]. Flat plate collectors have been used widely in the large-scale solar district heating plants in Denmark. Flat plate collectors have a bit lower efficiency at high temperature levels compared to evacuated tube collectors [27], Fresnel collectors and parabolic trough collectors [28]. Parabolic trough collectors are the more cost-effective at high temperature ranges such as 80–200 ˚C among these collectors [28]. Parabolic trough collectors are mainly used for solar power plants with oil or molten salt as heat transfer fluid. Parabolic trough collector with water as heat transfer fluid for direct steam generation also is an attractive option in electricity generation or industrial process [29]. Leiva-Illanes et al. [30] analyzed a solar poly-generation plant with parabolic trough collectors for electricity, water, cooling and heating in

high direct normal irradiation conditions. More and more small-scale parabolic trough collectors are optimized to supply heat to industrial process [31] and hot water production. A preliminary case study of parabolic trough collectors for district heating networks at high latitudes with low solar radiation resources was first carried out in 2000 [32]. The economic comparison indicated that parabolic trough collector systems could be competitive with flat plate collectors. But few practical projects with parabolic trough collectors for district heating are found during the last decades. The Danish company Aalborg CSP A/S [33] and Technical University of Denmark (DTU) [34] started in 2013 to investigate the feasibility of parabolic trough collectors for district heating networks in large solar heating plants supported by the Danish Energy Agency through the Energy Technology Development and Demonstration Program (EUDP). A hybrid solar heating field with both flat plate collectors and parabolic trough collectors in series has been constructed and connected to the existing district heating network in Taars [35]. It was found that the flat plate collector field was oversized. To avoid too high temperature in the system, the parabolic trough collectors therefore were often defocused in the summer [36]. This reduces the cost efficiency of the plant dramatically. All the potential benefits of the hybrid plant can only be experienced if the design, size and operation of the whole integrated system is consistently optimized [37]. The optimization of such hybrid solar district heating plants with different solar collector technologies is a major issue for large solar heating plants.

1.2. Levelized cost of heat

Designing solar heating plants is a multivariable optimization task because many design parameters should be varied and optimized on a project-specific basis, especially the area of the collectors and storage size. Cost of application of solar energy systems in district heating networks has been discussed for a long time. The levelized cost of energy (LCOE) has become the most popular and common criteria to identify the most cost-effective energy production technologies on a consistent basis [38]. The LCOE not only considers the cost of the energy systems, but also depends on the energy production of the investigated system simultaneously. Levelized cost of heat (LCOH), derived from LCOE, is used to evaluate the solar heat from the solar district heating plants in this study. The LCOH concept can be used as a tool to help to make decisions on systems planning and design based on the optimization routine [39].

1.3. Scope

Based on a comprehensive literature survey and data collected from detailed country reports from IEA-SHC over the past decades, the previous literatures were mainly focused on small solar heating systems [16,40], including domestic hot water systems for single-family homes and multi-family homes, small combined hot water and space heating systems. Only a limited number of publications on both energy and economic optimizations of large-scale solar district heating plants including natural gas boilers simultaneously in detail were found [41].

The novelty of this study is summarized as followed: (1) The optimized objective is a hybrid 9999 m^2 solar district heating plant with both flat plate collector and parabolic trough collector technologies, which is a novel design concept for solar district heating systems; (2) Two kinds of boundary conditions for LCOH optimization are compared in this study. The main goal of this study is to investigate ways to reduce the cost of the installation and increase the thermal performance of large solar heating plants simultaneously. Optimal area of different collectors for hybrid solar district heating plants in this study were figured out. Sensitivity analysis on storage size, orientation of PTC, different heat demands, fuel price trend and PTC price trend in the nearby future, are also investigated. This study could provide information on the optimal design of such combined solar district heating plants with both flat plate collectors and parabolic trough collectors.

2. Method

TRNSYS-GenOpt model, objective functions and cost investigations are introduced in this section.

2.1. TRNSYS-GenOpt model

A TRNSYS model on hybrid solar district heating plants has been developed in the TRNSYS 17 and validated [42]. Dynamic simulated daily (typical cloudy and sunny days) and monthly energy outputs of the hybrid solar heating plants have good agreements with the measured data. The TRNSYS model includes flat plate collectors, parabolic trough collectors, the storage tanks, natural gas boilers and so on. The quasi-dynamic model was used to simulate the energy output of both collector fields. Fig. 1 shows the basic process flow of the investigated plant in TRNSYS 17. GenOpt, developed by Lawrence Berkeley National Laboratory [39], was used to carry out the multivariable optimization. The general methodology of TRNSYS-GenOpt is summarized in Fig. 2. When the simulation results reach maximum or minimum objective value, the model will stop, such as minimum LCOH or maximum energy

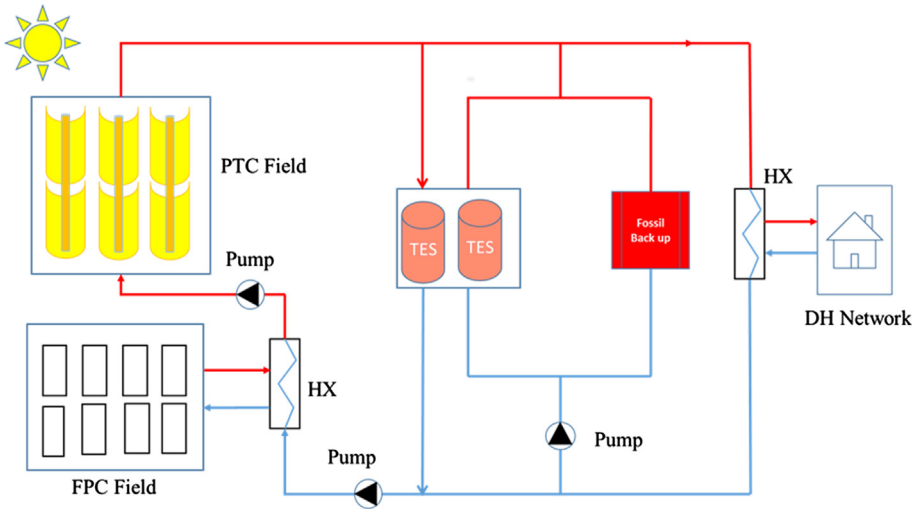

Fig. 1. Simplified process flow diagram of the hybrid solar heating plant model.

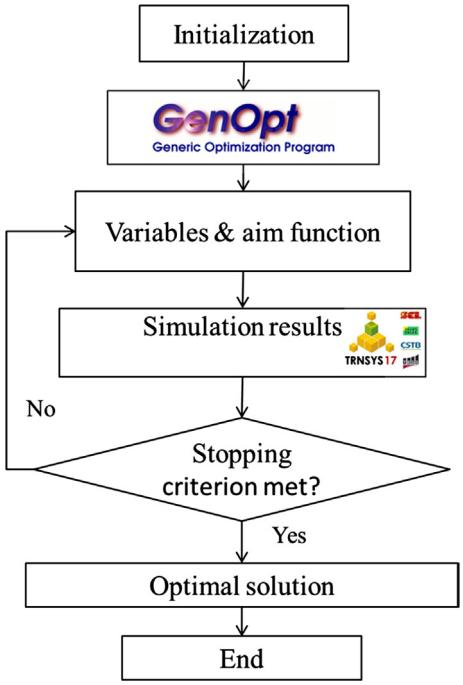

Fig. 2. Flow-chart of the TRNSYS-GenOpt model.

output. The flat plate collector field consists of two types of flat plate collectors without/with foils in series. The main components in the TRNSYS model can be found in the Table 1.

2.2. Objective functions

Two different kind of objective functions for optimizations are shown. In addition, two different boundary conditions of levelized cost of heat are also discussed.

2.2.1. Energy output

The energy output of the hybrid solar heating plant is expressed as Eq. (1). The maximum energy output per square meter of the plant can be used to determine the most efficient solar heating plant during the optimization. The energy output of the solar heating plant per m^2 aperture area in this study is the solar heat generated by the hybrid solar collector field minus heat loss from pipe loops and heat storages.

$$Q_0 = (Q_{ptc} \times A_{ptc} + Q_{fpc} \times A_{fpc} - Q_{loss})/(A_{ptc} + A_{fpc}) \quad (1)$$

2.2.2. Levelized cost of heat

Levelized cost of heat (LCOH) was used in this study. For end-use consumers, the final and optimal heat price which consumers would pay for the district heating is interesting for the commercial market. LCOH is a fair index to use both for parabolic trough and flat plate collectors in large solar heating plants for district heating networks. The general Equation of LCOH can be found in Eq. (2) [44].

$$LCOH = \frac{I_0 - S_0 + \sum_{t=1}^{T} \frac{C_t \cdot (1 - TR) - DEP_t \cdot TR}{(1+r)^t} - RV \cdot (1+r)^{-T}}{\sum_{t=1}^{T} E_t \cdot (1+r)^{-t}} \quad (2)$$

Two boundary conditions are applied for calculations of LCOH for the solar district heating plants in this study. One boundary condition is elaborated only for the solar collector fields and heat storage. The other boundary condition not only includes the solar collector fields and heat storage, but also takes conventional heat supply into consideration at the same time. The former is called by net LCOH and the latter is called by system LCOH respectively in this study. The DEP_t and TR are regarded as zero in the residential sector [39]. The simplified approach (Eqs. (3) and (4)) is derived from the exhaustive approach (Eq. (2)), by making a series of assumptions in the optimization; There is no residual value; There are no incentives; Operation and maintenance costs do not change from year to year; The yearly heat generation remains constant throughout the lifetime of the system [45].

1. Net LCOH (*nLCOH*)

Eq. (3) can be used to determine *nLCOH*. The lifetimes of both flat plate collector and parabolic trough collector field in Denmark are assumed as 30 years. Assumption of calculation discount rate is 3% [41]. With the increase or decrease of discount rate, the LCOH will increase or decrease slowly.

$$nLCOH = \frac{I_s + C_{storage} + \sum_{t=1}^{T} P_s \cdot (1+r)^{-t}}{\sum_{t=1}^{T} SE \cdot (1+r)^{-t}} \quad (3)$$

2. System LCOH (*sLCOH*)

The conventional natural gas boiler system is existing and quite common in Denmark. The integration of solar heating plants in existing district heating networks is a more and more common practice in Denmark. The system LCOH including the natural gas boiler system is expressed as Eq. (4). The lifetime of natural gas boilers is assumed as 30 years. The main operation cost of the backup boiler systems is regarded as the operation cost of the fuel consumption.

$$sLCOH = \frac{I_s + C_{storage} + I_b + \sum_{t=1}^{T} (P_s + P_b) \cdot (1+r)^{-t}}{\sum_{t=1}^{T} (SE + NE) \cdot (1+r)^{-t}} \quad (4)$$

2.3. Cost investigations

The heat price from the natural gas boiler system is assumed to be 0.57 DKK/kWh in this study. The assumed cost of the flat plate collector field with collectors without FEP foils is shown by Eq. (5). The cost of

Table 1
Main TRNSYS components and parameter settings (default condition) [43].

Name	Component type	Main Parameters	Descriptions
Weather data	Type 15	North Jutland of Denmark, Design Reference Year	Tracking model 1: fixed surface for FPC; Tracking model 2: the surface rotates about a fixed (user-defined) axis for PTC
FPC	Type 1290	5960 m^2	Flat plate collectors without/with FEP foils
PTC	Type 1290	4039 m^2	Parabolic trough collectors
Shadow	Type 30	Model 1: row distance: 5.67 m; Model 2: row distance: 12.6 m	Model 1: flat plate collectors; Model 2: Parabolic trough collectors.
Tank	Type 4	2430 m^3	Short-term storage.
Boilers	Type 659	9100 kW	Natural gas boiler systems
Pump	Type 3	Varied parameters	–
Heat load	Type 9	Return temperature and Heat load	Measured return temperature and heat load from the district heating system (approximately 850 buildings with about 1900 residents).

the flat plate collector field with collectors with FEP foils is assumed to be 7.6% higher than that of the flat plate collector field with collectors without FEP foils. The cost of the parabolic trough collector field and the storage tank is expressed by Eq. (6) [46] and (7) [40] respectively. The cost of parabolic trough collector field is 40–70% higher than the cost of flat plate collector field regarding of the size. The operation and maintenance cost of the flat plate collector field every year is assumed as follows: (a) 2 DKK/MWh heat produced for maintenance fee [47]; (b) 1.5 kWh electricity/100 kWh heat produced for operation (2.3 DKK/kWh electricity) [40]. The operation and maintenance cost of the parabolic trough collector field every year is assumed to be 0.8% of the initial cost [33].

$$C_{fpc} = \begin{cases} 2400\ \text{DKK/m}^2 \text{ for } 500\ \text{m}^2 < A_{fpc} \leqslant 1000\ \text{m}^2 \\ 2300\ \text{DKK/m}^2 \text{ for } 1000\ \text{m}^2 < A_{fpc} \leqslant 3000\ \text{m}^2 \\ 2180\ \text{DKK/m}^2 \text{ for } 3000\ \text{m}^2 < A_{fpc} \leqslant 10{,}000\ \text{m}^2 \end{cases} \quad (5)$$

The cost function of the parabolic trough collector field is as Eq. (6) [46]

$$C_{ptc} = 13925 \times A_{ptc}^{-0.17} \quad (6)$$

The cost function of the tank is assumed as Eq. (7) [40]

$$C_{storage} = (11680 \times V_{storage}^{-0.5545} + 130) \times 7.44 \quad (7)$$

3. Case study

A hybrid solar district heating plant with flat plate collectors and parabolic trough collectors is used as the reference case in the optimization. Details about the hybrid solar heating plants, climate data and heat demand are shown in Sections 3.1 and 3.2.

3.1. Taars solar heating plant

Taars plant with flat plate collectors and parabolic trough collector was constructed in August 2015. The hybrid plant is supported by the Danish Energy Agency through the Energy Technology Development and Demonstration Program (EUDP). Main design and technical parameters for the plant can be found in Tables 2 and 3 respectively. The solar collector field consists of flat plate collectors and parabolic trough collectors in series. In the flat plate collector subfield, on average half of the collectors are without FEP foils (HTHEATboost 35/10) and the other half of the collectors are with FEP foils (HTHEATstore 35/10). The flat plate collectors are delivered by Arcon-Sunmark A/S [48]. The collectors without the foils are placed first in the rows, while the collectors with the foils are placed last in the rows. The tilt of flat plate collectors is 50°. The return water from the district heating network is preheated by the flat plate collector field. Then the preheated water is heated up to a required temperature by the parabolic trough collectors. The parabolic trough collectors were delivered by Aalborg CSP A/S [33]. The orientation of parabolic trough collectors is N-S orientation with 13.4° towards west. The existing natural gas boilers are the backup systems for the district heating network. The efficiency parameters of the investigated solar collectors based on the aperture area can be found in Table 4.

$$\frac{Q}{A} = \eta_0 K_{\theta b}(\theta) G_b + \eta_0 K_{\theta d}(\theta) G_d - c_1(T_m - T_a) - c_2(T_m - T_a)^2 - c_3 \frac{dT_m}{dt} \quad (8)$$

$$K_{\theta b}(\theta) = 1 - b_0\left(\frac{1}{\cos\theta} - 1\right) - b_1\left(\frac{1}{\cos\theta} - 1\right)^2, \quad \theta \leqslant 60° \quad (9)$$

When θ (incident angle) $> 60°$, the IAM is linearized from the value at 60° to a value of zero at 90°. Where, Q is energy output, W; A is aperture area, m^2; K is incidence angle modifier; G_b is beam radiation on the collector plane, W/m^2; G_d is diffuse radiation on the collector plane, W/m^2; T_m is mean temperature, degrees Celsius; dT_m/dt is the time derivative of T_m, K/s.

3.2. Climate data and heat demand

Fig. 3 shows the monthly global radiation, DNI and average ambient temperature in the Design Reference Year (DRY) of Northern Jutland of Denmark [49]. Yearly DNI and global radiation in the DRY are 1150 and 1030 kWh/m^2 respectively. The district heating network consists of approximate 850 buildings with about 1900 consumers. The typical design heat demand of the district heating network is shown in Fig. 4. The heat demand was measured from the district heating network as the typical design parameter for the hybrid solar heating plant during the planning stage. The total heat demand is 20,167 MWh per year. The heat demand is quite low in the summer and high in the winter.

4. Results

Influence of storage size, orientation of PTC, different heat demands, fuel price trend and PTC price trend in the nearby future, are investigated and analyzed in this section.

4.1. The influence of storage volume

Areas of both collector fields and volume of the storage tanks are important design parameters for the hybrid solar heating plant. The optimal storage volume and solar collector areas of the solar collector fields depend strongly on each other. Fig. 5 shows the influence of the storage volume on the *nLCOH* and solar energy output in the reference case. The *nLCOH* of the Taars plant is 0.420 DKK/kWh. The *nLCOH* almost has the same level of 0.420 DKK/kWh when the storage volume varies between 2430 m^3 and 5000 m^3. The energy output of the plant delivered to the district heating network can increase from 422 kWh/m^2 to 434 kWh/m^2. When the heat storage volume is 7000 m^3, the energy output delivered to the district heating network almost peaks at 438 kWh/m^2. For further increased storage volumes, the thermal performance is not much increased. 5000–7000 m^3 could be the reasonable storage volume for the Taars plant.

4.2. Area of both collector fields

It appears from Fig. 5 that a larger storage tank not only can increase the energy output of the plant, but also keeps the *nLCOH* at a low constant level. So optimal areas of the collector fields based on four heat storage scenarios, including 2430 m^3 – scenario 1a/b, 5000 m^3 – scenario 2 a/b, 7500 m^3 – scenario 3a/b and 10000 m^3-– scenario 4a/b, are investigated and compared to the reference case. In the whole scenarios, the tilt of the flat plate collectors and the orientation of the parabolic trough collectors are also optimized to reach the minimum *nLCOH*. The optimal tilt of the flat plate collectors is 35° and the optimal orientation of the parabolic trough collectors is E-W orientation in the scenarios 1a-4a and 1b-4b. The areas of both flat plate collector field and parabolic trough collectors are between 100 and 10000 m^2 in the optimizations. Fig. 6 shows the optimal collector areas of different collectors based on the objective function of maximum energy output

Table 2
Main design parameters of the Taars plant.

Parameters	Taars (Denmark)
Latitude	57.39 °N
Longtitude	10.11 °E
Altitute	48 m
Parabolic trough collector field (Aperture area)	4039 m^2
Flat plate collector field (Aperture area)	5960 m^2
Fossil backup -Natural gas boilers	9.1 MW
Storage tank (2)	2430 m^3

Table 3
Main technical parameters of the collector fields.

Parameters	PTC	FPC
Solar collector fluid	Water	35% propylene glycol/water
Collector row distance, m	12.6	5.67
Azimuth, °	−13.4	0
Tilt, °	–	50

Table 4
Parameters of the investigated solar collectors.

η_0	b_0	b_1	$K_{\theta d}$	c_1, [W/(m^2·K)]	c_2, [W/(m^2·K^2)]	c_3, [kJ/(m^2·K)]	
0.839	0.1	0	0.98	2.596	0.016	7.321	HEATboost 35/10
0.802	0.1	0	0.93	2.226	0.010	7.876	HEATstore 35/10
0.75	0.27	0	0.038	0.04	0	4.00	PTC

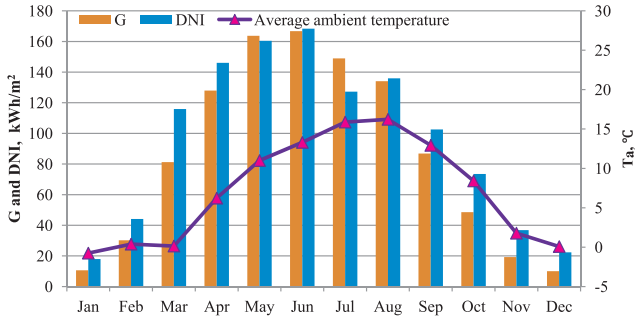

Fig. 3. Monthly global radiation, DNI and average ambient temperature in the DRY (Northern Jutland, Denmark).

delivered to the consumers. It is suggested that the optimal collector field should consist of mainly parabolic trough collectors without flat plate collectors for four scenarios. Fig. 7 shows the optimal collector areas of different collectors based on the objective function of minimum *nLCOH*. It is suggested that the optimal collector field should integrate flat plate collectors and parabolic trough collectors in series to reach minimum *nLCOH* points with the range 0.367–0.400 DKK/kWh. The solar fraction of the Taars plant is 21.0%. The solar fractions of the investigated four scenarios 1b-4b in Fig. 7 are placed in the interval from 18% to 23%. The comparison of Taars plant and scenario 1b in Fig. 7 shows that the solar collector fields was oversized during the design phase, which causes that the net LCOH of the Taars plant is higher than that of scenario 1b. But the net LCOH of Taars plant is still lower than the price for natural gas boiler systems. In addition, the comparison of Taars plant and scenario 4b in Fig. 7 shows that if there were a 10000 m^3 large storage volume, the optimal solar fraction could have increased to 23% with lower heat price, then the cost performance of such large-scale solar heating plants increases a lot.

Based on the results in Figs. 6 and 7, it is seen that quite different conclusions appear from different objective functions for the 4 scenarios. Various target groups would use different objective functions to benefit from the results. On the one hand, parabolic trough collectors are more efficient than flat plate collectors for high temperature levels. On the other hand, the price of parabolic trough collectors is higher than the price of flat plate collectors for high temperature levels. From the scenarios 1–4 in Fig. 7, it is shown that the combination of flat plate collectors and parabolic trough collectors in series can increase the cost-performance of the solar district heating plants, which is interesting for the commercial market and end-use consumers.

4.3. Orientation of the parabolic trough collectors

The orientation of the PTC fields affects the way of tracking and the received beam radiation. The N-S orientation is always regarded as the optimal orientation of concentrating solar power plants [50]. The typical E-W and N-S orientations are compared in Fig. 8. Fig. 8a and b shows the reference case (the Taars plant) and the optimal case of scenario 1 with both typical orientations in Fig. 7 respectively. The comparison between Fig. 8a and b indicates that the parabolic trough collectors are defocused a lot from May to August in the reference case. The defocus of the parabolic trough collector field causes a low heat production of the plant and a high *nLCOH*. Furthermore, Fig. 8 shows that the PTC field with N-S orientation produces higher heat in the summer months than the PTC field with E-W orientation. As shown in Fig. 4, the heat demand of the district heating network in the summer is very low. The PTC field with N-S orientation may cause excess heat production if the PTC works normally in the summer. It can be seen that in Fig. 8b that the monthly energy output of the PTC field with N-S orientation can be higher than 100 kWh/m^2. So the PTC field with N-S orientation has to be defocused a lot in sunny days in the summer. On the contrary, the PTC field with E-W orientation produces lower heat in the summer due to large incidence angle losses. In addition, the PTC field with E-W orientation produces more solar heat in the spring, autumn and winter seasons while the heat demand is also high during the peroid. In order to avoid the heat overproduction of the PTCs in the summer and harvest the thermal performance of the PTC in spring and autumn, E-W orientation is the suggested orientation for the PTC field for the district heating network in this study.

4.4. Heat demand

The heat demand of the district heating network influences the operation strategy of the solar heating plant directly, especially in the summer. Larger heat demand could improve the operation of parabolic trough collectors in the summer. Seven heat demand scenarios varying from 0% to 60% extra demand compared to the demand in Taars are shown in Table 5. All the other variables are kept constant as in the

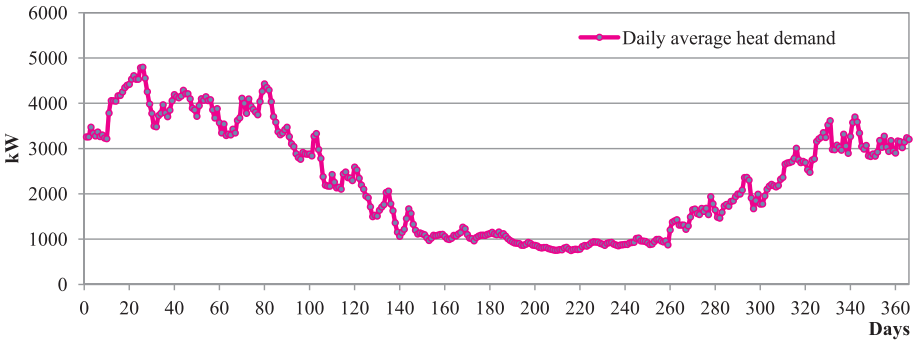

Fig. 4. Typical daily average heat demand of the district heating network [33].

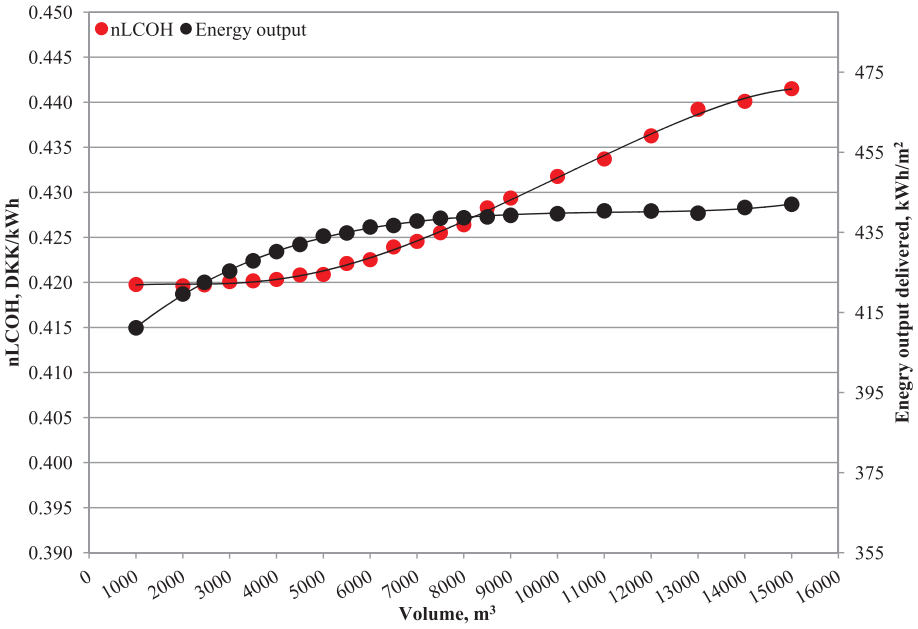

Fig. 5. The influence of the storage volume on net LCOH and yearly solar energy output of the Taars plant (All the other variables are kept constant as in the Taars plant).

Taars plant. Compared to existing flat plate collector plants in Denmark, the energy output of the flat plate collector field in Taars produces higher solar heat. That is due to the fact that the flat plate collectors work at relatively low operation temperature in the hybrid solar heating plant. With the increase of the heat demand, the energy output of the flat plate collector field increases slowly. But the energy output of the parabolic trough collector field increases sharply with larger heat demand. That is because the parabolic trough collector field is defocused and not used fully in the summer in the reference case. When the heat demand increases by 60%, the yearly output of the PTC field can increase from 418 kWh/m^2 to 528 kWh/m^2 and the *nLCOH* can be reduced from 0.420 to 0.363 DKK/kWh. So the collector field is oversized and should be smaller based on the heat demand in Taars. Another solution for the reference case is that a larger storage tank should be used, as indicated in Fig. 5.

4.5. Fuel price trend

The price of natural gas for household consumers in Denmark fluctuates a lot year by year, even month by month [25,26]. Four increased fuel price scenarios varying from 0% to 30% price increase are shown in Table 6 to determine the system LCOH. The system LCOH of the Taars plant is 0.54 DKK/kWh. The system LCOH is 5–9% lower than traditional natural gas boiler systems because of the application of the solar heating collectors in Table 6.

4.6. Price trend of parabolic trough collectors

The high price is the main barrier for the parabolic trough collectors to be applied widely in the market compared to the flat plate collectors. With the commercial development of PTC just started in 1970s [51], there is huge decrease potential of the cost of PTC. So four PTC price scenarios varying from 0% to −50% reduction in price were investigated to obtain an overview of the development for PTC technology in district heating networks in the future. Areas of the collectors, tilt of the FPC and orientation of the PTC were optimized simultaneously to reach minimum *nLCOH*. Fig. 9 shows the optimal design points for all the PTC price scenarios. The optimal tilt of flat plate

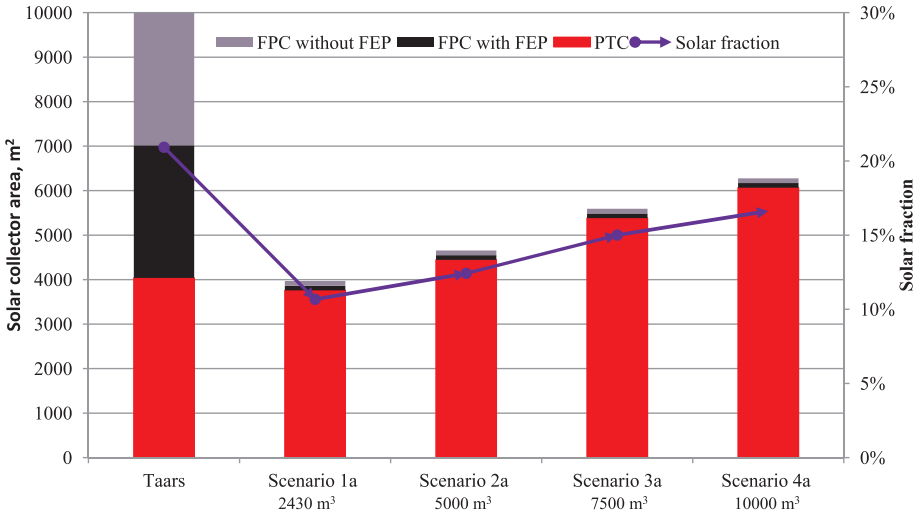

Fig. 6. Optimal solar collector area and solar fraction of the investigated scenarios 1a-4a based on the objective function of maximum energy output (All the other variables are kept constant as the Taars plant).

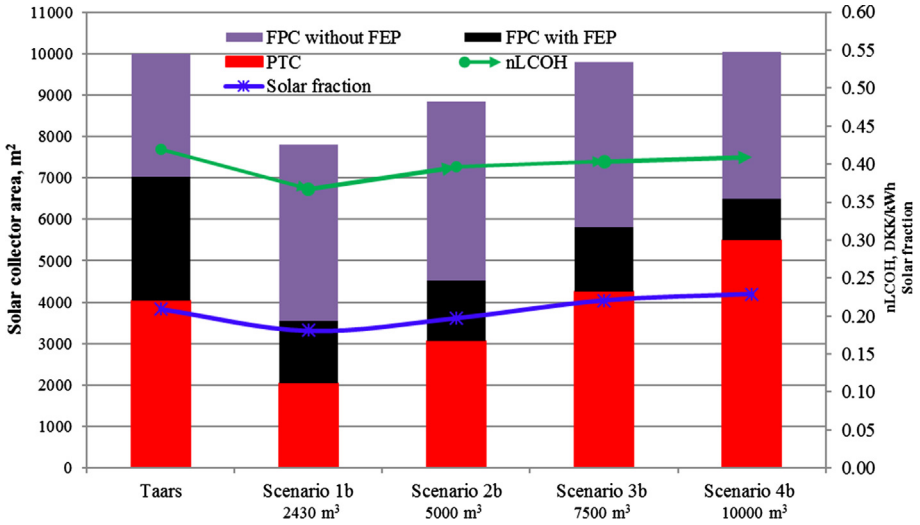

Fig. 7. Optimal solar collector area, *net LCOH* and solar fraction of the investigated scenarios 1b-4b based on the objective function of minimum *nLCOH* (All the other variables are kept constant as in the Taars plant).

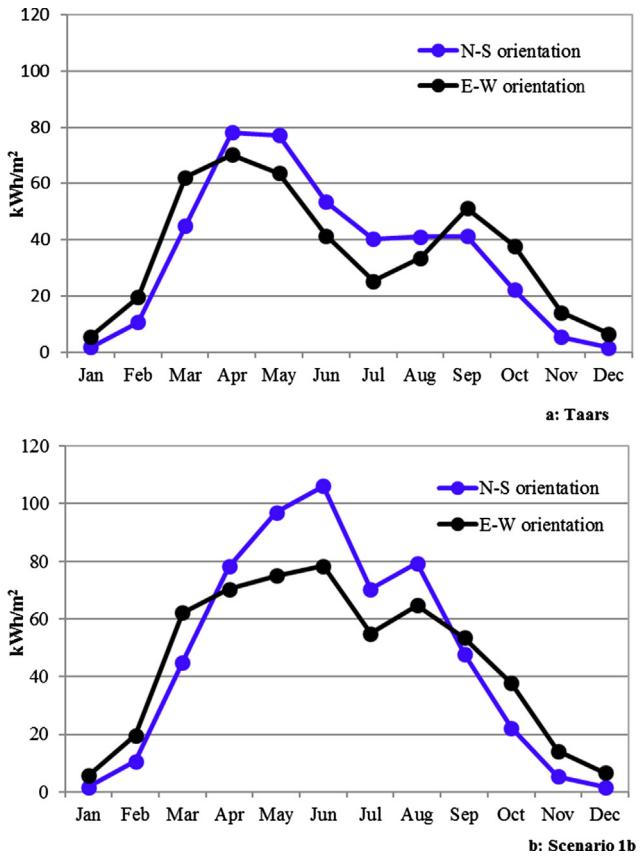

Fig. 8. The influence of typical orientation on the energy output of the parabolic trough field (a: the reference Taars plant; b: Scenario 1b- optimal case for Taars plant).

collectors is 35°. The optimal orientation of parabolic trough collectors is E – W orientation. All the other variables are kept as in the Taars plant. When the price of PTC decreases by 50%, the optimal *nLCOH* of the plant can be reduced from 0.367 DKK/kWh to 0.247 DKK/kWh. It can be found that the design strategy of flat plate collectors and parabolic trough collectors in series is feasible and optimal in order to reach minimum net LCOH in all the scenarios.

Table 5
nLCOH based on different heat demands.

Heat demand	Annual energy output, kWh/m²			*nLCOH*, DKK/kWh
	FPC field	PTC field	The whole plant excluding heat loss	
0 (Taars)	449	418	422	0.420
+10%	454	447	437	0.405
+20%	458	472	449	0.395
+30%	460	487	457	0.388
+40%	463	506	466	0.380
+50%	465	521	474	0.374
+60%	467	528	478	0.363

Table 6
sLCOH based on different fuel fees.

Price of the fuel, DKK/kWh	*sLCOH*, DKK/kWh
0.57 (Taars)	0.54
0.63	0.59
0.68	0.63
0.74	0.67

5. Discussion

The studied plant is the first pilot large-scale solar heating plant with flat plate collectors and parabolic trough collectors in series for district heating networks in Europe, even worldwide. The boiling problem for solar district heating plants in the summer is one of main factors to limit the size of plants, if there are not seasonal storage. On the one hand, the application of parabolic trough collectors can easily be defocused to avoid the overheat production, which can increase the flexibility of solar heating plants in the whole energy system, compared to evacuated tube collectors and compound parabolic collectors. On the other hand, the defocus of the parabolic trough collector reduces the cost-effective competitiveness of the hybrid solar heating plants. The integration of parabolic trough collectors can also guarantee that flat plate collectors work at relatively low operation temperature and produce more than the normal solar heating plants. The investigations in this study figure out the optimal solar collector areas for the Taars plant.

In addition, Fresnel collectors is another line-focusing collector, which arouses increasing interests in the last decade. Fresnel collectors

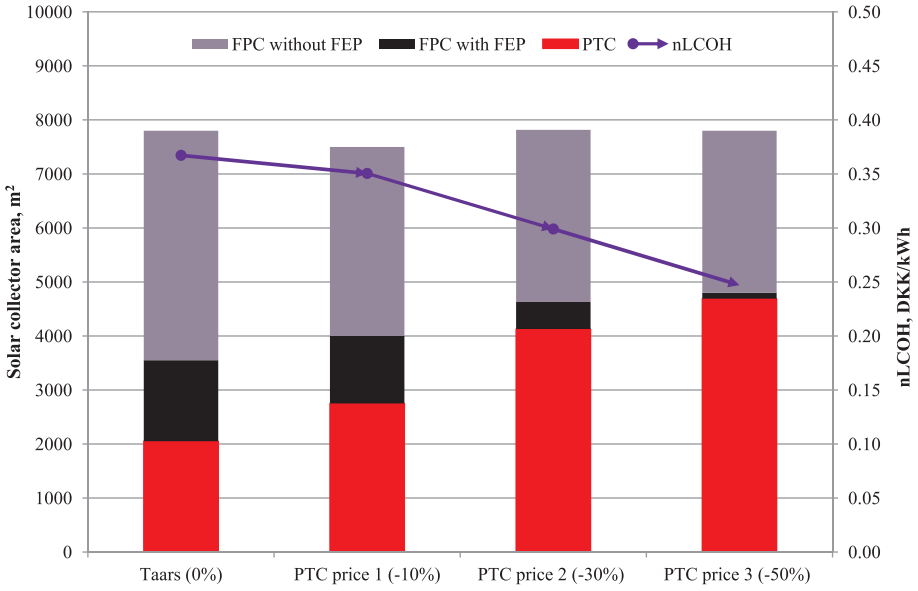

Fig. 9. Minimum *nLCOH* and optimal design collector areas based on different prices of the PTC.

have cheaper price and higher land use efficiency than parabolic trough collectors, while it has lower solar-to-power efficiency. If the advantages of Fresnel collectors were enough strong to the low efficiency, the Fresnel collectors could be an optional alterative collector type to parabolic trough collectors for such hybrid solar district heating plants. All in all, the integration of evacuated tube collectors, compound parabolic collectors, or Fresnel collectors with flat plate collectors due to the cheaper price could also be interesting to investigate for large-scale hybrid solar district heating plants in the future work.

6. Conclusions and future work

Analyses based on levelized cost of heat for large scale solar district heating plants have been carried out. An optimization approach based on TRNSYS-GenOpt was introduced. Multi variable and function optimizations of a hybrid solar heating plant were carried out. The LCOH of hybrid solar heating plants for different scenarios in the near future was also figured out. The following conclusions can be drawn:

The net LCOH of the Taars plant is 0.42 DKK/kWh. The lowest net LCOH of the optimized hybrid solar heating plant is much lower than the average price of heat from the natural gas boilers (0.57 DKK/kWh). The use of parabolic trough collector in the solar district heating systems is cost effective.

The system LCOH of the Taars plant can be reduced by about 5–9% by using solar collectors in district heating networks in this study.

For the investigated district heating network, parabolic trough collectors with E-W orientation are more suitable than that with N-S orientation due to the high solar fraction during the summer. The low heat demand/collector area ratio limits the potential of parabolic trough collectors as long as the plant is not equipped with large heat stores. Heat stores with large volumes are needed in order to fully utilize the parabolic trough collectors.

The concept with flat plate collectors and parabolic trough collectors in series for district heating networks is technical-economic feasible in Denmark compared to the heat price of conventional natural gas boiler systems. The optimization of area of the collectors and storage size based on the heat demand should be addressed in the planning and design phase of hybrid solar heating plants. The results not only can provide useful recommendations to designers, but also result in the lowest heat price for the end-use domestic consumers.

Acknowledgements

The first author really appreciates the China Scholarship Council (No. 201506120074) for the financial support for the PhD study at the Technical University of Denmark. Special thanks are expressed to Aalborg CSP A/S (Andreas Zourellis, Jan Holst Rothman, Steffen Rovsing Møller and Per Aasted) for the information provided. This work is a part of an EUDP project financed by the Danish Energy Agency and the IEA-SHC Task 55 “Towards the Integration of Large SHC Systems into DHC Networks”.

References

[1] Rad FM, Fung AS. Solar community heating and cooling system with borehole thermal energy storage – review of systems. Renew Sustain Energy Rev 2016;60:1550–61.
[2] Hazami M, Naili N, Attar I, Farhat A. Solar water heating systems feasibility for domestic requests in Tunisia: thermal potential and economic analysis. Energy Convers Manage 2013;76:599–608.
[3] Deng J, Tian Z, Fan J, Yang M, Furbo S, Wang Z. Simulation and optimization study on a solar space heating system combined with a low temperature ASHP for single family rural residential houses in Beijing. Energy Build 2016;126:2–13.
[4] Çomaklı K, Çakır U, Kaya M, Bakirci K. The relation of collector and storage tank size in solar heating systems. Energy Convers Manage 2012;63:112–7.
[5] Kaçan E, Ulgen K, Kaçan E. What is the effect of optimum independent parameters on solar heating systems? Energy Convers Manage 2015;105(November):103–17.
[6] Li H, Xu W, Yu Z, Wu J, Yu Z. Discussion of a combined solar thermal and ground source heat pump system operation strategy for office heating. Energy Build 2018;162:42–53.
[7] Bellos E, Tzivanidis C, Moschos K, Antonopoulos KA. Energetic and financial evaluation of solar assisted heat pump space heating systems. Energy Convers Manage 2016;120(July):306–19.
[8] Pardo García N, Zubi G, Pasaoglu G, Dufo-López R. Photovoltaic thermal hybrid solar collector and district heating configurations for a Central European multi-family house. Energy Convers Manage 2017;148(September):915–24.
[9] Ramos A, Chatzopoulou MA, Guarracino I, Freeman J, Markides CN. Hybrid photovoltaic-thermal solar systems for combined heating, cooling and power provision in the urban environment. Energy Convers Manage 2017;150(October):838–50.
[10] Bava F, Dragsted J, Furbo S. A numerical model to evaluate the flow distribution in large solar collector fields in different operating conditions. Sol Energy 2016;143:11–4.
[11] Bava F, Furbo S. A numerical model for pressure drop and flow distribution in a solar collector with horizontal U-connected pipes. Sol Energy 2016;134:264–72.
[12] Bava F, Furbo S. Development and validation of a detailed TRNSYS-Matlab model for large solar collector fields for district heating applications. Energy 2017;135:698–708.
[13] Wang J, Yang Y. Energy, exergy and environmental analysis of a hybrid combined cooling heating and power system utilizing biomass and solar energy. Energy Convers Manage 2016;124(September):566–77.
[14] International Energy Agency. IEA solar heating & cooling programme; 2017. https://www.iea-shc.org/. [Online]. Available: Mar. 2017.

[15] Dalenbäck Jan-Olof. IEA SHC task 7 central solar heating plants with seasonal storage – CSHPSS 1981–1990. Edited status report.
[16] Mauthner F, Weiss W. Solar heat worldwide: markets and contribution to the energy supply 2014. IEA Solar Heating and Cooling Programme; 2016.
[17] Fish M, Guigas M, Dalenback J. A review of large-scale solar heating systems in Europe. Sol Energy 1998;63(6):355–66.
[18] De Guadalfajara M, Lozano MA, Serra LM. Evaluation of the potential of large solar heating plants in Spain. Energy Procedia 2012;30:839–48.
[19] Bauer D, Marx R, Nußbicker-Lux J, Ochs F, Heidemann W, Müller-Steinhagen H. German central solar heating plants with seasonal heat storage. Sol Energy 2010;84(4):612–23.
[20] Olsthoorn D, Haghighat F, Mirzaei PA. Integration of storage and renewable energy into district heating systems: a review of modelling and optimization. Sol Energy 2016;136:49–64.
[21] Tulus V, Boer D, Cabeza LF, Jimenez L, Guillen-Gosalbez G. Enhanced thermal energy supply via central solar heating plants with seasonal storage: a multi-objective optimization approach. Appl Energy 2016;181:549–61.
[22] Guerreiro L, Canavarro D, Collares Pereira M. Efficiency improvement and potential LCOE reduction with an LFR-XX SMS plant with storage. Energy Procedia 2015;69:868–78.
[23] Sartor K, Quoilin S, Dewallef P. Simulation and optimization of a CHP biomass plant and district heating network. Appl Energy 2014;130:474–83.
[24] Drake landing solar community. Drake landing solar community; 2017. http://www.dlsc.ca/. [Online]. Available: July 2017.
[25] Furbo S, Fan J, Perers B, Kong W, Trier D, From N. Testing, development and demonstration of large scale solar district heating systems. Energy Procedia 2015;70:568–73.
[26] PlanEnergi, “planenergi”; 2017. http://planenergi.eu/activities/fjernvarme/solar-heating/. [Online]. Available: 2017.
[27] Liu Z, Li H, Liu K, Yu H, Cheng K. Design of high-performance water-in-glass evacuated tube solar water heaters by a high-throughput screening based on machine learning: a combined modeling and experimental study. Sol Energy 2017;142(January):61–7.
[28] Kalogirou S. The potential of solar industrial process heat applications. Appl Energy 2003;76(4):337–61.
[29] Biencinto M, González L, Valenzuela L. A quasi-dynamic simulation model for direct steam generation in parabolic troughs using TRNSYS. Appl Energy 2016;161:133–42.
[30] Leiva-Illanes R, Escobar R, Cardemil JM, Alarcón-Padilla D-C. Thermoeconomic assessment of a solar polygeneration plant for electricity, water, cooling and heating in high direct normal irradiation conditions. Energy Convers Manage Nov. 2017;151:538–52.
[31] Silva R, Perez M, Fernandez-Garcia A. Modeling and co-simulation of a parabolic trough solar plant for industrial process heat. Appl Energy 2013;106:287–300.
[32] Krueger D, Heller A, Hennecke K, Duer K, Energietechnik S, Zentrum D, Höhe L. Parabolic trough collectors for district heating systems at high latitudes. In: Proceedings of Eurosun; 2000.
[33] Aalborg CSP A/S. Aalborg CSP; 2017. http://www.aalborgcsp.com. [Online]. Available: July 2017.
[34] Perers B, Furbo S, Dragsted J. Thermal performance of concentrating tracking solar collectors. DTU Rep 2013;292(August).
[35] Perers B, Furbo S, Tian Z, Egelwisse J, Bava F, Fan J. Tårs 10000 m^2 CSP + flat plate solar collector plant – cost-performance optimization of the design. Energy Procedia 2016;91:312–6.
[36] Tian Z, Perers B, Furbo S, Fan J. Annual measured and simulated thermal performance analysis of a hybrid solar district heating plant with flat plate collectors and parabolic trough collectors in series. Appl Energy 2017;205:417–27.
[37] Buoro D, Pinamonti P, Reini M. Optimization of a distributed cogeneration system with solar district heating. Appl Energy 2014;124:298–308.
[38] Zhao Z-Y, Chen Y-L, Thomson JD. Levelized cost of energy modeling for concentrated solar power projects: a China study. Energy 2017;120:117–27.
[39] Louvet Y, Fischer S, Furbo S, Giovanetti F, Mauthner F, Mugnier D, et al. LCOH for solar thermal applications LCOH for solar thermal applications conventional reference system; 2017. http://task54.iea-shc.org. [Online]. Available: July 2017.
[40] Mauthner F, Herkel S. Classification and benchmarking of solar thermal systems in urban environments. TECHNOLOGY AND DEMONSTRATORS: technical report subtask C – Part C1; 2016. http://task52.iea-shc.org/publications. [Online]. Available: March 2017.
[41] Weiss Werner, Spörk-Dür Monika, Mauthner Franz. Solar heat worldwide-global market development and trends in 2016-detailed market figures 2015 (2017 version); 2017. http://www.iea-shc.org/solar-heat-worldwide.
[42] Tian Z, Perers B, Furbo S, Fan J. Analysis and validation of a quasi-dynamic model for a solar collector field with flat plate collectors and parabolic trough collectors in series for district heating. Energy 2018;142:130–8.
[43] TRNSYS. TRNSYS 17-a TRaNsient SYstem Simulation program – volume 4 mathematical reference; 2017. http://web.mit.edu/parmstr/Public/TRNSYS/04-MathematicalReference.pdf. [Online]. Available: June 2017.
[44] Louvet Y, Fischer S, Furbo S, Giovannetti F, Mauthner F, Mugnier D. Entwicklung eines Verfahrens für die Wirtschaftlichkeitsbe- rechnung solarthermischer Anlagen: die LCOH Methode. In: OTTI conference; 2017 [in German].
[45] Baez MJ, Martinez TL. Technical report on the elaboration of a cost estimation methodology; 2016. http://www.front-rhc.eu/wp-content/uploads/2014/11/FROnT_D3.1_elaboration-of-a-cost-estimation-methodology_2015.07.22.pdf, p. 1–28.
[46] Egelwisse J. Solar heating plants based on CSP and FP collectors. DTU master thesis; 2015.
[47] Bava F, Furbo S, Perers B. Simulation of a solar collector array consisting of two types of solar collectors, with and without convection barrier. Energy Procedia 2015;70(May):4–12.
[48] Arcon-Sunmark. Arcon-Sunmark A/S; 2017. http://arcon-sunmark.com/products. [Online]. Available: March 2017.
[49] Dragsted J, Furbo S. Solar radiation and thermal performance of solar collectors for Denmark. DTU Rep 2012;275.
[50] Nation DD, Heggs PJ, Dixon-Hardy DW. Modelling and simulation of a novel electrical energy storage (EES) receiver for solar parabolic trough collector (PTC) power plants. Appl Energy 2017;195(June):950–73.
[51] Fernández-García A, Zarza E, Valenzuela L, Pérez M. Parabolic-trough solar collectors and their applications. Renew Sustain Energy Rev Sep. 2010;14(7):1695–721.

Paper V

Fabienne Sallaberry, **Zhiyong Tian**, Odei Goñi Jauregi, Simon Furbo, Bengt Perers, Andreas Zourellis and Jan Holst Rothmann.

Evaluation of the Tracking Accuracy of Parabolic-Trough Collectors in a Solar Plant for District Heating

Proceedings of SolarPACES 2017 conference.

This page is intentionally left blank.

Evaluation of the Tracking Accuracy of Parabolic-Trough Collectors in a Solar Plant for District Heating

Fabienne Sallaberry[1,a)], Zhiyong Tian[2], Odei Goñi Jauregi[1,3], Simon Furbo[2], Bengt Perers[2], Andreas Zourellis[4], Jan Holst Rothmann[4]

[1]*CENER (National Renewable Energy Centre of Spain), Solar Thermal Energy Department, Ciudad de la Innovación 7, 31621 Sarriguren, Navarra (Spain). Phone: +34 948 25 28 00*
[2]*DTU (Technical University of Denmark), Department of Civil Engineering, Technical University of Denmark, Nordvej Building 119, Kgs. Lyngby, 2800 (Denmark).*
[3]*UPNA (Public University of Navarra), C/ Arrosadia s/n; 31006 - Pamplona (Spain)*
[4]*Aalborg CSP A/S, Hjulmagervej 55, 9000 Aalborg (Denmark)*

[a)]Fabienne Sallaberry: fsallaberry@cener.com

Abstract. The solar tracking system is a device which orientates solar concentrating systems in order to allow the focusing of the solar radiation on the receiver along the day. The accuracy of the solar tracker is a key parameter when compared to the acceptance angle of the concentrator in order to maximize the optical efficiency. The Taars solar heating plant was put into operation in Denmark in summer 2015 with a PTC solar field. The accuracy of the tracking system of the 6 PTC rows has been studied.

INTRODUCTION

Denmark is the country with the highest use of solar plants for district heating applications[1]. Most of the collectors used in existing large solar heating systems are flat plate collectors (FPC). Meanwhile, parabolic-trough collectors (PTC) are the most mature and prominent technologies for solar thermal power plants. A novel solar heating plant was put into operation in July 2015 in Taars, Denmark, combining 4039 m^2 of parabolic-trough collectors (PTC) with 5960 m^2 of flat plate collectors (FPC). Previous studies show the performance of the plant, both the PTC and FPC collectors [2-4].

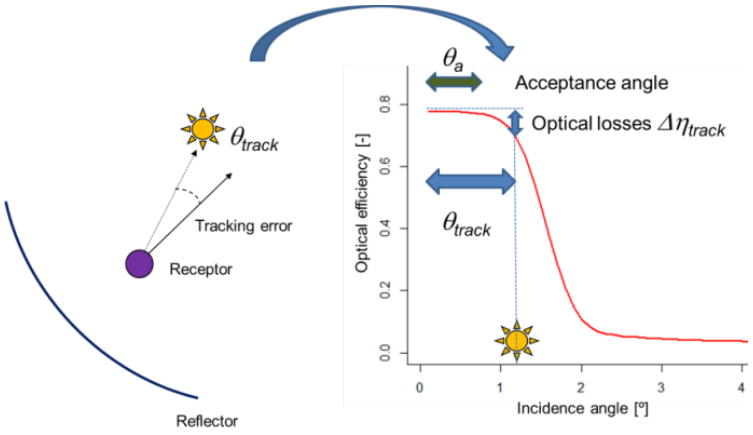

FIGURE 1: Scheme of the tracking error analysis

In the present study only the PTCs were studied. Many studies done in the last decade have already characterized the PTC efficiency [5-8], but few on site efficiency studies focused on the tracking error estimation of the PTC trackers [9-11]. Fig. 1 presents a summary of the acceptance angle as described in [11] as the angle until which the tracking errors do not have a significant impact on the PTC efficiency.

Previous studies also give the state-of-the-art of the methodologies available to characterize the tracking error of concentrating-tracking collectors and its influence on the solar collector efficiency [12-13].

The acceptance angle is a key parameter of the concentrator. The suitability between the acceptance angles with the tracking angles was checked and the tracker was determined to be accurate.

MATERIAL

A solar heating plant with 4039 m^2 PTC, in series with FPC collector field, has been constructed by Aalborg CSP A/S in Taars, in the northern part of Denmark [3,4] (longitude 10.11ºE, latitude 57.39ºN). This study analyses the tracking error of this PTC solar field. See Fig. 2 for a general view of the plant and the PTC collectors. The PTCs are manufactured by Aalborg CSP A/S, using receiver tubes manufactured by Archimede Solar Energy [14], and reflectors manufactured by Rioglass [15]. The receiver model is the product name HCEOI-12, with a nominal length of the receiver tube of 4060 mm (at ambient temperature); an absorber tube outer diameter of 70 mm, and a glass tube thickness of 2 mm. The reflector type is Mirror Type LS-3. Each collector length is 12 m, each row length is 124.457 m, and the collector aperture width is 5.774 m (See Fig. 2 for a view of the collectors and Table 1 for more specifications).

FIGURE 2. Schematic view of the plant; (b) View of the Taars plant (Denmark)

The PTCs track the sun in the transversal direction of the tube, and are oriented close to North-South direction. The orientation of the PTCs is slightly deviated from the North-South direction by 13.35º-13.37º. The exact orientation of each PTC row was estimated by topography study with a precision of ±0.001º. The inclinometer used to measure the PTC rotation is manufactured by Gemac. The data for the position of each of the 6 collectors were registered every 2 minutes by an inclinometer, positioned on the collector structure at the drive station in the center of the row.

TABLE 1. Geometrical parameters for the PTC collector

Parameters	Value
Absorber tube outer diameter d (m)	0.070
Absorber tube inner diameter (m)	0.066
Absorber tube solar absorptance (%)	96.0
Glass tube with anti-reflective solar transmittance (%)	96.5
Glass envelope outer diameter (m)	0.125
Glass envelope inner diameter (m)	0.119
Parabola width w (m)	5.77
Reflectors reflectance (%)	94,5
Numbers of modules per row	10
Mirror length in each module (m)	12
Geometrical concentration ratio $C_{geo} = w/(\pi\, d)$	26.24

METHODOLOGY

This study presents an analysis of the accuracy of six single-axis solar trackers of the PTC field in a solar plant for district heating.

First, the estimation is based on the measurement of inclinometers α mounted on the collector structure, as defined in Standard IEC 62862-3-2 [17]. The data analyzed are for more than one year (10/08/2015 to 17/11/2016) with a large range of incidence angles. For all data points the transversal and the longitudinal angles were calculated based on the sun position using the algorithm given by Blanco-Muriel [18]. A filter was applied to select the daily data (solar elevation h_s>0º; α >-100º; θ_T<20º; DNI > 0 W/m^2).

In order to check the accuracy of the solar tracker with a solar concentrator a definition of the acceptance angle should be defined. As for an ideal concentrating system, all the solar radiation entering with an incident angle smaller than this acceptance angle goes directed towards the receiver; whereas in a real solar collector, some optical losses exist due to optical properties, imperfections of materials, the size of the sun, the intercept factor, and the geometric imperfections. For this reason, using an accurate enough solar tracker is of high interest for the solar concentrator. The beam radiation IAM $K_b(\theta_T)$ crosses a limit threshold when exceeding the acceptance angle θ_a. The theoretical acceptance angle θ_a is defined for a PTC as described in Eq. 1, where Φ_r is the rim angle of the parabola and C_{geom} is the geometric concentration ratio [19]. The defocus angle θ_d is defined as the limit angle at which all the rays will miss the receiver, and is calculated by Eq. 2

$$\theta_a = \frac{\sin(\Phi_r)}{\pi C_{geom}} \tag{1}$$

$$\theta_d = \sin^{-1}\left(\frac{2\cdot\tan(\frac{\Phi_r}{2})}{\pi C_{geom}}\right) \tag{2}$$

Thus, the dependency of tracking error angle on the optical efficiency has also been determined by ray-tracing simulations. A ray-tracing model was implemented in the software Tonatiuh, previously presented and validated experimentally [20]. Thus, the transversal and longitudinal incidence angle modifier IAM, $K_b(\theta_T,\theta_L)$, are estimated using a ray-tracing program. See Fig. 3 for a view of the PTC of the collector and its model in Tonatiuh.

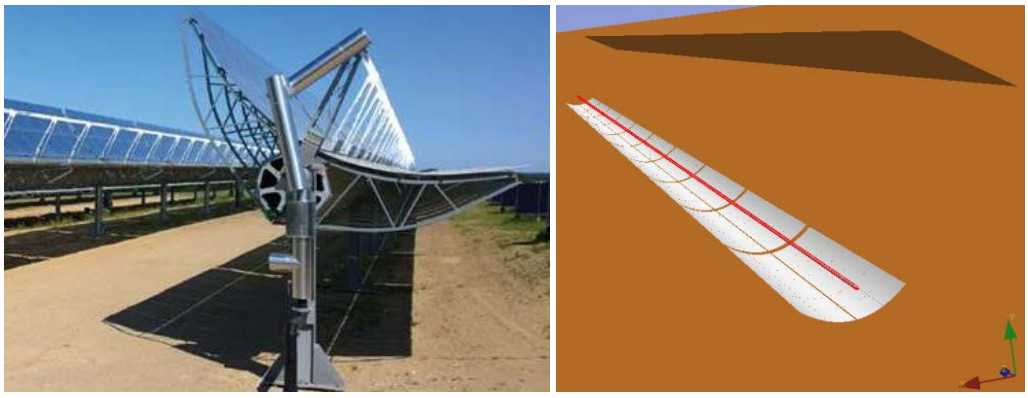

FIGURE 3. Picture and simulation of the PTC collector in Tonatiuh

In the ray-tracing program developed, the geometry of the solar concentrator is described by discrete elements with triangular surfaces. In this program four kinds of surfaces have been introduced: specular surfaces, opaque surfaces, interface surfaces (to implement glasses) and absorber surfaces (the receiver). The program calculates ray trajectories from one source (called the sun window) that emits to all the surfaces of the system, and only beam radiation is taken into account. The angular size of the sun has been modeled according to the Buie equations [21], and Fresnel effects are handled using a Monte Carlo approach. This program can calculate the optical efficiency and the radiation flux distribution on the absorber.

For the estimation of the optical efficiency of the collector, first angle dependencies of optical properties are considered. The collector is simulated fixing the longitudinal angle and changing the transversal angle, in order to see how these dependencies affect the efficiency. The angular dependencies of the optical properties are calculated with the next expressions. The transmittance of the cover $\tau(\theta)$ dependence curve of the incidence angle is according to [22], and the normal value according to manufacturer $\tau(0^o)=0.99$, as in Eq. 3.

$$\frac{\tau(\theta)}{\tau(0^o)} = 1 - \tan^{5.1}\left(\frac{\theta}{2}\right) \quad (3)$$

The reflectance of the reflectors dependence curve of the incidence angle is according to [23], and the normal value according to manufacturer $\rho(0^o)=0.94$. The absorptance of the receiver dependence curve of the incidence angle is according to [24], and the normal value according to manufacturer $\alpha(0^o)=0.94$, as in Eq. 4.

$$\frac{\alpha(\theta)}{\alpha(0^o)} = 1 - 0.017\left(\frac{1}{\cos\theta}\right)^{1.8} \quad (4)$$

The collector behaviour is simulated for angles from 0° to 90° in intervals of 10° in the longitudinal angle axis and from 0° to 2° in intervals of 0.2° in the transversal angle axis and the simulation is made with 10 million rays per iteration. The results are calculated with the information about photons that intersect with the receiver.

The optical efficiency is calculated with Eqs. 5 and 6:

$$\eta_{opt} = \frac{P_{receiver}(\theta_i)}{P_{incident}(\theta_i)} \quad (5)$$

$$P_{incident}(\theta_i) = G \cdot A_G \cdot \cos(\theta_i) \quad (6)$$

The IAM for any incidence angles, transversal and longitudinal $K_b(\theta_T,\theta_L)$, is calculated with Eq. 7:

$$K_b(\theta_T,\theta_L) = \frac{\eta_{opt}(\theta_T,\theta_L)}{\eta_{opt}(0°,0°)} \quad (7)$$

RESULTS

From the PTC dimensions, and according to the theoretical formulas Eqs. 1 and 2, the acceptance angle θ_a is 3.8 mrad (0.22º) and the defocus angle θ_d is 6.1 mrad (0.35º). The distribution of different incidence angles (tracking/transversal angle versus longitudinal angles) are presented in Fig. 4 with green dots, and the acceptance angle and defocus angle are shown with un-continuous lines. The longitudinal incidence angle change along the day from values from 0º to more +/-80º.

As seen in Fig. 4, the green dots are within the limit of the defocus angle lines, which means that for the 6 trackers, the tracking error (transversal angle) are mostly within the defocus angle θ_d (0.35º). However, some tracking errors higher than θ_d and up to 1º were observed (in the part top left of each graph inside the red ellipse). But those points were detected to be for days before 18/09/2015 when some tracking adjustment were done. It was observed that the behaviour of trackers nº 1–4 was similar, and that the trackers nº 5 and 6 had a similar behaviour too. Comparing to previous studies [16, 24], the tracking error lower than 0.5º is in line with normal PTC trackers behaviour.

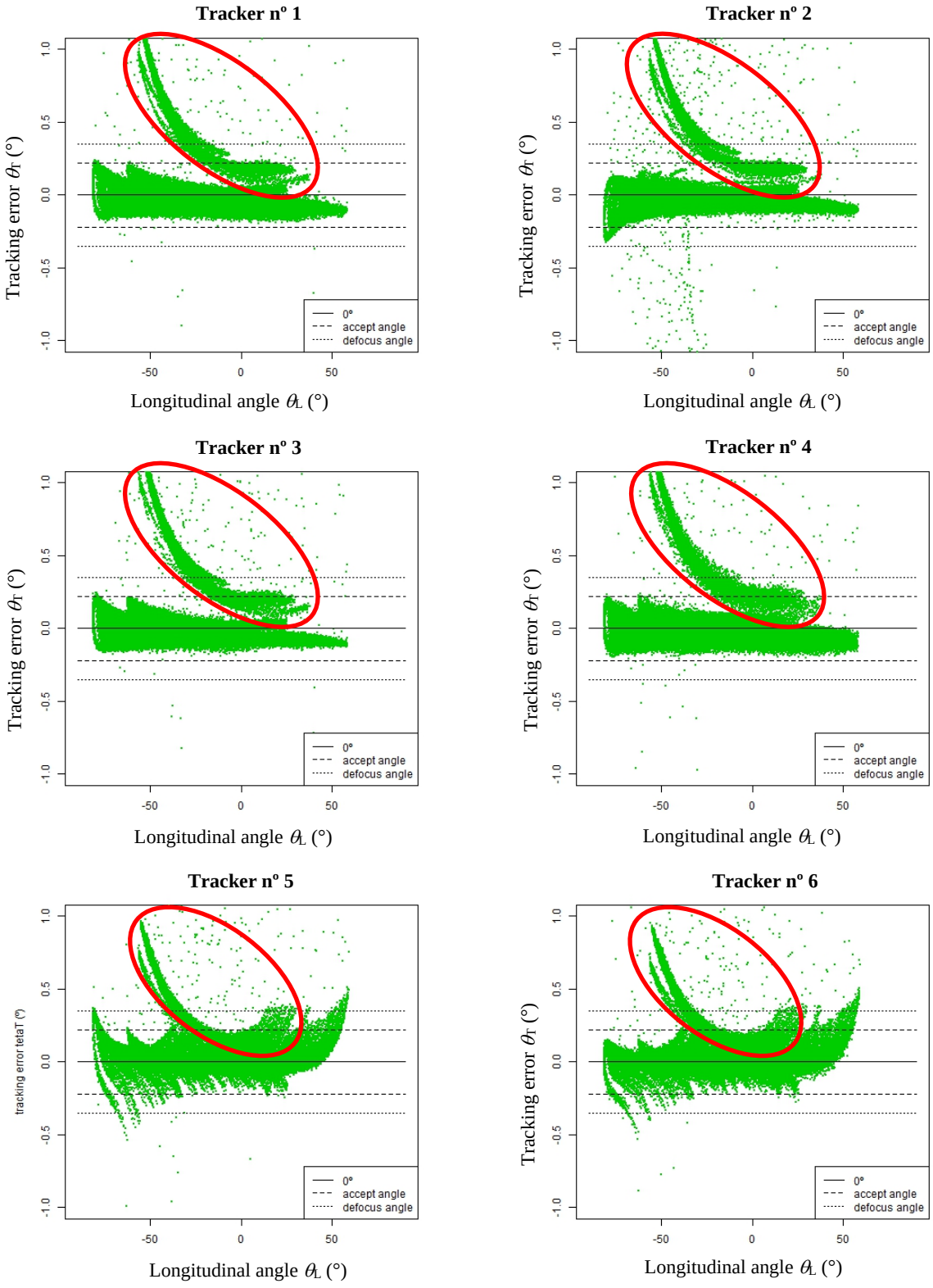

FIGURE 4. Tracking error distribution for the six solar trackers

Table 2 gives an overview of the maximum, minimum, mean and standard deviation of the tracker error along the day. From the standard deviation, it is seen than the tracking error is mostly lower than ±0.5º.

TABLE 2. Summary of tracking error for the 6 PTC trackers

Tracker nº	Min θ_T [º]	Max θ_T [º]	Mean θ_T [º]	Stand. dev. θ_T [º]
1	-0.55	0.48	-0.25	0.47
2	-1.47	1.30	-0.26	0.31
3	-0.49	0.67	-0.23	0.49
4	-0.53	0.20	-0.24	0.49
5	-0.51	0.87	-0.22	0.52
6	-0.62	0.50	-0.25	0.50

From the optical simulation with Tonatiuh, the values of IAM of different longitudinal and transversal angles were calculated and shown in Fig.5.

IAM is represented as functions of the longitudinal and transversal angle independently for a clearer view of the IAM variation.

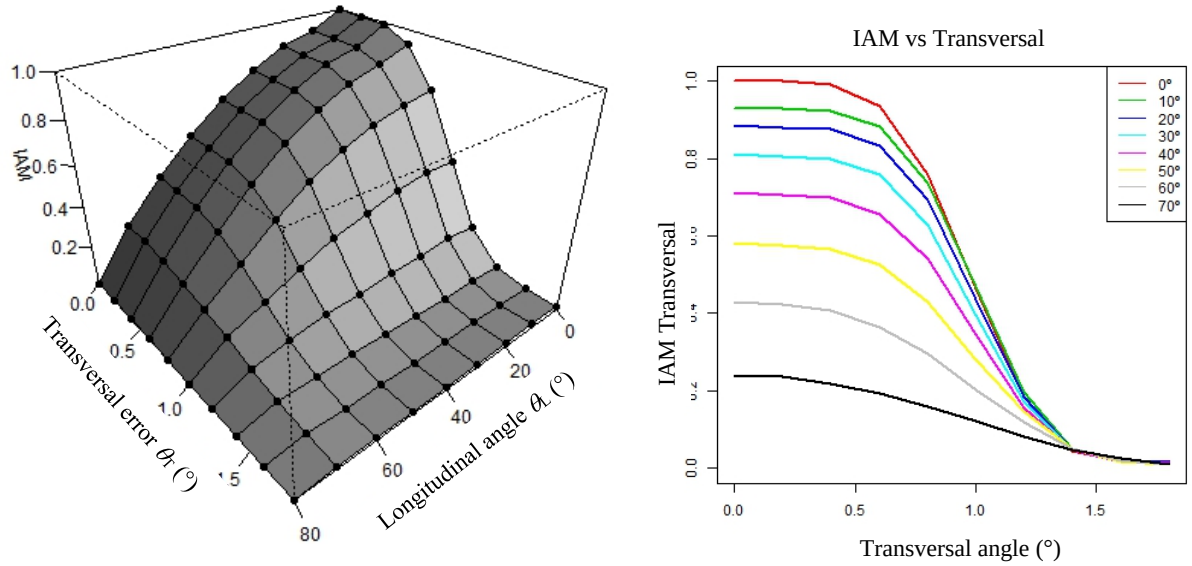

FIGURE 5. (a) 3D view of the longitudinal and transversal IAM obtained by ray-tracing (b) View of the IAM as function of transversal incidence angle for different longitudinal angles

The simulated transversal IAM $K_b(\theta_T)$ is presented in Fig. 5b and it can be seen that it decreases for transversal angles θ_T between 0.5º and 1º, which is a much larger range than the theoretical defocus angle calculated from Eq. 2. From this curves and the value from Fig. 4 it is estimated that the optical losses due to tracking error would be neglected.

Fig. 6 shows the power flux diagram on the perimeter of the receiver tube. It is seen in Fig. 6b how the distribution of the flux is moving around the tube perimeter while the transversal incidence angle is increasing.

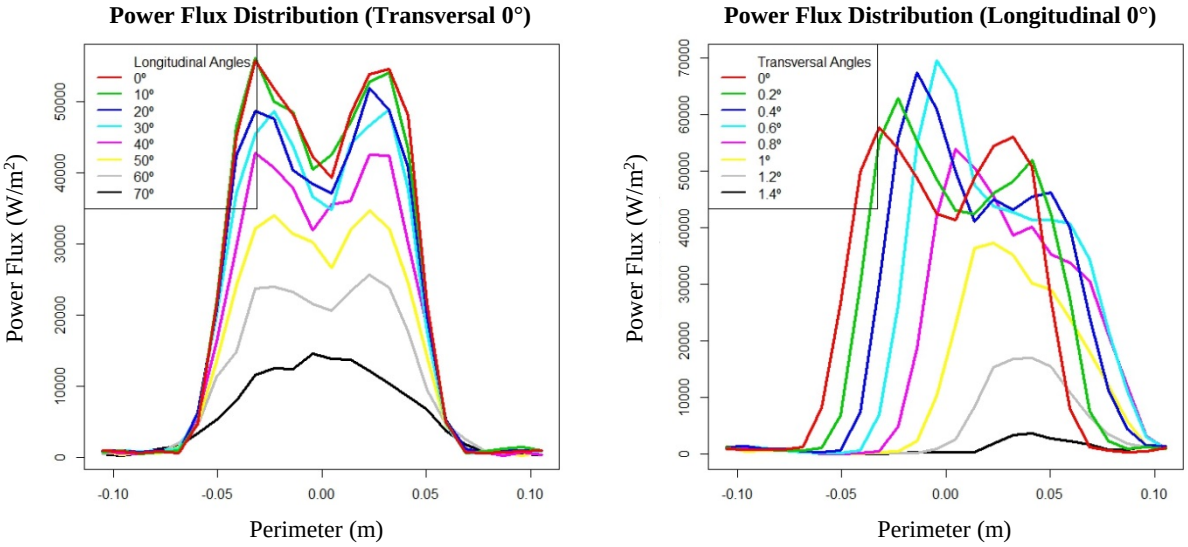

(a) (b)

FIGURE 6. (a) View of the perimeter flux distribution for different longitudinal angles, (b) View of the perimeter flux distribution for different transversal angles

CONCLUSIONS

Six PTCs rows with solar tracker used for district heating in Denmark were analyzed. The IAM was determined by optical simulation, in particular for transversal incidence angles in order to estimate the impact of the missfocusing of the tracker on the collector efficiency. The results show that the tracking error was most of the time lower than ±0.2º which is lower than the theoretical defocus angle of the concentrator. But, in some cases, the tracking error reaches more than 1º, which could cause some optical losses reducing the PTC performance.

ACKNOWLEDGEMENTS

The research leading to these results is thanks to collaboration between CENER and DTU during the year 2016-2017 and to the Danish Energy Agency due to the support through the EUDP program. Great thanks to Aalborg CSP making all measured data avaiable and giving all detailed facts about the collectors.

REFERENCES

1. W. Weiss, M. Spörk-Dür, F. Mauthner, 2017. Solar Heat Worldwide. Global Market Development and Trends 2016. Detailed Market Figures 2015. SHC Solar Heating & Cooling Programme, International Energy Agency, Edition 2017.
2. B.Perers, S.Furbo, J.Dragsted. Thermal performance of concentrating tracking solar collectors. DTU R-292. Technical University of Denmark, DTU Byg. August 2013
3. B. Perers, S. Furbo, Z. Tian, J. Egelwisse, F. Bava, and J. Fan, "Tårs 10000 m2 CSP + Flat Plate Solar Collector Plant - Cost-Performance Optimization of the Design," Energy Procedia, vol. 91, pp. 312–316, 2016.
4. Z. Tian, B. Perers, S. Furbo and J. Fan., Annual measured and simulated thermal performance analysis of a hybrid solar district heating plant with flat plate collectors and parabolic trough collectors in series, Manuscript, July, 2017.
5. N. Janotte, E. Lüpfert, R. Pitz-Paal, 2012. Acceptance Testing and advanced Evaluation Strategies for Commercial Parabolic Trough Solar Fields. 18th SolarPACES Conference, 11 - 14 September 2012, Marrakech, Morocco.
6. D. Kearney, 2011. Utility-scale parabolic trough solar systems: performance acceptance test guidelines

7. L. Valenzuela, R. López-Martín, E. Zarza, 2014. Optical and thermal performance of large-size parabolic-trough solar collectors from outdoor experiments: A test method and a case study. Energy 70, 456–464. doi:http://dx.doi.org/10.1016/j.energy.2014.04.016
8. MC Bhatnagar, JC Joshi, AK Mukerjee. Determination of tracking error in an automatic sun tracking system. Sol Wind Technol 1987;4(3):399–403.
9. M. Minor, P.García High-precision solar tracking system. London, U.K.: World Congress on Engineering; 2010.
10. M. Oliveira Análise do desempenho de um gerador fotovoltaico com seguidor solar azimutal. Porto Alegre; 2008. http://hdl.handle.net/10183/14737
11. F. Sallaberry, F. Alberti, J.-L. Torres, L. Crema, M. Roccabruna and R. Pujol Nadal. Characterization of a medium temperature concentrator for heat process – tracking error estimation. EuroSun Conference, 16 – 19 September 2014, Aix-les-Bains, France.
12. F. Sallaberry, A. García de Jalón, J.-L. Torres, R. Pujol-Nadal, Optical losses due to tracking error estimation for a low concentrating solar collector. Energy Conversion and Management 92 (2015) 194–206
13. F. Sallaberry, Ramón Pujol-Nadal, Bengt Peres. Optical losses due to tracking on solar thermal collectors. EuroSun Conference, 11 - 14 October 2016, Palma de Mallorca (Spain),
14. Archimede Solar Energy receiver tube datssheet, http://www.archimedesolarenergy.it/en_specifiche-prodotto-hceoi-12.htm
15. Rioglass Mirror Type LS-3 datssheet, http://rioglass.com/parabolic-trough-mirrors/
16. F. Sallaberry, R. Pujol-Nadal, M. Larcher, M. H. Rittmann-Frank, Direct tracking error characterization on a single-axis solar tracker, Energy Conversion and Management 105 (2015) 1281–1290
17. Standard draft IEC 62862-3-2 “Solar thermal electric plants - Part 3-2: Systems and components - General requirements and test methods for parabolic-trough collectors” (publication planned in 2017).
18. M. Blanco-Muriel, D.C. Alarcón-Padilla, T. López-Moratalla, M. Lara-Coira. Computing the solar vector. Solar Energy. 70 (2001) 431-41.
19. Bendt, P., Rabl, A., Gaul, H., and Reed, K. Optical analysis and optimization of line focus solar collectors. Tech. rep., Solar Energy Research Inst., Golden, CO (USA), 1979
20. Blanco, M., Mutuberria, A., Monreal, A., Albert, R., 2011. Results of the empirical validation of Tonatiuh at Mini-Pegase CNRS-PROMES facility. 17th SolarPACES Conference, 20 - 23 September 2011, Granada, Spain.
21. Buie D., Monger A. G., Dey C. J., 2003, “Sunshape distributions for terrestrial solar simulations”
22. S. Furbo, Z. Chen, J. Fan and J. M. Schultz, “Solar transmittances for glass covers with and without anti reflection treatment under real climatic conditions”.
23. Marco Montecchi, 2013, “Approximated method for modelling hemispherical reflectance and evaluating near-specular reflectance of CSP mirrors”.
24. Tesfamichael T. Wäckelgard E., 2000, “Absorptance and incident angle modifier of selective absorbers for solar thermal collectors”F. Sallaberry, L. Valenzuela, A. García de Jalón, J. Leon, Ig. D. Bernad, 2015. Towards Standardization of in-Site Parabolic Trough Collector Testing in Solar Thermal Power Plants. 21st SolarPACES Conference, 13 - 16 October 2015, Capetown, South-Africa.

Paper VI

Benjamin Ahlgren, **Zhiyong Tian**, Bengt Perers, Janne Dragsted, Emma Johansson, Kajsa Lundberg, Jonatan Mossegård, Joakim Byström, Olle Olsson.

A simplified model for linear correlation between annual yield and DNI for parabolic trough collectors.

Energy Conversion and Management, vol. 174, pp. 295–308, 2018.

This page is intentionally left blank.

Energy Conversion and Management 174 (2018) 295–308

Contents lists available at ScienceDirect

Energy Conversion and Management

journal homepage: www.elsevier.com/locate/enconman

A simplified model for linear correlation between annual yield and DNI for parabolic trough collectors

Benjamin Ahlgren[a], Zhiyong Tian[b,*], Bengt Perers[b], Janne Dragsted[b], Emma Johansson[a], Kajsa Lundberg[a], Jonatan Mossegård[c], Joakim Byström[c], Olle Olsson[c]

[a] Umeå University, SE-901 87 Umeå, Sweden
[b] Department of Civil Engineering, Technical University of Denmark, Brovej Building 118, Lyngby 2800, Denmark
[c] Absolicon Solar Collector AB, Fiskaregatan 11, SE-871 33 Härnösand, Sweden

ARTICLE INFO

Keywords:
Simplified methods
Parabolic trough collectors
DNI
Annual yield

ABSTRACT

This paper proposes a simple method for estimating annual thermal performance of parabolic trough collectors (PTCs) based on a linear relation with annual DNI for a certain latitude. A case study with simulations for a novel concentrating solar collector in 316 locations for three operating temperature scenarios worldwide was carried out and showed promising results for the latitudes and continents investigated. For a certain latitude and mean operating temperature, the annual yield of a PTC was found to be linearly proportional to yearly DNI. The proposed method will serve as a simplified alternative to the steady-state and quasi-dynamic methods already used. Estimating performance based on yearly DNI can be used by design engineers to do quick preliminary planning of solar plants. Customers can also use this method to evaluate existing solar collector installations. A TRNSYS/TRNSED tool that uses a steady-state model has been developed to carry out the simulations and it has been validated against a PTC array at Technical University of Denmark (DTU). The results show that the simplified method can give reliable estimates of long-term performance of parabolic trough collectors.

1. Introduction

The building sector consumes about 40% of the total society energy in the developed countries [1]. Space heating and domestic hot water systems account for more than 50% of the energy consumption in the building sector. Solar thermal energy systems are one of the most promising ways to reduce the fossil energy consumption. Large-scale solar collector arrays gain more and more interest in the district heating networks or industry processes. Small-size concentrating solar collectors with high efficiency is suitable for these applications.

Sweden was the first country to apply large solar collector arrays into district heating systems in the 1980s. Then solar district heating plants gained success in Denmark [2], Germany, and Austria. Denmark is presently the front-runner worldwide in the solar district heating plants [3]. By the end of 2016, more than 1.3 million m^2 of solar collectors were in operation in Denmark. China is an emerging market for large-scale solar thermal plants, reducing the air pollution in the winter.

Most solar collectors in existing plants are ground-mounted flat plate collectors and previous research is mainly on flat plate collector arrays. Parabolic trough collectors have shown more and more advantages in the low temperature level 70–150 °C [4]. The heat loss of concentrating solar collectors is much lower than the flat plate collectors so higher temperature heat can be produced with good efficiency. This guarantee better performance in industry applications and charging of heat storages compared to flat plate collector arrays.

Traditionally, complicated procedures or expensive software is used to calculate the performance of the parabolic trough collector array. To make qualified assumptions on the thermal performance of a PTC array, it is important to simulate the performance in a quick and cost-effective way.

1.1. Previous simulation work

TRNSYS is used widely in solar thermal energy systems simulation [5]. Most users of TRNSYS are researchers, focusing on the research purpose [6]. Bava et al. [7] developed a MATLAB-TRNSYS model on large solar collector fields for district heating networks. Kong et al. [8,9] proposed a new transfer function method for flat plate collectors. Deng et al. [10–12] developed a second-order transfer function model for dynamic test on the flat plate collectors. Tian et al. [13–15] applied the quasi-dynamic model to simulate the short and long-term performance for both large-scale flat plate collector fields and parabolic trough collector fields.

* Corresponding author.
E-mail addresses: tianzy0913@163.com, zhiytia@byg.dtu.dk (Z. Tian).

https://doi.org/10.1016/j.enconman.2018.08.008
Received 27 April 2018; Received in revised form 24 July 2018; Accepted 4 August 2018

Nomenclature

Variables	Description	Unit
Q/A	collector yield per area	[W/m^2]
G_b	beam solar radiation in the collector plane	[W/m^2]
G_d	diffuse solar radiation in the collector plane	[W/m^2]
T_m	mean fluid temperature (T_{in} + T_{out})/2	[°C]
T_a	ambient temperature close to collector (in the shade)	[°C]
θ_L, θ_T	biaxial incidence angles for beam radiation onto the collector plane in longitudinal (L) and transversal (T) direction from the normal	[°]

Parameters	Description	Unit
$F'(\tau\alpha)$	zero loss efficiency of the collector for beam radiation, at normal incidence angle	[–]
$K_{\theta b}(\theta_L, \theta_T)$	incidence angle modifier (IAM) for beam solar radiation. This can be generalized to $K_{\theta b}(\theta_L)$ in the case of a tracking concentrating collector with north to south tracking axis	[–]
b_0	incidence angle modifier coefficient	[–]
$K_{\theta d}$	incidence angle modifier for diffuse solar radiation	[–]
c_1	heat loss coefficient	[W/(m^2·K)]
c_2	temperature dependence in heat loss coefficient	[W/(m^2·K^2)]

Vela Solaris [16] has developed a commercial simulation tool for designing engineers and energy consultancies that is called Polysun. The RISE Research Institutes of Sweden has developed a user-friendly standardized open source tool for calculating the annual energy output for solar collectors available in the market – ScenoCalc [17]. The tool is now being used within the Solar Keymark, the quality labeling of solar thermal products in Europe for calculating certified annual collector output. The tool was developed within the EU-project *Quality Assurance in Solar Thermal Heating and Cooling Technologies* (QAIST) and uses a Microsoft Excel interface. Even though ScenoCalc is further developed by Berberich et al. [18], one drawback of ScenoCalc is that the shadow between the collector rows, in a field, is not taken into consideration.

Many existing publications on the parabolic trough collectors are on the detailed optical models and heat transfer models [19,20]. Reddy et al. [21] did sensitivity studies of thermal performance characteristics based on optical parameters for direct steam generation from parabolic trough collectors. Xu et al. [22] developed a numerical model to quantify several important factors affecting heat losses, and reveal the relationship between heat losses and the overall performance of parabolic trough solar collectors under various boundary conditions. Monte Carlo Ray Tracing method (MCRT) and Finite Volume Method have been widely used to determine optical performance or thermal performance of parabolic trough collectors [23–28]. ANSYS – Fluent was also widely used by the researchers to calculate the performance of parabolic trough collectors [29–32]. These research may be useful to develop single parabolic trough collector components for the manufactures. However, publications on the accurate and quick estimation of the performance of large PTC arrays are limited, as far as we know. A simple model is necessary for the solar industry and end-users to guarantee the thermal performance of parabolic trough collectors.

1.2. Scope

Parabolic trough collectors mainly use the beam radiation to produce heat [33]. This study proposes a simple prediction model of annual performance of large parabolic trough array based on a linear relation to yearly DNI, at a certain latitude worldwide. That model makes it possible also for non-experts to plan and evaluate collector fields since annual DNI data is easily accessible for most locations, e.g. through Global Solar Atlas [34]. It enables solar companies and engineers to speed up their preliminary planning of solar thermal plants. It also enables end-users around the world to better understand the potential of implementing solar energy.

This study aims to verify the hypothesis of linearity between annual output and total yearly DNI by running a big set of simulations, 316 locations under three operating temperature scenarios (948 cases). The simulations are done using a self-developed and validated TRNSYS/TRNSED simulation tool.

2. Methods

The methods of this study can be divided into two parts. The first one is to get simulated data based on the solar collector model. This includes both developing a TRNSYS/TRNSED tool for multiple simulations and validation against measured collector data. The second part is comparing the annual output with the yearly DNI to test the hypothesis of linearity.

2.1. Solar collector model

The solar collector modelling, testing and simulation methodologies can be divided into steady-state (SST), quasi-dynamic (QDT) and fully dynamic (DT) methods. The method of modelling and performance was carefully analyzed in [35] which is the fundamental basis for the simulation tool used in this paper. The basic collector model concept was analyzed and validated for a full operating season by Perers [36].

The simplified SST model for collector yield used in this study can be expressed as Eqs. (1)–(3) [37].

$$Q/A = F'(\tau\alpha)K_{\theta b}(\theta_L, \theta_T)G_b + F'(\tau\alpha)K_{\theta d}G_d - c_1(T_m - T_a) - c_2(T_m - T_a)^2 \quad (1)$$

where

$$K_{\theta b}(\theta_L, \theta_T) = K_{\theta b}(\theta_L)K_{\theta b}(\theta_T) \quad (2)$$

and

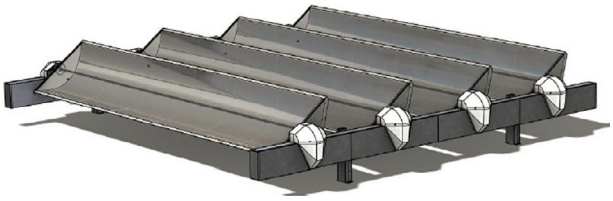

Fig. 1. Concentrating solar collector Absolicon T160 [40].

Table 1
Dimensions of T160 collector unit [41].

Length	5.490 m
Width	1.056 m
Absorber area	0.44 m^2 (specified by Absolicon)
Gross area	5.8 m^2 (measured by RISE)

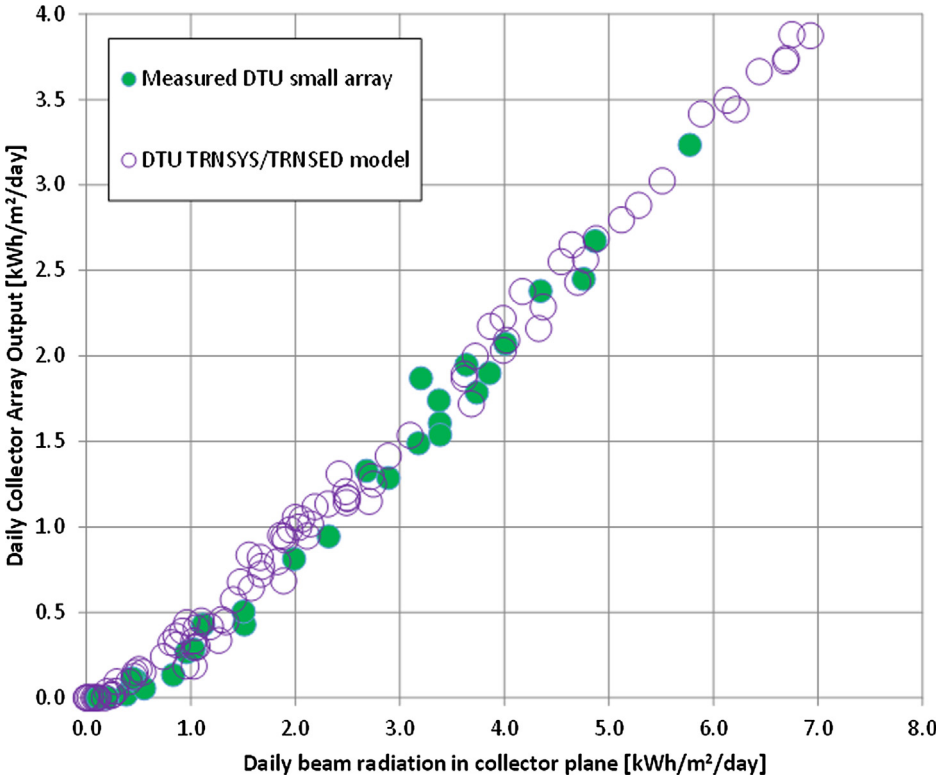

Fig. 2. Validation of the simulation tool used versus measured data for a four troughs-array at DTU in Copenhagen Denmark. Measurements during July to mid-September 2017. Green dots represent measured performance and purple rings is simulated performance with the tool used in this study. (For interpretation of the references to colour in this figure legend, the reader is referred to the web version of this article.)

$$K_{\theta b}(\theta_L) = 1 - b_0\left(\frac{1}{\cos\theta_L} - 1\right) \quad (3)$$

In this paper, the collector is tracking the sun with the tracking axis aligned north to south so that $K(\theta_T) = 1.0$. When the θ_L approaches 90°, the IAM ($K_{\theta b}(\theta_L)$) decreases. Since the IAM reaches zero before $\theta_L = 90°$, negative IAM values were set to 0.

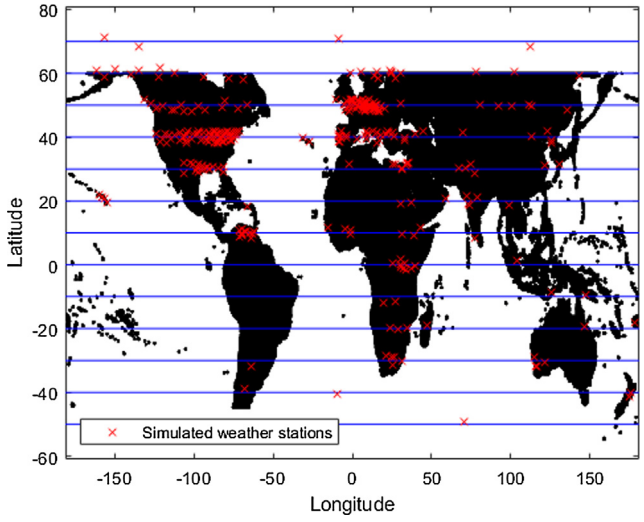

Fig. 3. The locations where the performance was simulated is shown with red crosses. More locations were chosen on some latitudes due to easier access to accurate weather data. Locations where interpolated annual DNI can be obtained from e.g. Global Solar Atlas [34] are indicated in black. The investigated latitudes are marked with blue lines. (For interpretation of the references to colour in this figure legend, the reader is referred to the web version of this article.)

The simplified SST model was used to get very fast annual simulations since many locations and three operating temperatures were to be investigated. The sky radiance and wind terms was assumed to be zero [37] since the PTC used here is covered with glass which makes those terms small. The capacitance term was neglected since one-hour resolution data was used and capacitance is insignificant on that time resolution [38]. The simplification without thermal capacitance term is also chosen in the ScenoCalc tool [17] used in the Solar Keymark.

The principle of TRNSYS Type 30 [39] was used to simulate the shadows between the solar collector troughs in an array. The collector length was assumed to be infinite, hence only shadowing between rows were accounted for.

2.1.1. Validation of solar collector model

The Absolicon T160 collector, see Fig. 1, was used in both simulations and validation of the collector model. T160 is a tracking concentrating collector with parabolic mirrors and a selective absorber tube placed in the focal line position. It is covered with glass that also is part of the mechanical structure. The design is optimized and adapted to fast robot manufacturing.

Table 2
Collector parameters from preliminary SPF test results for Absolicon T160 [25]. The parameters are based on aperture area.

Parameter	Value	Unit
$F'(\tau\alpha)$	0.7661	[–]
b_0	0.210	[–]
$K_{\theta d}$	0.08586	[–]
c_1	0.3677	[W/(m^2·K)]
c_2	0.003224	[W/(m^2·K^2)]
Aperture width	1.056	[m]

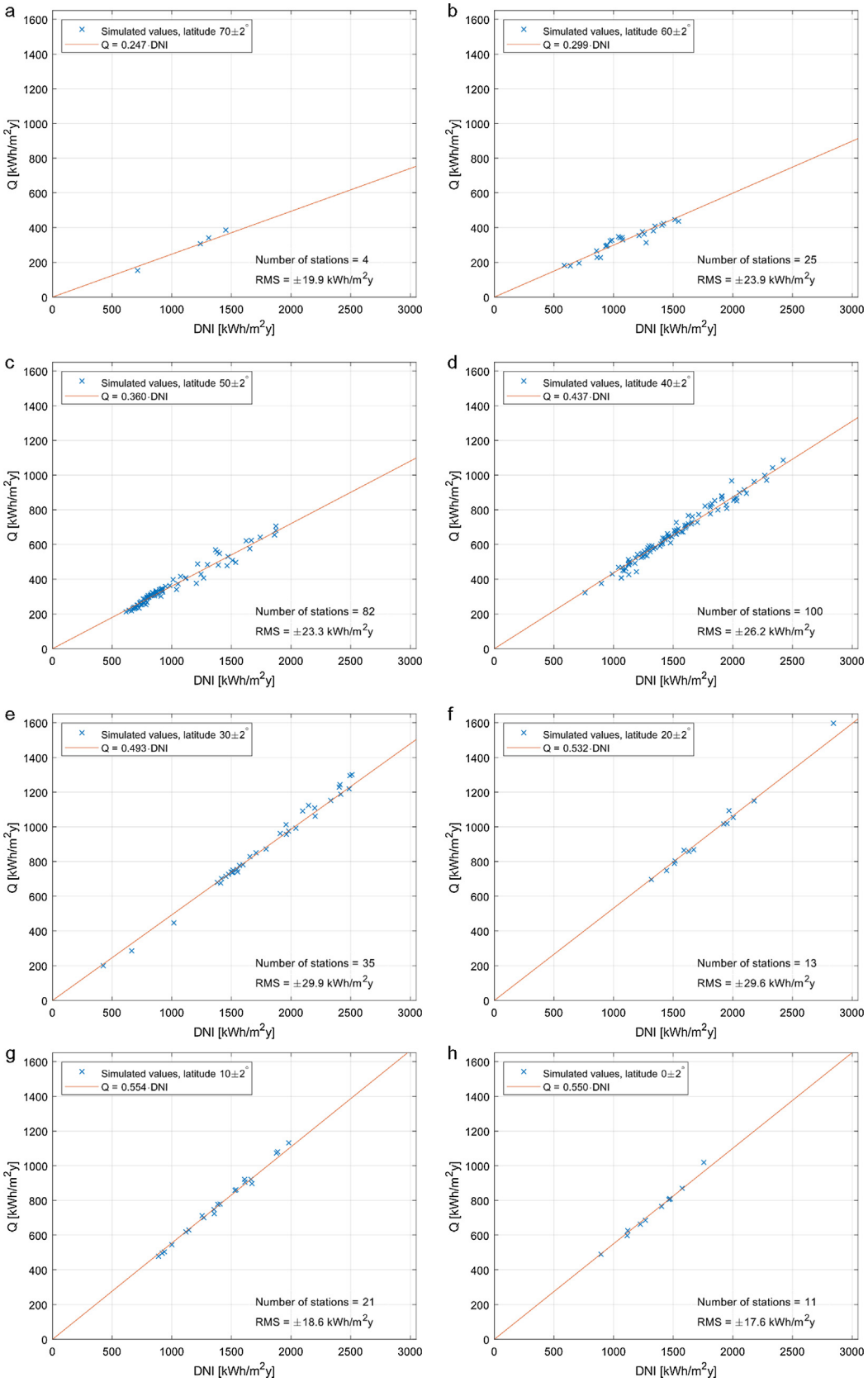

Fig. 4a–h. Simulated values for annual T160 collector yield compared to DNI around latitudes 70°, 60°, …, 0°. Collector yield simulations based on a mean operating temperature of 85 °C. A linear regression is shown with a red line. (For interpretation of the references to colour in this figure legend, the reader is referred to the web version of this article.)

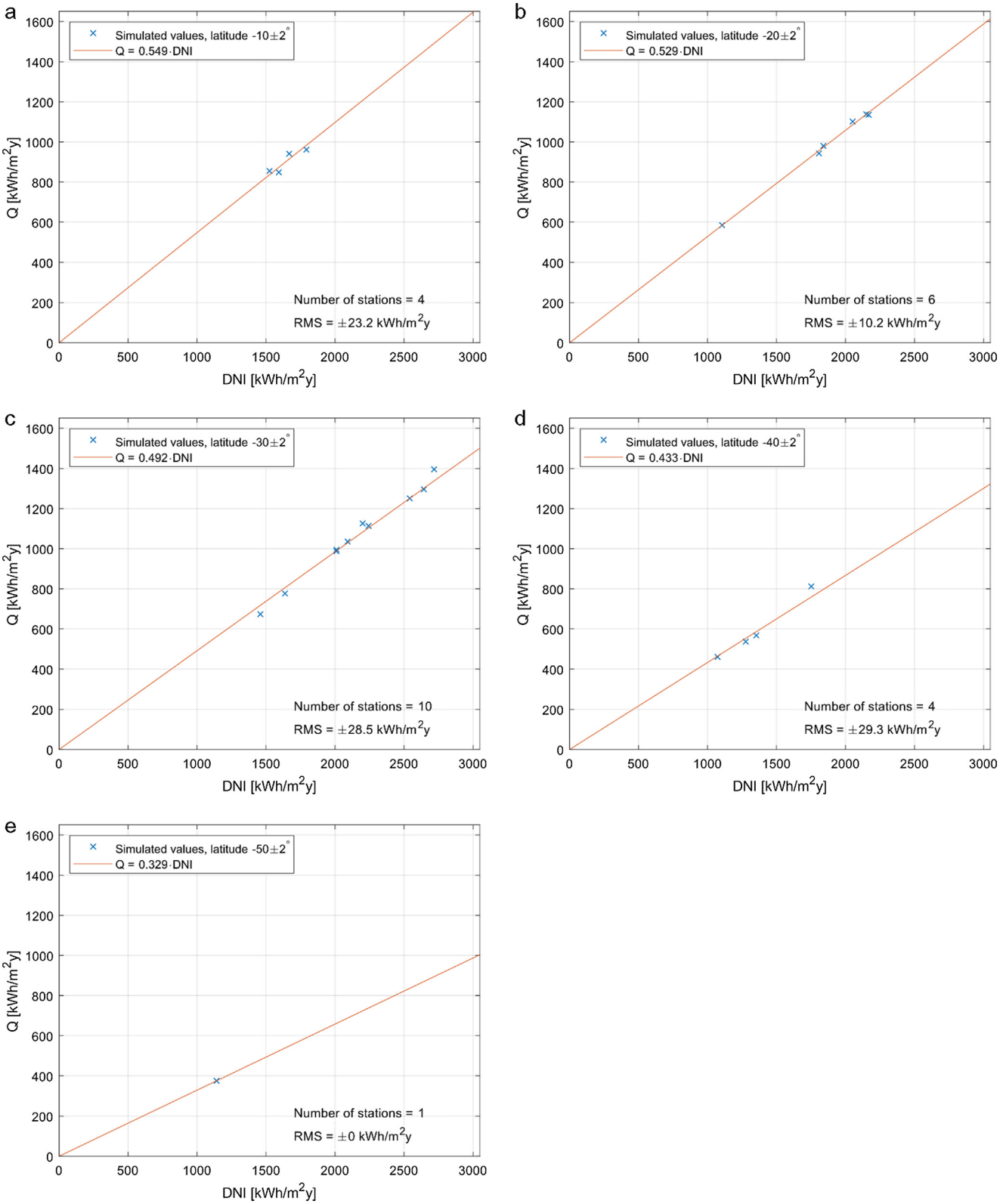

Fig. 5a–e. Simulated values for annual T160 collector yield compared to DNI around latitudes −10°, −20°, …, −50°. Collector yield simulations based on a mean operating temperature of 85 °C. A linear regression is shown with a red line. (For interpretation of the references to colour in this figure legend, the reader is referred to the web version of this article.)

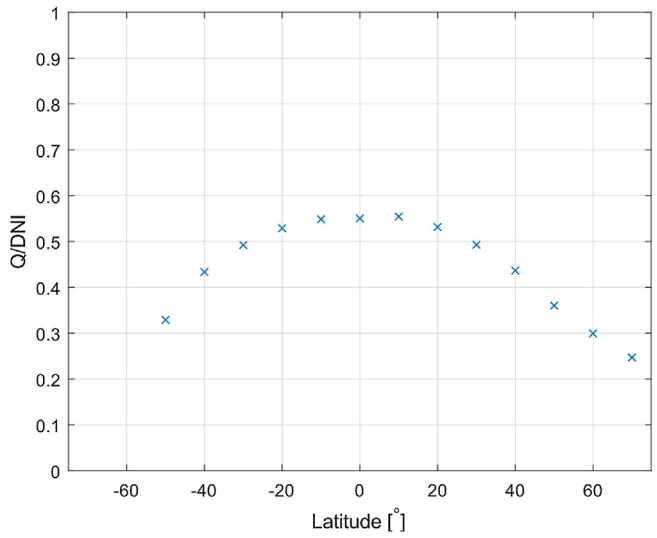

Fig. 6. Energy output per DNI plotted against latitude. Collector yield simulations based on a mean operating temperature of 85 °C.

In the basic installation design, the tracking axis is horizontal and can be installed in any azimuthal direction depending on local conditions like available roof or ground area direction. Load distribution over the day and year is also a factor.

The dimensions of T160 parabolic trough collector are listed in Table 1. The troughs are quite short so that the collector can have tracking axis tilt, which has been found to increase the annual performance significantly, especially at higher latitudes.

The solar collector model used for the simulations in this paper was validated in a case study against measurements for an array of 4 troughs at DTU in Copenhagen. The measurements lasted for 2.5 months starting July 2017. The parameters of T160 collector has been tested (QDT) at RISE (Research Institutes of Sweden) during 2016 [41] and the test results from RISE was used in the collector model when validating against measured data at DTU, see Fig. 2.

Fig. 2 gives a solid indication that the simulations in this paper should be realistic and give accurate long-term performance results. The measured and simulated energy outputs have good agreements in both sunny and cloudy days.

2.2. Simplified model based on DNI

The hypothesis was that the annual collector array performance would depend linearly on annual DNI, as expressed in Eq. (4)

$$Q = k_1 \times DNI \tag{4}$$

where Q is the annual yield, k_1 is a constant and DNI is the yearly DNI. A significant latitude effect was found for a horizontal north-south tracking axis so the formula was elaborated to Eq. (5) as

$$Q = k_1(latitude) \times DNI \tag{5}$$

where $k_1$is dependent on the latitude. This is a very simple relation that can be used quickly if just the local DNI and latitude is known.

There is also an operating temperature dependence in k_1. The full basic formula should then be Equation (6)

$$Q = k_1(latitude, T_m) \times DNI \tag{6}$$

where k_1 is dependent on both latitude and mean operating temperature, T_m.

2.2.1. Verification of simplified model

To confirm the hypothesis described above (Eqs. (4)–(6)), a set of 862 climate conditions was generated as typical meteorological years (TMY) from weather stations (non-interpolated data) in TRNSYS 17 [42]. The time resolution of the climate files was one hour. Climates closer than ± 2° to latitudes −50°, −40°, …, 60°, 70° was selected to define k_1 for all 13 latitudes worldwide. Due to lack of weather stations at some latitudes the number of climates selected for each latitude varied between 1 (at latitude −50°) and 100 (at latitude 40°), see Tables 3–5. The climate at −50° was kept even though it was the only one for the latitude. It was done to see whether it followed the pattern of decreasing k_1 at higher or lower latitudes.

Totally 316 climate stations were selected and investigated to confirm the hypothesis of the simplified model. The selected climate locations are indicated with red crosses in Fig. 3.

Simulations were done with the TRNSYS/TRNSED tool for a T160 array of 20 collectors for three mean operating temperatures (T_m), 85 °C, 120 °C and 160 °C. The TRNSYS/TRNSED tool was validated in Section 2.1.1. The collectors were tracking the sun movement from east to west with a horizontal north to south tracking axis. The center to center row distance of the troughs was 1.4 m and their azimuth angle (deviation from south) was 0°. The collector parameters used is from preliminary test results at SPF [43] for the latest T160 model and can be seen in Table 2.

The simulated yield for each weather station and operating temperature was grouped by latitude and compared to DNI. Linear regression then gave k_1 in Eq. (6).

2.3. Offset at zero DNI

When the simplified model was developed there was a discussion about whether to include an offset term, related to the heat losses from the collector array. The normal Input-Output curves have such an offset [44] if daily values are plotted. The motivation to make the analysis without offset is that the collector heat losses are very small for a concentrating collector and the annual operating time will also vary systematically with available annual solar radiation, DNI in this case [35]. Therefore, in a tentative zero DNI case, the operating time and thereby the heat losses would also be close to zero and the offset will not be a relevant parameter in the model.

Previous studies of this kind of very simple annual performance relations, for flat plate and vacuum tube collector's performance [45], indicated a negative zero offset when applying a similar collector model. They plotted annual collector output versus global horizontal radiation instead of DNI. In that case the variation in global radiation was due to small changes among different real years and different locations. The heat losses of the concentrating collectors studied in this paper are in the range of 5–10 times lower (around 0.5–1.0 W/(m^2 K) for a medium concentrating collector, compared to 3–4 W/(m^2 K) for a typical flat plate collector) than for flat plate collectors so the offset should be very small. Collector test parameters including heat losses for various collector types, can be found in the Solar Keymark Database [46].

A full verification of the zero-offset assumption cannot be done by statistical methods as there are no locations with climates that has even close to zero annual DNI on earth. Therefore, it was decided to make a model design freeze for the simplified tool at this level and constrain the model to pass the origin.

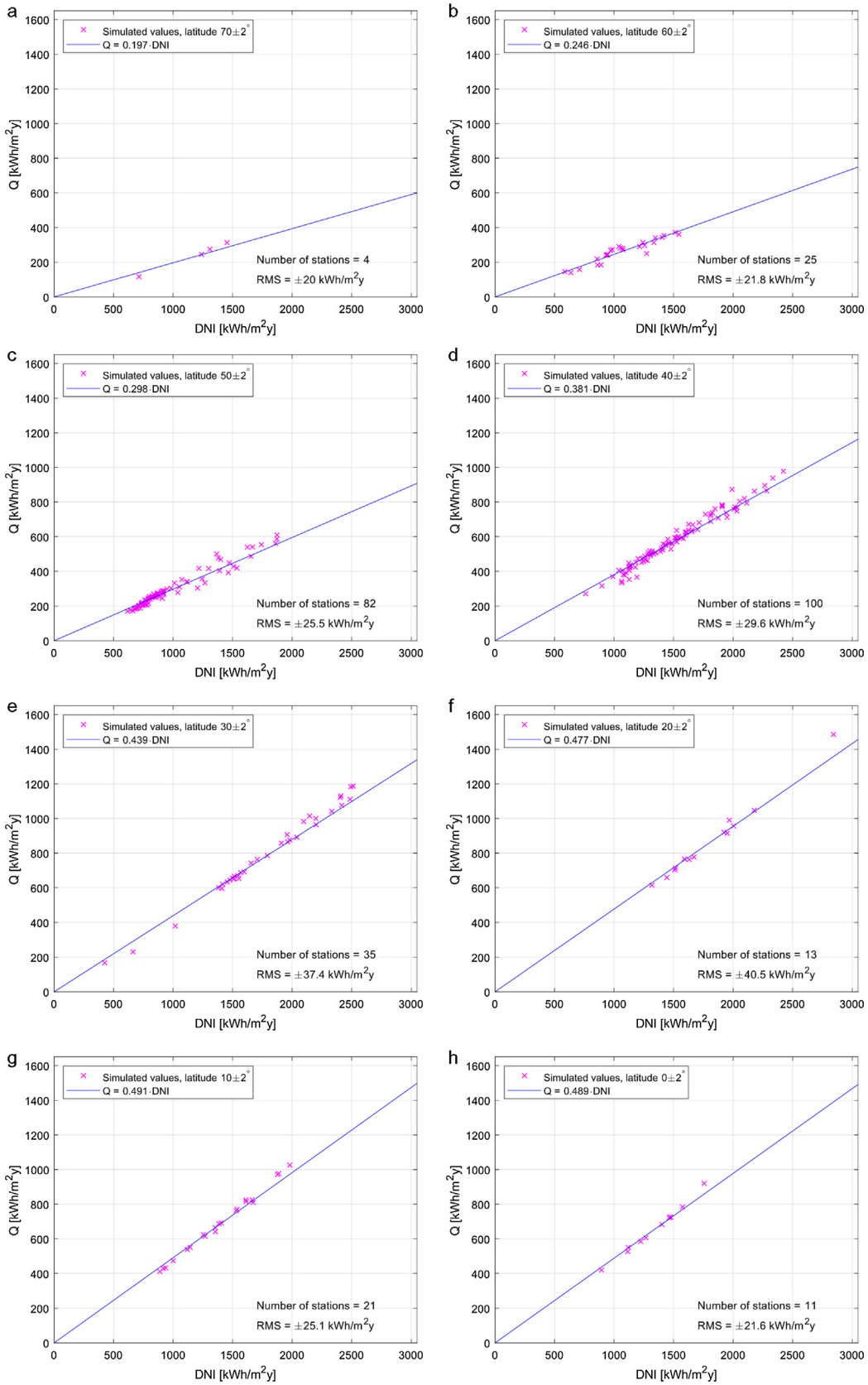

Fig. 7a–h. Simulated values for annual T160 collector yield compared to DNI around latitudes 70°, 60°, …, 0°. Collector yield simulations based on a mean operating temperature of 120 °C. A linear regression is shown with a blue line. (For interpretation of the references to colour in this figure legend, the reader is referred to the web version of this article.)

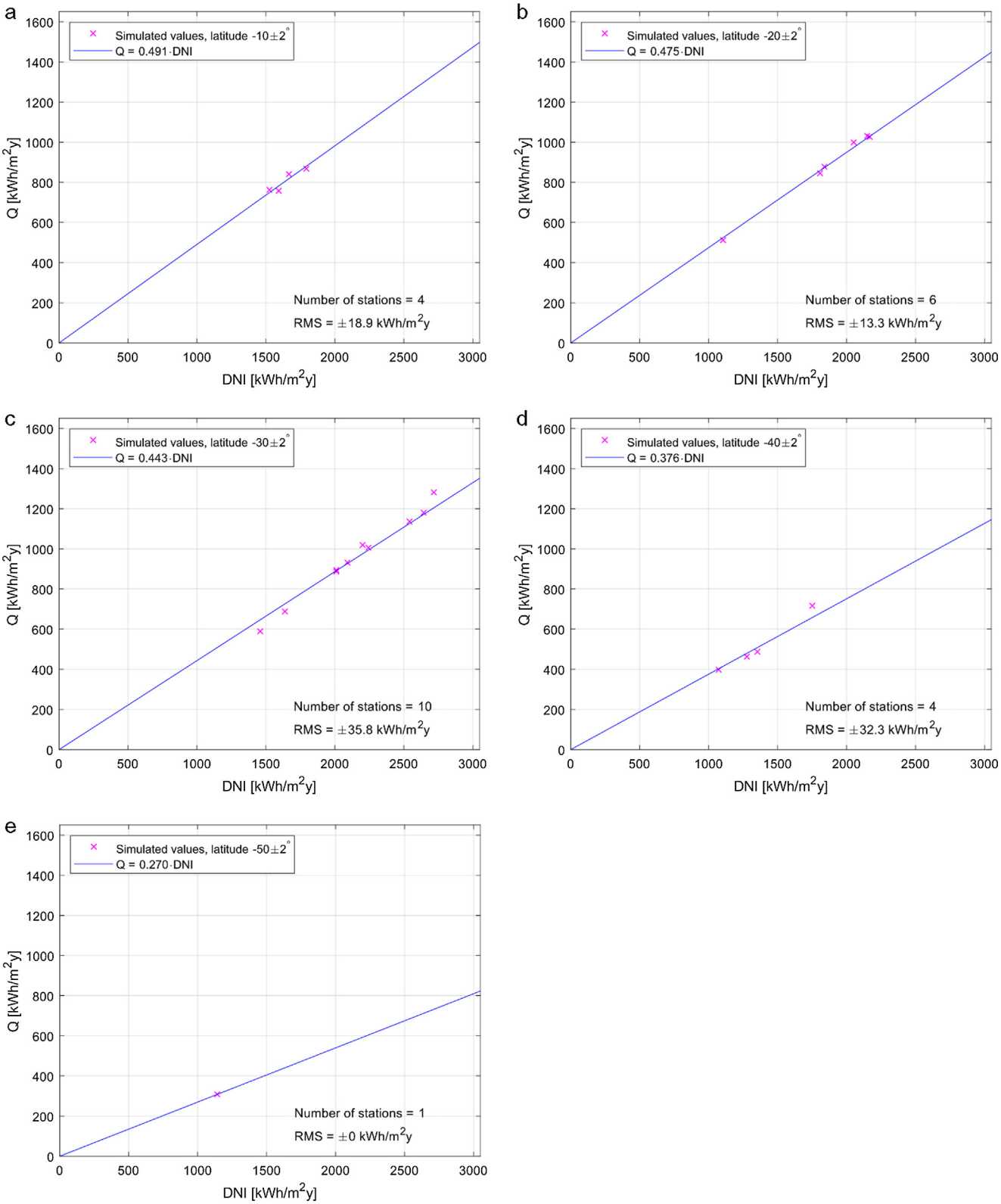

Fig. 8a–e. Simulated values for annual T160 collector yield compared to DNI around latitudes −10°, −20°, …, −50°. Collector yield simulations based on a mean operating temperature of 120 °C. A linear regression is shown with a blue line. (For interpretation of the references to colour in this figure legend, the reader is referred to the web version of this article.)

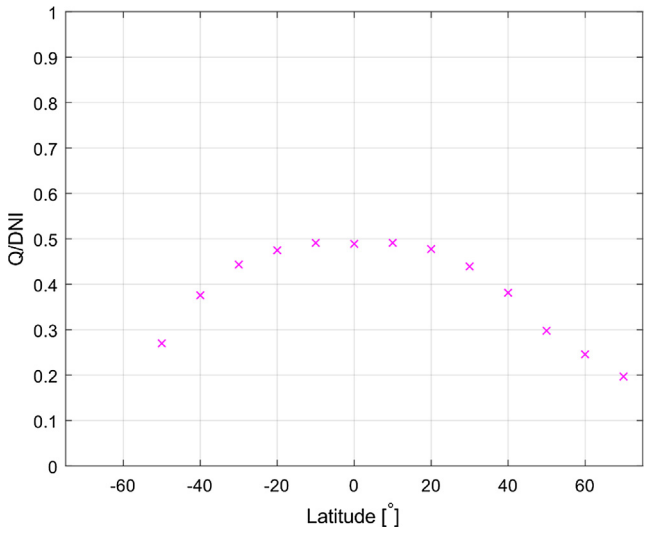

Fig. 9. Energy output per DNI plotted against latitude. Collector yield simulations based on a mean operating temperature of 120 °C.

3. Results and discussions

Plots of the results for mean operating temperature 85 and 120 °C, divided by latitude, is displayed in Figs. 4–9 in this section. Plots for T_m = 160 °C can be seen in Appendix. All the results indicate a strong linearity around all investigated latitudes except at −50° where no conclusions can be drawn due to lack of data. The biggest difference between the mean operating temperatures is the lower k_1 and the slight increase in model error at higher temperature. Both are most likely due to the increased heat loss. T_m = 85 °C and T_m = 120 °C will here be discussed more in detail.

3.1. Strong linearity

3.1.1. Mean operating temperature 85 °C

At 40° north (Fig. 4d) there were 100 weather stations available. The simplified model predicts an annual yield of 43.7% of available DNI there. As shown in the Fig. 4d the root-mean-square error (RMS) of the prediction was ± 26.2 kWh/(m^2 y). Most locations at the latitude were in the span of DNI 1100–1600 kWh/(m^2 y) and in that range the error was even smaller.

The widest span of DNI was found around 30° north and that is also where the RMS error was biggest, ± 30 kWh/(m^2 y). Fig. 4e indicates that the linearity holds over the whole span. Since the annual yield ranges from about 200–1300 kWh/(m^2 y), an RMS error of ± 30 kWh/(m^2 y) represents a relative error of 2.3–15% depending on whether the DNI was low or high on the location.

The longer from the equator, the lower the DNI, k_1 and hence the yield. At 50° north most of the 82 weather stations received DNI in the range of 500–1000 kWh/(m^2 y) and k_1 was found to be 0.360. The simulated yield was between 200 and 400 kWh/(m^2 y). An RMS of ± 23.3 kWh/(m^2 y) then represent 5.8–11.7% relative error. As one can see in Fig. 4c, the variation around the regression line was bigger at higher DNI so the relative error was smaller where most of the 82 stations are.

There are fewer weather stations at the south of the equator, as shown in Fig. 8a–e. The simulations based on the data available indicates strong linearity.

Fig. 6 shows the slope (k_1) of the regression lines for latitudes −50° to 70° and the very systematic variation with latitude. The slope is steepest at the equator and goes down towards the polar regions like a cosine curve. The relation is also quite symmetrical between north and south of the equator.

3.1.2. Mean operating temperature 120 °C

The linearity between annual energy output and total yearly DNI is clear at this temperature scenario as well, see Figs. 7 and 8. The deviation from the linear regression is slightly bigger compared to the results in Section 3.1.1. The biggest RMS error is ± 40.5 kWh/(m^2 y) and is here found at latitude 20° north.

The model is underestimating the yield at higher DNI at this mean operating temperature and is even more clear in the results for T_m = 160 °C in Appendix if the results for latitude 40° north in Figs. 4d, 7d and 10d are compared.

Figure 9 summarizes the slopes in the plots above and the same decrease when moving away from the equator can be seen here as in Fig. 6. The trends are similar in Figs. 6 and 9, but the size differs a bit due to decreased efficiency at the higher temperature.

3.2. Error analysis

The models displayed in Figs. 4, 5 and 7, 8 is summarized in Tables 3 and 4 respectively. The t-ratios indicate that the relation between annual yield and DNI is well described by the linear model for all the investigated T_m and latitudes, except for −50° where no conclusions can be drawn due to lack of data. The slopes of the regression lines are steepest close to the equator as one would expect as the tracking axis is horizontal. The mean residuals of the regressions for T_m = 85 °C were below 7% for all latitudes.

Comparing Tables 3 and 4 gives a signal on how the efficiency from *DNI* to *Q* (k_1) decreases with increasing T_m. It also indicates the increasing difficulty of modelling collector yield at higher mean operating temperatures. Even so, the mean residual for T_m = 120 °C is still below 9% and for T_m = 160 °C it is below 12.5% (see Appendix).

4. Conclusions and future work

The simulation tool used in this study has been validated against long-term measurements on a small T160 collector array installed and carefully monitored at DTU in Denmark. DNI measurements were available at the test installation at DTU and the whole chain of calculations was validated. The thermal performances of the studied parabolic trough collector array with 316 climate station conditions in 13 latitudes worldwide for three temperature scenarios were simulated based on the validated tool. These conclusions may be drawn:

(1) The hypothesis of a linear relation between annual PTC yield and DNI for a certain latitude was confirmed on 12 of the 13 investigated latitudes under three temperature scenarios. For the 13th latitude, 50° south, only one weather station was found so no conclusions can be drawn there. The general conclusion is that the annual performance of a tracking concentrating collector of type Absolicon T160 can be predicted quite accurately based on the proposed simplified model. Within accuracy 7% for T_m = 85 °C, 9% for T_m = 120 °C and 12.5% for T_m = 160 °C, annual thermal performance can be calculated based on only latitude and total yearly DNI. Simulation values like the ones listed in Table 3 could easily be used to determine collector performance and to do quick estimates.

Table 3
Results and error analysis of the linear models describing annual yield based on annual DNI for a certain latitude and a mean operating temperature, T_m = 85 °C. Note that for latitude −50° only one climate was simulated.

Figure	Latitude (± 2°)	k_1	Number of weather stations	RMS error [kWh/(m^2·y)]	Mean residual [%]	t-ratio
4a	70	0.247	4	19.9	6.92	35
4b	60	0.299	25	23.9	6.34	70
4c	50	0.360	82	23.3	4.81	149
4d	40	0.437	100	26.2	3.02	261
4e	30	0.493	35	29.9	2.61	197
4f	20	0.532	13	29.6	1.89	124
4g	10	0.554	21	18.6	1.87	206
4h	0	0.550	11	17.6	1.36	144
5a	−10	0.549	4	23.2	2.56	78
5b	−20	0.529	6	19.2	0.80	240
5c	−30	0.492	10	28.5	2.08	125
5d	−40	0.434	4	29.3	3.42	43
5e	−50	0.329	1	0.00	0.00	∞

Table 4
Results and error analysis of the linear models describing annual yield based on annual DNI for a certain latitude and a mean operating temperature, T_m = 120 °C. Note that for latitude −50° only one climate was simulated.

Figure	Latitude (± 2°)	k_1	Number of weather stations	RMS error [kWh/(m^2·y)]	Mean residual [%]	t-ratio
7a	70	0.197	4	20.0	8.95	28
7b	60	0.246	25	21.8	7.08	63
7c	50	0.298	82	25.5	6.14	117
7d	40	0.381	100	29.6	3.87	207
7e	30	0.439	35	37.4	3.88	149
7f	20	0.477	13	40.5	2.53	84
7g	10	0.491	21	25.1	2.93	141
7h	0	0.489	11	21.6	2.17	107
8a	−10	0.491	4	18.9	2.27	85
8b	−20	0.475	6	13.3	1.35	171
8c	−30	0.443	10	35.8	2.95	91
8d	−40	0.376	4	32.3	4.34	34
8e	−50	0.270	1	0.00	0.00	∞

There is a possibility to save both time and money by continuing developing simple prediction models that can be used in various manners where an accuracy of 12.5% is enough. All kinds of modelling based on normal years involve uncertainties, both traditional solar collector model simulations and this simple prediction model. The real year DNI is for example expected to deviate in the range of ± 8 to ± 15% according to [34].

(2) Based on the plots for T_m = 160 °C in Appendix one can argue whether it was a good decision to constrain the model to pass the origin. There is a trend that signals an offset in the plots. Higher mean operating temperatures increases the heat losses and hence undermine the arguments for keeping the constraint. In future work one should again consider whether an offset is needed, especially if even higher temperatures are modelled. It seems that at higher T_m, the model now tends to underestimate at high DNI and overestimate at low DNI.

At present, only the case of horizontal north-south axis direction has been investigated. But the relatively small collector array module design, is also suitable for application with tilt of the tracking axis and change of the azimuth according to local weather and installation conditions. This can be investigated by simulations in the future and preliminary simulations indicates a large performance improvement potential. It will therefore be of future interest to construct similar models that can handle tilts and rotations of collector fields.

The cosine behavior of k_1, see Figs. 6, 9 and 12, will also be analyzed more in future work. The spans around latitudes are likely to cause a minor scatter in the model. This could be minimized by analyzing the cosine behavior in detail.

Acknowledgements

Absolicon Solar Collector AB.

Appendix

See Figs. 10–12 and Table 5.

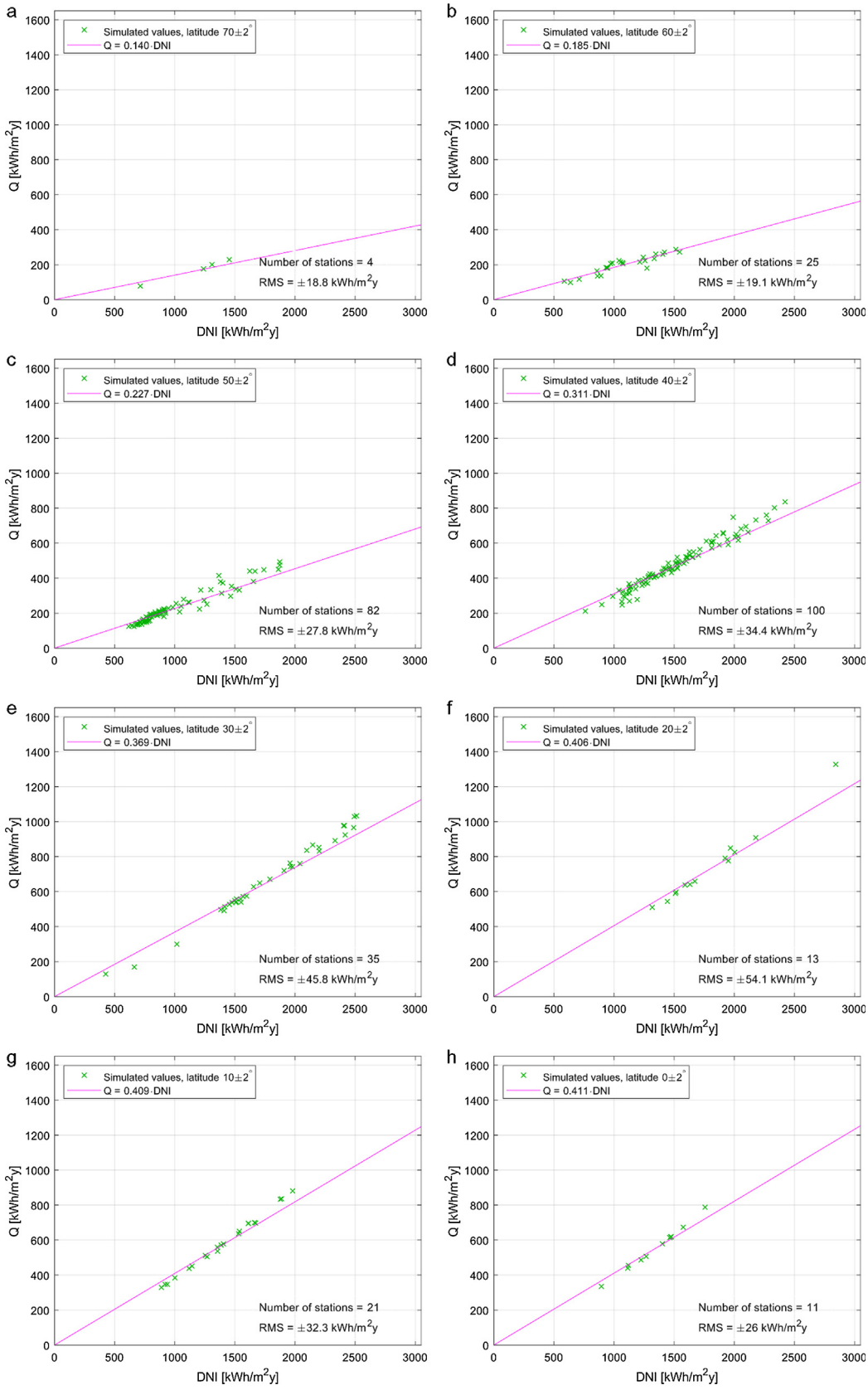

Fig. 10a–h. Simulated values for annual T160 collector yield compared to DNI around latitudes 70°, 60°, …, 0°. Collector yield simulations based on a mean operating temperature of 160 °C. A linear regression is shown with a magenta line. (For interpretation of the references to colour in this figure legend, the reader is referred to the web version of this article.)

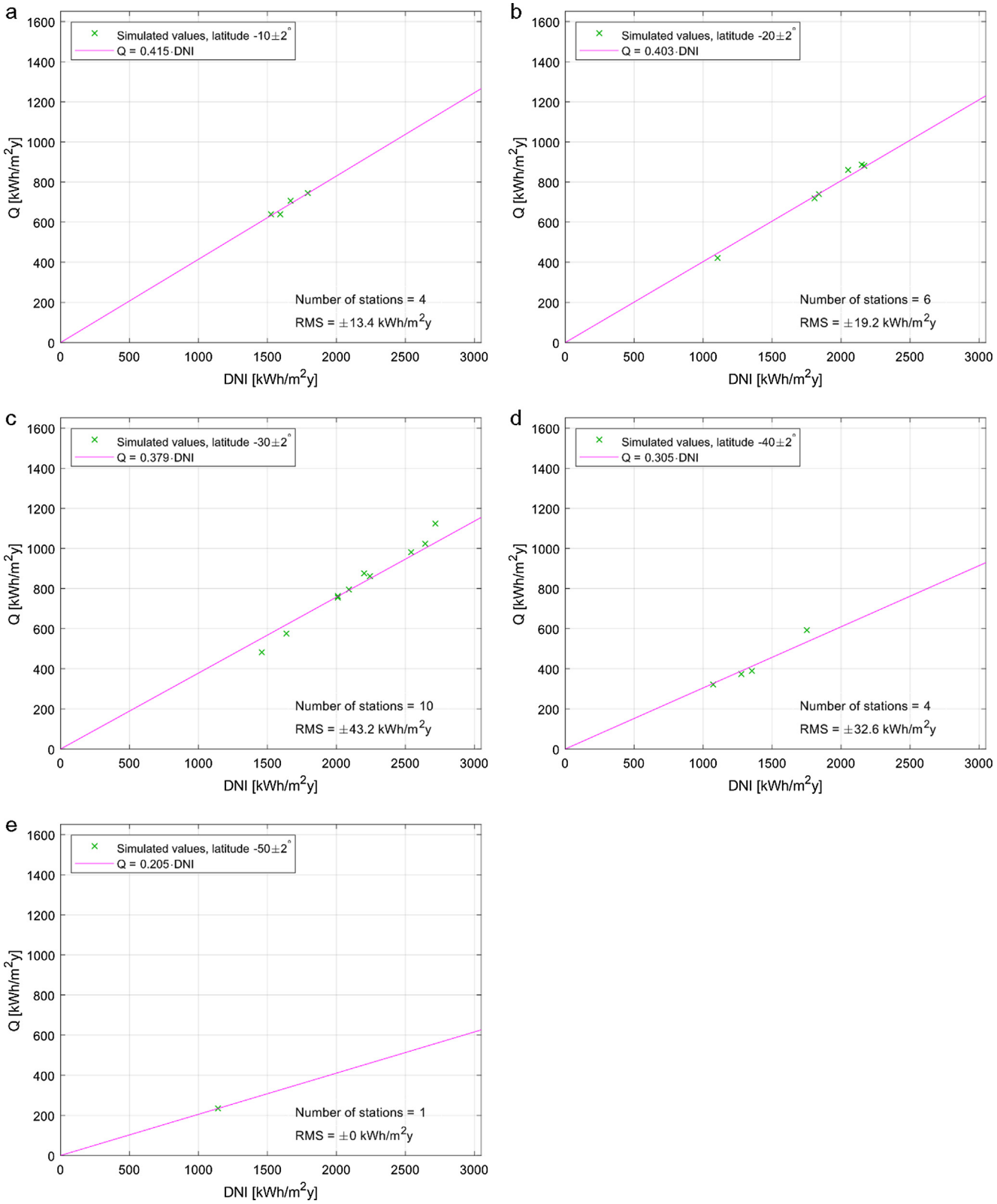

Fig. 11a–e. Simulated values for annual T160 collector yield compared to DNI around latitudes −10°, −20°, …, −50°. Collector yield simulations based on a mean operating temperature of 160 °C. A linear regression is shown with a magenta line. (For interpretation of the references to colour in this figure legend, the reader is referred to the web version of this article.)

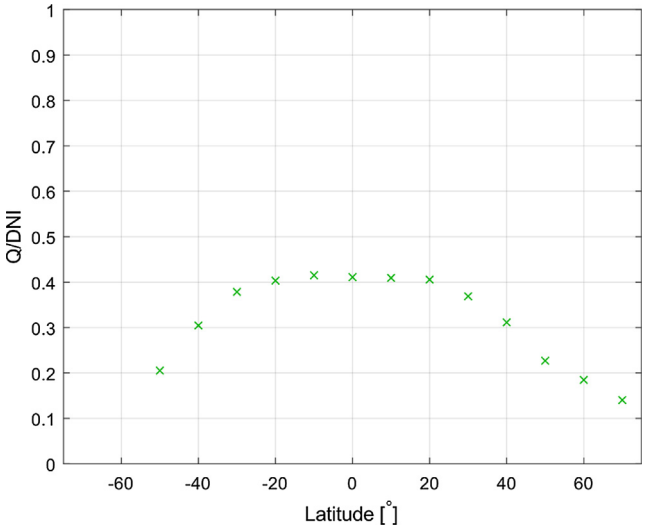

Fig. 12. Energy output per DNI plotted against latitude. Collector yield simulations based on a mean operating temperature of 160 °C.

Table 5
Results and error analysis of the linear models describing annual yield based on annual DNI for a certain latitude and a mean operating temperature, T_m = 160 °C. Note that for latitude −50° only one climate was simulated.

Figure	Latitude (± 2°)	k_1	Number of weather stations	RMS error [kWh/(m^2 y)]	Mean residual [%]	t-ratio
10a	70	0.140	4	18.8	12.3	22
10b	60	0.185	25	19.1	8.53	54
10c	50	0.227	82	27.8	8.30	86
10d	40	0.311	100	34.4	5.52	150
10e	30	0.369	35	45.8	6.26	106
10f	20	0.406	13	54.1	4.10	54
10g	10	0.409	21	32.3	4.56	94
10h	0	0.411	11	26.0	3.65	76
11a	−10	0.415	4	13.4	1.64	102
11b	−20	0.403	6	19.2	2.35	105
11c	−30	0.379	10	43.2	4.24	65
11d	−40	0.305	4	32.6	5.36	27
11e	−50	0.205	1	0.00	0.00	∞

References

[1] Tian Z, et al. Investigations of nearly (net) zero energy residential buildings in Beijing. Procedia Eng 2015;121:1051–7.
[2] Noussan M, Jarre M, Degiorgis L, Poggio A. Data analysis of the energy performance of large scale solar collectors for district heating. Energy Procedia 2017;134:61–8.
[3] Weiss Werner, Spörk-Dür Monika, Mauthner Franz. Solar heat worldwide-global market development and trends in 2016-detailed market figures 2015 (2017 version). <http://www.iea-shc.org/solar-heat-worldwide>; 2017.
[4] IEA. IEA-SHC Task 49; 2016. [Online]. Available: <http://task49.iea-shc.org/publications>.
[5] Khan MSA, Badar AW, Talha T, Khan MW, Butt FS. Configuration based modeling and performance analysis of single effect solar absorption cooling system in TRNSYS. Energy Convers Manag 2018;157:351–63.
[6] Tashtoush B, Alshare A, Al-Rifai S. Hourly dynamic simulation of solar ejector cooling system using TRNSYS for Jordanian climate. Energy Convers Manag 2015;100:288–99.
[7] Bava F, Furbo S. Development and validation of a detailed TRNSYS-Matlab model for large solar collector fields for district heating applications. Energy 2017;135:698–708.
[8] Kong W, et al. An improved dynamic test method for solar collectors. Sol Energy 2012;86(6):1838–48.
[9] Kong W, Wang Z, Li X, Li X, Xiao N. Theoretical analysis and experimental verification of a new dynamic test method for solar collectors. Sol Energy 2012;86(1):398–406.
[10] Deng J, Yang X, Wang P. Study on the second-order transfer function models for dynamic tests of flat-plate solar collectors Part I: a proposed new model and a fitting methodology. Sol Energy 2015;114:418–26.
[11] Deng J, Yang X, Wang P. Study on the second-order transfer function models for dynamic tests of flat-plate solar collectors Part II: experimental validation. Sol Energy 2017;141:334–46.
[12] Deng J, Xu Y, Yang X. A dynamic thermal performance model for fl at-plate solar collectors based on the thermal inertia correction of the steady-state test method. Sol Energy 2015;76:679–86.
[13] Tian Z, Perers B, Furbo S, Fan J. Analysis and validation of a quasi-dynamic model for a solar collector field with flat plate collectors and parabolic trough collectors in series for district heating. Energy 2018;142:130–8.
[14] Tian Z, Perers B, Furbo S, Fan J. Annual measured and simulated thermal performance analysis of a hybrid solar district heating plant with flat plate collectors and parabolic trough collectors in series. Appl Energy 2017;205:417–27.
[15] Tian Z, Perers B, Furbo S, Fan J. Thermo-economic optimization of a hybrid solar district heating plant with flat plate collectors and parabolic trough collectors in series. Energy Convers Manag 2018;165:92–101.
[16] Vela Solaris. Polysun; 2018. [Online]. Available: <http://www.velasolaris.com/english/home.html>.
[17] ScenoCalc. ScenoCalc - a program for calculation of annual solar collector energy output; 2018. [Online]. Available: <https://www.sp.se/en/index/services/solar/ScenoCalc/Sidor/default.aspx>.
[18] Berberich M. SCFW - solar yield prediction tool for solar district heating systems based on scenocalc. In: 5th international solar district heating conference; 2018.
[19] Salgado Conrado L, Rodriguez-Pulido A, Calderón G. Thermal performance of parabolic trough solar collectors. Renew Sustain Energy Rev 2017;67:1345–59.
[20] Halil Yılmaz İ, Mwesigye A. Modeling simulation and performance analysis of parabolic trough solar collectors: a comprehensive review. Appl Energy 2018;225:135–74.
[21] Reddy KS, Ajay CS, Nitin Kumar B. Sensitivity study of thermal performance characteristics based on optical parameters for direct steam generation in parabolic trough collectors. Sol Energy 2018;169:577–93.
[22] Xu L, et al. Analysis of the influence of heat loss factors on the overall performance of utility-scale parabolic trough solar collectors. Energy 2018.
[23] Cheng ZD, He YL, Cui FQ, Xu RJ, Tao YB. Numerical simulation of a parabolic

trough solar collector with nonuniform solar flux conditions by coupling FVM and MCRT method. Sol Energy 2012;86(6):1770–84.
[24] Cheng ZD, He YL, Cui FQ. A new modelling method and unified code with MCRT for concentrating solar collectors and its applications. Appl Energy 2013;101:686–98.
[25] Agagna B, Smaili A, Falcoz Q. Coupled simulation method by using MCRT and FVM techniques for performance analysis of a parabolic trough solar collector. Energy Procedia 2017;141:34–8.
[26] Cheng Z-D, He Y-L, Wang K, Du B-C, Cui FQ. A detailed parameter study on the comprehensive characteristics and performance of a parabolic trough solar collector system. Appl Therm Eng 2014;63(1):278–89.
[27] Shadmehri M, Narei H, Ghasempour R, Shafii MB. Numerical simulation of a concentrating photovoltaic-thermal solar system combined with thermoelectric modules by coupling Finite Volume and Monte Carlo Ray-Tracing methods. Energy Convers Manag 2018;172:343–56.
[28] He Y-L, Xiao J, Cheng Z-D, Tao Y-B. A MCRT and FVM coupled simulation method for energy conversion process in parabolic trough solar collector. Renew Energy 2011;36(3):976–85.
[29] Wu Z, Li S, Yuan G, Lei D, Wang Z. Three-dimensional numerical study of heat transfer characteristics of parabolic trough receiver. Appl Energy 2014;113:902–11.
[30] Wang Y, Liu Q, Lei J, Jin H. Performance analysis of a parabolic trough solar collector with non-uniform solar flux conditions. Int J Heat Mass Transf 2015;82:236–49.
[31] Tijani AS, Bin Roslan AMS. Simulation analysis of thermal losses of parabolic trough solar collector in malaysia using computational fluid dynamics. Procedia Technol 2014;15:841–8.
[32] Qiu Y, Li M-J, He Y-L, Tao W-Q. Thermal performance analysis of a parabolic trough solar collector using supercritical CO_2 as heat transfer fluid under non-uniform solar flux. Appl Therm Eng 2016.
[33] Tian Z, Perers B, Furbo S, Fan J, Deng J, Dragsted J. A comprehensive approach for modelling horizontal diffuse radiation, direct normal irradiance and total tilted solar radiation based on global radiation under danish climate conditions. Energies 2018;11(5):1315.
[34] Solargis. Global Solar Atlas. [Online]. Available: <http://globalsolaratlas.info>. [Accessed: 20-Apr-2018].
[35] Perers B. Optical modelling of solar collectors and booster reflectors under non stationary conditions. Uppsala: Uppsala University; 1995.
[36] Perers B. Dynamic method for solar collector array testing and evaluation with standard database and simulation programs. Sol Energy 1993;50(6):517–26.
[37] Perers B, Kovacs P, Olsson M, Persson M, Pettersson U. A tool for standardized collector performance calculations including PVT. Energy Procedia 2012;30:1354–64.
[38] Perers B, Karlsson B, Wallentun H. Simulation and evaluation for solar energy systems. D20:1990. Swedish Council for Building Research; 1990.
[39] TRNSYS. TRNSYS 17 - Volume 7 Programmer's Guide. Solar Energy Laboratory, University of Wisconsin-Madison; 2014.
[40] Absolicon Solar Collector AB. Absolicon Solar Collector AB; 2018.
[41] SP Technical Research Institute of Sweden. Test of Solar Collector Thermal Performance and Pressure Drop according to ISO 9806:2013 Ref:6P06089; 2016.
[42] TRNSYS. TRNSYS 17; 2017.
[43] SPF. SPF; 2018. [Online]. Available: <http://www.spf.ch/Testing.52.0.html?&L=6>.
[44] Perers B, Zinko H, Holst P. Analytical model for the input output energy relationship. In: First ec conference on solar heating, Amsterdam; 1984.
[45] Adsten M, Perers B, Wäckelgård E. The influence of climate and location on collector performance. Renew Energy 2002;25(4):499–509.
[46] Keymark S. Solar keymark database. [Online]. Available: <http://www.solarkeymark.dk/CollectorCertificates>. [Accessed: 20-Apr-2018].

Denmark has the most successful market worldwide for large solar district heating plants. It is interesting to analyse the potential of parabolic trough collectors in solar district heating plants in Denmark. The focus of this PhD study is on hybrid solar heating plants with flat plate collectors and parabolic trough collectors. The investigations show that hybrid solar district heating plants are technical-economically attractive in Denmark.

DTU Civil Engineering
Technical University of Denmark

Brovej, Bygning 118
2800 Kongens Lyngby
Tel. 45 25 17 00

www.byg.dtu.dk

ISBN 9788778774910
ISSN 1601-2917